STUDIES ON THE DEVELOPMENT OF STRUCTURE AND MORPHOLOGY IN NYLONS

Thesis submitted to the

UNIVERSITY OF PUNE

for the degree of

DOCTOR OF PHILOSOPHY

in

CHEMISTRY

by

Smitha S. Nair

Division of Polymer Science and Engineering

National Chemical Laboratory

PUNE: 411 008

INDIA

August 2006

DECLARATION

Certified that the work incorporated in this thesis entitled **"Studies on the Development of Structure and Morphology in Nylons"** submitted by **Smitha S. Nair** was carried out under my supervision. Such material as obtained from other sources has been duly acknowledged in this thesis.

August 2006
Pune

Dr. C. Ramesh
(Research Guide)

DECLARATION

I hereby declare that the thesis entitled **"Studies on the Development of Structure and Morphology in Nylons"** submitted for Ph. D. degree to the University of Pune has been carried out under the supervision of **Dr. C. Ramesh** at the Division of Polymer Science and Engineering, National Chemical Laboratory, Pune, India. The work is original and has not been submitted in part or full by me for any degree or diploma to this or any other University.

August 2006 (**Smitha S. Nair)**

Pune

Dedicated to my Parents…

"The whole of science is nothing more than a refinement of everyday thinking."

— Albert Einstein.

ACKNOWLEDGEMENTS

During the course of my thesis work, there were many people who were instrumental in helping me. I would like to take this opportunity to thank all those people who made this thesis possible and an enjoyable experience for me.

Firstly, my heartfelt gratitude to Dr. C. Ramesh, my research supervisor, mentor, for his guidance, fruitful discussions, valuable advice, constant support and encouragement throughout the course of this work. My sincere regards and reverence are for him, forever.

I am grateful to Dr. S. Sivaram, Director, NCL, who gave me an opportunity to work in this prestigious research institute. I am very lucky to have got the opportunity to associate with him many times.

I am extremely grateful to my collaborator Prof. Kohji Tashiro, Department of Future Industry-oriented Basic Science and Materials Graduate School of Engineering, Toyota Technological Institute, Nagoya, Japan for his valuable suggestions.

My special thanks to Drs. C. V. Avadhani, T. P. Mohandas, P. P. Wadgaonkar, S. P. Vernekar, S. Ponrathnam, M.G. Kulkarni, R. A. Kulkarni, D. Baskaran, R. P. Singh, A. K. Lele, K. Guruswamy, V. Natarajan, C. R. Rajan and Jayant Gadgil (Wadia College), for their needful help. I am also thankful to Mrs. D. A. Dhoble, Dr. (Mrs). A. N. Bote, Mr. S. K. Menon, Dr. R. S. Khisti, Dr. (Mrs). S. B. Idage, Mrs. Gracy Mathew and Mr. A. B. Gaikwad (SEM facility) for their help during the course of this work.

I am forever indebted to all my teachers for guiding me to embrace the good in everything I see.

I owe deeply to my ever-trustful friends in lab Dr. Bhoje Gowd, Mallikarjuna, Raghunath Reddy, Govindaiah, Tony Mathew, and Dr. V. Raghunadh, for all their affection and help. I must thank Bhoje especially for the constant support and encouragement he has given me.

My sincere thanks to my colleagues and all the members of Polymer Science and Engineering division, for their cooperation, and for providing me with an excellent working ambience during the course of this work.

I thank the members of PPC and NMR facility of NCL for their timely help. Many thanks are due to the Library staff, Administrative staff and the members of Glass Blowing, Engineering Services, Stores and Purchase for their cooperation. The award of research fellowship by CSIR, New Delhi is duly acknowledged.

I acknowledge an appreciation that extends beyond any words for the love and support of my friend Katherine. I wholeheartedly thank my friends Jinu, Nachiappan, Kailash, Anuji, Panchami, Mahima, Jainy, Sony, Manoj, Lisha, Virginia, Nilakshi, Poorvi, Sonu, Sharmili, Suman, Sabitha, Sreedevi, Priya, Harsha, Snehalata, Neeta, Sunita, Gnaneshwar, Pratheep, Rana, Bhalchandra, Bhaskar, Easwar, Balaji, Dhanya, Kavitha, Anesh, Lijo, Vinod, Sreeprasanth, and many others who made my stay at NCL pleasant. Their friendship shall always be remembered.

I express my deep sense of gratitude to Dr. Mrs. Lisi Nair for her continuing encouragement and affection.

I find no words to express my feelings for my parents and my brother Suraj. Their infallible love and support has always been my strength. Their patience and sacrifice will remain my inspiration throughout my life.

Above all I thank God the almighty for guiding me in my life.

Though, many have not been mentioned, none is forgotten.

(Smitha S. Nair)

CONTENTS

* Abstract i
* Glossary iii
* List of Tables iv
* List of Schemes v
* List of Figures vi

CHAPTER 1. GENERAL INTRODUCTION

1.1 Introduction 1
1.1.1 Synthetic Methods 1
1.1.1.1 Direct Amidation by Melt Polymerization 1
1.1.1.2 Reaction of Acid Chlorides with Amines 2
1.1.1.3 Ring Opening Polymerization 2
1.1.2 Crystal Structure 3
1.2 Crystalline Transitions in Nylons 5
1.2.1 Nylon-6,6 5
1.2.1.1 X-ray Diffraction Studies 5
1.2.1.2 Infrared Spectroscopy Studies 8
1.2.1.3 Crystalline Transitions in Nylon-6,6–clay Nanocomposites 8
1.2.2 Nylon-6 9
1.2.2.1 Crystalline Transitions in Nylon-6–clay Nanocomposites 14
1.2.3 Even-Even Nylons 16
1.2.3.1 Nylons -6,10 and -6,12 16
1.2.3.2 Nylons -4,6 -6,8 -8,10 and -10,12 [2N,2(N+1) Nylons] 19
1.2.3.3 Nylon-10,10 21
1.2.3.4 Nylons-X,4 (X = 4, 6, 8, 10, and 12) 25
1.2.3.5 Nylons-X,18 (X = 2, 4, 6, 8, 10, and 12) 26
1.2.3.6 Nylons-2,Y (Y = 6, 8, 10, and 12) 27
1.2.3.7 Nylons -4,8, -4,10, -4,12, -6,10, -6,12, -6,18 and -8,12 28
1.2.3.8 Nylons -6,6, -8,6, -8,8, -10,6, -10,8, -10,10, -12,6, -12,8, -12,10 and -12,12 29
1.2.3.9 Nylons -2,16, -4,16, -6,16, -8,16, -10,16, -12,16 30
1.2.3.10 Nylons -10,20 and -12,20 32

1.2.3.11 Nylon-12,12 33
1.2.3.12 Nylon-4,14 36
1.2.3.13 Nylon-10,14 36
1.2.4 Even Nylons 37
1.2.4.1 Nylon-8 37
1.2.4.2 Nylon-12 37
1.2.5 Even-Odd Nylons 39
1.2.5.1 Nylon-6,5 39
1.2.5.2 Nylon-6,9 40
1.2.5.3 Nylon-12,5 41
1.2.6 Odd-Even Nylons 41
1.2.6.1 Nylon-5,6 41
1.2.6.2 Nylon-5,10 42
1.2.6.3 Nylon-9,2 42
1.2.6.4 Nylons -11,10 and -11,12 43
1.2.7 Odd Nylons 44
1.2.7.1 Nylon-11 44
1.2.8 Odd-Odd Nylons 49
1.2.8.1 Nylon-5,5 49
1.3 References 49

CHAPTER 2. SCOPE AND OBJECTIVES OF THE PRESENT WORK

2.1 Introduction 56
2.2 Objectives of the present work 57
2.2.1 Crystalline phases in Nylon-11: Studies using HTWAXS and HTFTIR 57
2.2.2 Studies on the Crystalline Phases of Nylons -6,7 and -6,9 57
2.2.3 Studies on the Crystallization Behavior of Nylon-6 in the presence of Layered Silicates using Variable Temperature WAXS and FTIR 57
2.3 References 58

CHAPTER 3. CRYSTALLINE PHASES IN NYLON-11: STUDIES USING HTWAXS AND HTFTIR

3.1 Introduction 60
3.2 Experimental Section 61

3.3 Results and Discussion 64
3.4 Conclusion 85
3.5 References 85

CHAPTER 4. STUDIES ON THE CRYSTALLINE PHASES OF NYLONS -6,7 AND -6,9

4.1 Introduction 88
4.2 Experimental Section 88
4.2.1 Materials 88
4.2.2 Synthesis of Nylon-6,7 88
4.2.2.1 Melt Polymerization technique 89
4.2.2.2 Interfacial Polymerization technique 89
4.2.3 Sample Preparation 89
4.2.4 Characterization 90
4.3 Results and Discussion 90
4.3.1 Studies on Nylon-6,7 90
4.3.1.1 NMR Studies 90
4.3.1.2 Thermal Analysis 92
4.3.1.3 Variable Temperature WAXS Studies 93
4.3.1.4 Variable Temperature FTIR Studies 98
4.3.2 Studies on Nylon-6,9 104
4.3.2.1 NMR Studies 104
4.3.2.2 Thermal Analysis 106
4.3.2.3 Variable Temperature WAXS Studies 107
4.3.2.4 Variable Temperature FTIR Studies 112
4.4 Conclusion 118
4.5 References 119

CHAPTER 5. STUDIES ON THE CRYSTALLIZATION BEHAVIOR OF NYLON-6 IN THE PRESENCE OF LAYERED SILICATES USING VARIABLE TEMPERATURE WAXS AND FTIR

5.1 Introduction 121
5.2 Experimental Section 122
5.3 Results and Discussion 123

5.3.1 Variable Temperature WAXS Studies 123
5.3.2 Variable Temperature FTIR Studies 129
5.4 Conclusion 137
5.5 References 137

CHAPTER 6. SUMMARY AND CONCLUSIONS

6.1 Summary 139
6.2 Conclusions 140
6.3 Perspectives 141

ABSTRACT

The thesis presents the results on the crystalline studies made on the various crystalline phases of nylons and more specifically on the γ phase. To that end three different types of nylons were chosen: i) even nylon, nylon-6 ii) odd nylon, nylon-11 iii) even-odd nylons, nylons -6,7 and -6,9. These nylons were crystallized into the α, γ and psuedohexagonal phases by appropriate methods.

Nylon-11 was crystallized into different crystalline phases by appropriate methods. The change in the structure during heating was monitored *in situ* by wide-angle X-ray scattering (WAXS). The α phase obtained by precipitating nylon-11 in 1,4-butanediol started transforming into the pseudohexagonal phase on heating, but the transformation was not fully completed before melting. The melt-crystallized sample at 175 °C gave the pseudohexagonal phase, which transformed into the α' phase on cooling to room temperature at about 100 °C. The *d* spacing of the 001 reflection also showed a change at the transition temperature. The melt-quenched sample showed the pseudohexagonal phase, which did not change during heating but on cooling transformed into the α' phase. The γ phase was obtained by casting nylon-11 in trifluoro acetic acid (TFA), and it changed into the pseudohexagonal phase at about 110 °C on heating. The *d* spacing of the 001 reflection depended on the way in which it was obtained. The studies have shown that nylon-11 is one of the few nylons that exhibit extensive degree of polymorphism. High temperature Fourier transform infrared spectroscopy (HTFTIR) studies revealed, apart from the conformational differences between various phases of nylon-11, some information on the formation of the γ phase.

Nylon-6,7 was synthesized by interfacial and melt polymerization techniques, and a detailed study was carried out on its crystalline phases on heating and cooling using HTWAXS and HTFTIR. Crystalline transition studies were also carried out on nylon-6,9, a known even-odd nylon, with a chemical repeat unit close to nylon-6,7 using HTWAXS and HTFTIR. The results obtained were compared with that of nylon-6,7.

Nylon-6,7 precipitated in 1,4-butanediol crystallized in the γ phase with a small amount of α phase which transformed into the γ phase above 140 °C and the sample melted in the γ phase. The melt-crystallized sample at 220 °C gave the γ phase, which was retained on

cooling to the room temperature. However, an additional peak was observed close to the main γ phase peak, which was due to the metastable phase and it transformed into the γ phase on cooling at about 150 °C. The melt-quenched sample showed the pseudohexagonal phase, and at about 190 °C, the metastable phase started appearing and coexisted with the psuedohexagonal phase until melting. If the psuedohexagonal phase was cooled without allowing it to melt, it transformed into the γ phase.

The α phase obtained by precipitating nylon-6,9 in 1,4-butanediol transformed into the γ phase at about 190 °C on heating, which was stable up to melting. During this transition a small amount of the material transformed into the metastable phase and was stable until melting. Melt-quenched nylon-6,9 crystallized into the psuedohexagonal phase and similar to nylon-6,7, the metastable phase was formed at about 160 °C. On cooling the psuedohexagonal phase transformed into the γ phase immediately.

The HTFTIR studies indicated that in the case of nylon-6,7, the molecular conformation in the γ phases obtained by 1,4-butanediol crystallization and melt crystallization were different. On the other hand nylon-6,9 crystallized in 1,4-butanediol showed spectra typical of the α phase, while the melt-crystallized sample showed spectra due to the γ phase.

The crystallization of nylon-6 clay nanocomposite was studied by variable temperature wide-angle X-ray scattering (WAXS) and Fourier transform infrared spectroscopy (FTIR). Nylon-6 was found to crystallize into the γ phase at 210 ^{o}C, as indicated by its characteristic peaks in WAXS. However, an additional peak was observed close but on the lower angle side of the main γ phase peak indicating the presence of a metastable phase. The metastable phase transformed into the γ phase on cooling. The transformation was reversed on heating. The clay content in the nanocomposite, as well as the crystallization conditions dictated the extent of metastable phase that developed. The behavior of the *d* spacing of the γ phase obtained in the presence of clay layers showed subtle difference from the γ phase obtained by treating nylon-6 in KI/I_2 solution. Variable temperature FTIR studies were conducted on the γ phases for the first time and it showed minor differences in the spectra of the phases obtained by the two methods.

GLOSSARY

DSC	Differential scanning calorimetry
DTA	Differential thermal analysis
DTGS	Deuterated triglycine sulfate
FTIR	Fourier transform infrared spectroscopy
FWHM	Full width at half maximum
ΔH	Enthalpy of melting
HTFTIR	High temperature Fourier transform infrared spectroscopy
HTWAXS	High temperature wide-angle X-ray scattering
KBr	Potassium Bromide
KI/I_2	Potassium Iodide / Iodine
MMT	Montmorillonite
NMR	Nuclear magnetic resonance
SAXS	Small-angle X-ray scattering
SEM	Scanning electron microscopy
T_B	Brill temperature
T_c	Crystallization temperature upon cooling
TEM	Transmission electron microscopy
TFA	Trifluoro acetic acid
T_g	Glass transition temperature
T_m	Melting temperature
TMS	Trimethyl silane
WAXS	Wide-angle X-ray scattering
XRD	X-ray diffraction
η_{inh}	Inherent viscosity

List of Tables

1.1	Crystallization/Holding temperature (T_c) and Brill temperature (T_B) of Nylon-6,10.	18
1.2	Thermal data and Brill spacings for 2N,2(N+1) Nylons.	21
1.3	Thermal data and Brill spacings for the X,4 Nylons.	26
1.4	T_B and T_m for the X,18 Nylons.	27
1.5	Thermal data and Brill spacings for the 2,Y Nylons.	28
1.6	Thermal data and Brill spacings for Nylons -4,8, -4,10, -4,12, -6,10, -6,12, -6,18 and -8,12.	29
1.7	Thermal data and Brill spacings for Nylons -6,6, -8,6, -8,8, -10,6, -10,8, -10,10, -12,6, -12,8, -12,10 and -12,12.	29
1.8	T_B and T_m values of Nylons -2,16, -4,16 and -6,16.	31
1.9	T_B and T_m values of Nylons -8,16, -10,16 and -12,16.	31
3.1	Crystallization/Holding Temperature (T_c) and Transition Temperature (T_B) of Nylon-11.	72

List of Schemes

1.1	Reaction of diamine with dicarboxylic acid.	1
1.2	Reaction of diamine with diacid chloride.	2
1.3	Ring opening polymerization of caprolactam.	3

List of Figures

1.1 Hydrogen-bonded sheets in (a) nylon-6,6 and (b) nylon-6. Unit cell face shown dotted. 4

1.2 (a) Progressive shear in nylon-6,6 α phase. (b) Staggered shear in nylon-6 α phase and nylon-6,6 β phase. 4

1.3 Temperature dependence of *d* spacings observed for (100) and (010/110) reflections of nylon-6,6 in the heating process (O) and cooling process (,). 6

1.4 Schematic of hydrogen bonding within α and γ phases of nylon-6 as seen from end and side-view of each crystal. Closed and open circles represent chain axes projecting out of and into the page, respectively. Dashed lines represent hydrogen bonds between nylon chains. The upper left hand portion of this figure was adopted from the work of Aharoni. 10

1.5 Variation of *d* spacing of (a) a quenched amorphous nylon-6,10 sample on heating and (b) during cooling from various holding temperatures. 18

1.6 (a) An energetically minimized crystal structure model of nylon-10,10 α phase used for the molecular dynamics simulation and (b)-(d) the snapshots extracted on the way of molecular dynamics calculation at the various temperatures. 25

1.7 The XRD patterns of the α phase of nylon-12,12 drawn with different ratios at 90 °C. 35

1.8 The XRD patterns of the α phase of nylon-12,12 drawn with different ratios at 160 °C. 35

1.9 Crystal transitions of nylon-11: (a) quenching into ice bath, (b) heating to high temperature (>95 °C), (c) heating to high temperature (>95 °C), (d) isothermal crystallization at high temperature (>95 °C), (e) drawing at low temperature (<95 °C), (f) annealing at high temperature (>95 °C), (g) cooling to high temperature (>95 °C), (h) quenching into ice bath, and (i) isothermal crystallization at high temperature (>95 °C). 46

1.10 XRD patterns of (a) nylon-11 molten at 205 °C and then melt-crystallized at room temperature, (b) nylon-11 casting from the trifluoroacetic acid solution, (c) nylon-11–MMT nanocomposite molten at 205 °C and then melt-crystallized at room temperature, and (d) nylon-11–MMT nanocomposite molten at 205 °C, melt-crystallized at room temperature, and then annealed at 160 °C for 24h. 48

1.11 IR spectra of (a) nylon-11 molten at 205 °C and then melt-crystallized at room temperature, (b) nylon-11 casting from the trifluoroacetic acid solution, and (c) nylon-11–MMT nanocomposite molten at 205 °C and then melt-crystallized at room temperature in the region of 900-550 cm^{-1}. 48

3.1 The DSC thermograms obtained during the first heating for 1,4-butanediol crystallized, melt-crystallized, quenched and TFA-cast nylon-11. 64

3.2 Behavior of (a) XRD patterns and (b) *d* spacings on heating from room temperature to melt for the α phase of nylon-11 crystallized in 1,4-butanediol. 65

3.3 (a) Isothermal crystallization behavior for nylon-11 at 175 ^{o}C. (b) Degree of crystallinity and the variation of amorphous peak position during isothermal crystallization at 175 ^{o}C. 67

3.4 Behavior of (a) XRD patterns and (b) *d* spacings of nylon-11 melt-crystallized at 175 °C on cooling to room temperature. 69

3.5 Behavior of the *d* spacings of the 001 reflection on cooling from T_c to room temperature and on heating from room temperature to melting. 70

3.6 Behavior of (a) XRD patterns and (b) *d* spacings on heating from room temperature to melt for quenched nylon-11. 71

3.7 The behavior of the *d* spacings of the melt quenched sample on heating to 170 °C and on cooling from the holding temperatures 170 °C, 150 °C and 120 °C to room temperature. The arrows indicate the direction of heating/cooling. 72

3.8 Behavior of (a) XRD patterns and (b) *d* spacings on heating from room temperature to melt for γ phase obtained by casting nylon-11 film from TFA. The indexing is based on *c* axis along the chain direction. 74

3.9 Variable temperature FTIR spectra of the region 500–800 cm^{-1} of nylon-11 during heating from room temperature to melt: (a) α phase (1,4-butanediol crystallized), (b) α' phase (melt-crystallized), and (c) γ phase obtained by casting in TFA. The variation of the wave number of amide V and amide VI bands during heating for (d) α phase, (e) α' phase, and (f) γ phase. 76

3.10 Variable temperature FTIR spectra of the region 1100–1400 cm^{-1} of nylon-11 during heating from room temperature to melt: (a) α phase, (b) α' phase, and (c) γ phase. The variation of the wave number and normalized absorbance of bands 1160 and 1190 cm^{-1} during heating for (d) α phase, and (e) α' phase. (f) The variation of the wave number and normalized absorbance of bands 1160 and 1198 cm^{-1} during heating for γ phase. 78

3.11 Variable temperature FTIR spectra of the region 1500–1800 cm^{-1} of nylon-11 during heating from room temperature to melt: (a) α phase, (b) α' phase, and (c) γ phase. The variation of the wave number and normalized absorbance of amide I and amide II bands during heating for (d) α phase, (e) α' phase, and (f) γ phase. 80

3.12 Variable temperature FTIR spectra of the region 3000–3600 cm^{-1} of nylon-11 during heating from room temperature to melt: (a) α phase, (b) α' phase, and (c) γ phase. The variation of the wave number and normalized absorbance of amide A band during heating for (d) α phase, (e) α' phase, and (f) γ phase. 81

3.13 Variable temperature FTIR spectra of the TFA-cast nylon-11 film with 5% TFA during heating from room temperature to melt: (a) 3000–3600 cm^{-1}, (b) 1500–1800 cm^{-1}, and (c) 1100–1400 cm^{-1}. The variation of the wavenumber and normalized absorbance of the characteristic bands (d) 3000–3600 cm^{-1}, (e) 1500–1800 cm^{-1}, and (f) 1100–1400 cm^{-1}. 84

4.1 ^{1}H NMR spectrum of nylon-6,7. 91

4.2 ^{13}C NMR Spectrum of nylon-6,7. 91

4.3 The DSC thermograms obtained during (a) first heating, (b) cooling, and (c) reheating, for nylon-6,7 crystallized in1,4-butanediol. 92

4.4 Behavior of (a) XRD patterns and (b) *d* spacings on heating from room temperature to melt for nylon-6,7 crystallized in 1,4-butanediol. 93

4.5 Behavior of (a) XRD patterns and (b) *d* spacings of nylon-6,7 melt-crystallized at 220 °C on cooling to room temperature. 95

4.6 Behavior of (a) XRD patterns and (b) *d* spacings on heating from room temperature to melt for quenched nylon-6,7. 96

4.7 Behavior of XRD patterns of the melt-quenched nylon-6,7 sample on cooling from the holding temperatures (a) 200 °C, and (b) 170 °C to room temperature. The behavior of *d* spacings of the melt-quenched sample on cooling from the holding temperatures (c) 200 °C, and (d) 170 °C to room temperature. 97

4.8 Variable temperature FTIR spectra of the region 500–800 cm^{-1} of nylon-6,7 during heating from room temperature to melt for (a) 1,4-butanediol crystallized, and (b) melt-crystallized samples. The variation of the wavenumber of amide V and amide VI bands during heating for (c) 1,4-butanediol crystallized, and (d) melt-crystallized samples. 99

4.9 Variable temperature FTIR spectra of the region 1100–1400 cm^{-1} of nylon-6,7 during heating from room temperature to melt for (a) 1,4-butanediol crystallized, and (b) melt-crystallized samples. 100

4.10 Variable temperature FTIR spectra of the region 1500–1800 cm^{-1} of nylon-6,7 during heating from room temperature to melt for (a) 1,4-butanediol crystallized, and (b) melt-crystallized samples. The variation of the wavenumber of amide I and amide II bands during heating for (c) 1,4-butanediol crystallized, and (d) melt-crystallized samples. 102

4.11 Variable temperature FTIR spectra of the region 3000–3600 cm^{-1} of nylon-6,7 during heating from room temperature to melt for (a) 1,4-butanediol crystallized, and (b) melt-crystallized samples. The variation of the wavenumber and normalized absorbance of amide A band during heating for (c) 1,4-butanediol crystallized, and (d) melt-crystallized samples. 103

4.12 ^{1}H NMR spectrum of nylon-6,9. 105

4.13 ^{13}C NMR Spectrum of nylon-6,9. 105

4.14 The DSC thermograms obtained during (a) first heating, (b) cooling, and (c) reheating, for nylon-6,9 crystallized in1,4-butanediol. 106

4.15 Behavior of (a) XRD patterns and (b) *d* spacings on heating from room temperature to melt for nylon-6,9 crystallized in 1,4-butanediol. 108

4.16 Behavior of (a) XRD patterns, (b) *d* spacings of nylon-6,9 melt-crystallized at 205 °C on cooling to room temperature, and (c) *d* spacings of the 001 reflection on cooling from T_c to room temperature. 109

4.17 Behavior of (a) XRD patterns and (b) *d* spacings on heating from room temperature to melt for quenched nylon-6,9. 111

4.18 Behavior of (a) XRD patterns and (b) *d* spacings of the melt-quenched nylon-6,9 sample on cooling from the holding temperature 175 °C to room temperature. 112

4.19 Variable temperature FTIR spectra of the region 500–800 cm^{-1} of nylon-6,9 during heating from room temperature to melt for (a) 1,4-butanediol crystallized, and (b) melt-crystallized samples. The variation of the wavenumber of amide V and amide VI bands during heating for (c) 1,4-butanediol crystallized, and (d) melt-crystallized samples. 113

4.20 Variable temperature FTIR spectra of the region 1100–1400 cm^{-1} of nylon-6,9 during heating from room temperature to melt for (a) 1,4-butanediol crystallized, and (b) melt-crystallized samples. 115

4.21 Variable temperature FTIR spectra of the region 1500–1800 cm^{-1} of nylon-6,9 during heating from room temperature to melt for (a) 1,4-butanediol crystallized, and (b) melt-crystallized samples. The variation of the wavenumber of amide I and amide II bands during heating for (c) 1,4-butanediol crystallized, and (d) melt-crystallized samples. 116

4.22 Variable temperature FTIR spectra of the region 3000–3600 cm^{-1} nylon-6,9 during heating from room temperature to melt for (a) 1,4-butanediol crystallized, and (b) melt-crystallized samples. The variation of the wavenumber and normalized absorbance of amide A band during heating for (c) 1,4-butanediol crystallized, and (d) melt-crystallized samples. 117

5.1 (a) Behavior of XRD patterns and (b) *d* spacings on cooling from T_c to room temperature of nylon-6 cloisite 25A nanocomposite (6%). 124

5.2 Behavior of XRD patterns on heating from room temperature to melt of nylon-6 cloisite 25A nanocomposite (5.5%) crystallized in a silicone oil bath at 100 ^oC. (Note: Sample prepared in Haake Rheocord). 127

5.3 XRD patterns at the end of crystallization at 210 ^oC for various clay contents of nylon-6–clay nanocomposites. Inset shows the ratio of the 200 peaks of the metastable and γ phases at 210 ^oC. 127

5.4 Behavior of (a) XRD patterns and (b) *d* spacings of clay at low 2θ ranges on cooling from T_c (210 ^oC) to room temperature for nylon-6 cloisite 25A nanocomposite (6%). 129

5.5 Variable temperature FTIR spectra of the region 400–800 cm^{-1} of nylon-6 during heating from room temperature to melt: (a) α phase; (b) γ phase obtained by treating α phase in KI/I_2 solution at room temperature; (c) γ phase obtained by melt crystallization of nylon-6–clay nanocomposite; (d) variation of the wavenumber of amide V band at 690 cm^{-1} for all the three phases during heating; (e) variation of the wavenumber of amide VI bands at 585 cm^{-1} and 623 cm^{-1} for the γ phases during heating. 131

5.6 Variable temperature FTIR spectra of the region 900 to 1050 cm^{-1} of nylon-6 during heating from room temperature to melt: (a) α phase (b) γ phase obtained by treating α phase in KI/I_2 solution at room temperature (c) γ phase obtained by melt crystallization of nylon-6–clay nanocomposite. The variation of (d) wave number (e) full width at half maximum (f) normalized absorbance for the 962 and 975 cm^{-1} bands for the γ phases during heating. 133

5.7 Variable temperature FTIR spectra of the region 1150 to1300 cm^{-1} of nylon-6 during heating from room temperature to melt: (a) α phase (b) γ phase obtained by treating α phase in KI/I_2 solution at room temperature (c) γ phase obtained by melt crystallization of nylon-6–clay nanocomposite. The variation of (d) wave number (e) full width at half maximum (f) normalized absorbance for the 1234 cm^{-1} band for the γ phases during heating. 134

5.8 Variable temperature FTIR spectra of the region 2750 to 3750 cm^{-1} of nylon-6 during heating from room temperature to melt: (a) α phase (b) γ phase obtained by treating α phase in KI/I_2 solution at room temperature (c) γ phase obtained by melt crystallization of nylon-6–clay nanocomposite (d) The variation of the wave number of amide A band at 3301 cm^{-1} with temperature for all the three samples. 136

CHAPTER 1

GENERAL INTRODUCTION

1.1 Introduction

Dr. Wallace Hume Carothers of Du Pont, USA, invented aliphatic polyamide or nylon as the first "engineering thermoplastic" in the 1930's.[1] Nylons can be synthesized by condensation of amino acids (nylons *n)* or diamines and dibasic acids (nylons *m,n).* Nylons are important semicrystalline polymers with many useful properties. The properties are dictated by the structure consisting of flexible methylene segments and rigid amide groups connected in an alternate manner along the chain axis. Among nylons, nylon-6,6 and nylon-6 are commercially successful and have been extensively explored scientifically.

1.1.1 Synthetic Methods

Although nylons have been prepared by many methods, only melt polycondensation, ring-opening, and low temperature solution polymerization have gained commercial importance.[2]

1.1.1.1 Direct Amidation by Melt Polymerization

In direct amidation by melt methods a diamine reacts directly with a dicraboxylic acid to form a polymer with elimination of water, as shown in Scheme 1.1.

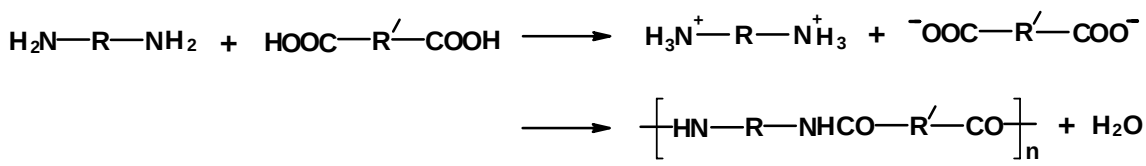

Scheme 1.1: Reaction of diamine with dicarboxylic acid.

The reactive groups may be part of a single molecule, (e.g., an amino acid) or they may be on different molecules (e.g., diamines and dicarboxylic acids). In the latter case, a precise balance of reactive groups must be present to ensure that high molecular weight is achieved. Isolating and purifying the salt formed by mixing the intermediates in balanced proportions or by controlling the pH of an aqueous common solution of both reactants achieve the precise balance of the acid and amine groups. This is not necessary for amino acids because there is a natural balance of amine and carboxylic groups.

1.1.1.2 Reaction of Acid Chlorides with Amines

Low temperature polycondensation of acid chlorides with diamines is a particularly useful method of preparing polyamides from aromatic diamines of relatively low basicity. It is also useful for preparing polymers from amines that are not thermally stable or in reactions in which there is a danger of cross-linking at elevated temperatures.

Interfacial polymerization was the initial low temperature route for the preparation of polyamides from diamines and diacid chlorides. Basically, the method consists in reacting a diacid chloride in a water-immiscible solvent with a diamine in water containing a detergent and an organic base as hydrogen chloride acceptor. The reaction takes place at the organic side of the interface. Fast stirring maximizes the amount of interface and maximizes the efficiency of the reaction. Overall balance of the reactants is not critical because the balance at the interface is the important feature. The polymerization works well for aliphatic (highly basic) amines but not for aromatic amines. The inorganic base (HCl acceptor) can be hydroxide, carbonate, or bicarbonate, depending on the basicity or reactivity of the amine (i.e., weak acid acceptor for weak amines).

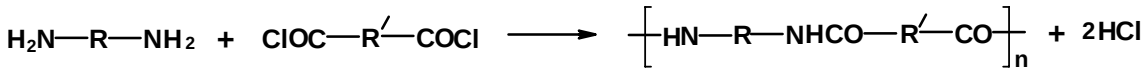

Scheme 1.2: Reaction of diamine with diacid chloride.

The interfacial method is useful for preparation of small polymer samples for evaluation, but has limited commercial utility because of broad molecular weight distribution and difficulty in removing salt and detergent contaminants.

1.1.1.3 Ring Opening Polymerization

Ring opening polymerization is an effective and commercially important route for preparing aliphatic polyamides from lactams. The ring opening occurs without elimination of another molecule. This is the major commercial route for preparing nylon-6 from caprolactam.[3] Water, amino acid, or amine carboxylate is used as an initiator. The water hydrolyzes some of the lactam to amino acid, which is the true initiator. Pure, dry caprolactam does not polymerize, even on prolonged heating at elevated temperatures. Polyamides from lactams are also readily prepared by anionic ring opening polymerization

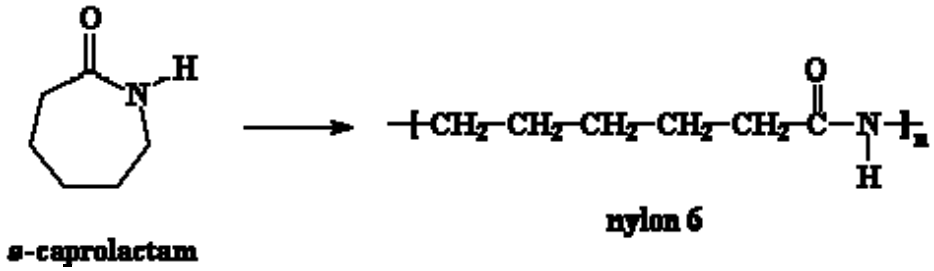

Scheme 1.3: Ring opening polymerization of caprolactam.

using strong bases, such as sodium hydride as initiator, and an acylating cocatalyst (e.g., acetic anhydride). A most effective, commercially available cocatalyst is *N*-acetylcaprolactam, which can be used in most anionic polymerizations of lactams. Temperature of polymerization depends on the lactam-polyamide equilibrium, and the ceiling temperature and varies with ring strain.

1.1.2 Crystal Structure

Hydrogen bonding dominates the crystal structure of nylons; hydrogen-bonded sheets are the main feature of the nylon structure and the two strong reflections arise from this feature. The *d* spacings of these reflections at 0.37 and 0.44 nm are due to the inter-sheet distance between the sheets and the projected inter-chain distance within the sheet, respectively. The structure is called the α phase if the hydrogen-bonded sheets are sheared and stacked progressively by weak van der Waals interactions, while the β phase results if it is in alternating shear. The chains in the α phase are in fully extended zigzag conformation with hydrogen bonds between antiparallel chains.

Nylons -6,6,[5] -6,10, and -6,12[6] exist in the triclinic α phase at room temperature. The α phase of nylon-6 has a monoclinic structure.[4] In both nylon-6 and nylon-6,6 the normal method of packing involves a shear of 3/14 *b* between the hydrogen-bonded sheets (*b* = 17.2 A°).[4] The appearance of hydrogen-bonded sheets for nylon-6 and nylon-6,6 is shown in Figures 1.1a and b. In nylon-6,6 α phase the shear is progressive (Figures 1.2a) while in nylon-6,6 β phase and nylon-6 α phase the shear is staggered (Figures 1.2b). The projected cell bases of the two structures are identical except for the doubling of both axes, which occurs in nylon-6 α phase. The *a*-axis is doubled because of the inversion of successive molecular chains to perfect the hydrogen bonding (Figures 1.1b) and the *c*-axis is doubled

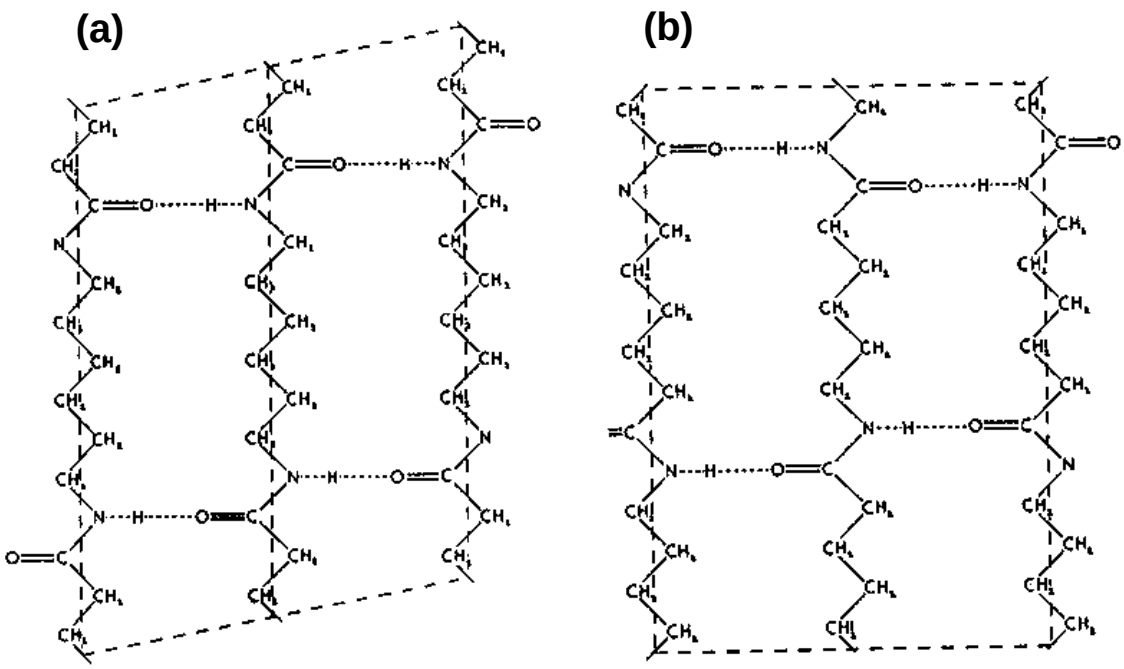

Figure 1.1: Hydrogen-bonded sheets in (a) nylon-6,6 and (b) nylon-6.[4] Unit cell face shown dotted.

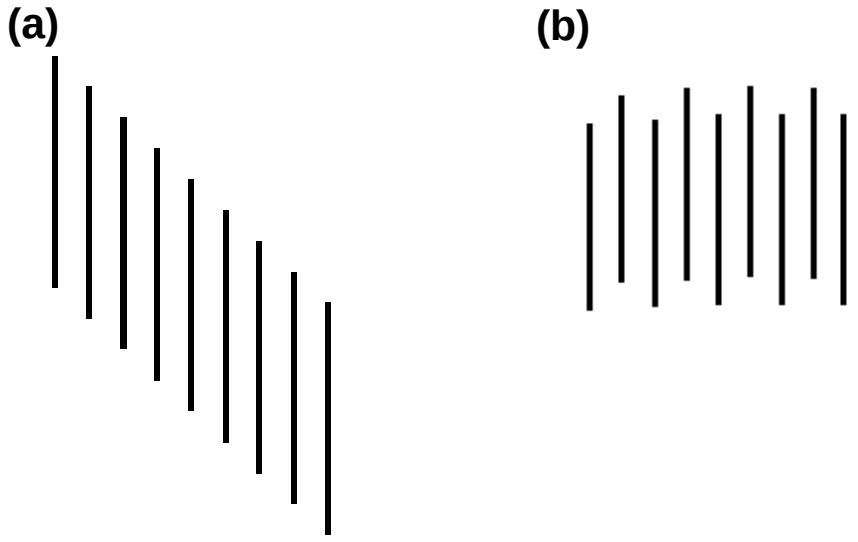

Figure 1.2: (a) Progressive shear in nylon-6,6 α phase. (b) Staggered shear in nylon-6 α phase and nylon-6,6 β phase.[4]

because of the staggered rather than progressive shear. The structure of solution grown nylon-4,6 single crystal mats[7] is like nylon-6 α phase, rather than like nylon-6,6 α phase.

The high temperature pseudohexagonal structure is called the γ phase and is observed when the amide groups are tilted 60° off the sheet plane. As a consequence, a characteristic shortening in the chain axis repeat is noticed when compared with the fully extended conformation of the α phase. The twisted chains allow hydrogen bonds to be formed between parallel chains.[8] The sheets of hydrogen-bonded chains are stacked together in a similar way with that of the α phase. The γ phase is considered to be a less ordered phase than the α phase. The characteristic of the γ phase is that it exhibits only one strong reflection and the *d* spacing is 0.42 nm. The γ phase is characteristic of nylons with high methylene content in their chemical repeat units or nylons for which linear hydrogen bonds between adjacent chains cannot be established when an extended conformation is considered (even-odd, odd-even, and odd-odd nylons). In many even or even-even nylons, the α phase can be converted to the γ phase (or vice versa) or both can coexist in various proportions. Transformations between both kinds of structures can be engineered in some cases by solvent or swelling agents,[9] rates of fiber spinning,[10] and temperature.[11] Structural variations can be envisaged as a consequence of different possible balances between the van der Waals attractions, hydrogen bonds, dipole-dipole forces, and torsion about covalent bonds. Thus in nylons derived from ω-amino acids and with more than six methylene groups between the amide groups, the dominance of the van der Waals forces over the hydrogen bonds is such that the extended conformation seldom exists.[12] Recently, it has been found that the γ phase is readily formed in nylon-6 nanocomposites, primarily the nylon-6–montmorillonite clay nanocomposites.[13-16]

1.2 Crystalline Transitions in Nylons

1.2.1 Nylon-6,6

1.2.1.1 X-ray Diffraction (XRD) Studies

Most nylons show a crystal-to-crystal transition on heating. This phenomenon was first observed in nylon-6,6 by Brill in 1942.[17] The room temperature triclinic α phase transforms into a pseudohexagonal (hexagonally packed) phase at elevated temperatures, and the transition is reversible. The Brill transition is most clearly displayed in XRD studies, as the two strong reflections at room temperature of nylon-6,6 seen at diffracting angles ~20° (100) and 24° (010/110), upon heating merge into a single reflection above a transition temperature of about 160 ^{o}C. From this transition temperature, which was called as the Brill temperature (T_B), only one reflection was seen at higher temperatures up to

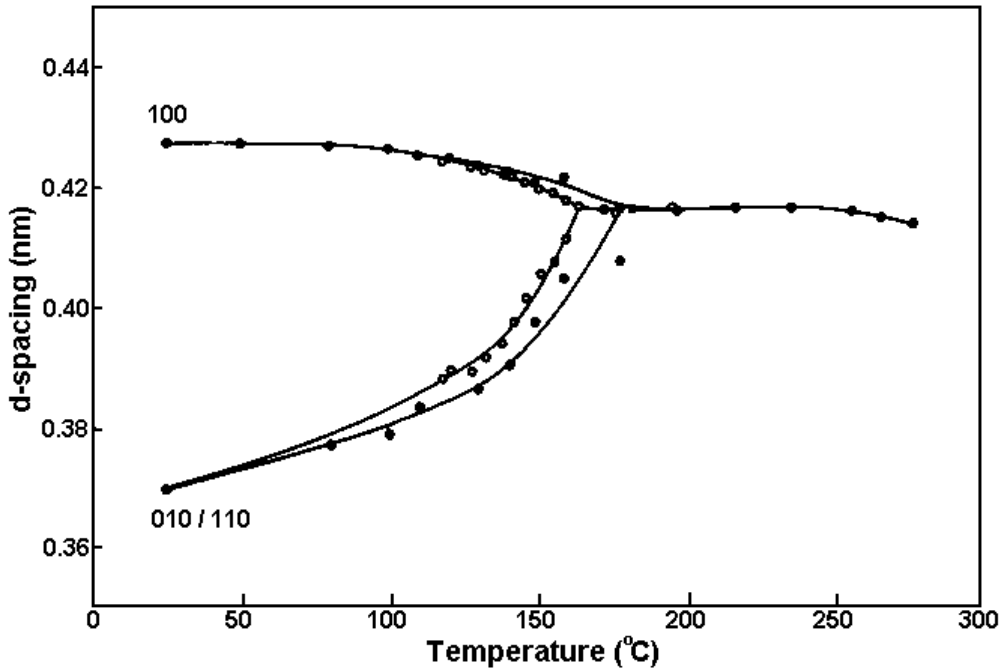

Figure 1.3: Temperature dependence of *d* spacings observed for (100) and (010/110) reflections of nylon-6,6 in the heating process (O) and cooling process (,).[18]

melting at 265° C. The Brill transition in nylon-6,6 has been the most extensively studied.[17-23] Ramesh et al. have shown that the T_B in nylon-6,6 strongly depends on the crystallization temperature (T_c).[18] They followed the isothermal crystallization process from the melt in nylon-6,6 *in situ* by XRD. At all the T_c's studied (196 °C, 232 °C, 260 °C) the samples crystallized into the pseudohexagonal Brill structure, which transformed into the triclinic structure on subsequent cooling to room temperature from the T_c. The transition occurred at about 40 °C lower than the respective T_c. The T_B also displayed a hysteresis effect on heat cycling, with T_B being higher on heating than on cooling as shown in Figure 1.3, which affirmed the first-order transition character of T_B,[18] contrary to some previous suggestions.[19,21,24] The dependence of T_B on T_c also implied a gradation in perfection and/or crystal size while in the Brill structure.[18] As crystallization always occurred in the Brill structure it followed further that any difference in structure and property, as determined at room temperature, must reside in the Brill structure at the stage of formation and can only be reflected indirectly by the transformed structures observed at room temperature. In the case of solution-crystallized samples a small endothermic peak around 200 °C in the differential scanning calorimetry (DSC) trace corresponding to T_B was observed on heating and it appeared that the crystals grow directly into the triclinic Bunn structure.[18,20,24] This has been attributed[24] to the better defined T_B which results from

the more uniform crystals obtained by crystallization from dilute solution, as opposed to the crystallization from the melt. Chain-folded lamellar single crystals of nylon-6,6 grown from 1,4-butanediol[25] showed Brill transition on heating at 220 °C.

Variable-temperature solid-state nuclear magnetic resonance (NMR) data confirm the structural changes during Brill transition in nylon-6,6.[22] Variable-temperature XRD measurements confirm the NMR results that the Brill transition is very broad and that the transition temperature is probably dependent on the size and perfection of the crystals. The integrity of the hydrogen-bonded sheet structure, present in the room temperature structure, is maintained during the Brill transition, and up to the melting point.[19,22,23,26,27] An NMR study coupled with line-shape simulations performed on deuterium labelled nylon-6,6 polymer over a wide temperature range showed that the N-D groups undergo rapid, but quite restricted, librational motion at all temperatures below the melting point, thus reflecting the preservation of the hydrogen bonds.[22] XRD showed that the inter-sheet inter-amide distance in the pseudohexagonal structure of nylon-6,6 was too great to permit hydrogen bond formation.[19] Another argument is[28-33] that the transformation into the pseudohexagonal structure must have been driven by a partial rearrangement of hydrogen bonds into inter-sheet directions, similar to that first postulated by Brill. This model offered an explanation for the inter-chain distances remaining nearly constant between the T_B and melting temperature (T_m).

Extruded nylon-6,6 displayed an XRD pattern close to, albeit nonidentical, the pseudohexagonal phase.[34] Upon storage at room temperature and relative humidity of 60% the polymer underwent a slow polymorphic transition toward the triclinic phase, without reaching it. This phenomenon was reversible under temperature treatment. Modeling study provided a detailed molecular comprehension of how such a transition may be induced by water; the existence of stable structural intermediates is obviously required in such a solid-state transition. Further modeling of water interaction with an assembly of nylon-6,6 chains indicated that water did not penetrate the crystalline region but instead reacted with the crystalline surfaces, more preferentially with the *bc* plane, and induced the structural evolution.

Synchrotron small-angle X-ray scattering (SAXS) was used to characterize the lamellar structures in nylon-6,6 at several temperatures and the changes during the Brill transition at ~160 °C were monitored.[35] During heating the integrated intensity and the coherence

length of the lamellar stacks increased above T_B. In contrast, during cooling, the intensity increased below T_B whereas the coherence length increased up to T_B and remained unchanged upon further cooling. The increase in SAXS intensity observed above T_B during heating was attributed to the enhanced contrast resulting from a decrease in the packing density of the amorphous chain segments. It was suggested that the changes in the packing of the crystalline stems, such as the ones that occur during crystalline phase transitions, are accompanied by changes in the packing of the amorphous chain segments in the interlamellar regions.

1.2.1.2 Infrared Spectroscopy Studies

Vasanthan et al. have reported the first observation of the changes in the infrared spectra of nylon-6,6 at the T_B.[36] They have shown that some of the weaker infrared bands ("Brill bands") in the nylon-6,6 spectra disappeared abruptly at the Brill transition. The changes in the structure could be attributed to the onset of librational motions that bought about changes in the packing of the crystalline segments within the lamellae rather than the large scale conformational changes.

Polarized transmission Fourier transform infrared spectroscopy (FTIR) microscopy studies have been performed on a monodisperse 3-amide oligomer, which is a model compound for nylon-6,6 having essentially the same room temperature crystal structure, and it underwent the Brill transition, prior to melting.[37] The extensive parallel dichroism exhibited by the NH stretch and amide I bands was retained right up to the melting. This proved that the Brill transition did not involve major rearrangement of hydrogen bonds. These results strongly suggested that the equivalent Brill transition in nylon-6,6 also proceeded without significant hydrogen bond rearrangement.

1.2.1.3 Crystalline Transitions in Nylon-6,6–clay Nanocomposites

Nylon-6,6–clay nanocomposites showed a lower T_B than neat nylon-6,6 which was attributed to the strong interaction between nylon-6,6 chains and surfaces of silicate layers.[38,39] It is known that the Brill transition is induced by the thermal expansion of a crystalline lattice, and the room temperature stable α phase transformed into the high temperature stable pseudohexagonal phase. The addition of silicate layers favored the formation of pseudohexagonal phase. With increasing annealing temperature, the mobility of the molecular chains increased; the transition from the α phase to the pseudohexagonal

phase was easier under the existence of silicate layers. However Zhang et al. observed that the Brill transition in nylon-6,6–clay nanocomposite occurred at a higher temperature than neat nylon-6,6 which they attributed to the strong interaction between the silicate layers and the nylon-6,6 molecules, which decreased the mobility of the molecules and suppressed the molecular oscillations.[40] Wu et al. used XRD methods and DSC thermal analysis to investigate the structural changes in nylon-6,6–clay nanocomposites.[41] They showed only the presence of α phase in nylon-6,6–clay nanocomposites.

1.2.2 Nylon-6

Nylon-6 is a low cost and high performance polymer, which has found wide applications in the field of fibers and engineering plastics. There are two major crystalline phases in nylon-6, monoclinic α phase and γ phase.[4,8,42-45] The α phase consists of fully extended planar zigzag chains, in which adjacent anti-parallel chains are joined by the hydrogen bonds as shown in Figure 1.4. Therefore, it is the thermodynamically most stable crystalline phase, and can be obtained by slowly cooling from the melt. The γ phase is composed of pleated sheets of parallel chains joined by the hydrogen bond (Figure 1.4). It is less stable and can be obtained by fiber spinning at a high speed or by fast cooling from the melt.[46] The γ phase can be converted into α phase by melting followed by recrystallization, by annealing at 160 °C in a saturated-steam atmosphere without any significant loss of orientation and by applying stress at room temperature.[47,48] Murthy et al. first reported the presence of Brill transition in nylon-6 on heating using variable-temperature XRD and NMR measurements.[23] They showed that nylon-6 underwent crystalline transitions between the glass transition temperature (T_g) and the T_m. These transitions bought about a crystalline transition between 80° and 170 °C from a monoclinic structure to a new crystalline structure, which was also most likely monoclinic. As observed in nylon-6,6, in nylon-6 also the integrity of the hydrogen-bonded sheets was maintained during this transition and up to the T_m. The low and high temperature crystalline phases coexisted during the transformation, and the transition from the low temperature to the high temperature phase was diffuse, occurring over a temperature range of about 100 °C. The phenomenon was further studied by infrared spectra during transition.[36] DSC and DMA could not detect such a transition at least in the melt-crystallized samples.

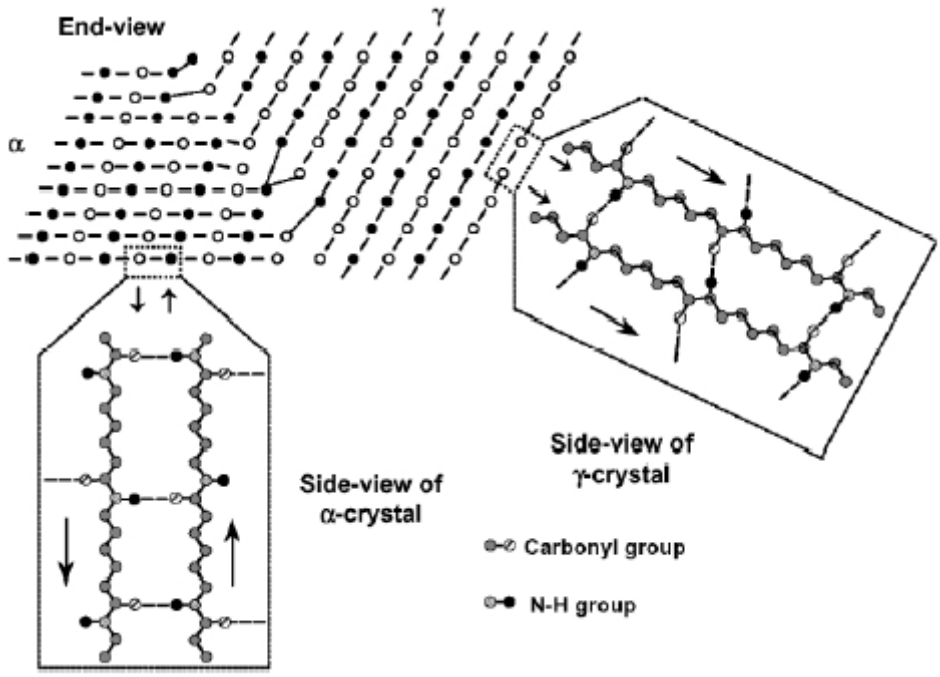

Figure 1.4: Schematic of hydrogen bonding within α and γ phases of nylon-6 as seen from end and side-view of each crystal.[49] Closed and open circles represent chain axes projecting out of and into the page, respectively. Dashed lines represent hydrogen bonds between nylon chains. The upper left hand portion of this figure was adopted from the work of Aharoni.[50]

Ramesh et al. monitored the crystallization of nylon-6 from the melt *in situ* by XRD.[51] The nylon-6 crystallized into a high temperature α' phase if crystallized in a narrow temperature range between 200 °C and $T_{m.}$ On cooling from the T_c to room temperature, the structure transformed into the low temperature α phase at ~180 °C. On heating, the α phase transformed into the α' phase at about 190 °C and melted in that phase. The transition took place over a temperature range where both phases coexisted. However, samples crystallized from the melt at temperatures 140 and 180 °C showed the α phase at room temperature, but on heating the α phase first transformed into a pseudohexagonal phase, and before melting the pseudohexagonal phase further transformed into the α' phase. The α phase of nylon-6 was transformed into the γ phase, by potassium iodide-iodine treatment, and the behavior of the γ phase with temperature was studied for the first time. The γ phase did not show any crystalline transition on heating and melted in the γ phase.

A metastable crystalline phase was observed in uniaxially stressed nylon-6 fibers with a significant γ crystalline fraction.[52] It was investigated using XRD and shown to be distinct

from both the conventional α and γ phases. The fraction of the metastable phase increased at the expense of the γ phase when the fibers were stretched. Upon releasing the stress, the metastable phase transformed into the α phase or reverted back to the γ phase depending on whether the stress was below or above a critical value. Further, the metastable phase could be converted back to γ by immersing in boiling water for <1min. It was also shown that in the metastable phases analysed, the chain-axis repeat was ~ 17 A°, and the amide planes were not coplanar. These observations suggested that in addition to hydrogen bonds within a sheet of extended antiparallel chains, there might also be inter-sheet hydrogen bonds between parallel chains. Such an intermediate structure would enable the metastable phase to be transformed either into the α or γ phases under a suitable sequence of thermomechanical treatments.

The MSXX force field (derived from ab initio quantum calculations)[53] was used to carry out theoretical calculations to determine the details of the various structures of nylon-6 and the conversion between them by Li et al.[54] Assuming infinite chains and evaluating the free energy for all 112 regular crystal structures, they found three classes of regular crystal structures: α phase (with amide bonds parallel to the methylene sheets), γ phase (with amide bonds ~ perpendicular to the methylene sheets), and δ phase (somewhat intermediate between α and γ). They found that the thermostability of α phase over other phases came from intramolecular hydrogen bonds in α phase, which were dynamically and entropically favored. They also found that the γ phase had a more linear hydrogen bond than the α phase, which was consistent with the conclusion from solid NMR.[55]

The effect of pressure on the melting and transformation behavior of the γ phase of nylon-6 obtained by iodine-treatment was studied.[48] The crystalline structures which resulted in the endothermic and exothermic peaks in the differential thermal analysis (DTA) thermogram were examined using XRD measurement. Under relatively low pressure (170-2000 $kgcm^{-2}$), two endothermic peaks were found in the DTA thermogram. With increasing pressure, the lower endotherm due to melting of the γ phase crystal became small, while the higher one due to the melting of the converted α phase crystal became large. Under high pressure (above 2000 $kgcm^{-2}$) an endotherm due to the melting of the converted α phase crystal and an exotherm were observed. This exotherm was attributed to the γ to α phase transformation. Solid-state ^{I3}C and ^{15}N NMR results relevant to the

structure of iodinated nylon-6 and its conversion into the γ phase were presented by Murthy et al.[56] Experimental evidence was presented that indicated that the γ phase was formed during initial KI/I_2 desorption even while the amorphous chain segments remained complexed. This suggested that the γ phase evolved from the complex without going through an identifiable, intermediate, native amorphous phase.

The Brill transition in nylons corresponds to the transformation of an ordered crystalline structure at low temperature into a less ordered crystalline phase at high temperature. This transition spans a large temperature domain, and depends on crystallization conditions. For some nylons, it does not occur before melting. This transition should have a tremendous effect on the mechanical properties, notably on plasticity, which is expected to largely improve with crystalline disorder. So, understanding the plastic behavior of nylon-6 implies to recognize which class it belongs to. The crystalline phase of nylon-6 films produced using various physical treatments were investigated by thermal analysis, XRD and infrared spectroscopy.[57] Melt-cast and quenched films displayed a mesomorphic β phase that was thermally stable up to about 120 °C. This structure partly reorganized into the stable monoclinic α phase above 120 °C. Films in the major γ phase produced by iodine treatment were thermally stable up to 200 °C. No evidence was given for Brill transition at about 170 °C, which was an important factor for further understanding of the drawing behavior of nylon-6 at temperatures above and below this domain. The plastic behavior of nylon-6 films under uniaxial and biaxial tensile drawing was studied in relation to structural features.[58] Quenched films in the mesomorphic β phase were more ductile than films in the predominant stable α phase. Films in the major γ phase were intermediate between films in the β and γ phases. Under uniaxial drawing, a great part of the β phase underwent strain-induced phase change into the α phase, involving strain hardening of the material. The β to α phase change was more pronounced above 120 °C because of additional thermal reorganization. The γ phase that was thermally stable up to 200 °C also underwent a strain-induced phase change above 120 °C, but the reorganization was much less important than for the β phase. The disordered distribution of the hydrogen bonds in the mesomorphic β phase of the quenched films was more appropriate for biaxial drawing. The strain-induced β to α phase reorganization, proved to be much reduced during biaxial drawing below 120 °C.

Vasanthan et al. used FTIR methods for quantitative analysis of phase changes during thermal treatment and the drawing of nylon-6 fibers.[59] The results showed that the γ phase was stable to heat treatment in these fibers and that thermally induced crystallization took place only from the amorphous phase. It involved increases in both α and γ phases, and did not involve crystal-to-crystal transformation. However, drawing or strain-induced structure changes involved both crystallization of the amorphous phase in the α phase and γ to α transformation. Murthy et al.[60] showed that upon annealing nylon-6 fibers, the α phase is produced primarily by γ to α transformation in high-orientation fibers, while additional α phase can also crystallize from the amorphous phase in low-orientation fibers. Rhee et al.[61] showed that extrusion cast nylon-6 films, which were either unstretched or stretched at low temperature, exhibited poorly defined β (pleated α) phase if cooled down to room temperature and aged for more than two weeks. By increasing the stretch temperature from 40 to 180 °C, the β (pleated α) phase is transformed to the monoclinic α phase. Annealing the films, which had been stretched at 65 °C, in boiling 20% formic acid solution perfected the crystal transformation to the well-defined α phase. A procedure based on a combination of XRD and deconvolution data was used to study the structural changes accompanying the melt spinning, annealing, and drawing of nylon-6 filaments.[62] Higher spin draw ratios resulted in higher crystallinity, greater relative amounts of γ phase, and higher orientation. Annealing for ≤2 h in boiling water or a 20% aqueous formic acid solution decreased the γ phase content, increased the α phase content and total crystallinity, but did not eliminate all of the γ phase in samples spun with high spin draw ratios. Annealing in vacuum also increased the α phase content when annealing was carried out at temperatures above 120 °C, but there was little effect below this temperature. Drawing of as-spun and conditioned filaments at 90 °C also increased the α phase content and decreases the γ phase content. In drawing nylon-6 fibers at 80 °C with a draw ratio of 3.75 atmospheric pressure to 200 k/cm^2 it was found that by increasing the pressure, structural conversion from the γ phase to the α monoclinic phase occurred, and that crystallinity and orientation increased.[63]

The films obtained after each of the four production steps involved in the manufacture of bioriented nylon-6 films which are extrusion, blowing, stabilization, and finishing were studied by XRD, infrared analysis, and density measurements.[64] Quenching, after extrusion, generated an unstable γ phase and an amorphous phase. Blowing transformed

the unstable γ phase into the thermodynamically stable α phase and increased the chain orientation; stabilization increased α phase crystals, favored hydrogen bond formation and, therefore, the mechanical properties, leaving unchanged the chain orientation; the final treatment increased the mechanical properties.

1.2.2.1 Crystalline Transitions in Nylon-6–clay Nanocomposites

XRD methods and DSC thermal analysis showed the presence of polymorphism in nylon-6 and in nylon-6–clay nanocomposites prepared by the intercalation of ε-caprolactam and then exfoliaton of the layered hosts (saponite or montmorillonite) by subsequent polymerization. [65-67] This polymorphic behavior was dependent on the cooling rate of nylon-6–clay nanocomposites from melt and the content of saponite or montmorillonite in nylon-6–clay nanocomposites. The quenching from the melt induced the crystallization into the γ phase. The addition of clay increased the crystallization rate of the α phase at lower saponite content and promoted the heterophase nucleation of γ phase at higher saponite or montmorillonite content. Thermal treatment of nylon-6 and nylon-6–clay nanocomposites at various temperatures promoted mostly the formation of α phase. But the 5 wt% nylon-6–montmorillonite nanocomposites showed the presence of more unstable γ phase after annealing at the temperature close to the higher temperature of the Brill transition in nylon-6. [65] This phenomenon was probably due to the presence of montmorillonite induced heterophase nucleation of γ phase, the fast cooling from the melt preferred forming less stable γ phase, and the high treated temperature eliminated the structural memory of α phase. The effect of isothermal crystallization process on the crystal structure of nylon-6 and nylon-6–montmorillonite nanocomposite between 0 and 180 °C was examined using XRD.[68] With increasing T_c the γ phase in nylon-6, transformed gradually into α phase. The α phase crystals expanded and a high temperature crystallization peak appeared at $2\theta = 28.5°$ in the XRD pattern for nylon-6 crystallized at 180 °C. The addition of montmorillonite at various temperatures (0-180 °C) promoted the crystalline transition from α to γ phase and increased the perfection of crystallization. The diffraction patterns of the nanocomposites exhibited the high temperature crystalline diffraction features of pure nylon-6 even at lower temperature. The α phase was predominant in the whole temperature range as indicated by its strong crystalline peaks. The unknown high temperature crystalline peak at $2\theta = 28.5°$ maintained unchanged in intensity.

The γ to α crystalline phase transition in nylon-6–clay nanocomposite prior to melting was investigated by XRD.[69] The phase transition took place at 160 °C, which was 40 °C higher than that of nylon-6 at 120 °C. The lower transition extent in the nanocomposite than in nylon-6 was supposed to be due to strongly confined spaces between the silicate layers, which constrained the mobility of the polymer chains, and the favorable environment for the formation of the γ phase in the presence of clay. Further Liu et al.[70] examined the influence of nanodispersed clay on the crystalline structure of nylon-6 using *in situ* XRD between room temperature and melting. They showed that as compared to the crystalline transition in the α phase of nylon-6[51] the α phase in nylon-6–clay nanocomposite obtained by slow cooling from melt did not show crystalline transition on heating but only continuous intensity variation due to increase in the annealing temperature. This was due to constrained mobility of the polymer chains in the presence of silicate layers. They also showed that the γ phase in nylon-6[51] or γ phase in nylon-6–clay nanocomposite[71] was a stable crystalline phase that did not show any crystalline transition prior to melting. Lincoln et al.[72] showed using simultaneous small and wide-angle X-ray scattering (WAXS) and modulated DSC that the presence of aluminosilicate layers in nylon-6 stabilized a dominant γ phase, essentially unmodified, until melting. The temperature dependence of the relative fractions of α and γ phases was strongly dependent on the layered silicate content and the interaction between nylon-6 and the aluminosilicate layers. Nylon-6–clay nanocomposites with various cooling histories from the melt, including medium-rate cooling (air cooling) and rapid cooling (water-quenched) crystallized in the γ phase in the presence of clay.[73]

The influence of zinc oxide (ZnO) nanoparticles on the crystalline structure of nylon-6 was examined under different crystallization conditions (annealing at different temperatures, isothermal crystallization, crystallization from the melt at different temperatures, and crystallization from solution) using DSC, XRD and scanning electron microscopy (SEM).[74] ZnO nanoparticles could induce the crystallization of the nylon-6 into γ phase from the melt and during the annealing of the amorphous solid. The inducing effect was found to increase with decreasing ZnO particle size.

Nylon-6 and nylon-6–clay nanocomposite films were stretched uniaxially below the T_m and the influence of draw temperature (100-140-180 °C) on the structure was investigated

by XRD.[75] The as-cast films were in γ phase. Stretching promoted the formation of α phase at all draw temperatures for nylon films. At low draw temperatures the nanocomposite films also assumed α phase, while at 180 °C they displayed a mixture of α and γ phases. The effect of melt temperature on the phase behavior in nylon-6–montmorillonite nanocomposite fibers melt-spun at extrusion temperatures ranging from 230 to 250 °C was investigated. The fibers spun at 240 °C were found to exhibit primarily the γ phase.[76,77] As the take-up speed was increased a small population of oriented α phase was observed. At comparable take-up speeds, the amount of α phase formed diminished as the spinning temperature increased from 230 to 250 °C. For both nylon-6 and nylon-6–clay nanocomposites it was found that drawing was more effective than annealing in producing the γ to α transition.[78] Liu et al.[79] showed that in nylon-6–clay nanocomposites with different cooling histories (cooled in oil bath naturally and quenched in liquid nitrogen) undefined crystalline structures remained in the substantially molten polymer matrix up to 300 °C. All the neat nylon-6 samples with the different cooling histories presented amorphous XRD patterns when heated up to the melting range.

1.2.3 Even-Even Nylons

1.2.3.1 Nylons -6,10 and -6,12

Unlike nylon-6,6, which can exist as a stable modification below the T_c,[18] nylon-6,12 has been reported to crystallize into the pseudohexagonal phase[80] and transform into the triclinic α phase immediately below T_c on subsequent cooling. The γ phase was obtained by heating an amorphous sample above the T_g near 40 °C and was stable only at high temperatures. Cooling of the pseudohexagonal phase immediately resulted in the Brill transition into the α phase. From the XRD measurements and the FTIR investigations it was shown that the Brill transition temperature was identical with the annealing or T_c of the γ phase. Brill transition on heating solution grown crystals of nylon-6,10 and nylon-6,12 have been shown to coincide with the T_m.[32]

The crystallization of nylons -6,10 and -6,12 were monitored *in situ* by XRD from the melt.[81] They were found to crystallize into the α phase when crystallized from the melt in a narrow temperature range between 200 °C and T_m. On cooling from the T_c to room temperature, the structure transformed from the high temperature α phase to the low temperature α phase below 200 °C and this transition was independent of T_c. Amorphous

nylons -6,10 and -6,12 crystallized in the pseudohexagonal structure when heated from room temperature and transformed into the high temperature α phase above 190 °C. But if cooled before this transition, these samples exhibited pseudohexagonal to α phase transitions (Brill transitions). In nylon-6,10 the transition occurred 30 °C below the holding temperature and in nylon-6,12 it occurred within 10 °C below the holding temperature.

The structural change in the Brill transition of nylons -6,10 and -6,12 was investigated by carrying out the temperature dependent infrared spectral measurement as well as by DSC and the analyzed results were compared with that of nylon-10,10.[82] Since these polymer samples have different methylene sequential lengths, they were useful for the clarification of the role of the methylene segments in the Brill transition phenomenon of nylons. They took the crystal structure of α phase at room temperature. The structural change was of the order to disorder type. The conformation of all-*trans* zigzag methylene segments was shortened by an invasion of gauche bonds. This tendency was more remarkable for the $NH(CH_2)_mNH$ part than the $CO(CH_2)_nCO$ part. Such a conformational disordering in the methylene segment was related strongly with the twisting motions about the amide–CH_2 bonds. The intermolecular hydrogen bonds were kept but became weaker. So far the change of XRD pattern from triclinic to pseudohexagonal type was considered to be useful for tracing the Brill transition phenomenon. But the structural change was not a real transformation of the triclinic packing to the hexagonal mode. The intermolecular hydrogen bonds were kept in the transition region, making the real hexagonal packing of the rotating chains impossible. Therefore the XRD profile change was not needed to complete in the Brill transition.[21] A more important and essential structural feature was conformational disordering in both the methylene and CH_2–amide parts of the molecular chains. They spontaneously resulted in the change of the XRD pattern. The conformational disordering occurred in a wide temperature region. This was not because of the broad molecular weight distribution and many structural defects. In fact, the broad transition behavior was detected even for the low molecular weight model compounds with explicitly defined chemical formulae.[83] Therefore the Brill transition of nylons may be assumed as a structural disordering process, which occurred in an appreciably wide temperature region.

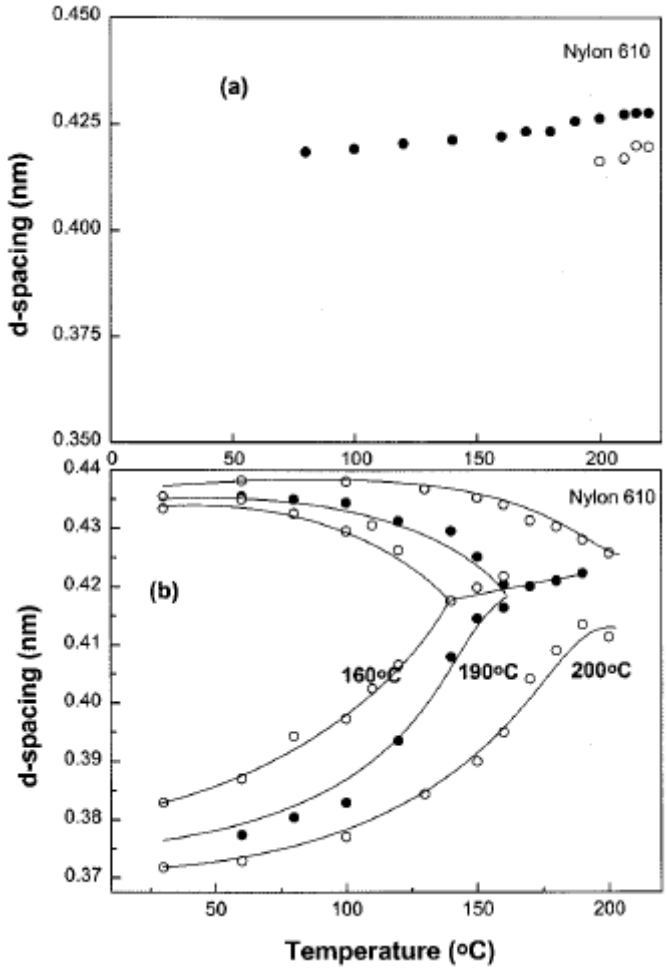

Figure 1.5: Variation of *d* spacing of (a) a quenched amorphous nylon-6,10 sample on heating and (b) during cooling from various holding temperatures.[81]

Table 1.1: Crystallization/Holding temperature (T_c) and Brill temperature (T_B) of Nylon-6,10

T_c, °C	T_B, °C	T_c-T_B, °C
130	100	30
160	140	20
180	150	30
190	160	30

1.2.3.2 Nylons -4,6 -6,8 -8,10 and -10,12 [2N,2(N+1) Nylons]

Nylons -4,6 -6,8 -8,10 and -10,12 are special since each has an equal number of methylene units in both the diamine alkane and diacid alkane chain segments, allowing two different types of chain-folded hydrogen-bonded sheet structures possible: progressive or alternating shear. The chains have opposite polarity. Single crystals of nylon-4,6[7] and nylon-6,8[84] grown from solution in 1,4-butanediol and examined in the transmission electron microscope (TEM) showed similar crystal structures. Both had monoclinic unit cells at room temperature. Both nylon-4,6 and nylon-6,8 reached a T_B before melting. The two strong diffraction signals at 0.435 and 0.375 nm gradually came together and transformed from the monoclinic phase to the pseudohexagonal phase on heating. The T_B for nylon-4,6 was 245 °C, and melting took place at 295 °C and the T_B for nylon-6,8 was at 203 °C and it melted at 234 °C. Nylon-6,8 crystals quenched in a non solvent from the T_c[84] grew in the pseudohexagonal phase and could be frozen into that phase by quenching below T_g. They could be reverted to the monoclinic phase on heating above T_g.

The structures and morphologies of nylons -8,10 and -10,12 synthesized and crystallized from 1,4-butanediol in the form of chain-folded lamellae have been studied and compared with nylons -4,6 and -6,8.[85] It has been shown that they can crystallize in two types of sheets: p-sheet (progressive) or a-sheet (alternating) and the sheets can stack with either a progressive shear to form α phase crystals, or alternating shear to form β phase crystals. Thus, four different crystal structures were possible which were described as α_p, α_a, β_p and β_a. The results for nylons -8,10 and -10,12 showed that the crystals were predominantly in the α_p phase, i.e., in the progressive sheet structure and with alkane groups in the adjacent re-entry fold. In contrast, nylons -4,6 and -6,8 with alkane segments containing six or less methylene units, were found to crystallize from 1,4-butanediol in the β_a phase, i.e., in the alternating sheet structure and with amide groups in the fold. As the length of alkane segments in the 2N,2(N + 1) nylons increased, a change in the sheet structure occurred, with a consequent change in the chemical nature of the lamellar surface. This transition occurred in passing from nylon -6,8 to -8,10. Thus the p-sheet structure had a slightly lower energy than the a-sheet. The melting points of solution grown crystals of nylons -4,6 -6,8 -8,10 and -10,12 decreased with decreasing intrachain amide density. When lamellar crystals of these nylons were heated, the two characteristic inter-chain diffraction signals moved together and met at their Brill temperature (Table 1.2); for nylon-10,12 it appeared to be close to the melting point.

Nylon-10,12 is a newly industrialized polyamide.[86] It has attracted much attention because of its prominent properties, including a lower melting point, a slightly lower density, excellent impact properties, plus the lower dielectric constant and water affinity in comparison with nylon-6,6. Yan et al.[87] examined the Brill transition in nylon-10,12 crystallized from the melt by XRD and FTIR and found that the Brill transition behavior was much different from that reported by Atkins and coworkers[85] for single crystals of nylon-10,12 grown from solution as mentioned above. The difference may be due to different preparation conditions of the samples. Nylon-10,12 samples crystallized from the melt underwent Brill transition from the α phase to the pseudohexagonal phase at about 120 °C on heating. On cooling the transition occurred at about 110 °C (a little lower than the transition temperature on heating), thus suggesting a completely reversible transition. The infrared spectra also showed that a sequence of bands at 897 cm^{-1}, 986 cm^{-1}, 1165 cm^{-1}, 1189 cm^{-1}, 1224 cm^{-1} and 1338 cm^{-1} which were "α-bands" disappeared abruptly during Brill transition. Further Yan and coworkers[88] investigated the crystal structure of nylon-10,12 prepared under different conditions using FTIR and XRD. The γ phase was obtained for nylon-10,12 cast from trifluoro acetic acid, which was independent of the cast temperature. The α phase was found when nylon-10,12 was crystallized from the melt or cast from *m*-cresol at low temperature. The crystal structure for the film cast from *m*-cresol varied with increasing cast temperature, and the γ phase was formed when the cast temperature was 170 °C.

The crystallization of nylon-4,6 was monitored *in situ* by XRD from the melt.[81] It crystallized with a single peak, which was characteristic of the γ phase (hexagonal structure). Nylon-4,6 showed two crystalline transitions on cooling from the T_c (280 °C). It transformed into the high temperature α phase about 40 °C below the T_c and showed a further transition at about 140-150 °C below the T_c. The second transition was from the high temperature α phase to the room temperature α phase.

Table 1.2: Thermal data and Brill spacings for 2N,2(N+1) Nylons

Nylon	Brill temperature (T_B °C)	Melting point (T_m °C)	Brill spacing (nm)
4,6	245	295	0.420
6,8	203	234	0.420
8,10	185	210	0.420
10,12	-	193	-

1.2.3.3 Nylon-10,10

Nylon-10,10 has a molecular structure analogous to nylon-6,6 as both belong to the family of 2N,2N nylons with equal carbon numbers in the diacid and diamine parts. It also has a crystal structure similar to nylon-6,6 except for a longer *c*-axis. Generally for nylon molecules in the same series as nylon 2N,2(N + 1) or 2N,2N, it is believed[85] that the T_m is dependent on the length of the diamine or diacid alkane segment. The melting point decreases as the length of the alkane segment increases. Consequently, the melting point of nylon-10,10 is 202 °C, which is much lower than that of nylon-6,6 which melts at 260 °C. Therefore it is easy to process and especially useful in a low temperature environment thus making it another important commercial polyamide. Nylon-10,10 also has a higher dimensional stability and a lower moisture absorption than nylon-6,6. The T_B also decreases as the length of the alkane segment increases, but the rate is less than that of the melting point. As a result, the T_B disappears when the length of the diamine or diacid alkane segment reaches a certain value.

However, the crystallization conditions can also change the T_B in a wide range.[18,89] The Brill transition could not be observed for melt-crystallized nylon-10,10.[90] The change in lattice spacings of nylon-10,10 crystals with temperature examined by variable-temperature XRD during heating and cooling demonstrated a gradual and continuous transition with temperature. However, melting took place before the two peaks merged completely. Crystallization from melting resulted directly in crystals of the triclinic α phase rather than the material passing first through the pseudohexagonal phase and then transforming to the α phase on subsequent cooling like other nylons. The transition was thermodynamically reversible. From a comparison of the transition of nylon-10,10 to that

of nylon-6,6, it was concluded that no hydrogen-bonded network was formed either during or after the transition. This transition in melt-crystallized nylon-10,10 was attributed to asymmetrical structural disorder rather than to a truly first order phase transition. The pattern of change in the lattice spacings of lamellar crystals of nylon-10,10 grown from a very dilute solution, by using a new solvent dimethyl formamide, was different from that of melt-crystallized spherulitic crystals during the heating process, especially after 180 °C.[91] The continuous approach of the two main spacings was replaced by their slight separation. This was a novel phenomenon observed in nylon crystals. It favored the idea that the T_B increased as the crystal became more perfect. The single crystals of nylon-10,10 grown from dimethyl formamide inhabited a more perfect structure and regular shape than crystals grown from 1,4-butanediol. However, the usual pattern of change in spacing was observed during the cooling process. At room temperature, the spacings of (002) and (010/100) reflections were smaller than those of melt-crystallized spherulites, whereas the spacings of the (100) reflection of the two crystals were identical. By its combination with the effect of temperature on the spacings of the crystal, it was concluded that the structure of nylon-10,10 crystals was dependent on the regularity of chain packing and hydrogen bonds. Nylon-10,10 crystals with different size and perfection were prepared under various crystallization conditions.[92] The XRD and TEM results showed that the crystal structure at room temperature as well as its thermal behavior on heating was strongly influenced by the crystallization conditions. The pseudohexagonal phase of nylon-10,10 was obtained by heating the quenched sample to high temperatures, where this phase was stable. Cooling of the pseudohexagonal phase sample immediately resulted in the Brill transition into the triclinic phase. No T_B was observed for melt-crystallized spherulitic crystals and lamellar single crystals grown from dilute solution in both the heating and the cooling process as the crystals obtained were large or perfect. However, the crystals obtained by post annealing (150 °C for 24h) of the quenched sample were rather small and always introduced more defects into their structure. This showed that the Brill transition depended on the size and perfection of the crystal. Yang and coworkers[93] also studied the Brill transition of nylon-10,10 cold-crystallized at various temperatures from the melt-quenched state. The transition was observed for the cold-crystallized specimens, and their transition temperatures were greatly dependent on the T_c. Cold crystallization from the amorphous state at different temperatures resulted in crystals with different lamellar thickness. The sizes of these crystals were determined by SAXS and correlated with the T_B. It was found that the T_B had a linear relationship with the size of

crystals, which was used to predict the T_B for those crystals with thick lamella and to calculate the size for crystals showing T_B below room temperature. Nylon-10,10 crystal possessed the pseudohexagonal phase rather than the α phase at room temperature if its size became small enough. It was believed that the behavior of the *d* spacings of the nylon crystal during Brill transition was the result of balance between the thermal motion and packing tendency of polymer stems within crystals. For large crystals, a great tendency for the crystal to maintain its original stable packing order was observed. Therefore, a higher temperature was necessary to break such a balance. On the other hand, the motion of polymer stems even at a rather low temperature easily destroyed the packing order of a small crystal. The small size of the hydrogen-bonded sheets resulted in weak action between the sheets and thus an easy movement of sheets during thermal expansion as the temperature increased. Therefore, the smaller the crystal size, the lower was the T_B. For the melt-crystallized spherulites or solution-grown lamellar crystals, their size was larger than the critical size of nylon-10,10 needed to show T_B. It was definite that no real Brill transition was achieved. In contrast, for a crystal with an especially small size, such as some "crystals" in the quenched nylon-10,10, T_B was lower than room temperature. Therefore, the crystal exhibited a pseudohexagonal phase even at room temperature. Variable temperature XRD studies on the crystalline transition of nylon-10,10 showed that the well crystallized α phase of nylon-10,10 transformed into a γ phase at about 135 °C, on heating from room temperature to a high temperature which was the so called Brill transition of nylon-10,10.[94] Nylon-10,10 crystallized directly in a kind of α phase when isothermally crystallized from the melt at high temperature (190 °C), which was much different from the behavior of nylon-6,6 and nylon-10,12. Upon further cooling to room temperature, nylon-10,10 transformed into the normal α phase. However, if the nylon-10,10 sample with the γ phase was not melted, but immediately cooled from a temperature between T_B and T_m, the reverse transition from γ phase to α phase was observed at about 130 °C, indicating reversible Brill transition of nylon-10,10.

Structural changes in the Brill transitions of nylon-10,10 and its model compounds were investigated by Tashiro et al.[83] by carrying out the temperature-dependent measurements of XRD and infrared spectra along with the DSC measurement. At room temperature the crystal structure was found to be the α phase with the all-*trans* zigzag methylene segments. In the Brill transition region, the progression bands assigned to the vibrational

modes of all-*trans* zigzag methylene segments were found to disappear. At the same time new progression bands appeared and increased in intensity, which were found to correspond to the progression bands of $(CH_2)_7$ - $(CH_2)_5$ methylene segments. These spectral changes indicated that the all-*trans* methylene segments were conformationally disordered by a generation of *gauche* bonds and as a result the effective length of *trans*-zigzag segments became shorter. This conformational disordering was found to occur more remarkably in the methylene segment of the NH–$(CH_2)_{10}$–NH part than the CO–$(CH_2)_8$–CO part. The infrared bands of amide groups, particularly the bands sensitive to the twisting angles about the CH_2–amide bonds were found to show remarkable change, indicating the local conformational change from the planar-zigzag to the twisted form in the CH_2–amide moiety. The frequency shift of the amide A band (NH stretching mode) indicated a weakening of intermolecular hydrogen bonds. From these data combined with the XRD data, the structural disordering in the Brill transition phenomena was deduced concretely. To confirm the structural features in the Brill transition of aliphatic nylons, molecular dynamics calculation was performed at various temperatures for nylon-10,10 crystal as a model.[95] With an increase in temperature, the torsional motions around the methylene–amide and methylene–methylene bonds were activated. These motions became more remarkable above 420 K and the interconversion between *trans* and *gauche* forms occurred frequently, resulting in the disordered conformation of the methylene sequences and the pseudohexagonal packing of these parts. However, the hydrogen bonds were kept alive during the drastic structural disordering although the bond strength became weaker. These calculations were found to be consistent with the experimental results by the temperature-dependent XRD and infrared spectral measurements. Another important purpose to perform the molecular dynamics calculation of nylon was to clarify the relation between the structural change in the Brill transition and the change in the mechanical property such as the Young's modulus along the chain axis or the crystallite modulus. The Young's modulus along the chain axis was also calculated as a function of temperature: it decreased remarkably from 250 GPa at 0 K to180 GPa at 300 K due to a small contraction of the skeletal chain by only about 0.2 – 0.5 % through the torsional motion of the skeletal chains, and it further decreased to 80 Gpa at 550 K because of the larger conformational disordering of the skeletal chains. The Young's modulus in the direction perpendicular to the chain axis was also found to decrease remarkably in parallel to the change of the chain packing mode. X-ray fiber diagram of uniaxially-oriented nylon-10,10 sample was measured at various temperatures.[96] The 11th layer line reflections originating from the

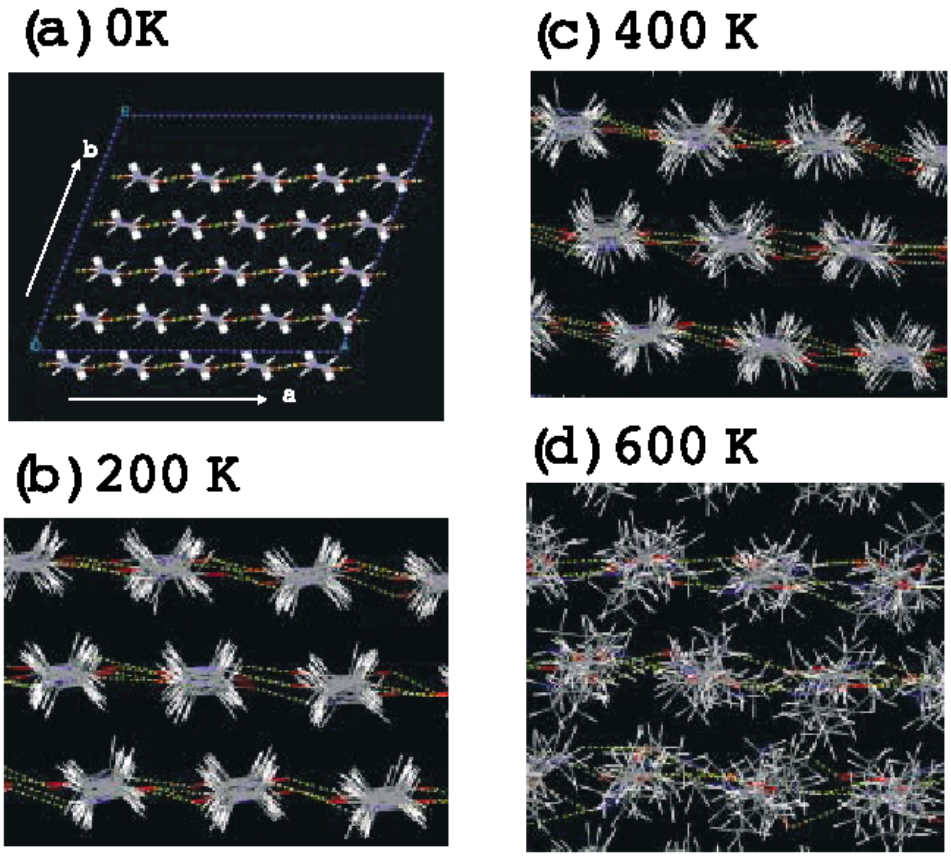

Figure 1.6: (a) An energetically-minimized crystal structure model of nylon-10,10 α phase used for the molecular dynamics simulation and (b)-(d) the snapshots extracted on the way of molecular dynamics calculation at the various temperatures.[95]

methylene zigzag sequences became diffuse above the Brill transition region (140-170 °C), while the layer reflections corresponding mainly to the original repeating period of the parent nylon chains were almost unchanged. This observation confirmed that the conformational disordering occurred in the methylene sequential parts in the Brill transition region, while keeping the repeating period of the whole skeletal chain or keeping the intermolecular hydrogen bonds between the amide groups of the neighboring chains. This order-to-disorder structural change was consistent with the conclusion deduced from the infrared spectral data, and was also supported by the computer simulation of the X-ray fiber pattern.

1.2.3.4 Nylons-X,4 (X = 4, 6, 8, 10, and 12)

Chain-folded lamellar single crystals of nylons -4,4, -6,4, -8,4, -10,4 and -12,4 grown from solution behaved similarly with respect to their room temperature crystal structures and behavior on heating.[97] At room temperature the crystals were composed of chain-folded,

hydrogen-bonded sheets; the hydrogen bonds within the sheets formed a progressive shear pattern, and the sheets themselves were sheared progressively parallel to the sheet plane so that the unit cells were triclinic. The magnitude of the inter-sheet shear for the nylons was dependent on the details of the amide decoration pattern on the hydrogen-bonded sheet faces. The five nylons had crystal structures closely related to nylon-6,6. The two strong and characteristic diffraction signals of the room temperature triclinic structure, at spacings 0.44 and 0.37 nm moved together and merged at temperatures between 140 and 198 °C, similar to the single crystals of other even-even nylons. In each case the triclinic structure gradually transformed into the pseudohexagonal phase on heating and the T_B was well below the T_m. The melting points of the solution grown crystals of this series of even-even nylons decreased, with decreasing linear hydrogen bond density. This series of nylons is unique as in each case the chain folds must be in the diamine alkane segment.

Table 1.3: Thermal data and Brill spacings for the X,4 Nylons

Nylon	T_B, °C	T_m, °C	Brill spacing, nm
4,4	170	degrades	0.415
6,4	190	275	0.42
8,4	190	254	0.42
10,4	160	242	0.42
12,4	140	237	0.42
6,6	220*	265	0.42*

*Data from ref. 32

1.2.3.5 Nylons-X,18 (X = 2, 4, 6, 8, 10, and 12)

The series of even-even nylons -2,18, -4,18, -6,18, -8,18, -10,18, and -12,18 showed three different crystalline transition behaviors when studied by variable temperature XRD.[98] Both, the melt-crystallized and solution-crystallized samples of nylons -2,18 and -4,18 underwent the Brill transition on heating. For nylon-6,18 the solution-crystallized sample melted prior to the complete crystalline transition, while the melt-crystallized sample did show the Brill transition before melting. The T_B's could not be detected perfectly in

advance of melting in either melt-crystallized or solution-crystallized samples for nylons -8,18, -10,18 and -12,18. The crystalline conditions and the melting temperatures of polyamides both play an important role in the Brill transition behavior of the even-even nylons under consideration.

Table 1.4: T_B and T_m for the X,18 Nylons

Nylon	T_B, °C		T_m, °C
	Melt-crystallized	Solution-crystallized	
12,18	175 (extrapolated)	≥ T_m	172
10,18	180 (extrapolated)	≥ T_m	176
8,18	185 (extrapolated)	≥ T_m	184
6,18	191	≥ T_m	199
4,18	215	220	218
2,18	150	175	233

The real-time FTIR results indicated that the change of the crystalline structure was related to the twisting of the CH_2-amide bonds and the enhanced vibration of the methylene sequences. The planar hydrogen bonds transformed gradually into the three-dimensional hydrogen bond network.

1.2.3.6 Nylons-2,Y (Y = 6, 8, 10, and 12)

The structures of chain-folded lamellar single crystals of nylons -2,6, -2,8, -2,10 and -2,12 grown from 1,4-butanediol were different from nylon-6,6 and many other even-even nylons.[31] At room temperature each nylon in the 2,Y series formed crystals with unit cells that were triclinic, but the characteristic room temperature signals were at 0.42 and 0.39 nm (compared with 0.44 and 0.37 nm observed for nylon-6,6 and most even-even nylons at ambient temperature). On heating the crystals from room temperature to melt, the triclinic structures transformed into pseudohexagonal structures and the two diffraction signals met at the T_B, which occurred at temperatures between 158 and 181 °C, significantly below the melting point. The diamine alkane segments of 2,Y nylons are too

short to sustain chain folds; thus, the chain folds must be in the diacid alkane segments in all cases. The room temperature structures and behavior on heating of the nylon 2,Y family was noticeably different from that of the nylon X,4 family, although the only difference between these families of polyamides

Table 1.5: Thermal data and Brill spacings for the 2,Y Nylons

Nylon	T_B, ±5°C	T_m, ±2°C	Brill spacing, ±0.003 nm
2,6	174	315	0.415
2,8	177	294	0.409
2,10	181	280	0.427
2,12	158	262	0.419

was the relative disposition of the amide groups within the chains. Thus the detailed chemistry strongly influenced the properties of nylons.

1.2.3.7 Nylons -4,8, -4,10, -4,12, -6,10, -6,12, -6,18 and -8,12

Single crystals of the seven nylons: -4,8, -4,10, -4,12, -6,10, -6,12, -6,18 and -8,12 were grown from 1,4-butanediol.[32] They had similar properties, both at room temperature and at elevated temperatures. The crystals were composed of chain-folded, hydrogen-bonded sheets; the linear hydrogen bonds within the sheets generated a progressive shear of the chains. The sheets were found to stack in two different ways; some progressively to form α phase crystals and others alternately to form β phase crystals. Both, the α and β crystals gave two strong diffraction signals at spacings of 0.44 and 0.37 nm at room temperature. Some crystals also showed an additional diffraction signal at 0.42 nm at the room temperature, characteristic of the pseudohexagonal phase usually only found at high temperatures. On heating, the two strong diffraction signals in both the α and β phase crystals moved together and met, as in the case of other even-even nylons. For all the nylons in this series of even-even nylons the T_B was coincident with the T_m, and the two strong signals met at the spacing of 0.42 nm of the pseudohexagonal phase. The melting points of the nylons decreased with decreasing linear hydrogen bond density.

Table 1.6: Thermal data and Brill spacings for Nylons -4,8, -4,10, -4,12, -6,10, -6,12, -6,18 and -8,12

Nylon	4,8	4,10	4,12	6,10	6,12	6,18	8,12	6,6
T_B, ±5°C	250	240	235	220	215	190	202	220
T_m, ±3°C	253	243	237	223	215	192	205	265
Brill spacing, ±0.003 nm	0.423	0.431	0.427	0.423	0.422	0.427	0.433	0.418

1.2.3.8 Nylons -6,6, -8,6, -8,8, -10,6, -10,8, -10,10, -12,6, -12,8, -12,10 and -12,12

Chain-folded lamellar single crystals of nylons -6,6, -8,6, -8,8, -10,6, -10,8, -10,10, -12,6, -12,8, -12,10 and -12,12 grown from 1,4-butanediol revealed that at room temperature three crystalline forms were present in different ratios.[25] The crystals were composed of chain-folded, hydrogen-bonded sheets; the linear hydrogen bonds within the sheets generated a progressive shear of the chains (p-sheets). The sheets were found to stack in two different ways. Some p-sheets stacked with a progressive shear to form the α_p structure and other sheets stacked with and alternate stagger, to form the β_p structure. Both, the α_p and β_p structures gave two strong diffraction signals at spacings of 0.44 and 0.37 nm at room temperature.

Table 1.7: Thermal data and Brill spacings for Nylons -6,6, -8,6, -8,8, -10,6, -10,8, -10,10, -12,6, -12,8, -12,10 and -12,12

Nylon	6,6	8,6	8,8	10,6	10,8	10,10	12,6	12,8	12,10	12,12
T_B, °C	220	194	213	184	222	200	183	213	188	181
T_m, °C	265	250	227	240	222	200	229	213	188	181
T_m-T_B, °C	45	56	14	56	0	0	46	0	0	0
Brill spacing, nm	0.422	0.426	0.423	0.428	0.429	0.430	0.428	0.430	0.430	0.428

Preparations of nylons -6,6, -8,6, -8,8, -12,6, and -12,8 consisted almost entirely of material with the α_p structure, with only a trace of material with the β_p structure. In contrast, nylons -10,6, -10,8, -10,10, -12,10 and -12,12 contained substantial quantities of both α_p and β_p structure material, with the α_p structure material always being in the majority. Preparations of nylons -10,8, -12,10 and -12,12 also showed an additional diffraction signal at 0.42 nm at the room temperature, characteristic of the pseudohexagonal phase usually only found at high temperatures On heating, the strong diffraction signals gradually moved together and merged at the T_B to form a single diffraction signal at 0.42 nm. This single diffraction signal remained until melting. For nylons -6,6, -8,6, -8,8, -10,6, and -12,6, the T_B's were substantially below the respective T_m's and the single diffraction signal at 0.42 nm was stable over temperature ranges of 14 °C to 56 °C, depending on the nylon. Conversely, nylons -10,8, -10,10, -12,8, -12,10 and -12,12 had coincident melting and extrapolated T_B's. The T_m of solution grown lamellae of these even-even nylons decreased with decreasing linear amide density.

1.2.3.9 Nylons -2,16, -4,16, -6,16, -8,16, -10,16, -12,16

Nylons -2,16, -4,16, -6,16 underwent Brill transition before melting upon heating.[99] The T_B values measured by variable-temperature XRD corresponded to 195 °C, 205 °C and 185 °C for Nylons -2,16, -4,16, -6,16 respectively.

The Brill bands were also identified based on real-time FTIR. The bands at 1297, 1227, 1068, 1040, 1018 and 988 cm^{-1} disappeared abruptly around 190 °C for nylon-6,16. The bands at 1068, 1040 and 1018 cm^{-1} originated from the skeletal C–C stretch vibration and the band at 988 cm^{-1} corresponded to –NH– rocking pattern.[36] The band at 1227 cm^{-1} was defined as a 'fold band' due to the wagging and twisting of $–CH_2–$ as well as the amide III mode. In addition, the band at 1297 cm^{-1} was correlated with –NH– twisting. Changes of these bands around the T_B reflected the changes of crystal structure in nylon-6,16. The T_B's determined by FTIR were about 200 °C for both nylons -2,16 and -4,16. The real-time FTIR results were entirely consistent with those of variable-temperature XRD measurements.

Table 1.8: T_B and T_m values of Nylons -2,16, -4,16 and -6,16

Nylon	T_B, °C		T_m, °C
	Determined by XRD	Determined by FTIR	Measured by DSC
-2,16	195	200	235
-4,16	205	200	218
-6,16	185	190	206

Table 1.9: T_B and T_m values of Nylons -8,16, -10,16 and -12,16

	Nylon-8,16	Nylon-10,16	Nylon-12,16
T_m, °C	189	176	170
T_B, °C (single crystals)	180	-	-
T_B, °C (melt-crystallized)	175	176 (extrapolated)	160

Crystalline transition behavior of nylons -8,16, -10,16, -12,16 was surprisingly found to be different from one another.[100] The measured T_B was dependent on crystallization conditions and varied with the perfection of the crystals. Both melt-crystallized samples and single crystals of nylon-8,16 grown from 1,4-butanediol showed Brill transition before melting upon heating. The T_B of sedimented mats (180 °C) was higher than that of the melt-crystallized sample (175 °C). The T_m of nylon-8,16 was 189 °C measured by DSC, which was high enough to allow the occurrence of Brill transition of the single crystals before melting. The difference between two T_B's of the single crystals and melt-crystallized samples came from the variation of the crystalline perfection. No crystalline transition was observed until melting in either melt-crystallized sample or single crystals grown from 1,4-butanediol for nylon- 10,16. The extrapolated T_B and T_m for melt-crystallized nylon-10,16 were coincident even though the crystalline perfection of melt-crystallized sample is usually poor. Since T_m of nylon-10,16 measured by DSC was as low

as 176 °C the single crystals had T_B higher than T_m. The authors found that nylon-10,16 was the only one of nylons for which no Brill transition could be observed below the T_m even for the melt-crystallized sample. Interestingly, the crystalline transition behavior of nylon-12,16 was situated between those of nylon-8,16 and nylon-10,16. The T_B of the melt-crystallized sample (160 °C) was lower than its melting point and the crystalline transition did not occur before melting on heating for single crystals grown from 1,4-butanediol. Since the T_m of nylon-12,16 was rather low (170 °C measured by DSC), the single crystals of nylon-12,16 had an extrapolated T_B higher than T_m. The variety in crystalline transition behavior of these nylons must have resulted from the difference in arrangement of hydrogen bonds within the crystal due to the different lengths of alkane segments between amine groups and acid groups.

The real-time FTIR studies were also carried out for nylons -8,16, -10,16, -12,16 and the results were all consistent with those of variable-temperature XRD measurements. The variation of hydrogen bonds with increasing temperature suggested that Brill transition originated from the 'local melting' of methylene between amide groups as mentioned above.

1.2.3.10 Nylons -10,20 and -12,20

In recent years, long alkane segment nylons have attracted much attention due to their special properties such as lower melting points, lower densities, lower dielectric constant, lower water affinity and considerable potential in the gel-spinning processes.[87,101-103] It was also suggested that long alkane segment nylons could be used as compatibilizers to bridge the gap between polyamides and polyolefins[104] For this reason, the investigation of the crystalline transition behaviors of long segment nylons under high temperature is important.

The crystalline transition behavior of nylons -12,20 and -10,20 studied by variable-temperature XRD depended to a large extent on the crystal perfection of the samples.[105] The dilute solution-grown lamellar crystals (grown from 1,4-butanediol) that had the most orderly structure showed no distinct Brill transition before melting, because at high temperature the movement of the long alkane segments reduced the regularity of the crystal before the Brill transition took place. Unlike the lamellar crystals of many other even-even nylons, which displayed two crystal signals until T_m, they presented a broad amorphous-like signal when the temperature increased to around 10 °C below T_m. The

post-annealed samples of nylons -12,20 and -10,20 displayed Brill transition on heating at 155 and 157 °C respectively, which were about 20 °C below the T_m's of the samples. The solution-cast (*m*-cresol) samples showed transition behavior at 110 and 135 °C for nylon-12,20 and nylon-10,20, respectively. Their transition processes were different from those of the dilute solution-grown lamellar and post-annealed samples, i.e., on heating the location of 100 signal remained essentially unchanged while 010/110 signal closed to 100 signal and finally disappeared around T_B. The changes in the infrared spectra of nylons -12,20 and -10,20 were also studied by real-time FTIR. It revealed an unusual behavior at T_B: not only some α bands disappeared or shifted to γ bands as expected, but also the crystalline band, at 942 cm^{-1}, surprisingly completely disappeared. This change in crystal structure could be attributed to the local melting that long alkane segments of the diacid (18-octadecanedicarboxlyic acid) may have undergone near T_B.

Real-time FTIR was used to investigate the crystalline transition of nylon-10,20.[106] The long CH_2 sequences between the amide groups were helpful in exploring the changes in the CH_2 units by FTIR during the crystalline transition. The intensity of the hydrogen bonds became weak and dissolved to free NH groups with increase in temperature. The twisting of the C–CO and C–N bonds improved as the temperature increased and the vibrations of the methylene sequences were strengthened, indicating that the methylene units were mobile at high temperature. The ordered stacking of methylene segments with the *trans*-zigzag conformation (bands around 1440, 1335 and 1182 cm^{-1}) gradually became disordered by the insertion of the gauche conformation (bands around 1096 and 1130 cm^{-1}) of the methylene units upon heating.

1.2.3.11 Nylon -12,12

Nylon-12,12 is one of the important engineering thermoplastics in the family of even-even nylons. They have rather long alkane segments between amide groups. Jones et al.[25,107] observed the morphology and structure of solution-grown, chain-folded lamellar crystals of nylon-12,12. Two phases were identified at room temperature the triclinic α phase and the triclinic γ phase. Li et al.[108] observed by using variable temperature XRD that the α phase transformed into the γ phase at about 130 °C when the melt-crystallized nylon-12,12 sample was heated from room temperature to a higher temperature. This transformation temperature was much lower than that of the solution-crystallized nylon-12,12 samples,[25] which was at 181 °C coincident with it's T_m. In addition, nylon-12,12 was found to

isothermally melt-crystallize into the γ phase at higher temperature (175 °C). Upon further cooling from the T_c to room temperature, the γ phase transformed in to the α phase at about 120 °C.

Furthermore, *in situ* FTIR was also used to study the Brill transition of nylon-12,12 samples on both heating and cooling. Fast-heating FTIR showed that the hydrogen bond strength decreased dramatically during the Brill transition because of the mobility of the methylene groups. The fingerprint region (1350–800 cm^{-1}) for nylons represented mainly the mobility of the methylene groups. Therefore some bands were found to disappear at the T_B because of the local melting of the alkane segments. When a well-crystallized sample was heated from room temperature to the T_m (190 °C) the band at 943 cm^{-1} assigned to the crystalline bands became weaker and broader and disappeared when the sample was melted. In contrast, there was no change for the amorphous bands (i.e., 1021 and 1172 cm^{-1}) up to T_m. However, some bands at 833, 856, 978, 1076 and 1292 cm^{-1}, assigned as the "Brill bands" decreased in intensity with increasing temperature and disappeared at 130 °C. Dramatic changes in the normalized area and the shift of –NH– stretching bands were also observed at the T_B and T_m of nylon-12,12 in the –NH– stretching region (3100–3500 cm^{-1}). The changes were due to the decrease in the hydrogen strength. During the melting process of nylon-12,12 also, the hydrogen bond strength decreased because of the higher mobility of the methylene groups and the transformation of some of the hydrogen-bonded –NH– groups into "free" –NH– groups.

The crystal transition of nylon-12,12 under annealing and drawing was investigated using XRD.[109] The triclinic α phase could be obtained by isothermal crystallization from a melted state or by annealing the γ phase at high temperature (above 150 °C). The crystal structure of the α phase annealed at 90 °C didn't change with time except for the perfection of crystals and an increase in the degree of crystallinity. The pseudohexagonal phase could be produced by crystallizing from the melt state at low temperature (90 °C) or by drawing the α phase samples at 90 and 160 °C as seen in Figures 1.7 and 1.8. For the first time the Brill transition was observed under drawing conditions, instead of under the traditional conditions of thermal inducement (continuous heating and cooling). There was a competition between drawing inducement and thermal inducement. Experimental results confirmed that drawing inducement was preferable for the formation of the γ phase and

played an important role in determining the crystal structure. Thermal inducement was preferable for the formation of the α phase.

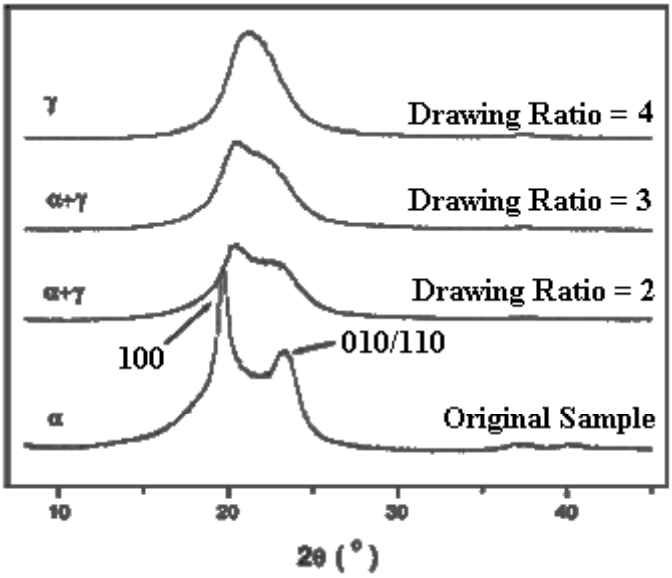

Figure 1.7: The XRD patterns of the α phase of nylon-12,12 drawn with different ratios at 90 °C.[109]

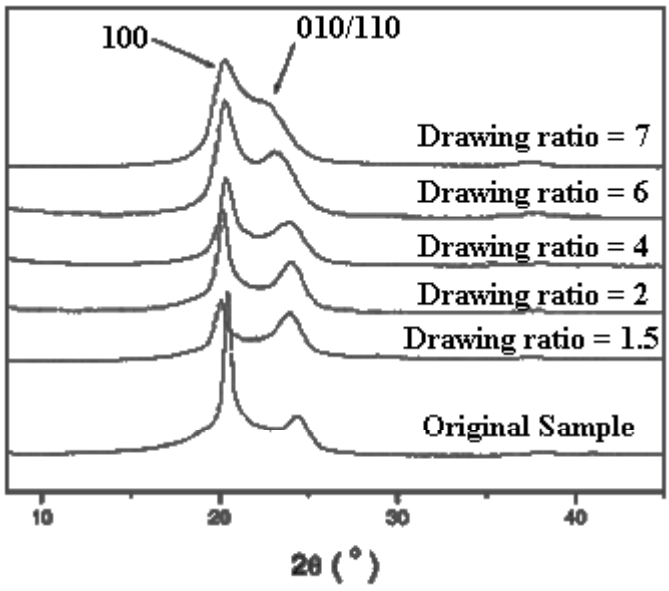

Figure 1.8: The XRD patterns of the α phase of nylon-12,12 drawn with different ratios at 160 °C.[109]

1.2.3.12 Nylon-4,14

A new nylon nylon-4,14 based on a short alkane diamine and a long alkane diacid was synthesized by melt polycondensation.[110] Variable-temperature XRD studies showed that well-melt-crystallized nylon-4,14 underwent Brill transition at 170 °C on heating. After Brill transition was recorded on heating, the temperature was further increased to above the T_m (230 °C) of the sample, and then cooled to 215 °C for isothermal crystallization. The diffraction pattern showed two distinct crystalline peaks at 2θ = 20.45° and 20.98°, which corresponded to the *d* spacings at 0.436 and 0.423 nm, respectively. The two peaks indicated that the crystalline phase was a kind of α phase. However, the high temperature α phase was much different from the room temperature α phase because the two *d* spacings were very close.

1.2.3.13 Nylon-10,14

Nylon-10,14 is a long alkane segment nylon. When crystallized from dilute solution it crystallized into the α phase.[111] Previous studies on the Brill transition behavior of melt-crystallized nylons -10,10,[94] -10,12[87,102] and -12,12[108] showed that the T_B of these long alkane segment nylon samples were much lower compared with those of the solution-crystallized nylons which were carefully studied by Jones and coworkers.[25,85] Li et al.[112] studied the influence of crystallization conditions on the crystalline transformation behavior of nylon-10,14. Three kinds of nylon-10,14 crystals with different perfections were prepared under various crystallization conditions. The Brill transition behavior of these nylon-10,14 crystals was investigated by variable-temperature XRD. The T_B of the lamellar crystals grown from dilute solution (1,4-butanediol) was so high that no T_B could be observed before melting. However, the Brill transition took place for the sample that was post annealed at different temperatures. The higher the post annealing temperature used, the higher the T_B that could be obtained. For crystals post annealed at 125 °C, the T_B was as low as 130 °C and for crystals post annealed at 160 °C, the T_B was as high as 170 °C, as the perfection of the crystal increased with increasing annealing temperature. The results showed that the Brill transition behavior of nylons was strongly dependent on the crystallization conditions, for example, the perfections of the crystals.

1.2.4 Even Nylons

1.2.4.1 Nylon-8

Nylon-8 crystallized from solution showed a peculiar structural modification reported as the $\alpha*$ phase.[113] The $\alpha*$ phase was prepared from 1 wt% solution of the γ phase of nylon-8 in formic acid (99 wt%) at 25 °C. The phase transition of the $\alpha*$ phase to the γ phase proceeded through melting and recrystallization, rather than a $\alpha* \rightarrow \gamma$ solid-solid transition. When the γ crystallization was concluded, the melting of this phase took place. DSC and XRD data demonstrated that this transition was irreversible.

Nylon-8 was crystallized from 1,4-butanediol in the form of chain-folded crystal lamellae and two crystal phases were observed when studied using TEM including selected area electron diffraction.[30] At room temperature single crystals were usually found in the monoclinic phase. Nylon-8 single crystals, which had been drastically quenched into non-solvent from the T_c showed a different structure, which was proposed to be a pseudohexagonal structure. The monoclinic crystals when heated in the hot stage of the TEM from room temperature to melting, gradually transformed into the pseudohexagonal structure. The process varied in detail with the crystal preparation before heating; the transformation was only completed if the crystals were originally imperfect and/or contained solvent. In others melting took place before the full pseudohexagonal phase was reached. The monoclinic phase was the low temperature phase and the pseudohexagonal phase was the stable phase at high temperatures. It was concluded that single crystals grew in this high temperature pseudohexagonal phase, but usually transformed into the monoclinic phase on cooling to room temperature. The high temperature pseudohexagonal phase could, however, be 'frozen in' by quenching very rapidly from the T_c into non-solvent below the T_g (50 °C); such 'frozen' crystals reverted to the low temperature, monoclinic phase on heating above 50 °C.

1.2.4.2 Nylon-12

The α phase of nylon-12 is monoclinic,[50,114] and the room temperature phase of nylon-12 appeared to depend on the crystallization conditions. The samples crystallized by slow cooling and rapid quenching from the melt showed γ phase at room temperature.[115] The single crystal mats[116] and drawn and rolled samples[116] showed α' phase at room temperature as the spacings were very close. However, nylon-12 crystallized at high temperature and pressure exhibited both α and γ phase at room temperature.[115,117] Nylon-

12 crystallized into the α' phase when crystallized from the melt at 170 °C.[118] The sample crystallized at 160 and 175 °C also showed behavior similar to the sample crystallized at 170 °C. On cooling from the T_c to the room temperature nylon-12 transformed into the γ phase. The high temperature α' phase was also assumed to be monoclinic. This finding of high temperature α' phase transformation into γ phase on cooling confirmed the earlier reports that nylon-12 had hexagonal structure at room temperature[7,50,119] when crystallized from the melt. Hiramatsu et al.[115] observed that the α phase obtained by high-pressure crystallization transformed into γ phase on annealing at 150 °C.

Li et al.[120] monitored the temperature dependence of the crystalline structure and morphology of nylon-12. XRD measurements revealed that the α' phase was a stable high temperature crystalline phase, independent of thermal history. Upon cooling, at temperatures around 100-130 °C, a hexagonal phase existed (single peak). This crystalline transition $\alpha' \leftrightarrow \gamma$ around 120 °C indicated a discontinuous change in density by SAXS. At low temperatures, two crystal reflections occurred at wide angles. This was interpreted as a monoclinic or an orthorhombic structure, which evolved from the hexagonal structure of the γ phase by an anisotropic thermal expansion. The evolution of the crystalline thickness during cooling and heating suggested the occurrences of partial surface crystallization and melting. This effect was superimposed on the crystalline transition and lead to crystal thickening and thinning during cooling and heating, respectively. The transition from γ to α' with increasing temperature arose from a "one-dimensional-melting" type of rupture between the hydrogen-bonded sheets. Fast quenching from the melt resulted in the γ' phase, which transformed upon annealing into either the γ or the α' phase. This process proceeded most probably through melting and recrystallization.

The formation conditions of the α phase of nylon-12 under high pressure from the melt and from the quenched state were investigated by high pressure DTA and XRD.[121] The α phase was formed by crystallization from the melt above 200 MPa, and the γ phase disappeared in the sample obtained above 500 MPa. The quenched state was transformed into the α phase at a temperature lower than the T_m of the α phase under high pressure, whereas the γ phase was hardly transformed at all. The thermal behavior of the α phase at atmospheric pressure was also studied. Two endotherms due to the meltings of the α and γ phase and one exotherm due to the α to γ transformation were observed. This

transformation occurred without melting of the α phase at a slow heating rate and was regarded as a monotropic transition. Hiramatsu at al.[122] further investigated the transformations among α, γ and γ' phases in nylon-12 using XRD, X-ray fiber patterns and DSC.[122] The γ' phase was distinguished from the γ phase, in spite of their very similar XRD patterns, because the γ phase could not be transformed into the α phase while the γ phase was so transformed under high pressure. The γ' to γ transformation occurred on annealing above 110 °C at atmospheric pressure. The γ to γ' and α to γ' transformation occurred on drawing at atmospheric pressure above 50 °C and above 70 °C, respectively.

Ishikawa et al. found that the α phase of nylon-12 could be obtained by casting γ nylon-12 from a phenol-ethanol mixture below 30 °C.[123] They also studied the transformation from the γ phase to the α phase by drawing and found that by using optimum conditions partial transformation from the γ phase to the α phase took place.[124] Further they studied in detail the drawing conditions influencing the α crystal formation.[125] Partial development of the α phase crystals in γ nylon-12 was found to take place by drawing near the melting point. The development of the α phase was confirmed by XRD, infrared absorption, and DSC. The amount of the α phase varied depending upon the temperature of drawing and draw ratio, whereas it was almost independent of the rate of drawing. The minimum draw ratio necessary to yield the α phase increased as the temperature of drawing decreased. The development of the α phase was ascribed to the transformation from the γ phase rather than crystallization from the amorphous region.

Nylon-12 crystallized from solution showed a peculiar structural modification reported as the $\alpha*$ phase.[113] The $\alpha*$ phase was prepared from 1 wt% solution of the γ phase of nylon-12 in formic acid (99 wt%) at 80 °C. The phase transition of the $\alpha*$ phase to the γ phase proceeded through melting and recrystallization, rather than a $\alpha* \rightarrow \gamma$ solid-solid transition. When the γ crystallization was concluded, the melting of this phase took place. DSC and XRD data demonstrated that this transition was irreversible.

1.2.5 Even-Odd Nylons

1.2.5.1 Nylon-6,5

A new type of polyamide structure was found for nylon-6,5 lamellar crystals which was different from the conventional α and γ phases of nylons.[126] Each molecule was linked to

its four neighbours by a network of hydrogen bonds made by amide groups in two different orientations. Results obtained by structural modeling pointed to a particular conformation for the glutaryl units characterized by a rotation angle about 52° between the two carbonyl directions, which stabilized the network of two hydrogen bond directions.
Temperature-induced structural changes were studied for nylon-6,5 fibers from 25 to 220 °C. The two strong equatorial reflections gradually merged into one peak as the temperature was increased. A single spot at 4.25 A° was observed at 190 °C corresponding to the pseudohexagonal packing. Modifications were believed to occur by thermal vibrations of the methylene groups without changes in the hydrogen bond system, in a way similar to that found in nylon-6,6.[127] There is a similarity between the chemical repeat units of nylon-6,5 and nylon-6,6.

1.2.5.2 Nylon-6,9

The predominant room temperature structure of nylon-6,9, both in chain-folded lamellar crystals and uniaxially oriented fibers, incorporated two inter-chain hydrogen bond directions.[128] The room temperature structure showed the two characteristic (inter-chain) diffraction signals at spacings of 0.43 and 0.38 nm, typical of α phase nylons. However, nylon-6,9 was unable to form the α phase hydrogen-bonded sheets without serious distortion of the all-*trans* polymeric backbone. The structure had c and c∗ noncoincident and two directions of hydrogen bonding. Optimum hydrogen bonding could only occur if consecutive pairs of amide units alternated between two crystallographic planes. This model offered a possible universal solution for the crystalline state of all odd-even nylons. The nylon-6,9 room temperature structure had a *C*-centered monoclinic unit cell (β = 108°) with the hydrogen bonds along the *C*-face diagonals. This structure was similar to the structure reported for nylon-6,5. In the case of nylon-6,5, it was suggested that the origin of the ‘‘two hydrogen bond direction’’ structure emanated from the relative shortness of the diacid alkane segment (the glutaryl unit). Atkins and coworkers believed that this was not the fundamental ingredient for this class of crystalline structures in odd-even nylons. It was argued that the underlying reason for this structure in nylon-6,9 was the direct consequence of directional pairing of consecutive amide units necessary for achieving an optimal arrangement of hydrogen bonds.

On heating nylon-6,9 lamellar crystals and fibers, the two characteristic diffraction signals at 0.43 nm and 0.38 nm converged to 0.42 nm and met at the T_B. The T_B for nylon-6,9

lamellar crystals was 202 °C which was slightly below the T_m (207 °C), whereas the T_B for nylon-6,9 fibers was ≅ 100 °C below T_m. The T_B increased with the degree of crystal perfection[30] and hence the variation in the T_B values for the crystal mat and fiber samples. Above T_B, nylon-6,9 had a hexagonal unit cell; the alkane segments existed in a mobile phase and equivalent hydrogen bonds populated the three principal (hexagonal) directions.

1.2.5.3 Nylon-12,5

Nylon-12,5 has a structure different from the conventional α and γ phases of nylons.[129] It was similar to the structure of nylon-6,5[126] with molecules packed in a network of hydrogen bonds with two spatial orientations. The structure was derived from a particular conformation of the glutaric units and appeared to be independent of the number of methylene groups present in the diamine residue.

The fibers obtained from the melt corresponded to a different pseudohexagonal phase characterized by a single equatorial spacing at 4.25 A° and a shortening around 0.52 A° per amide group with respect to an extended conformation. This structure was interpreted as a γ phase, but a higher degree of disorder could be present in this case. In contrast to nylon-6,5, where this pseudohexagonal phase could be transformed into the monoclinic one after annealing under stress, all the nylon-12,5 fibers broke when they were annealed.

1.2.6 Odd-Even Nylons

1.2.6.1 Nylon-5,6

Nylon-5,6 is an isomeric compound of nylon-6,5 and is also close to nylon-6,6. Two crystalline structures were studied for nylon-5,6, one was the γ phase and another corresponded to an α-like phase.[130] Structural modeling and energy calculations were carried out for the α-like phase and the results pointed out to a structure with two hydrogen bond directions. The methylene carbons existed in an all-*trans* conformation and the consecutive amide groups (those separated by the odd methylene segment) rotated in different senses from the methylene plane. The torsional angles for the CH_2-NH and CH_2-CO bonds of one residue were $\varphi = +152°$ and $\varphi = \pm 137°$. This model was similar to the α-like phase observed in both odd-even and even-odd nylons.

Temperature-induced structural changes were also studied for nylon-5,6 fibers which existed initially in an α-like phase from 25 to 220 °C and it was observed to be similar to

nylon-6,5. The pseudohexagonal packing was obtained near 220 °C in a process that took place without changes in the hydrogen bond system.

1.2.6.2 Nylon-5,10

Nylon-5,10 showed polymorphism with two different structures related to the γ phase obtained by either solution or melt crystallization.[131] Packing differences were due to the change in the hydrogen bonding system. In the case of the sample crystallized in 1,2,6-hexanetriol, the crystal morphology, unit cell dimensions, and the symmetry of the electron diffraction pattern suggested more than one hydrogen bonding direction. Two possibilities were compatible with the experimental data. One was based on an irregular structure where the amide units flipped ± 60° out of the plane defined by the methylene carbons. Another possibility was based on a regular structure with two hydrogen bonding directions and a molecular conformation like the one postulated for the α-like phase. The melt-crystallized sample had a structure similar to the conventional γ phase with a single hydrogen bond direction. In contrast with polymers with a low number of methylene groups (nylon-5,6), the α-like phase was difficult to obtain. It could be prepared by precipitation from strong acid solutions or from their mixtures with chloroform. A model with two hydrogen bonding directions was given for this phase, similar to that postulated for polyamides derived from odd diamine or odd diacid units.

Temperature-induced structural changes were studied for nylon-5,10 fibers annealed under stress from 25 to 205 °C. The two prominent equatorial reflections of the α-like phase gradually changed with temperature and they came together and met (4.27 A° at 195 °C) before the melting point was reached.

1.2.6.3 Nylon-9,2

Nylon-9,2[132] has a structure characterized by two hydrogen bond directions. From a conformational point of view this structure has an all-*trans* conformation, which was close to the characteristic α phase of nylons. The main difference was the different rotation of consecutive amide groups along the polymer chain from the plane defined by the methylene carbons. In the α phase of nylon-6,6 the torsion angles of the NH-CH_2 bonds deviated in the same sense ($\varphi_1 = -\varphi_2$), giving a structure with a single hydrogen bond direction. In nylon-9,2 the torsion angles of the NH-CH_2 bonds slightly deviated from

180 °C in order to optimize the hydrogen bonding interactions between neighbouring chains. Diffraction spacings were similar for both structures and clearly differed from those expected for a γ structure. The proposed conformation ($\varphi_1 = \varphi_2$) was also possible in other odd-even and even-odd nylons, since it allowed the establishment of all possible hydrogen bonds. The new structure was an alternative to the γ phase commonly postulated for this type of nylons.

Changes with temperature in the spacings of the two strong diffraction signals (020 and 110/110) of nylon-9,2, which at room temperature appeared at 4.34 and 3.68 A° were monitored using X-ray patterns of sedimented crystal mats. While the spacing of the first diffraction signal remained practically constant, the second one increased with temperature until a maximum spacing of approximately 4.05 A°, was reached at 215 °C (approximately 30 °C before melting). Thus a Brill transition in which both equatorial reflections merged into a single reflection had not been observed.

1.2.6.4 Nylons -11,10 and -11,12

The novel odd-even nylons, nylons -11,10 and -11,12 were synthesized by step-heating melting-polycondensation with 1,11-diaminoundecane of dodecanedioic acid and decanedioic acid.[133] The T_m of nylon-11,12 was at 188 °C, which was lower than that of nylon-11,10 at 195 °C. The difference in their T_m's was due to the difference in the concentration of hydrogen bond. The variable temperature XRD results indicated that nylon-11,10 underwent the Brill transition during heating before melting while nylon-11,12 did not. At room temperature, the XRD patterns of nylon-11,10 showed two characteristic diffractions at *d* spacings of 0.44 and 0.37 nm, indicating the α like phase which on heating gradually converged into one single reflection at *d* spacing of 0.42 nm, indicating the transformation into the high temperature pseudohexagonal phase. The real time FTIR spectra of nylon-11,10 showed results similar to that of nylon-10,20 during the Brill transition. It was found that the intensity of hydrogen bond became weak, and the twisting of the C–CO and C–N bonds were enhanced as the temperature increased. The vibration of the methylene units strengthened and the *trans*-zigzag conformation decreased. The ordered stacking of the methylene segments became gradually disordered by the insertion of the *gauche* conformation of the methylene units.

1.2.7 Odd Nylons

1.2.7.1 Nylon-11

Nylon-11 is a high-performance semicrystalline polymer. In the odd nylons group, nylon-11 has received considerable scientific attention because of its piezoelectric and ferroelectric properties. Early workers[134] reported only the stable triclinic structure for odd numbered amino acid nylons. Sasaki[135] reported that the nylon-11 film cast from trifluoro acetic acid solution showed a new crystal phase with one strong diffraction signal at 4.16 A° whereas the nylon-11 film cast from phenol-ethylene chlorohydrin solution showed an ordinary XRD pattern of the triclinic phase with two strong diffraction signals at 3.73 A° and 4.44 A°. The amide V and amide VI bands at 687 and 584 cm^{-1}, respectively [136,137] observed in the infrared spectrum of the film cast from a phenol-ethylene chlorohydrin solution disappeared in the spectrum of the film cast from a trifluoro acetic acid solution and a new band appeared at 627 cm^{-1}. The crystal phase obtained from the trifluoro acetic acid solution was stable against heat treatment (boiling in water for about 5 hrs) but was converted to the normal crystal phase by stretching.

XRD study of nylon-11 was carried out at high pressures and high temperatures.[138] A crystal transition at atmospheric pressure was observed to occur at 95 °C, the triclinic α phase changed to the pseudohexagonal structure. It was found that the increase in transition temperature with pressure dT_t/dP (~15 K/kbar) was greater than the T_m increase with pressure dT_m/dP (~9 K/kbar). The temperature of the transition increased until at 310 °C and 14.5 kbar a triple point was reached. Thus, at pressures above 14.5 kbar the α phase was stable until melting. Further Chen and coworkers[139] suggested that two species of crystals were involved in the melting of nylon-11 for samples crystallized at atmospheric pressure or when the environmental pressure was below 4 kbar. The sample melted at atmospheric pressure showed two melting peaks at 180 °C and 188 °C. At atmospheric pressure the high melting species was predominant. Under hydrostatic pressures, the high melting species underwent phase transition to the low melting species before melting. The amount of material involved in the transition depended on the pressure. The entire high melting species transformed to the low melting species at pressures of 4 kbar or greater. For samples crystallized at high pressures, the melting behavior at atmospheric pressure also showed two melting peaks for a crystallization pressure below 4 kbar. With increasing pressure the amount of low melting species increased, and at 4 kbar or higher, only melting of the low melting species was observed.

The XRD patterns taken at room temperature suggested that the samples crystallized between atmospheric pressure and 3 kbar contained both the α phase and the δ' phase crystals but the samples crystallized at 4 kbar and higher contained only the α phase crystal. The XRD patterns at high temperatures near the melting showed that the low melting species was of the δ phase and the high melting species of the δ' phase crystals for samples crystallized below 4 kbar. The α–δ transition at 95 °C resulted in the δ phase crystals. The melting at high pressures (<4 kbar) of samples crystallized at atmospheric pressure also appeared to involve a $\delta'-\delta$ transition. These results suggested that both the crystal phases δ and δ' were stable at high temperatures for pressures lower than 4 kbar, and that only the δ phase crystals were stable upto melting at pressures greater than 4 kbar.

Three crystal modifications were found for lamellar single crystals of nylon-11 obtained from solution.[140] Lamellar crystals of form I obtained from solution in diols, had a triclinic unit cell and were similar to the α phase of nylon-6,6 and 6,10. Lamellar crystals of form II were obtained from solution in water containing 5 % formic acid. Form II was monoclinic and was very similar to the α phase of nylon-6. Lamellar crystals of form III were obtained from solution in water and triethylene glycol. The crystal structure of this form was pseudohexagonal and was very similar to the γ phase of nylon-6.

Newman et al.[141] proposed that the melt-crystallized films of nylon-11 did not have the α phase structure despite the general similarity of their diffraction patterns to the solution cast (*m*-cresol) α phase. The smaller angle *d* spacing from the melt-crystallized film (which in the α phase corresponds to the 001 reflection) was larger: 11.95 as opposed to 11.33 A°. The *d* spacing of the reflection which in the α phase is indexed as 010 was 3.82 A° instead of 3.72 A°. The third strong reflection, in the α phase indexed as 100 showed the same *d* spacing in both melt-crystallized and solvent-cast films. After annealing, the *d* spacings of the melt-crystallized films did not approach those of the α phase. Further the temperature dependence of the *d* spacings of the two strongest peaks was studied. The intensity of the 010 reflection of the solution cast film gradually decreased with increasing temperature and was not observed at temperatures above 140 °C. The 100 reflection also decreased somewhat in intensity with increasing temperature but was observed at temperatures above 140 °C. However, the two peaks did not merge

into a single peak at any temperature. In the melt-crystallized sample the two peaks merged into a single peak characteristic of a pseudohexagonal structure at 100 °C.

To summarize nylon-11 exhibits five crystalline modifications including the α phase, resulting from annealing of the quenched polymer[140,142,143] or solution casting from *m*-cresol,[141] the α' phase obtained from melt crystallization,[141] the pseudohexagonal phase obtained above room temperature by heating α' phase, [138] smectic or δ' phase obtained by melt quenching,[144] and the γ phase obtained by solution casting from trifluoro acetic acid.[135]

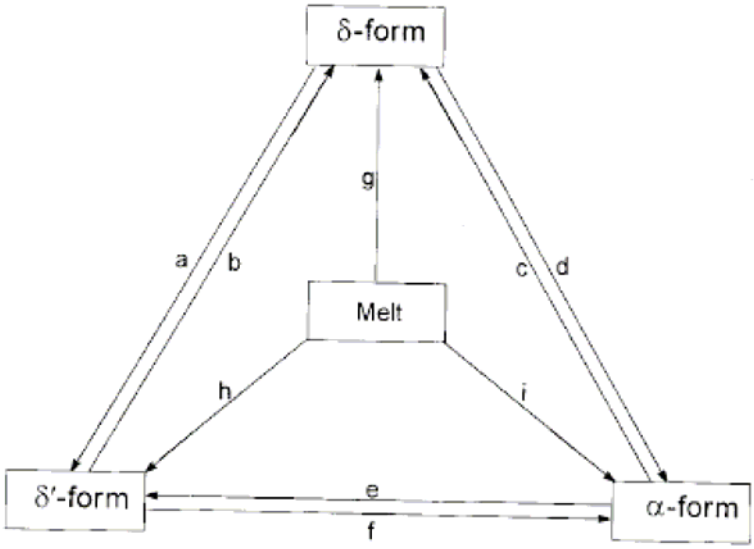

Figure 1.9: Crystal transitions of nylon-11: (a) quenching into ice bath, (b) heating to high temperature (>95 °C), (c) heating to high temperature (>95 °C), (d) isothermal crystallization at high temperature (>95 °C), (e) drawing at low temperature (<95 °C), (f) annealing at high temperature (>95 °C), (g) cooling to high temperature (>95 °C), (h) quenching into ice bath, and (i) isothermal crystallization at high temperature (>95 °C).[145]

Q. Zhang et al.[145] have studied the crystal transitions of nylon-11 at different drawing temperatures with different drawing ratios, and the results showed that they strongly depended on the thermal history and conditions of hot drawing. The δ' phase could be gradually transformed into the α phase when drawn at high temperature and the α phase was only partly transformed into the δ' phase when drawn at low temperature. This could be due to the effect of the competition between thermal inducement and drawing

inducement. The thermal inducement was favorable for producing the α phase, while the drawing inducement was favorable for producing the δ' phase.

Nylon-11 was synthesized with 99 + % ^{15}N labeling of the amide nitrogen and the roles of conformational order and hydrogen bond mobility in the α–δ transition were examined.[146] Polymer samples were thermally treated to give the stable triclinic α phase and the metastable δ' smectic phase and precipitated from trifluoro acetic acid to give the γ phase. ^{15}N CP/MAS NMR coupled with spin-lattice relaxation (T_{1N}) measurements clearly differentiated the polymer morphologies. The α phase transformed to the pseudohexagonal δ phase above 95 °C confirming the previously reported XRD and thermal analysis results. ^{15}N spin-lattice (T_{1N}) relaxation experiments confirmed decreasing relative mobility in the order $\delta' > \delta > \alpha$ consistent with increasing molecular rigidity and density. Unlike previous studies in which hydrogen bonds were postulated to break and reform rapidly above the 95 °C transition, ^{15}N chemical shift anisotropy spectra showed that the hydrogen-bonded amide units were rigidly oriented in the crystal lattice.

Melt-crystallized sample preparations of nylon-11, which were *m*-cresol cast, trifluoro acetic acid cast and sodium hydroxide treated, were examined by infrared analysis.[147] The *m*-cresol cast films appeared to be intermediate in conformational structure between melt-crystallized and trifluoro acetic acid cast films. The four spectral regions indicative of the crystal phase in nylons: amide V and VI, amide II and the CH_2 bending region were sensitive to the crystal phase transformation in nylon-11. Sodium hydroxide treatment promoted the α to γ conversion in melt-crystallized films of nylon-11. The infrared temperature response of melt-crystallized and *m*-cresol cast films, was entirely different when viewed in terms of frequency shifts and areas inspite of their similar crystal structures.[148] The melt-crystallized sample showed the Brill transition in the 68-88 °C range and the transition was virtually invisible in the *m*-cresol and trifluoro acetic acid cast films. The thermal transition observed in the 108-140 °C range in melt-crystallized sample and not observed in the *m*-cresol and trifluoro acetic acid cast films was assigned to the glass transition.

Nylon-11–montmorillonite (MMT) nanocomposite displayed polymorphism.[149] The XRD pattern of the nanocomposite molten at 205 °C and melt-crystallized at room temperature showed a new peak at $2\theta = 21.7°$ characteristic of the γ phase of nylon-11 along with the

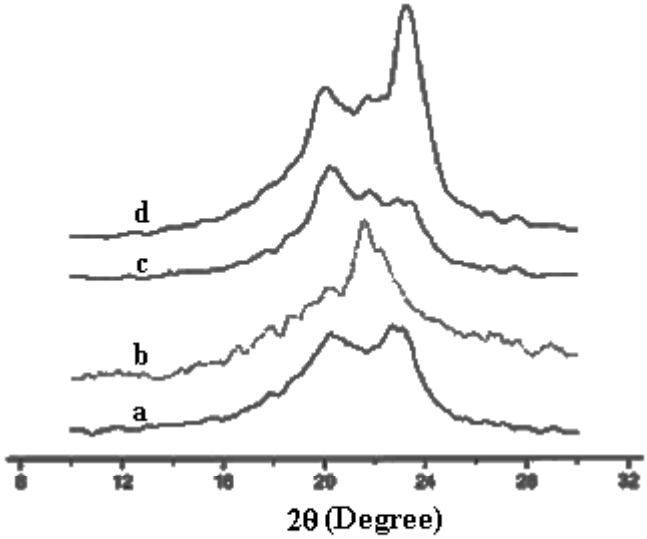

Figure 1.10: XRD patterns of (a) nylon-11 molten at 205 °C and then melt-crystallized at room temperature, (b) nylon-11 casting from the trifluoro acetic acid solution, (c) nylon-11–MMT nanocomposite molten at 205 °C and then melt-crystallized at room temperature, and (d) nylon-11–MMT nanocomposite molten at 205 °C, melt-crystallized at room temperature, and then annealed at 160 °C for 24h.[149]

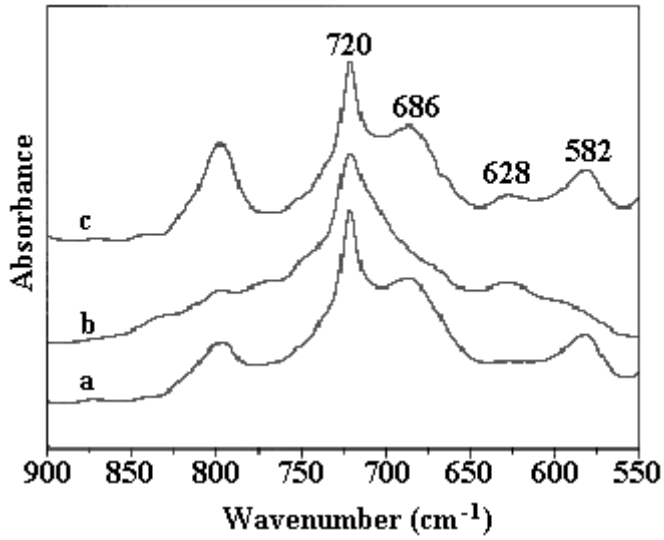

Figure 1.11: Infrared spectra of (a) nylon-11 molten at 205 °C and then melt-crystallized at room temperature, (b) nylon-11 casting from the trifluoro acetic acid solution, and (c) nylon-11–MMT nanocomposite molten at 205 °C and then melt-crystallized at room temperature in the region of 900-550 cm^{-1}.[149]

two peaks of the α' phase of nylon-11 at $2\theta = 20$ and 23° as seen in Figure 1.10. The γ phase peak was reserved after annealing the sample at 160 °C for 24h, which indicated that MMT induced and stabilized the γ phase of nylon-11. The FTIR results confirmed it by the investigation of the amide V, VI, and II bands of nylon-11. The spectrum of the melt-crystallized nylon-11 nanocomposite showed peaks at 686 and 582 cm^{-1} corresponding to the amide V and VI bands of the α phase respectively, and a peak at 628 cm^{-1} corresponding to the amide VI band of the γ phase as seen in Figure 1.11. The second derivative of the infrared spectrum for the melt-crystallized nylon-11 nanocomposite film displayed a peak at 1542 cm^{-1} corresponding to the amide II band of the α phase and also a shoulder peak on the higher wavenumber side at about 1560 cm^{-1} corresponding to the amide II band of the γ phase. This indicated that both α and γ phases coexisted in the nanocomposite. However, the hydrogen bonds of nylon-11 were weakened by the addition of MMT that restricted the formation of hydrogen-bonding sheets by forcing the amide groups of nylon out of the hydrogen-bonding sheet. Meanwhile, the temperature dependence of hydrogen bonds for the nanocomposite varied a lot as compared with neat nylon-11, which showed a slower weakening trend with increasing temperature.

1.2.8 Odd-Odd Nylons

1.2.8.1 Nylon-5,5

The nylon-5,5 structure seemed to be stable over the whole temperature range between room temperature and T_m, since no change of the measured *d* spacings was detected in the fiber diffraction patterns registered at different temperatures.[12] In nylon-5,5 the molecules were packed in a network of hydrogen bonds with two spatial orientations, similar to the proposed structure for nylon-6,5.

1.3 References

1. Bolton, E. K. *Ind. Eng. Chem.* **1942,** *34,* 53.
2. Sweeny, W.; Zimmerman, J. *Polyamides, in Encyclopedia of Polymer Science and Technology*, *Wiley-Interscience, New York,* **1969,** 10.
3. Synder, O. E.; Richardson, R. J. *Polyamide fibers, to DuPont, in Encyclopedia of Polymer Science and Technology*, *Wiley-Interscience, New York,* **1969,** *10,* 356.
4. Holmes, D. R.; Bunn, C. W.; Smith, D. J. *J. Polym. Sci*. **1955,** *17*, 159.
5. Bunn, C. W.; Garner, E. V. *Proc. R. Soc. (London)* **1947,** *189,* 39.

6. Dreyfuss, P.; Keller, A. *Macromol. Sci. Phys.* **1970,** *B4,* 811.
7. Atkins, E. D. T.; Hill, M.; Hong, S. K.; Keller, A.; Organ, S. *Macromolecules* **1992,** *25,* 917.
8. Arimoto, H.; Ishibashi, M.; Hirai, M.; Chatani, Y. *J. Polym. Sci. Part A:* **1965,** *3,* 317.
9. Arimoto, H. *J. Polym. Sci., Part A: Gen. Pap.* **1964,** *2,* 2283.
10. Ziabicki, A.; Kedzierska, A. *J. Appl. Polym. Sci.* **1959,** *2,* 14.
11. Stepaniak, R. F.; Garton, A.; Carlsson, D. J.; Wiles, D. M. *J. Polym. Sci., Polym. Phys.* **1979,** *17,* 987.
12. Navarro, E.; Aleman, C.; Subirana, J. A.; Puiggalı´, J. *Macromolecules* **1996,** *29,* 5406.
13. VanderHart, D. L.; Asano, A.; Gilman, J. W. *Chem. Mater*. **2001**, *13*, 3781.
14. Lincoln, D. M.; Vaia, R. A.; Wang, Z. G.; Hsiao, B. S. *Polymer* **2001**, *42*, 1621.
15. Cho, J. W.; Paul, D. R. *Polymer* **2001**, *42*, 1083.
16. Maiti, P.; Okamoto, M. *Macromol. Mater. Eng.* **2003,** *288,* 440.
17. Brill, R. J. *J. Prakt. Chem.* **1942**, *161*, 49.
18. Ramesh, C.; Keller, A.; Eltink, S. J. E. A. *Polymer* **1994,** *35*, 2483.
19. Colclough, M. L.; Baker, R. *J. Mater. Sci.* **1978,** *13,* 2531.
20. Starkweather, H. W., Jr.; Jones, G. A. *J. Polym. Sci., Polym. Phys. Edn.* **1981,** *19,* 467.
21. Itoh, T. *Jpn. J. Appl. Phys.* **1976,** *15*, 2295.
22. Hirschinger, J.; Miura, H.; Gardner, K. H.; English, A. D. *Macromolecules* **1990,** *23,* 2153.
23. Murthy, N. S.; Curran, S. A.; Aharoni, S. M.; Minor, H. *Macromolecules* **1991,** *24*, 3215.
24. Xenopoulos, A.; and Wunderlich, B. *Colloid Polym. Sci.* **1990,** *20,* 375.
25. Jones, N. A.; Atkins, E. D. T.; Hill, M. J. *J. Polym. Sci., Part B: Polym. Phys.* **2000,** *38,* 1209.
26. Cannon, C. G.; Chappel, F. P.; Tidmarsh, J. I. *J. Text. Inst.* **1963,** *54,* 210.
27. Itoh, T.; Yamagata, T.; Hasegawa, Y.; Hashimoto, M.; Konishi. T. *Jpn. J. Appl. Phys.* **1996,** *35,* 4474.
28. Schmide, G. F.; Stuart, H. A. *Naturforsch* **1958**, *13A***,** 222.
29. Olf, H. G.; Peterlin, A. *J. Polym. Sci. A2 (Polym Chem)* **1971,** *9,* 1449.
30. Atkins, E. D. T.; Hill, M. J.; Veluraja, K. *Polymer* **1995,** *36,* 35.

31. Jones, N. A.; Cooper, S. J.; Atkins, E. D. T.; Hill, M. J.; Franco, L. *J. Polym. Sci., Polym. Phys.* **1997,** *35,* 675.
32. Jones, N. A.; Atkins, E.D.T.; Hill, M. J.; Cooper, S. J.; Franco, L. *Polymer* **1997,** *38,* 2689.
33. Atkins, E. D. T.; Hill, M. J.; Jones, N. A.; Cooper, S. J. *J. Polym. Sci., Polym. Phys.* **1998,** *36,* 2401.
34. Vergelati, C.; Imberty, A.; Perez, S. *Macromolecules* **1993,** *26,* 4420.
35. Murthy, N. S.; Wang, Z.-G.; Hsiao, B. S. *Macromolecules* **1999,** *32,* 5594.
36. Vasanthan, N.; Murthy, N. S.; Bray, R. G. *Macromolecules* **1998,** *31*, 8433.
37. Cooper, S. J.; Coogan, M.; Everall, N.; Priestnall, I. *Polymer* **2001,** *42,* 10119.
38. Liu, X.; Wu, Q.; Berglund, L. A. *Polymer* **2002,** *43,* 4967.
39. Liu, X.; Wu, Q.; Zhang, Q.; Mo, Z. *J. Polym. Sci., Polym. Phys.* **2003,** *41,* 63.
40. Zhang, Q. X.; Yu, Z. Z.; Yang, M.; Ma, J.; Mai, Y. W. *J. Polym. Sci., Polym. Phys.* **2003,** *41,* 2861
41. Wu, T. M.; Wu, J. Y. *J. Macromol. Sci., Phys.* **2002,** *B41*, 17.
42. Vogelsong, D. C. *J. Polym. Sci., Polym. Chem*. **1963,** *1,* 1055.
43. Miyasaka, K.; Ishikawa, K. *J. Polym. Sci*. **1968**, *A-2, 6*, 1317.
44. Miyasaka, K.; Ishikawa, K. *J. Polym. Sci*. **1972**, *A-2, 10*, 1497.
45. Kyotani, M. *J. Macromol. Sci*., *Phys.* **1975,** *B11,* 509.
46. Brucato, V.; Grippa, S.; Piccarolo, S.; Titomanlio, G. *Polym. Eng. Sci.* **1991,** *24,* 1411.
47. Murthy, N. S.; Szollosi, A. B.; Sibilia, J. P.; Krimm, S. J. *J. Polym. Sci., Polym. Phys.* **1985,** *23,* 2369.
48. Hiramatsu, N.; Hirakawa, S. *Polym. J.* **1982,** *14,* 165.
49. Fornes, T. D.; Paul, D. R. *Polymer* **2003,** *44*, 3945.
50. Aharoni, S. M. *n-Nylons: their Synthesis, Stucture and Properties; John Wiley & Sons: Chichester, U.K.,* **1997;** Chapter 1.3.
51. Ramesh, C.; Gowd, E. B. *Macromolecules* **2001,** *34*, 3308.
52. Murthy, N. S. *Polym. Commun.* **1991**, *32*, 301.
53. Dasgupta, S.; Hammond, W. B.; Goddard, W. A. III. *J. Am. Chem. Soc.* **1996**, *118*, 12291.
54. Li, Y.; Goddard, W. A. III. *Macromolecules* **2002,** *35*, 8440.
55. Hatfield, G. R.; Glans, J. H.; Hammond, W. B. *Macromolecules* **1990**, *23*, 1654.
56. Murthy, N. S.; Hatfield, G. R.; Glans, J. H. *Macromolecules* **1990,** *23,* 1342.

57. Penel-Pierron, L.; Depecker, C.; Séguéla, R.; Lefebvre, J.-M. *J. Polym. Sci., Part B: Polym. Phys.* **2001,** *39,* 484.
58. Penel-Pierron, L.; Séguéla, R.; Lefebvre, J.-M.; Miri, V.; Depecker, C.; Jutigny, M.; Pabiot, J. *J. Polym. Sci., Part B: Polym. Phys.* **2001,** *39,* 1224.
59. Vasanthan, N.; Salem, D. R. *J. Polym. Sci., Part B: Polym. Phys.* **2001,** *39,* 536.
60. Murthy, N. S.; Aharoni, S. M.; Szollosi, A. B. *J. Polym. Sci., Polym. Phys. Ed.* **1985,** *23,* 2549.
61. Rhee, S.; White, J. L. *Polymer* **2002,** *43,* 5903.
62. Gianchandani, J.; Spruiell, J. E.; Clark, E. S. *J. Appl. Polym. Sci.* **1982,** *27,* 3527.
63. Miyata, S.; Balakov, I. *J. Macromol. Sci., Chem.* **1981,** *A16,* 1233.
64. Bianchi, F.; Cantagallo, S.; Consolati, G.; Laporta, M.; Pegoraro, M.; Tieghi, G.; Zanderighi, L. *J. of Appl. Polym. Sci.,* **2002,** *86,* 559.
65. Wu, T. M.; Liao, C. S. *Polym. Eng., Sci.* **2002,** *42,* 1141.
66. Wu, T. M.; Wu, J. Y. *J. Macromol. Sci., Phys.* **2002,** *B41,* 17.
67. Wu, T. M.; Liao, C. S. *Macromol. Chem. Phys.* **2000,** *201,* 2820.
68. Zhao, Z.; Yu, W.; Liu, Y.; Zhang, J.; Shao, Z. *Materials Letters* **2004,** *58,* 802.
69. Liu, X.; Wu, Q. *Polymer* **2002,** *43,* 1933.
70. Liu, X.; Wu, Q.; Zhang, Q.; Berglund, L. A.; Mo, Z. *Polymer Bulletin* **2002,** *48,* 381.
71. Liu, X.; Wu, Q. *Polymer* **2002,** *43,* 2445
72. Lincoln, D. M.; Vaia, R. A.; Wang, Z.-G.; Hsiao, B. S.; Krishnamoorti, K. *Polymer* **2001**, *42*, 9975.
73. Wang, S.; Hu, Y.; Li, Z.; Wang, Z.; Zhuang, Y.; Chen, Z.; Fan, W. *Colloid and Polym. Sci.* **2003,** *281,* 951.
74. Zheng, J.; Siegel, R. W.; Toney, C. G. *J. Polym. Sci., Part B: Polym. Phys.* **2003,** *4*1, 1033.
75. Ergungor, Z.; Cakmak, M.; Batur, C. *Annual Technical Conference - Society of Plastics Engineers, 60th,* **2002,** *2,* 1519.
76. Ergungor, Z.; Cakmak, M.; Batur, C. *Annual Technical Conference - Society of Plastics Engineers, 60th,* **2002,** *2,* 2280.
77. Ergungor, Z.; Cakmak, M.; Batur, C. *Macromol. Symp.* **2002,** *185,* 259.
78. Yoon, K.; Kumar, S.; Polk, M. B.; Min, B. G.; Schiraldi, D. A. *Polymer Preprints* **2002,** *43,* 1372.
79. Liu, X.; Breen, C. *Macromol. Rapid Commun.* **2005**, *26*, 1081.

80. Biangardi, H. J. *J. Macromol. Sci.-Phys. B* **1990**, *29* (2/3), 139.
81. Ramesh, C. *Macromolecules* **1999**, *32*, 3721.
82. Yoshioka, Y.; Tashiro, K.; Ramesh, C. *Polymer* **2003,** *44*, 6407.
83. Yoshioka, Y.; Tashiro, K. *Polymer* **2003,** *44*, 7007.
84. Hill, M. J.; Atkins, E. D. T. *Macromolecules* **1995,** *28,* 604.
85. Jones, N. A.; Atkins, E. D. T.; Hill, M. J.; Cooper, S. J.; Franco, L. *Macromolecules* **1997,** *30,* 3569.
86. Li, Y. J.; Zhu, X. Y.; Yan, D. Y. *Polym. Eng. Sci.* **2000,** *40,* 1989.
87. Yan, D. Y.; Li, Y. J.; Zhu, X. Y. *Macromol. Rapid Commun.* **2000,** *21,* 1040.
88. Li, Y. J.; Yan, D. Y.; Zhu, X. Y. *Eur. Polym. J.* **2001,** *37,* 1849.
89. Atkins, E. D. T.; Hill, M. J.; Veluraja, K. *Polymer* **1995,** *36,* 35.
90. Yang, X. N.; Kong, X. H.; Tan, S. S.; Li, G.; Zhou, E. L. *Polym. Int.* **2001,** *50,* 817.
91. Yang, X. N.; Tan, S. S.; Li, G.; Zhou, E. L. *J. Polym. Sci., Part B: Polym. Phys.* **2001,** *39,* 729.
92. Yang, X. N.; Li, G.; Zhou, E. L. *Macromol. Chem. Phys.* **2001,** *202,* 1631.
93. Yang, X. N.; Tan, S. S.; Li, G.; Zhou, E. L. *Macromolecules* **2001,** *34,* 5936.
94. Li, Y. J.; Yan, D. Y.; Zhu, X. Y. *Macromol. Rapid Commun.* **2000,** *21,* 1282.
95. Tashiro, K.; Yoshioka, Y. *Polymer* **2004,** *45*, 4337.
96. Tashiro, K.; Yoshioka, Y. *Polymer* **2004,** *45*, 6349.
97. Jones, N. A.; Atkins, E. D. T.; Hill, M. J.; Cooper, S. J.; Franco, L. M*acromolecules* **1996**, *29*, 6011.
98. Cui, X.; Li, W.; Yan, D. *Polym. Int.* **2004**, *53*, 2031.
99. Li, W. H.; Huang, Y.; Zhang G. S.; Yan, D. *Polym. Int.* **2003,** *52,* 1905.
100. Li, W. H.; and Yan, D. Y. *Polym. Bull.* **2003,** *49,* 387.
101. Li, Y. J.; Zhu, X. Y.; Tian, G. H.; Yan, D. Y.; Zhou, E. L. *Polym. Int.* **2001**, *50*, 677.
102. Li, Y. J.; Yan, D. Y.; Zhu, X. Y.; Jiang, X. L. *J. Chin. Univ. Chem.* **2000**, *20***,** 983.
103. Ehrenstein, M.; Sikorski, P.; Atkins, E.; Smith, P. *J. Polym. Sci., Polym. Phys.* **2002,** *40,* 2685.
104. Ehrenstein, M.; Dellsperger, S.; Kocher, C.; Stutzmann, N.; Weder, C.; Smith, P. *Polymer* **2000**, *41*, 3531.
105. Huang, Y.; Li, W.; Yan, D. *Eur. Polym. J.* **2003**, *39*, 1133.

106. Cui, X.; Yan, D. *J. Polym. Sci. Part B: Polym. Phys.* **2004,** *42*, 4017.
107. Jones, N. A.; Atkins, E. D. T.; Hill, M. J. *Macromolecules* **2000**, *33*, 2642.
108. Li, Y. J.; Yan, D. Y.; Zhou, E. L. *Colloid Polym. Sci.* **2002**, *280*, 124.
109. Song, J.; Zhang, H.; Ren, M.; Chen, Q.; Sun, X.; Wang, S.; Zhang, H.: Mo, Z. *Macromol. Rapid Commun.* **2005**, *26*, 487.
110. Li, Y. J.; Yan, D. Y. *Polymer* **2001**, *2*, 5055.
111. Li, Y. J.; Yan, D. Y. *J. Polym. Sci., Part B: Polym. Phys.* **2003**, *41*, 1422.
112. Li, Y.; Yan, D. *Colloid Polym. Sci.* **2002**, *280,* 678.
113. Cojazzi, G.; Fichera, A. M.; Malta, V.; Zannetti, R. *Makromol. Chem.* **1991,** *192,* 185.
114. Cojazzi, G.; Fichera, A.; Garbuglio, C.; Malta, V.; Zannetti, R. *Makromol. Chem*. **1973**, *168*, 289.
115. Hiramatsu, N.; Haraguchi, K.; Hirakawa, S. *Jpn. J. Appl. Phys.* **1982,** *21*, 335.
116. Dosiere, M. *Polymer* **1993**, *34*, 3160.
117. Stamhuis, E.; Pennings, A. J. *Polymer* **1977**, *18*, 667.
118. Ramesh, C. *Macromolecules* **1999**, *32*, 5704.
119. Northolt, M. G.; Tabour, B. J.; van Aartsen, J. J. *J. Polym. Sci*., *Part A-2* **1972,** *10*, 191.
120. Li, L; Koch, M. H. J.; de Jeu, W. H. *Macromolecules* **2003,** *36,* 1626.
121. Hiramatsu, N.; Hashida, S.; Hirakawa, S. *Jpn. J. Appl. Phys., Part 1* **1982,** *21,* 651.
122. Hiramatsu, N.; Hashida, S.; Hirakawa, S. *J. Appl. Phys., Part 1* **1983,** *22,* 335.
123. Ishikawa, T.; Nagai, S. *J. Polym. Sci., Polym. Phys. Ed.* **1977,** *15,* 1315.
124. Ishikawa, T.; Nagai, S.; Kasai, N. *Makromol. Chem.* **1979,** *180,* 2999.
125. Ishikawa, T.; Nagai, S. *Makromol. Chem.* **1981,** *182,* 977.
126. Navarro, E.; Franco, L.; Subirana, J. A.; Puiggalı´, J. *Macromolecules* **1995,** *28,* 8742.
127. Wendolowski, J. J.; Gardner, K. H.; Hirschinger, J.; Miura, H.; English, A. B. *Science* **1990**, *247*, 431.
128. Franco, L.; Cooper, S. J.; Atkins, E. D. T.; Hill, M. J.; Jones, N. A. *J. Polym. Sci., Part B: Polym. Phys.* **1998,** *36,* 1153.
129. Navarro, E.; Subirana, J. A.; Puiggalı´, J. *Polymer* **1997,** 3*8,* 3429.

130. Puiggalı´, J.; Franco, L.; Aleman, C.; Subirana, J. A.; *Macromolecules* **1998,** *31,* 8540.
131. Villasenor, P.; Franco, L.; Subirana, J. A.; Puiggalı´, J. *J. Polym. Sci., Part B: Polym. Phys.* **1999,** *37,* 2383.
132. Franco, L.; Subirana, J. A.; Puiggalı´, J. *Macromolecules* **1998,** *31,* 3912.
133. Cui, X. W.; Yan, D. Y. *Eur. Polym. J.* **2005**, *41*, 863.
134. Slichter, W. P. *J. Polym. Sci.* **1959**, *36*, 259.
135. Sasaki, T. *J. Polym. Sci. Polym. Lett.* **1965**, *3*, 557.
136. Miyake, A. *J. Polym. Sci.* **1960**, *44*, 223.
137. Matsubara, I.; Shinomiya, M. *Abstracts of papers, 16th Annual Meeting of the Chemical Society of Japan*, *March*, **1963**, 275.
138. Newman, B. A.; Sham, T. P.; Pae, K. D. *J. Appl. Phys.* **1977**, *48*, 4092.
139. Chen, P. K.; Newman, B. A.; Scheinbeim, J. I.; Pae, K. D. *J. Mater. Sci.* **1985**, *20*, 1753.
140. Kawaguchi, A.; Ikawa, T.; Fujiwara, Y.; Tabuchi, M.; Monobe, K. *J. Macromol. Sci. Phys.* **1981**, *B20*, 1.
141. Kim, K. G.; Newman, B. A.; Scheinbeim, J. I. *J. Polym. Sci. Polym. Phys. Ed.* **1985**, *23*, 2477.
142. Slichter, W. P. *J. Polym. Sci.* **1959**, *36*, 259.
143. Kinoshita, Y. *Macromol. Chem.* **1959**, *33*, 1.
144. Schmidt, C. F.; Stuart, Z. *Naturforsch* **1958**, *13A*, 222.
145. Zhang, Q. X.; Mo, Z. S.; Zhang, H. F.; Liu, S. Y; Cheng, S. Z. D. *Polymer* **2001**, *42*, 5543.
146. Mathias, L. J.; Powell, D. G. *Macromolecules*, **1990**, *23*, 963.
147. Yu, H. H. *Mater. Chem. Phys.* **1998**, *56*, 289.
148. Yu, H. H. *Mater. Sci. Engg.* **1998**, *A254*, 53.
149. Zhang, G. S.; Li, Y. J.; Yan, D. Y. *J. Polym. Sci., Part B: Polym. Phys.* **2004,** *42,* 253.

CHAPTER 2

SCOPE AND OBJECTIVES OF THE PRESENT WORK

2.1 Introduction

Nylons show two crystalline modifications at room temperature, namely the α phase[1] and the γ phase,[2] of which the α phase is most commonly observed at room temperature. In the case of even-even nylons or even nylons the principal phase is the α phase and is consisted of hydrogen-bonded sheets sheared progressively. The chains are in the all-*trans* conformation and the hydrogen bonds are confined to a plane. The γ phase is considered to be a less ordered phase than the α phase and is characteristic of nylons with high methylene content in their chemical repeat units or nylons for which linear hydrogen bonds between adjacent chains cannot be established when an extended conformation is considered (even-odd, odd-even, and odd-odd nylons).

Most nylons show a crystal-to-crystal transition on heating. This phenomenon was first observed in nylon-6,6 by Brill and hence is known as the Brill transition.[3] The room temperature triclinic α phase transforms into a pseudohexagonal phase at elevated temperatures, and the transition is reversible. Murthy et al.[4] suggested enhanced mobility of chains in the crystalline phase during transformation from one crystalline phase to another. The structural changes occurring in the Brill transition phenomenon for a series of nylons -*m,n* and its model compounds have been studied by Tashiro et al.[5-9] using high temperature wide-angle X-ray scattering (HTWAXS) and high temperature Fourier transform infrared spectroscopy (HTFTIR) techniques in combination with the computer simulation method.

Most of the existing studies on the crystalline transitions in nylons have been made on even-even and even nylons. Furthermore, these studies mainly revolved around the α phase. The primary focus of the present thesis is to study the characteristics of the γ phase and its behavior on heating and cooling. To that end three different types of nylons that exhibit the γ phase are chosen, namely, even, odd and even-odd nylons. They are nylon-6, nylon-11, nylon-6,7 and nylon-6,9. All these nylons exhibit the γ phase under appropriate conditions. Interestingly nylon-6, nylon-11 and nylon-6,9 exhibit the α phase as well providing an opportunity to compare the behavior of the α and γ phases under different conditions.

2.2 Objectives of the present work

2.2.1 Crystalline Phases in Nylon-11: Studies using HTWAXS and HTFTIR

Nylon-11 received considerable scientific attention in the odd-nylons group because of its piezoelectric and ferroelectric properties. Nylon-11 exhibits polymorphism, and several researchers[10-17] have studied the polymorphism of nylon-11. Nylon-11 can be crystallized into various polymorphs namely, α, γ and psuedohexagonal phases.

The primary objective of the present work is to study the crystalline transitions exhibited by the various polymorphs of nylon-11. The nylon-11 was crystallized in 1,4-butanediol and trifluoro acetic acid (TFA) to obtain the α and γ phases respectively. The γ phase was also obtained by melt crystallization. The α and γ phases were characterized at room temperature as well as on heating using HTWAXS and HTFTIR.

2.2.2 Studies on the Crystalline Phases of Nylons -6,7 and -6,9

The studies on the crystalline phases of even-odd or odd-even nylons are very scanty. The even-odd nylons present a different crystal structure from even-even nylons resulting in some different properties from even-even nylons.[18-21]

The objective of the present work is to synthesize nylon-6,7 polymer, as it is not available commercially, to explore its crystalline transitions by using HTWAXS and HTFTIR, and to compare the results obtained with a similar even-odd nylon. The studies were carried out on nylon-6,7 crystallized in 1,4-butanediol. We also report the results on the crystallization of nylon-6,7 at high temperature, from the melt state, and the crystalline transitions on cooling from the T_c and then on heating from room temperature to melting. The crystalline transition on heating melt-quenched nylon-6,7 has also been studied. Similar crystalline transition studies were carried out on nylon-6,9 with a chemical repeat unit close to nylon-6,7 using HTWAXS and HTFTIR. The results obtained were compared with that of nylon-6,7.

2.2.3 Studies on the Crystallization Behavior of Nylon-6 in the Presence of Layered Silicates using Variable Temperature WAXS and FTIR

Melt or solution crystallization of nylon-6 gives the α phase. However, the γ phase may be obtained under more severe conditions such as high speed spinning.[22] The α phase can be

transformed into the γ phase by treatment with aqueous potassium iodide–iodine solution.[2,22-24]

Recently, it has been found that the γ phase is readily formed when nylon-6 is melt crystallized in the presence of layered silicates.[25-28] The relative fraction of the α and γ phases is dependent on the content as well as the interaction between nylon-6 and the silicate layers.[29]

Another objective of the present work is to study the characteristics of the γ phase of nylon-6 obtained by melt crystallization in the presence of layered silicates. To that end the crystallization of nylon-6–clay nanocomposite from the melt has been monitored, by using a hot stage coupled to an X-ray diffractometer. The γ phases were obtained by two different routes, viz., melt crystallization of nylon-6 in the nylon-6–clay nanocomposite and the treatment of α phase in KI/I_2 solution, and were compared by HTFTIR.

2.3 References

1. Holmes, D. R.; Bunn, C. W.; Smith, D. J. *J. Polym. Sci*. **1955**, *17*, 159.
2. Arimoto, H.; Ishibashi, M.; Hirai, M.; Chatani, Y. *J. Polym. Sci., Part A:* **1965,** *3*, 317.
3. R. J. Brill, *J. Prakt. Chem.* **1942,** *161*, 49.
4. N. S. Murthy, S. A. Curran, S. M. Aharoni, H. Minor, *Macromolecules* **1991**, *24*, 3215.
5. Y. Yoshioka, K. Tashiro, C. Ramesh, *Polymer* **2003**, *44*, 6407.
6. Y. Yoshioka, K. Tashiro, *J. Phys.Chem. B* **2003**, *107*, 11835.
7. Y. Yoshioka, K. Tashiro, *Polymer* **2003**, *44*, 7007.
8. Y. Yoshioka, K. Tashiro, *Polymer* **2003**, *44*, 4337.
9. Y. Yoshioka, K. Tashiro, *Polymer* **2004**, *45*, 6349.
10. Lee, J. W.**;** Takase, Y.**;** Newman, B. A.**;** Scheinbeim, J. I. *J. Polym Sci., Polym. Phys.* **1991**, *29*, 273.
11. Slichter, W. P. *J. Polym. Sci.* **1959**, *36*, 259.
12. Kinoshita, Y. *Macromol. Chem.* **1959**, *33*, 1.
13. Kawaguchi, A.; Ikawa, T.; Fujiwara, Y.; Tabuchi, M.; Konobe, K. *J. Macromol. Sci. Phys. B* **1981**, *20* (1), 1.

14. Kim, K. G.; Newman, B. A.; Scheinbeim, J. I. *J. Polym. Sci. Polym. Phys. Ed.* **1985**, *23*, 2477.
15. Newman, B. A.; Sham, T. P.; Pae, K. D. *J. Appl. Phys.* **1977**, *48*, 4092.
16. Schmidt, C. F.; Stuart, Z. *Naturforsch* **1958**, *13A*, 222.
17. Sasaki, T. *J. Polym. Sci. Part B: Polym. Lett*. **1965**, *3*, 557.
18. Navarro, E.; Franco, L.; Subirana, J. A.; Puiggalı´, J. *Macromolecules* **1995,** *28,* 8742.
19. Navarro, E.; Subirana, J. A.; Puiggalı´, J. *Polymer* **1997,** 3*8*, 3429.
20. Franco, L.; Cooper, S. J.; Atkins, E. D. T.; Hill, M. J.; Jones, N. A. *J. Polym. Sci., Part B: Polym. Phys.* **1998,** *36,* 1153.
21. Kinoshita, Y. *Makromol. Chem.* **1959,** *33,* 1.
22. Murthy, N. S. *Polym. Commun.* **1991**, *32*, 301.
23. Miyasaka, K.; Makishima, K. *J. Polym. Sci., Part A-1* **1967,** *5*, 3017.
24. Stepaniak, R. F.; Garton, A.; Carlsson, D. J.; Wiles, D. M. *J. Polym. Sci., Polym. Phy. Ed.* **1979,** *17*, 987.
25. Kojima, Y.; Usuki, A.; Kawasumi, M.; Okada, O.; Fukushima, Y.; Kurachi, T.; Kamigaito, O. *J. Mater. Res.* **1993,** *8,* 1185.
26. VanderHart, D. L.; Asano, A.; Gilman, J. W. *Chem. Mater*. **2001**, *13*, 3781.
27. Lincoln, D. M.; Vaia, R. A.; Wang, Z. G.; Hsiao, B. S. *Polymer* **2001**, *42*, 1621.
28. Cho, J. W.; Paul, D. R. *Polymer* **2001**, *42*, 1083.
29. Lincoln, D. M.; Vaia, R. A.; Wang, Z. G.; Hsiao, B. S.; Krishnamoorti, R. *Polymer* **2001,** *42*, 9975.

CHAPTER 3

CRYSTALLINE PHASES IN NYLON-11: STUDIES USING HTWAXS AND HTFTIR

3.1 Introduction

Nylons are important semicrystalline polymers with many useful properties. Among nylons, nylon-6,6 and nylon-6 are commercially successful and have been extensively explored scientifically, while other nylons have received less attention. In the odd-nylons group, nylon-11 received considerable scientific attention because of its piezoelectric and ferroelectric properties. The piezoelectric and ferroelectric properties of nylon-11 have been studied in recent years[1-6] and are thought to originate from the polar structure such as in that of the α phase of odd nylon. Nylon-11 exhibits polymorphism, and several researchers[3,7-13] have studied the polymorphism of nylon-11.

The crystal structure of nylons is dominated by hydrogen bonds; hydrogen bonded sheets are the main feature of nylon structure, and the two strong reflections arise from this feature. The *d* spacings of these reflections at 0.37 and 0.44 nm are due to the inter-sheet distance between the sheets and the projected inter-chain distance within the sheet, respectively. The important feature of nylons is that the structure undergoes a crystalline transition when subjected to heating. The crystalline transition in nylon-6,6 has been well documented and is known as the Brill transition.[14] In nylon-6,6, the room temperature α phase transforms into a pseudohexagonal structure on heating. Crystalline transition is also reported for nylons -4,6,[15] -6,10,[15] and -6,12.[15, 16] Murthy et al.[17] have observed that the room temperature monoclinic structure of nylon-6 transforms into a high temperature monoclinic structure on heating from room temperature and considered it as the Brill transition. The changes observed in the infrared spectra of nylons -6 and -6,6 during heating have been correlated to the Brill transition.[17] Nylon-12 crystallizes[18] into the α phase on crystallization from the melt and transforms into the γ phase on subsequent cooling to room temperature.

Murthy et al.[19] suggested enhanced mobility of chains in the crystalline phase during transformation from one crystalline phase to another. Tashiro and coworkers[20-24] studied the crystalline transitions in nylons by using high temperature wide-angle X-ray scattering (HTWAXS) and high temperature Fourier transform infrared spectroscopy (HTFTIR) techniques in combination with the computer simulation method. Furthermore, they have used model compounds to understand the crystalline transition behavior in nylons. In the Brill transition region, the methylene segments are conformationally disordered with an invasion of gauche bonds, and the effective lengths of *trans*-zigzag methylene parts

become shorter. This information was obtained on the basis of systematic assignments of the infrared spectra observed for a series of nylons and their model compounds. The triclinic packing structure is kept in average, but it approaches gradually to the pseudohexagonal packing mode, as proved by the molecular dynamics calculations.

Nylon-11 exhibits five crystalline modifications, including the α phase, resulting from annealing of the quenched polymer[7-9] or solution casting from m-cresol,[10] the α' phase obtained from melt crystallization,[10] the pseudohexagonal phase obtained above room temperature by heating the α' phase,[11] smectic, or δ' phase obtained by melt quenching,[12] and the γ phase obtained by solution casting from trifluoro acetic acid (TFA).[13] Zhang et al. have studied the crystal form transitions of nylon-11 at different drawing temperatures with different drawing ratios.[25] The crystal structure of the α phase obtained by casting from *m*-cresol and lamellar crystals grown from glycerine[9] is triclinic,[8] the amide groups lie in a plane tilted to the chain axis, and the structure is similar to nylon-6,6.[26] In the α phase of nylon-6,6, the hydrogen bonds are formed between the parallel chains. A monoclinic cell similar to that of nylon-6 is also suggested[10] for nylon-11 grown from the solution in water containing 5% formic acid at 160 °C. In the monoclinic structure of nylon-6, the hydrogen bonds are formed between antiparallel chains. These authors also observed another form similar to the γ phase of nylon-6.

Variable temperature wide-angle X-ray scattering (WAXS) is perhaps one of the most appropriate tools to study the crystalline phases and their transitions. In the present chapter, we report the results of the detailed study made on the polymorphism of nylon-11. For the first time, we prepared the various crystalline forms of nylon-11 by different procedures and followed the crystalline transitions *in situ* by using a hot stage attached to an X-ray diffractometer. Furthermore, for the first time, we observed, in the case of nylon-11, the distinct changes in the *d* spacing of the 001 reflection during crystalline transition in the case of certain phases. Also, for the first time, we examined the FTIR spectra of the various phases at room temperature and on heating and correlated it with the HTWAXS data.

3.2 Experimental Section

Nylon-11 pellets were obtained from Aldrich, USA. The η_{inh} for the nylon-11 pellets measured at 30 ^{o}C in an automated Schott Gerate AVS 350 viscometer, using an

Ubbelohde suspended level viscometer in concentrated H_2SO_4 (98%) at a polymer concentration of 0.5% was 0.67 dl/g.

Nylon-11 was crystallized in the α phase by dissolving nylon-11 pellets in 1,4-butanediol at its refluxing temperature. On cooling very gradually to room temperature, the nylon-11 formed a precipitate, which was filtered and washed repeatedly in acetone to remove the 1,4-butanediol. This procedure gave a highly crystalline α phase in the form of fine powder. This powder was used for WAXS studies on the α phase of nylon-11. Room temperature WAXS pattern showed that the sample crystallized fully into α phase, and the crystallinity obtained by profile fitting of the peaks was 57%.

The X-ray diffraction experiments (XRD) experiments were performed using a Rigaku Dmax 2500 diffractometer with a copper target. The system consists of a rotating anode generator with a copper target and a wide-angle powder goniometer having a diffracted beam graphite monochromator, fitted with a high-temperature attachment. The generator was operated at 40 kV and 150 mA. All the experiments were performed in the reflection mode. The samples were scanned between 2θ = 5 to 30° at a scan speed of 2°/min. The sample holder was a copper block, and the nylon-11 powder in the α phase was pressed on the block. The diffraction pattern was collected while the sample temperature was held constant. The change in the diffraction pattern was monitored during heating by scanning at regular temperature intervals until the sample melted. To avoid degradation, the sample was kept under vacuum during experiment. The positions of the peaks were fixed by deconvoluting the peaks by profile fitting, using Rigaku multipeak separation software available with the diffractometer system.

For melt crystallization studies, a thin film of nylon-11 was formed on the copper block by melt pressing the sample. The sample was heated well above the melting temperature (T_m) and then cooled to 175 °C, the crystallization temperature (T_c). It was cooled/heated at the rate of 20 °C /min, and when the sample temperature reached within 20 °C of the required set temperature, the cooling/heating rate was automatically reduced to 2 °C/min to minimize the over shooting of the set temperature. The temperature was maintained within 1 °C of the set temperature thereafter. The development of crystalline structure during the isothermal crystallization process was studied by scanning at regular time intervals. After the crystallization was completed, the sample was cooled to room temperature and

scanned at different temperatures during cooling, and the change in crystal structure was monitored. The sample was again heated to melting, and the data were acquired at regular temperature intervals. In another experiment, a thin nylon-11 melt was formed on the copper sample holder and quenched in ice. During this procedure, it was made sure that ice or water was not allowed to get in contact with the nylon-11 sample. The melt-quenched nylon-11 sample was loaded in the X-ray hot stage and heated to melting, and the diffraction patterns were acquired at regular temperature intervals. In a few cases, instead of heating the sample to melt, the heating was stopped at a certain temperature and the sample was cooled back to room temperature.

Nylon-11 film was also cast from TFA. The film was stuck in the copper sample holder and heated to melting, and the diffraction patterns were acquired at regular temperature intervals. In one experiment, the heating was stopped at 150 °C and the sample was cooled back to room temperature.

Room temperature and high temperature infrared spectra of these samples were taken using a Perkin-Elmer FTIR Spectrometer (model: Spectrum GX) with a deuterated triglycine sulfate (DTGS) detector at a resolution of 2 cm^{-1} in the range of 400–4500 cm^{-1}. A total of 32 scans were used for signal averaging. The high temperature spectra were obtained by mounting the sample in the Mettler Toledo FP82HT hot stage and placing it in the sample compartment of the FTIR. The sample, in the form of powder, was sandwiched in the KBr pellet. The sample was heated at the rate of 5 ^{o}C/min. The spectra were collected while the sample temperature was held constant. The change in spectra was monitored during heating by scanning at regular temperature intervals until the sample melted. The selected regions of the spectra were profile-fitted by using Peakfit (Jandell) profile fitting program, and the profiles were assumed to be Gaussian. In the case of TFA-cast film, the film was initially heated to 120 ^{o}C to remove the residual TFA solvent from the film and then cooled to room temperature before starting the experiment.

The melting behavior of the various samples was analyzed by using a TA Instruments Q10 calorimeter. The sample weight was about 5 mg, and the heating rate was 10 °C/min. The calorimeter was calibrated using the standard protocol. The samples were scanned from 0 °C to 250 °C.

3.3 Results and Discussion

The calorimetric data on the nylon-11 samples will be presented first. Figure 3.1 shows the thermograms obtained during the first heating of nylon-11 samples crystallized by various techniques. The melt-crystallized, and 1,4-butanediol crystallized samples show T_m at 184 °C. The sample cast from TFA has a lower melting point at 181 °C. Apart from the melting endotherm, the 1,4-butanediol crystallized sample and the TFA-cast film show a broad endotherm at about 100 °C arising from the solvent retained in the samples even

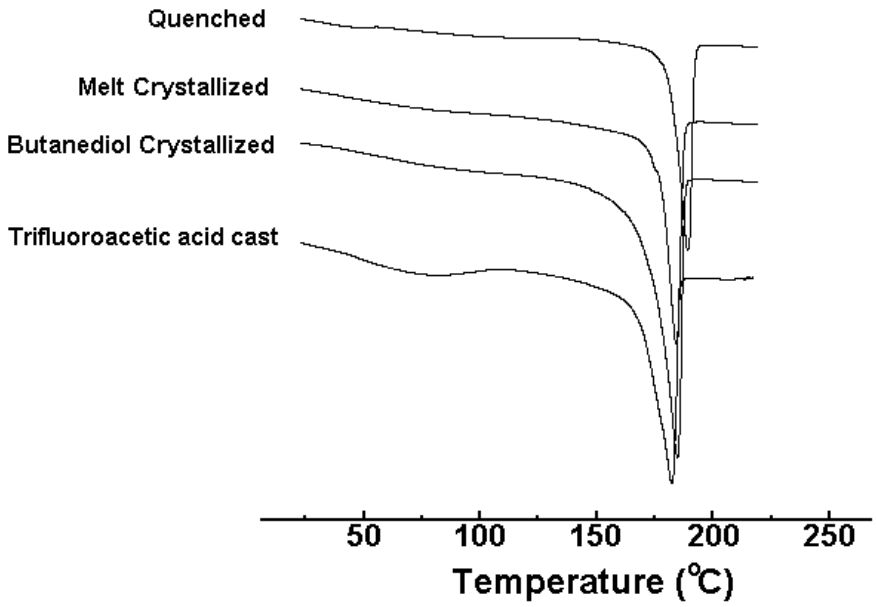

Figure 3.1: The DSC thermograms obtained during the first heating for 1,4-butanediol crystallized, melt-crystallized, quenched and TFA-cast nylon-11.

after drying in the vacuum oven at 30 °C overnight. TGA studies on the TFA-cast film showed the presence of about 5% solvent in the film. The melt-quenched sample does not exhibit crystallization exotherm, indicating that the sample crystallized despite rapid quenching. Interestingly, the quenched sample shows a higher T_m than the other samples and melts at 189 °C. In general, these thermograms do not exhibit any thermal event before melting.

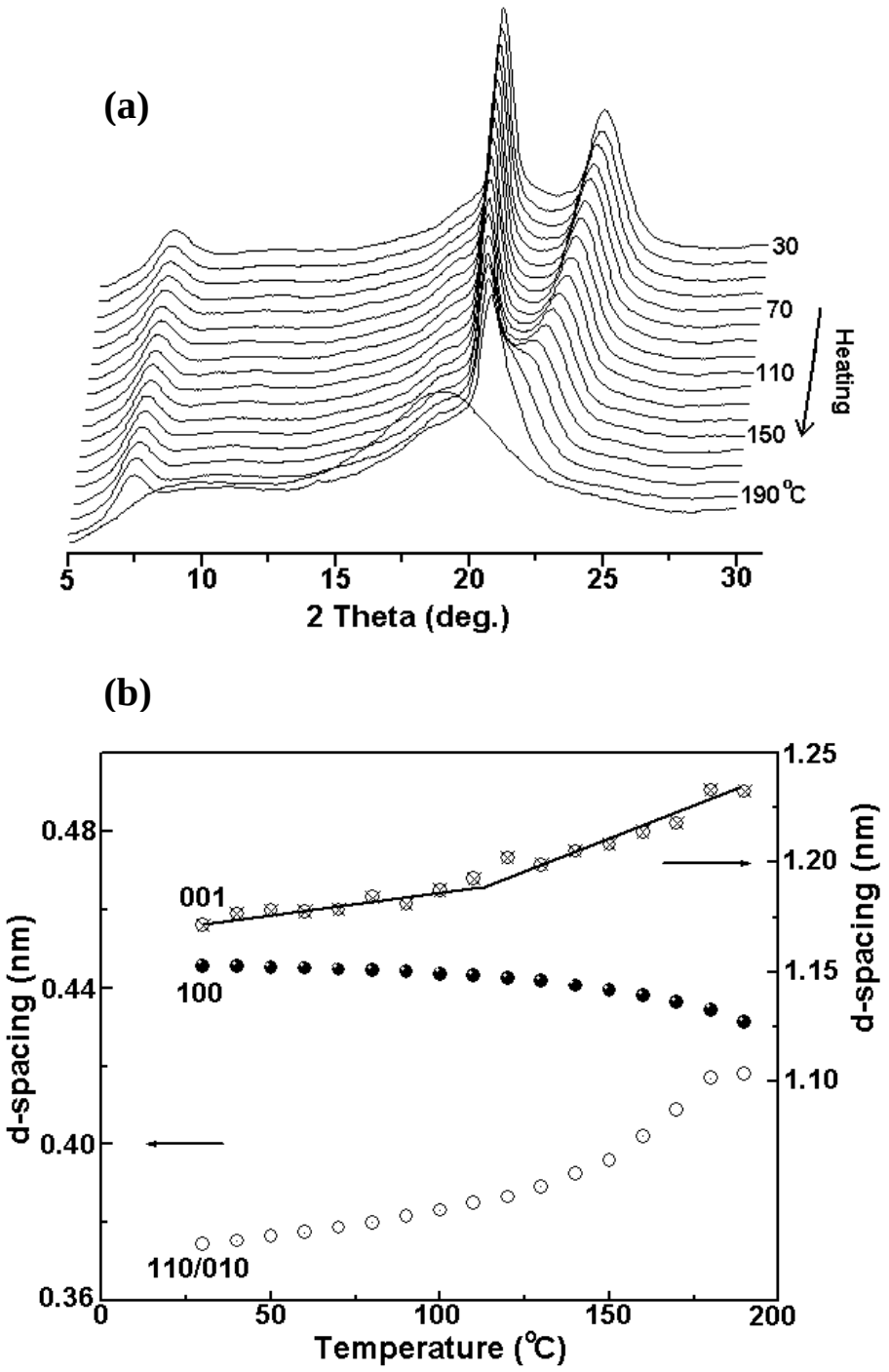

Figure 3.2: Behavior of (a) XRD patterns and (b) *d* spacings on heating from room temperature to melt for the α phase of nylon-11 crystallized in 1,4-butanediol.

The room temperature diffraction pattern of the nylon-11 sample crystallized in 1,4-butanediol shows the characteristic reflections of nylons at 2θ = 19.92 and 23.74°. The corresponding *d* spacings are 0.445 and 0.374 nm, respectively. These reflections may be indexed as 100 and 110/010 based on the α phase having a triclinic unit cell proposed by

Slichter[7], Kawaguchi et al.,[9] and Kim et al.[10] The *d* spacings 0.445 and 0.374 nm correlate to the projected inter-chain distance within the sheet and the inter-sheet distance between the sheets respectively. The 001 reflection occurs at 2θ = 7.54°, corresponding to a *d* spacing of 1.171 nm. The α phase may also be obtained by treating nylon-11 in glycerine at 160 °C[9] or by casting from *m*-cresol.[10] The behavior of the diffractograms and the *d* spacings of the α phase on heating from room temperature to melt is shown in Figure 3.2a and b, respectively. It is seen from the Figure 3.2 that, on heating, the two-peak nature of the diffractogram is preserved until melting. The change in the *d* spacings of 100 and 110/010 reflections with increase in temperature is reminiscent of the behavior of *d* spacings in the even-even nylons such as nylon-6,6, nylon-6,10, and nylon-6,12. The *d* spacing of the 110/010 reflection shows a rapid increase after 110 °C and approaches the 100 reflection, indicating the transformation of the α phase into the pseudohexagonal phase. However, the transformation is not fully completed before melting. Indeed, Tashiro and co-workers[20-24] have shown that the Brill transition does not occur at only one temperature point but it occurs over a temperature region. Another notable feature of the nylon-11 α phase is the behavior of the 001 peak on heating, as shown in Figure 3.2b. The *d* spacing of the 001 reflection increases with increase in temperature; the increase is more rapid at about 110 °C, similar to the *d* spacing of 110/010 reflections. In general, with an increase in temperature, a small decrease in the 001 reflection *d* spacing is expected because of the enhanced motion of the methylene segments.[20,21] The higher mobility of the methylene segments is a general feature of all nylons at elevated temperatures.[20,21] In the present case, the increase in the *d* spacing of the 001 reflection with an increase in temperature may be attributed to the decrease in the angle made by the normal of the 001 plane to the *c* axis. The variations in diffraction patterns and *d* spacings on heating from room temperature are found to be reversible if the sample is not allowed to melt, but held at temperatures below the T_m and then cooled to room temperature.

The behavior of the diffractograms and *d* spacings of the melt-crystallized sample is different from the sample crystallized from the 1,4-butanediol solution described above. The diffraction patterns obtained during isothermal melt crystallization of nylon-11 at 175 °C are shown in Figure 3.3a. The initially amorphous sample slowly crystallizes, and the diffraction pattern shows the development of crystalline peaks at 2θ = 6.93° and 20.69° with an increase in time. The corresponding *d* spacings are 1.274 and 0.429 nm. The

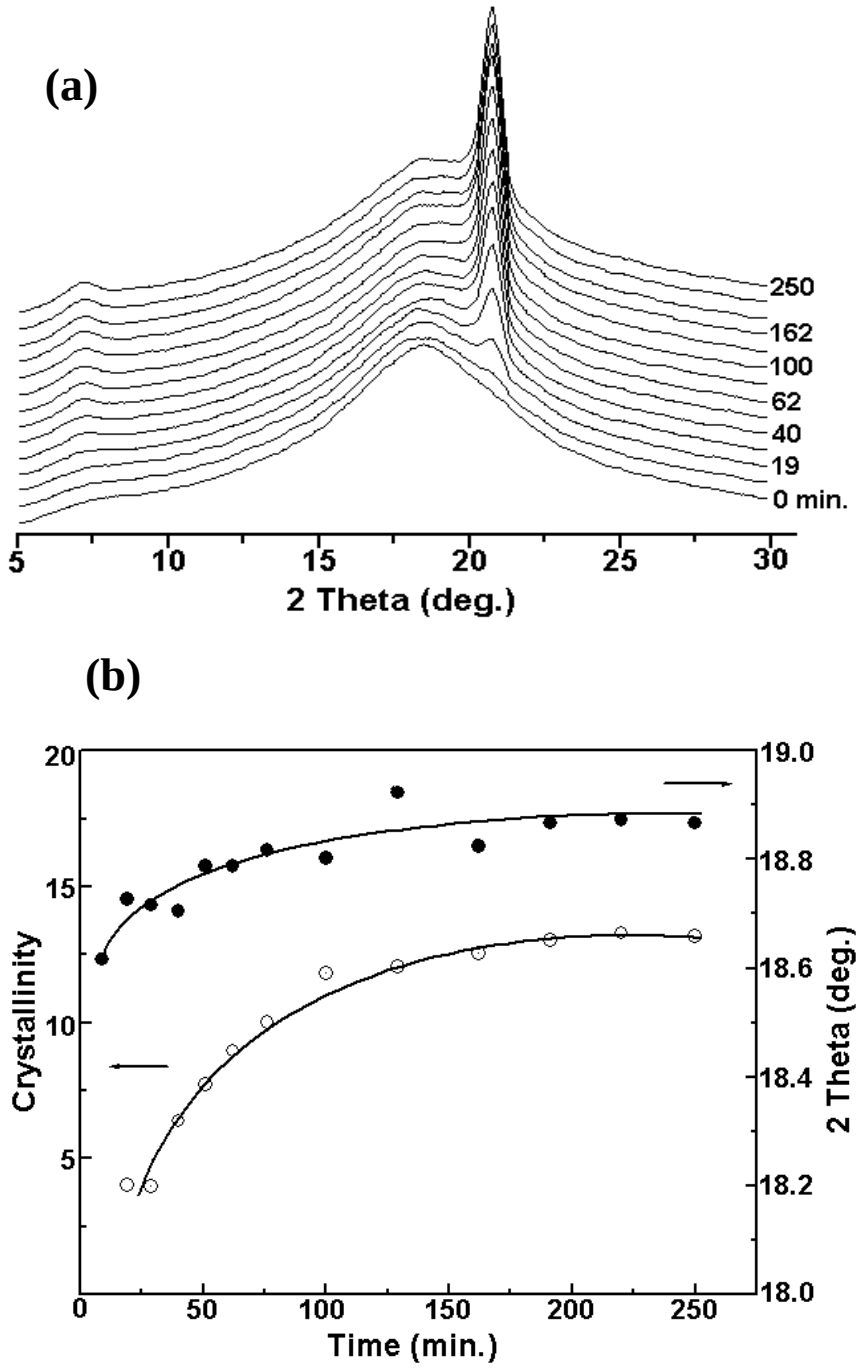

Figure 3.3: (a) Isothermal crystallization behavior for nylon-11 at 175 ^{o}C. (b) Degree of crystallinity and the variation of amorphous peak position during isothermal crystallization at 175 ^{o}C.

reflection at 2θ = 6.93° arises from the chain repeat unit and may be indexed to the 001 reflection. The *d* spacing value, 1.274 nm, which is much lower than the extended chain length of 1.5 nm, indicates that, in the melt crystallization also, the normal of 001 plane is tilted with respect to the *c* axis. Hence, the single single peak at 2θ = 20.69° indicates that the sample crystallized in the pseudohexagonal phase like nylon-6,6[14, 27] at 175 °C.

During isothermal crystallization, the degree of crystallinity increases with increase in crystallization time, and after about 3 h, it remains almost constant even with a further increase in crystallization time, as shown in Figure 3.3b. The figure also shows the shift in the amorphous peak position to higher angles with an increase in crystallization time. This indicates the densification of the amorphous region with an increase in crystallinity. Hence, caution should be exercised when assuming amorphous phase density for the quantitative determination of crystallinity using density techniques.

The behavior of the diffractograms and the *d* spacings on cooling from T_c to room temperature is shown in Figure 3.4a and b, respectively. It is seen from the Figure 3.4a that, on cooling from the T_c, the single-peak nature of the diffractogram is preserved and the *d* spacings of the pseudohexagonal phase show small decreases with further decrease in temperature. However, two new peaks at $2\theta = 20.89^o$ and 21.94° appear at about 100 ^{o}C. These peaks become prominent and separate out with further decrease in temperature, and concomitantly, the peak due to the pseudohexagonal phase decreases. This indicates a crystalline transition of the pseudohexagonal phase at about 100 °C. At room temperature, these new peaks appear at $2\theta = 20.17°$ and 23.13°, and the corresponding *d* spacings are 0.440 and 0.384 nm. The 001 reflection now occurs at $2\theta = 7.20^o$, and the corresponding *d* spacing is 1.227 nm. These *d* spacings at room temperature are different from the *d* spacings of the α phase discussed above. Furthermore, the behavior of the diffractograms with temperature is different from that of the α phase. Hence, we designate this phase as the α' phase[10] to distinguish it from the α phase obtained by crystallizing in 1,4-butanediol. The pseudohexagonal phase peak is not obvious in the diffraction pattern below 70 °C; however, the profile fitting of the peaks clearly shows the presence of the pseudohexagonal phase peak even at room temperature. At room temperature, the pseudohexagonal phase fraction is about 4% and that of the α' phase is about 46%. In the temperature range 30–100 °C, the peak at $2\theta = 6.93°$ is attributed only to the α' phase because the amount of the pseudohexagonal phase is too low to identify the position of the 001 reflection. The peak at $2\theta = 6.93°$, which is due to the 001 reflection, shows interesting behavior and is shown in Figure 3.4b. The *d* spacing of this reflection remains constant in the pseudohexagonal phase, but starts to decrease after its transformation to the α' phase at 100 °C. The variations in diffraction patterns and *d* spacings on cooling from

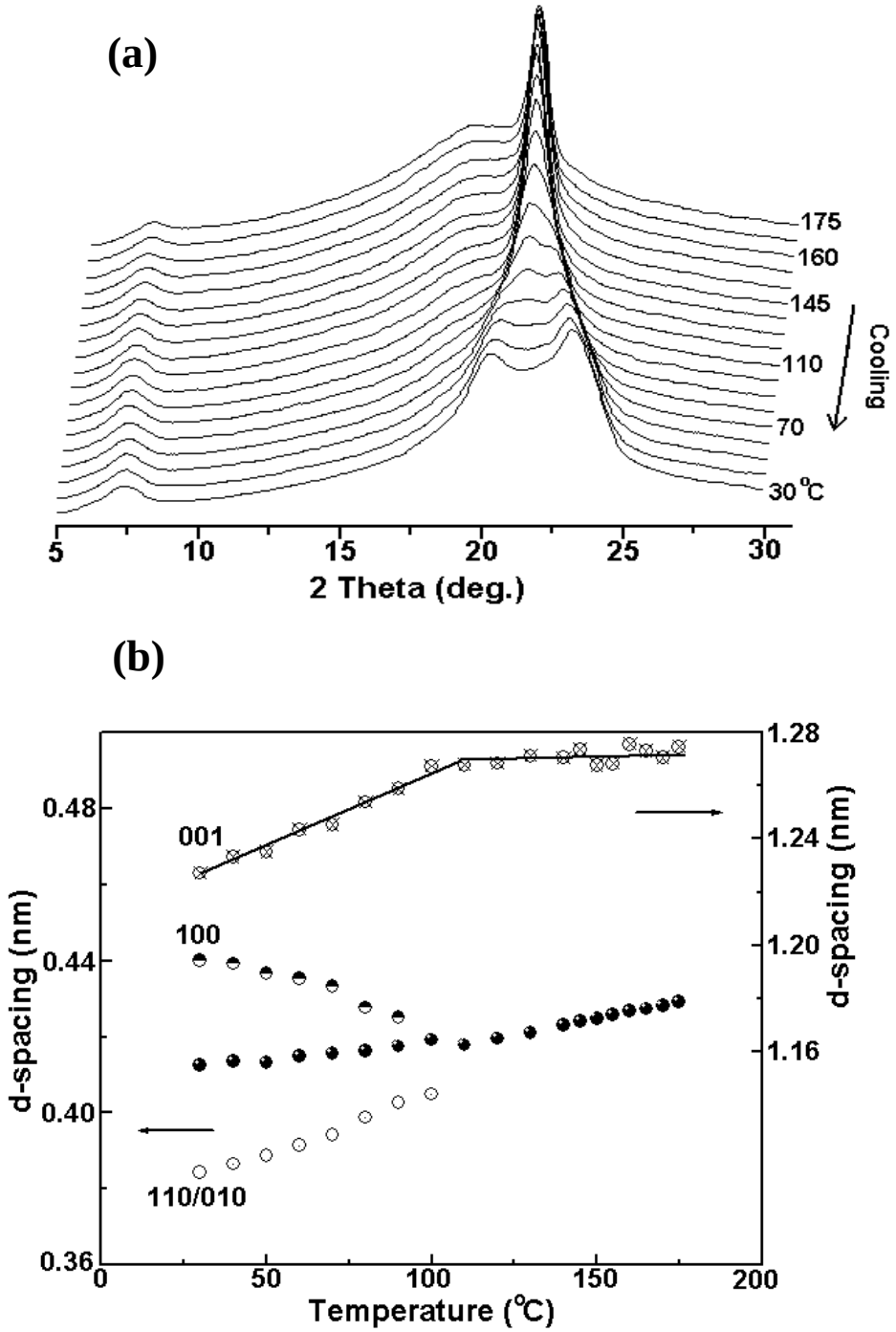

Figure 3.4: Behavior of (a) XRD patterns and (b) *d* spacings of nylon-11 melt-crystallized at 175 °C on cooling to room temperature.

the T_c are found to be reversible on heating the sample from room temperature to melting. However, a small shift in the transition temperature is noted between the cooling and heating cycle and is more clearly seen in the plot of the *d* spacing of the 001 reflection, shown in Figure 3.5. The transition temperature occurs at 100 °C on cooling and at 120

°C on heating. Such a hysteresis in the transition temperature is shown for nylon-6,6 and is indicative of first order transition.[27]

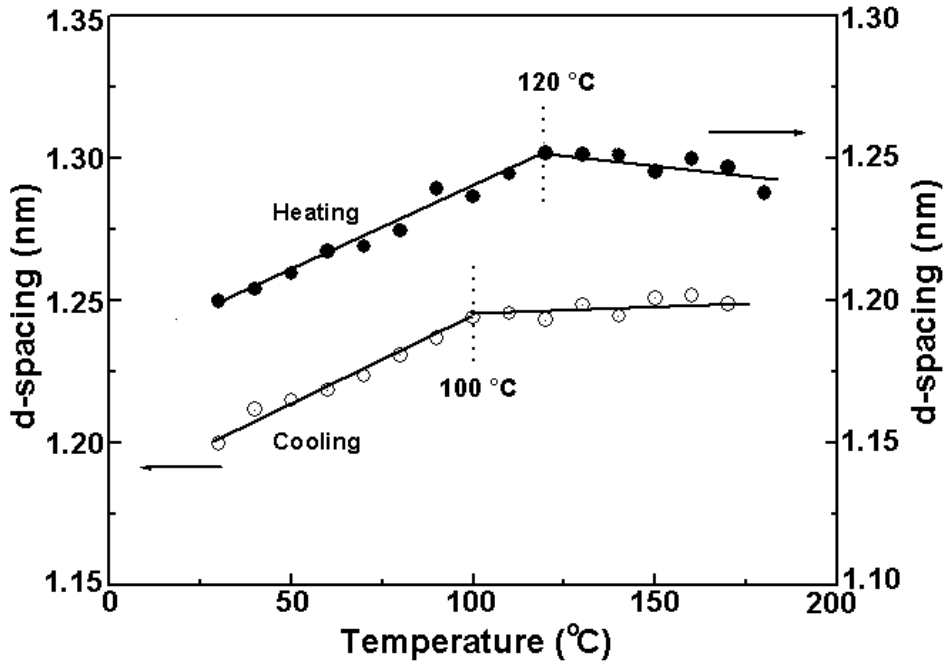

Figure 3.5: Behavior of the *d* spacings of the 001 reflection on cooling from T_c to room temperature and on heating from room temperature to melting.

Another phase reported for nylon-11 is the smectic phase or the δ' phase and is obtained by rapidly quenching the melt. Parts a and b of Figure 3.6 show diffractograms and *d* spacings of the melt-quenched sample on heating from room temperature. The room temperature diffractogram looks very broad, similar to the amorphous material, but the definite peak at 2θ = 7.11° arising from the 001 reflection shows that the material is indeed crystalline. Profile fitting the broad peak brings the crystalline peak at 2θ = 21.43°. On heating, the single peak at 2θ = 21.43° becomes sharper and shifts to lower angles, and the single-peak nature is preserved till melting. The position of the peak at 2θ = 7.11° does not vary with heating. These results indicate that the δ' phase progressively transforms into the pseudohexagonal phase, as discussed earlier in the text. Alternatively, it may be thought of that the smectic phase or the δ' phase is indeed the pseudohexagonal phase with highly defective crystals, and on heating, these crystals become more perfect. A similar behavior is also exhibited by rapidly quenched nylon-6,10.[28]

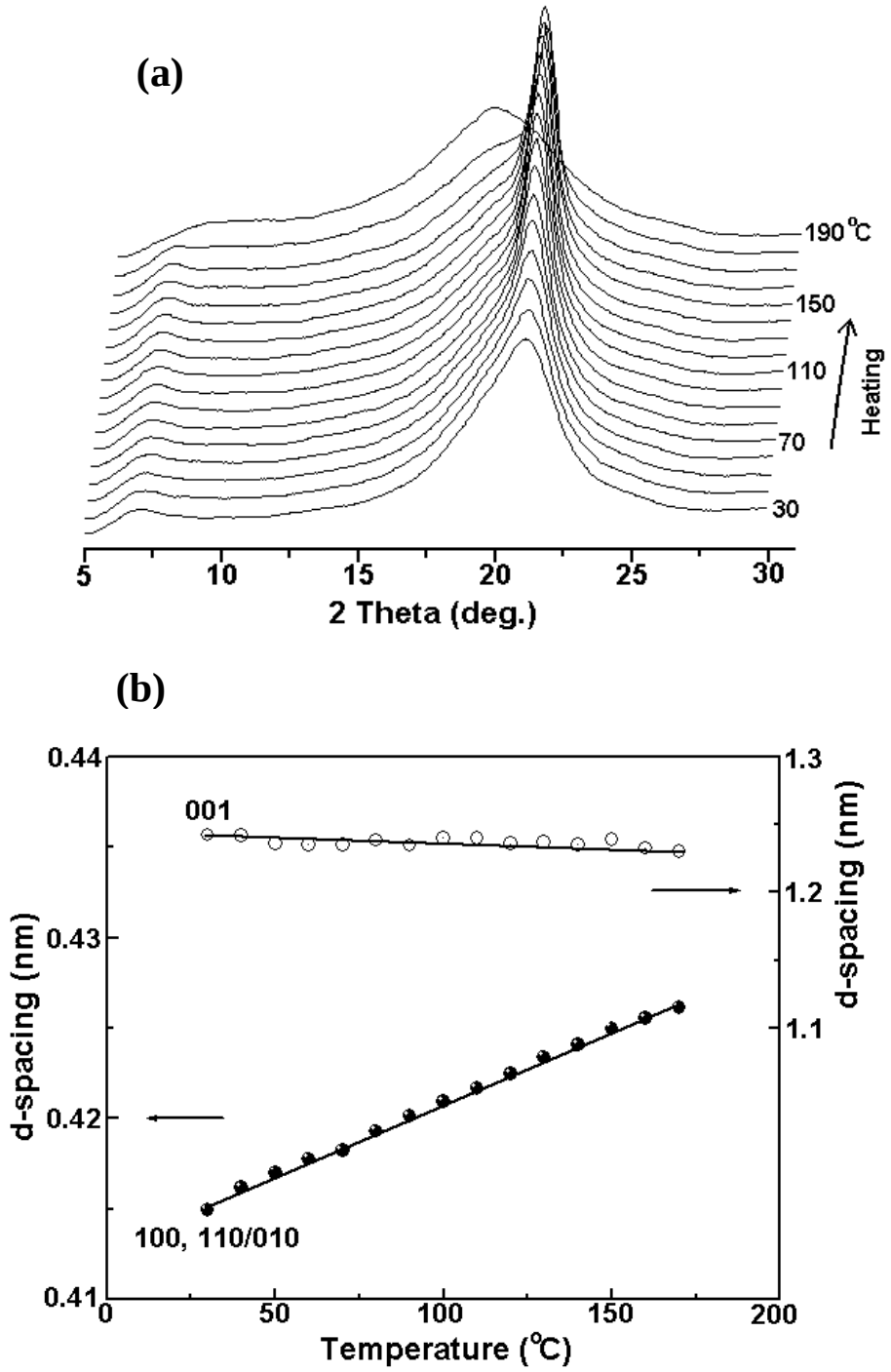

Figure 3.6: Behavior of (a) XRD patterns and (b) *d* spacings on heating from room temperature to melt for quenched nylon-11.

The behavior of the sample is different, however, if it is not allowed to melt but held at temperatures below the T_m and then cooled to room temperature. The diffractograms obtained on cooling from the holding temperature 170 °C show that the pseudohexagonal structure transformed into the α' phase by the appearance of its characteristic peaks at

Table 3.1: Crystallization/Holding Temperature (T_c) and Transition Temperature (T_B) of Nylon-11

T_c (°C)	T_B (°C)	T_c - T_B (°C)
175*	100	75
170	100	70
150	80	70
120	70	50

* Melt-crystallized sample. Others are melt-quenched and heated to the respective temperatures. The cooling rate of the hot stage is too limiting to study the crystallization behavior of the samples below 175 ^{o}C as the sample crystallizes very rapidly before reaching the intended T_c.

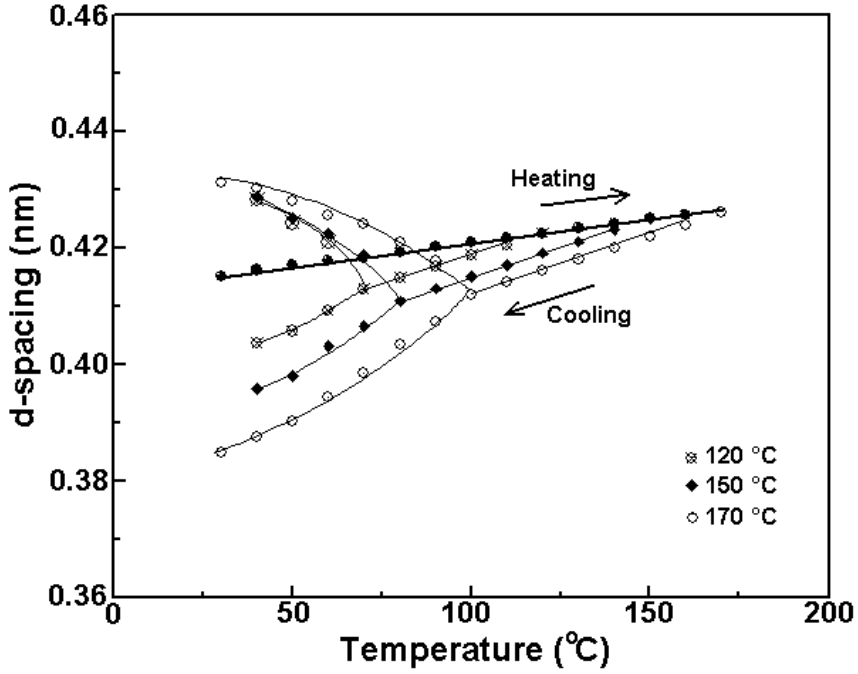

Figure 3.7: The behavior of the *d* spacings of the melt-quenched sample on heating to 170 °C and on cooling from the holding temperatures 170 °C, 150 °C and 120 °C to room temperature. The arrows indicate the direction of heating/cooling.

about 100 °C. However, in this sample, the pseudohexagonal phase is not very obvious below 100 °C, as in the case of the melt-crystallized sample at 175 °C, and hence, it is not

considered during the profile fitting procedure. A similar behavior is observed for holding temperatures 150 °C and 120 °C; however, the transition temperature shifts to lower temperatures. For holding temperatures below 100 °C, the peaks could not reliably be separated; the peaks show broadening on cooling. Table 1 shows the holding temperatures and the corresponding transition temperatures. Another important point to be noted is that on cooling from 170 to 100 °C, the characteristic *d* spacing of the pseudohexagonal phase does not retrace the *d* spacing obtained on heating, as shown in Figure 3.7. Instead, the *d* spacings on cooling depend on the T_c, and such a behavior is different from the behavior of nylons -6,6[27] and -6,10.[15] Furthermore, the observed difference in the *d* spacings of the pseudohexagonal phase at a given temperature depending on whether the temperature is approached on heating the quenched sample or on cooling from the holding temperatures, indicates that there exists a subtle difference in the pseudohexagonal phase during heating and cooling.

The nylon-11 cast from TFA exhibits the γ phase and appears similar to the γ phase of nylon-6 obtained by treating in KI/I_2 solution, and the room temperature diffraction pattern can be seen in Figure 3.8a. The γ phase may also be obtained by exposing melt-crystallized sample in 10% sodium hydroxide solution.[29] Though at room temperature the diffractogram appears to have a single peak at $2\theta = 21.34^o$, the profile fitting procedure clearly indicates the presence of a shoulder at $2\theta = 21.87^o$. The corresponding *d* spacings of these reflections are 0.416 and 0.406 nm, respectively. The peak due to the 001 reflection is seen at $2\theta = 5.91°$, and the *d* spacing is 1.495 nm. Because the fully extended repeat unit of nylon-11 is 1.5 nm, in the γ phase, the chain axis coincides with the *c*-axis of the unit cell. Although the detailed structure of the γ phase is not available in the literature, it can be thought of as monoclinic, but it is different from the monoclinic structure of form II discussed by Kawaguchi et al.[9] The changes in the diffraction pattern and the *d* spacings during heating from room temperature to melting are shown in Figure 3.8a and b. On heating, the peak at $2\theta = 21.87^o$ moves closer to the peak at $2\theta = 21.34^o$ and merges into a single peak at about 110 ^{o}C. On further heating, the single peak remains as a single peak until melting. Concomitantly the 001 reflection shows a small decrease in its d-spacing. These data indicate that the γ phase transforms into a pseudohexagonal phase at 110 ^{o}C, which is distinctly different from the pseudohexagonal phase discussed earlier based on the 001 *d* spacings.

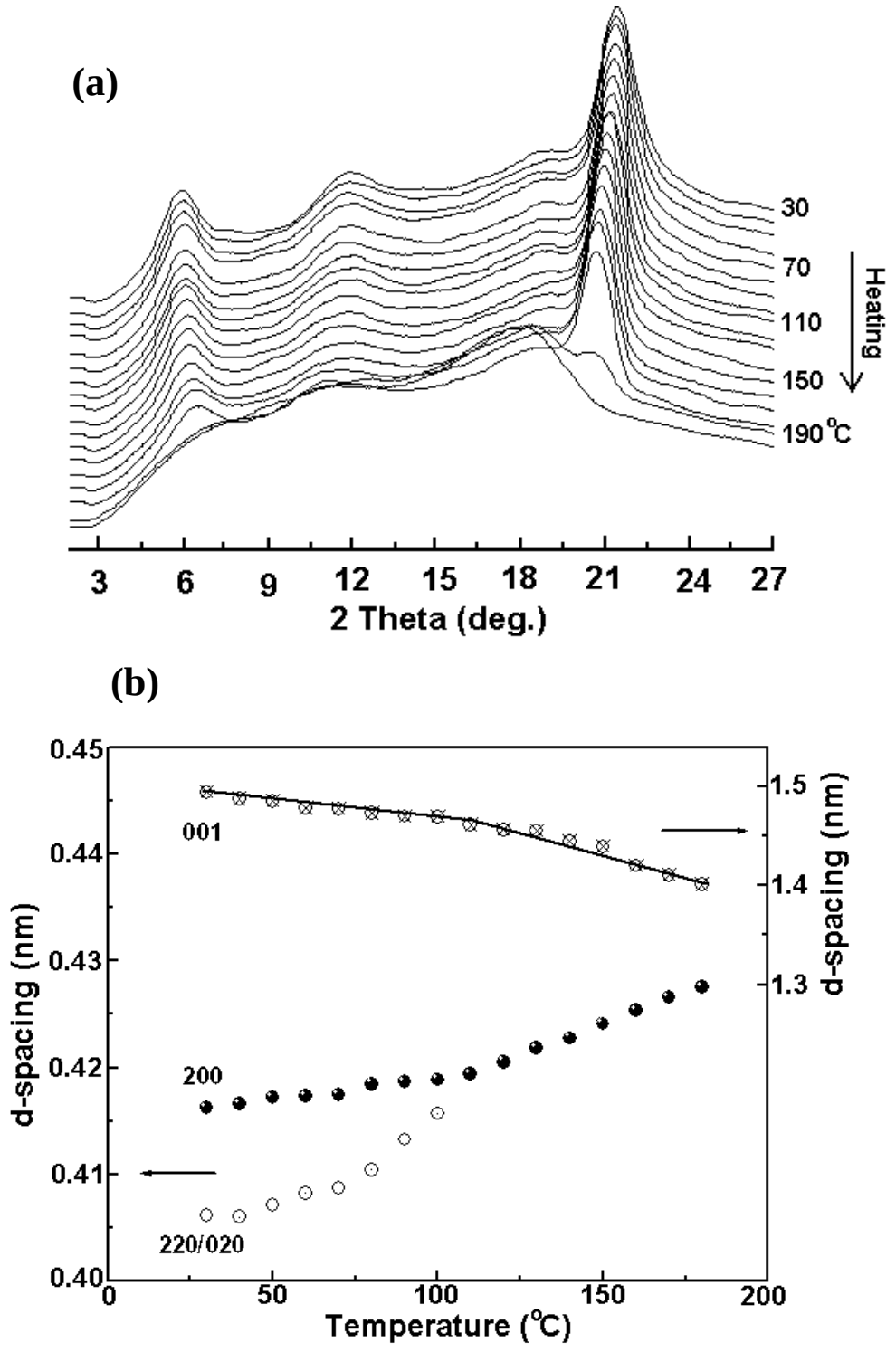

Figure 3.8: Behavior of (a) XRD patterns and (b) *d* spacings on heating from room temperature to melt for γ phase obtained by casting nylon-11 film from TFA. The indexing is based on *c* axis along the chain direction.

It is evident from the Figure 3.8 that the γ phase transforms into the pseudohexagonal phase at about 110 ^{o}C on heating and remains in the pseudohexagonal phase until melting.

Above 110 °C, the *d* spacing of the pseudohexagonal phase increases with increase in temperature. If the pseudohexagonal phase is not allowed to melt, but held at temperatures below the T_m and then cooled to room temperature, it transforms back into the γ phase at about 90 °C. The room temperature diffraction pattern of the γ phase, as obtained immediately after casting from the TFA, and the diffraction pattern taken at room temperature after heating to 150 °C appear very similar, indicating that the transformation is reversible. On heating, the 001 reflection shows a minor shift to a higher angle side, indicating a decrease in the *d* spacing. The *d* spacing of the 001 reflection and the change at the γ phase to pseudohexagonal phase transition at 110 °C is shown in Figure 3.8b.

The foregoing discussions indicate that nylon-11 exists in the pseudohexagonal phase at temperatures above 110 °C; however, 001 *d* spacing and its variation with temperature depends on the starting phase. It also means that the pseudohexagonal phase obtained from the different phases has a different packing mode. This is the first report on pseudohexagonal phases having different types of packing in a single nylon.

The forgoing discussions are primarily focused on the structure based on the data obtained from variable temperature WAXS studies, and in the following section, the discussion will be focused on the data obtained from variable temperature FTIR studies on the various phases of nylon-11. WAXS is sensitive to the changes in the unit cell, while FTIR is sensitive to conformational changes. FTIR spectra of nylons are well documented in the literature[30] and have four important regions. The region 500–800 cm^{-1} comprises two bands specific for the known nylon polymorphism[31], the amide V (N–H out-of-plane bending) and amide VI (C=O out-of-plane bending) bands. The 1000–1400 cm^{-1} region contains the so-called progression bands and is sensitive to the methylene segments. The region 1500–1700 cm^{-1} contains the amide I (C=O stretching) and amide II (C–N stretching and CO–N–H bending) bands. The amide A band occurs at about 3300 cm^{-1} and is assigned to the hydrogen-bonded N–H stretching vibration and is sensitive to the strength of the hydrogen bond.

Figure 3.9a-c shows the spectral region from 500 to 800 cm^{-1} for the various phases and comprises the amide V and amide VI bands. At room temperature the amide V and amide VI bands appear at 686 and 582 cm^{-1} respectively for the α phase (1,4-butanediol

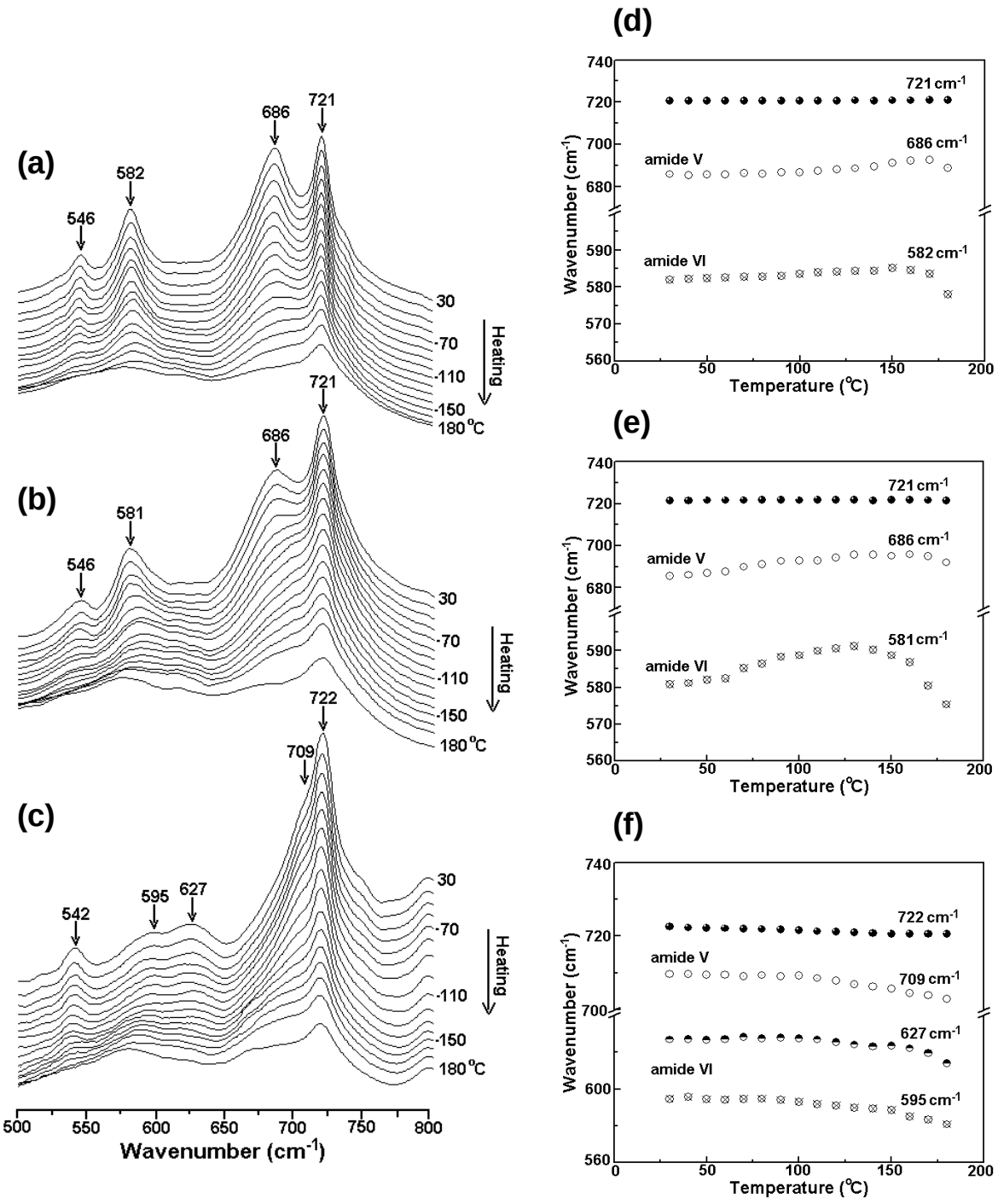

Figure 3.9: Variable temperature FTIR spectra of the region 500–800 cm^{-1} of nylon-11 during heating from room temperature to melt: (a) α phase (1,4-butanediol crystallized), (b) α' phase (melt-crystallized), and (c) γ phase obtained by casting in TFA. The variation of the wavenumber of amide V and amide VI bands during heating for (d) α phase, (e) α' phase, and (f) γ phase.

crystallized sample). These bands appear at 686 and 581 cm^{-1} for the α' phase (melt-crystallized sample). The amide V band shifts from 686 cm^{-1} to 709 cm^{-1} for the γ phase

(TFA-cast film). Furthermore in the case of the γ phase the amide VI band is shifted[31] from 582 cm^{-1} to 627 cm^{-1}. Similar to the γ phase of nylon-6[32] the spectra show a distinct additional band at 595 cm^{-1}, which is characteristic of the γ phase[32]. The variation of amide V and amide VI band positions on heating for α, α' and γ phases is shown in Figure 3.9d-f. On heating, the wavenumber of amide V band of the α phase remains constant up to 130 °C and then increases on further heating. However, close to the T_m the wavenumber starts to decrease. The α' phase also shows slightly different behavior; the wavenumber increases initially but above 120 °C it remains constant and towards the melting temperature it decreases. It may be pointed out here that the α' phase transforms into the pseudohexagonal phase at about 120 °C. In the γ phase, on the other hand, the wavenumber remains constant up to 100 °C and then it starts to decrease when the γ phase transforms into the pseudohexagonal phase. The amide VI band at 582 cm^{-1} in the case of the α phase, does not change position during heating but decreases towards the T_m. The amide VI band of the α' phase shows a behavior similar to the amide V band. On the other hand the amide VI bands at 595 and 627 cm^{-1} for the γ phase show a decrease with increasing temperature. The methylene rocking mode band at 721 cm^{-1} appears to be invariant towards heating for all the phases.

Another region of interest is from 1100 to 1400 cm^{-1} and is characterized by the progression bands from the methylene sequence. Figure 3.10a-c shows this region and the bands appear at 1126, 1159, 1190, 1223, 1240, 1279 and 1373 cm^{-1} for the α phase at room temperature. These bands appear essentially at the same position for the α' phase. These bands however appear at different position for the γ phase and occur at 1123, 1160, 1198, 1225, 1250, 1279 and 1371 cm^{-1} respectively. Upon heating almost all these bands show minor shift in position and decrease in absorbance but the major difference is observed between the α and γ phases. The 1160 and 1198 cm^{-1} bands are assigned to T_{10} and T_9 (CH_2 twisting) respectively and the 1190 cm^{-1} band arises from W_1 (CH_2 wagging).[30] Figure 3.10d-f depicts the variation of the band position and absorbance for various samples. In the case of the α phase the 1160 cm^{-1} shows a small shift towards the lower wavenumber with heating. The 1190 cm^{-1} band shifts to higher wavenumber with increase in temperature and the increment is more obvious above 120 °C. The absorbance decreases with increasing temperature for these bands and again the decrease is more prominent above 120 °C. The behavior of these bands shows minor variation for the α'

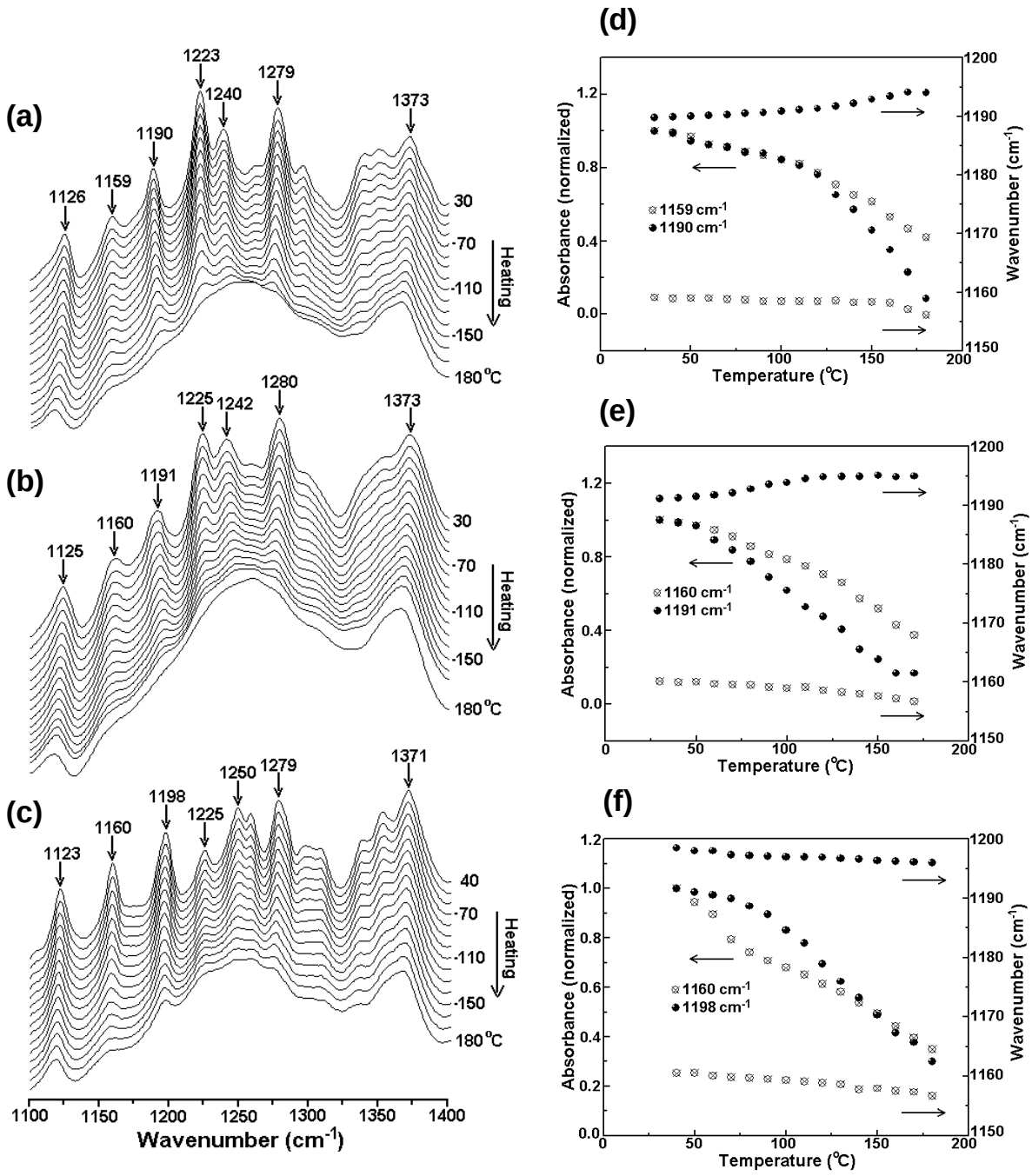

Figure 3.10: Variable temperature FTIR spectra of the region 1100–1400 cm^{-1} of nylon-11 during heating from room temperature to melt: (a) α phase, (b) α' phase, and (c) γ phase. The variation of the wavenumber and normalized absorbance of bands 1160 and 1190 cm^{-1} during heating for (d) α phase, and (e) α' phase. (f) The variation of the wavenumber and normalized absorbance of bands 1160 and 1198 cm^{-1} during heating for γ phase.

phase. The 1160 cm^{-1} band position decreases with increase in temperature and is similar to the behavior of this band in the α phase. The 1190 cm^{-1} band also increases with increasing temperature initially and exhibits a more pronounced change in the temperature

region 70 to 120 °C. Above this region the band position remains constant and from the HTWAXS data presented above, the sample exists in the pseudohexagonal phase above 120 °C. Such a behavior of progression bands is a common feature of nylons and is shown to arise due to the enhanced mobility of methylene segments with increasing temperature.[20,21] In the γ phase, the band at 1190 cm^{-1} is not obvious in the spectra but the band at 1198 cm^{-1} is prominent; furthermore, the behavior of 1160 and 1198 cm^{-1} bands with increasing temperature is different from that of the α and α' phases and is shown in Figure 3.10c. The wavenumber of these two bands decreases with increasing temperature but shows deviation at about 100 °C. The normalized integrated absorbance of 1160 and 1198 cm^{-1} band decreases with increasing temperature. The 1198 cm^{-1} band, which appears only for the γ phase, shows a rapid decrease above 100 °C, when the γ phase transforms into pseudohexagonal phase.

The regions sensitive to hydrogen bonding are from 1500 to 1800 cm^{-1} and from 3000 to 3600 cm^{-1}. The region 1500 to 1800 cm^{-1} is shown in Figure 3.11a-c for the α, α' and γ phases and contains the amide I and amide II bands. The amide I band appears at 1640 and 1637 cm^{-1} for α and α' phases respectively, while for the γ phase it is again at 1639 cm^{-1}. The amide I band arises from the stretching of the carbonyl groups and the band has contribution from the hydrogen bonded carbonyl groups in the crystalline region (ordered), the hydrogen bonded carbonyl groups in the amorphous region (disordered) and the non hydrogen bonded carbonyl groups (free). Because of the contribution from the different carbonyl groups outlined above, the band usually appears highly asymmetric. Visual inspection of the Figure 3.11a-c shows that the behavior of the amide I band looks very similar for the α and α' phases at room temperature and on heating. The amide I band of the γ phase, however, shows variance from the α and α' phases; the band is considerably sharper. The amide II band appears at 1537 and 1544 cm^{-1} for the α and α' phases respectively. The band shifts to 1555 cm^{-1} for the γ phase. The amide II band arises mainly from the in-plane N–H bending and has contributions from ordered, disordered and free N–H groups. Consequently, the amide II band also appears highly skewed. Deconvolution of the peak into individual components is not attempted due to the uncertainty in the position of the individual bands and hence the band is treated as a single peak. Figure 3.11d-f shows the behavior of the band position and the normalized

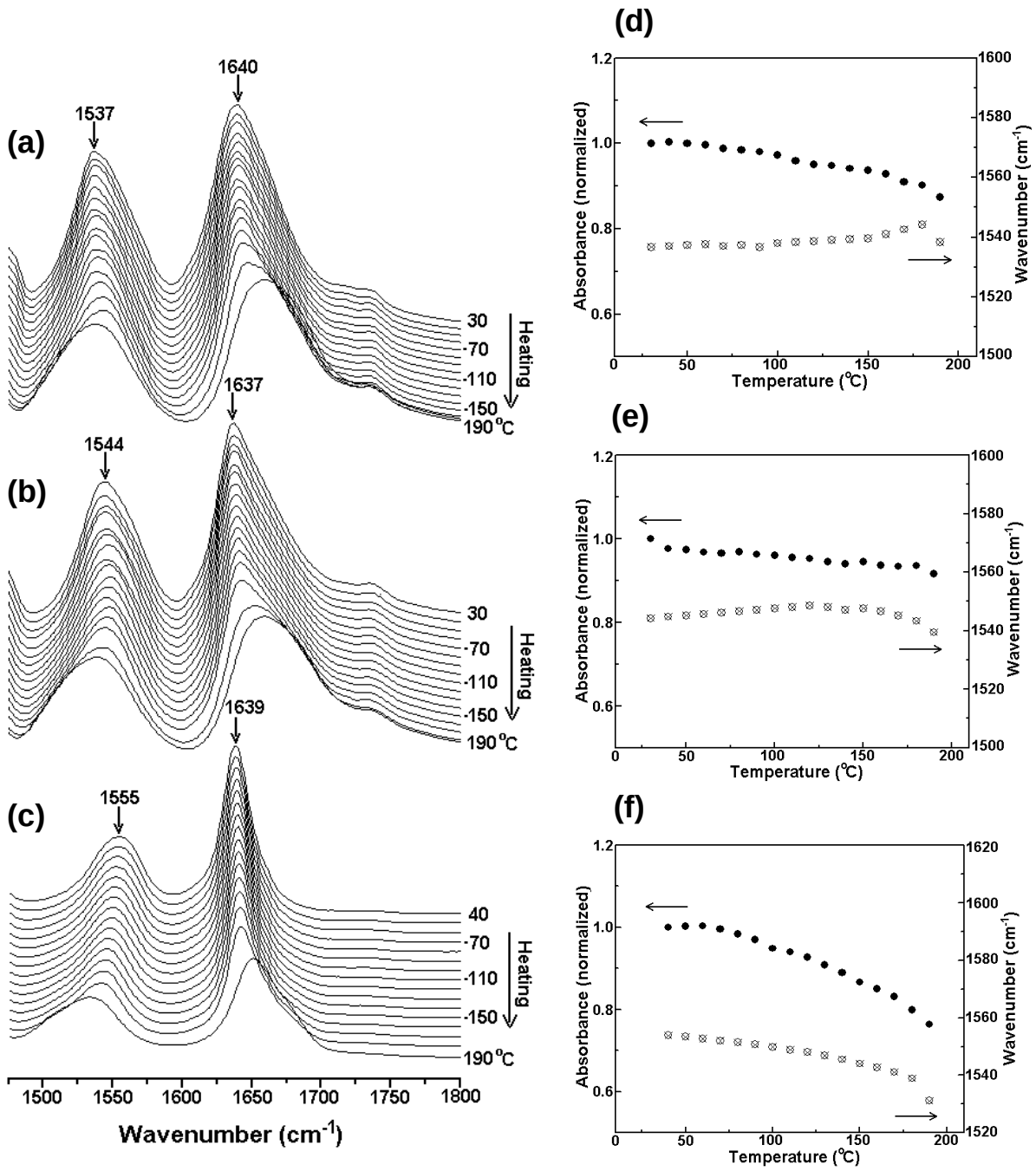

Figure 3.11: Variable temperature FTIR spectra of the region 1500–1800 cm^{-1} of nylon-11 during heating from room temperature to melt: (a) α phase, (b) α' phase, and (c) γ phase. The variation of the wavenumber and normalized absorbance of amide I and amide II bands during heating for (d) α phase, (e) α' phase, and (f) γ phase.

absorbance during heating for the various phases. The wavenumber increases slightly with increasing temperature for the α phase and the shift is more pronounced close to T_m. The wavenumber 1544 cm^{-1} of the α' phase increases up to 120 ^oC and then decreases. The normalized integrated absorbance progressively decreases with increasing temperature for

both the phases. The amide II band of the γ phase shows slightly different behavior. First of all, the band appears at 1555 cm^{-1}, at higher wavenumber than the α and α' phases. Secondly, the behavior of the band on heating is very different from the α phases. The band shifts to lower wavenumber on heating and becomes sharper.

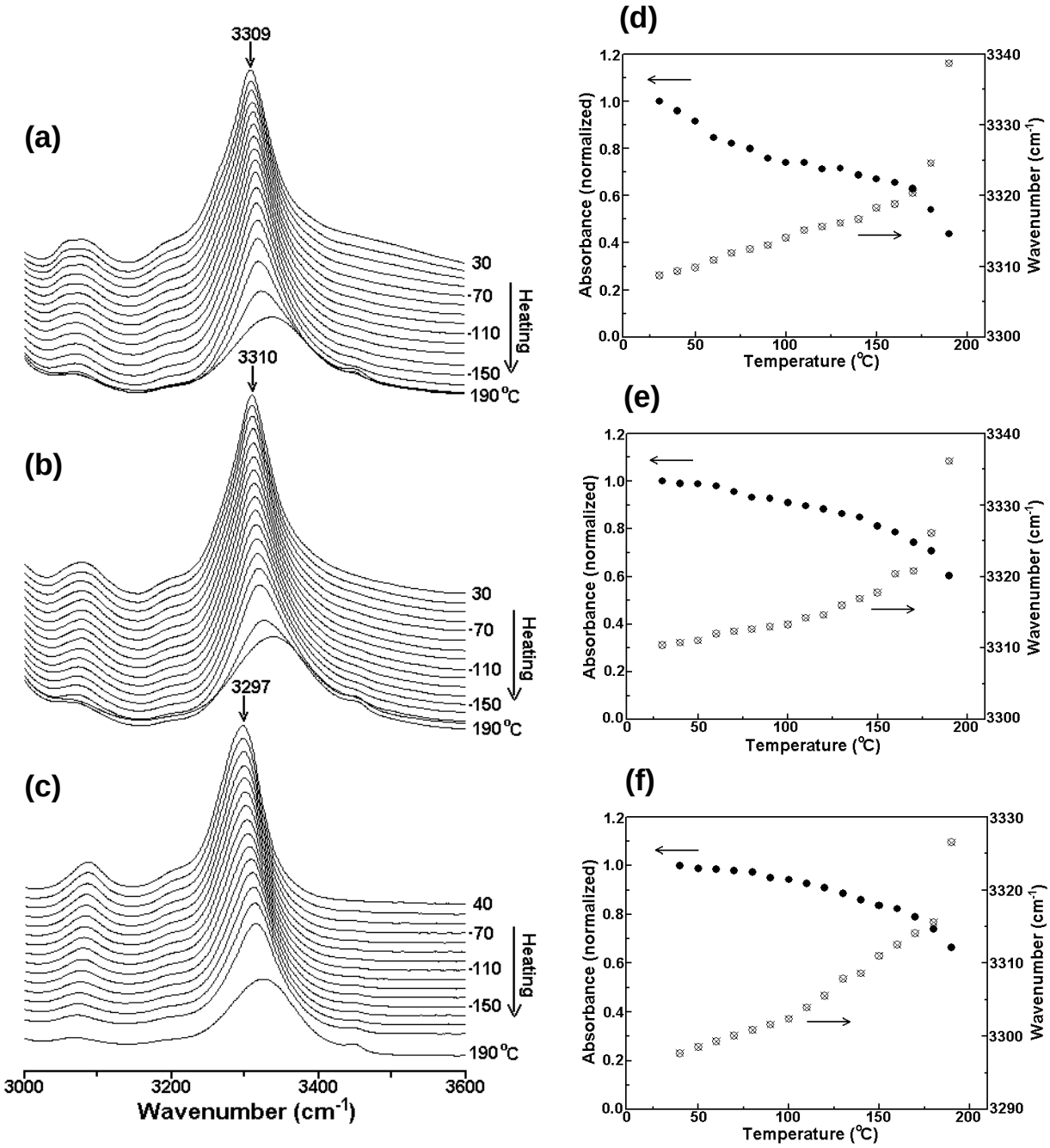

Figure 3.12: Variable temperature FTIR spectra of the region 3000–3600 cm^{-1} of nylon-11 during heating from room temperature to melt: (a) α phase, (b) α' phase, and (c) γ phase. The variation of the wavenumber and normalized absorbance of amide A band during heating for (d) α phase, (e) α' phase, and (f) γ phase.

The changes in the amide II band occurring during heating is also reflected in the amide A band and Figure 3.12a-c shows the variation in the spectra during heating for all the samples. The amide A band is assigned to N–H stretching vibration and is sensitive to the strength of the hydrogen bond. The contribution to the amide A comes from i) free N–H stretch at 3444 cm^{-1} ii) bonded N–H stretch at 3300 cm^{-1} arising out of crystalline fraction iii) bonded N–H stretch at 3310 cm^{-1} arising out of amorphous fraction. The region is too broad to deconvolute meaningfully into individual peaks and hence is discussed as a composite peak. The amide A band appears at 3309 and 3310 cm^{-1} for the α and α' phases respectively. In the case of the γ phase it shifts to 3297 cm^{-1}. Another noticeable difference between the α and γ phases is the absorbance of the amide A band in relation with the bands at 2851 and 2920 cm^{-1}, which are assigned to symmetric and anti-symmetric CH_2 stretch, respectively.[30,33] The amide A band of the α and α' phases has comparable peak height with the band at 2920 cm^{-1} but amide A band of the γ phase shows much reduced absorbance. The amide A band, in general is sharp and skewed and cannot be approximated to Gaussian profile. However, it may be noted that Skrovanek et al.[34] observed symmetrical profile in samples cast from 1,1,1,3,3,3-hexafloro-2-propanol. Figure 3.12d-f shows the variation of the wavenumber and absorbance of the amide A band during heating. In the case of the α phase, the peak position shifts to higher wavenumber in a linear fashion until melting and after melting the peak shifts to 3338 cm^{-1} and the band has Gaussian profile. The normalized area decreases with increasing temperature; initially the rate is more which slows down after 90 ^{o}C. Again close to melting it decreases more rapidly. The α' phase shows similar behavior with the α phase; nevertheless minor variations are seen. In the case of the γ phase, the wavenumber increases with increase in temperature but more pronounced increase is at about 100 ^{o}C when the γ phase transforms into the pseudohexagonal phase. The integrated absorbance decreases progressively with increase in temperature.

The WAXS studies presented above clearly indicate that the α and α' phases are distinctly different and on heating the α phase does not transform into the pseudohexagonal phase. The α' phase, however, transforms into the pseudohexagonal phase before melting. On the other hand FTIR spectra show subtle differences between these phases indicating these two phases have similar molecular conformation in the crystalline phase. The γ phase shows distinct differences in the FTIR spectra when compared with the α and α' phases.

Since the conformation in the amorphous phase is expected to be the same for all the phases, the differences may be attributed to different conformation in the crystalline phase of the γ phase.

The FTIR spectra of the γ phase of nylon-11 are similar to the spectra of the γ phase of nylon-6. In the case of nylon 6 the γ phase is obtained by KI/I_2 treatment or by melt crystallization with clay layers controlling the hydrogen bonds. In the case of the γ phase obtained by KI/I_2 treatment, the iodine forms a complex with the nylon-6 and the removal of iodine from the complex leads to the γ phase.[31] TGA studies have indicated that about 5% of the TFA is trapped in the nylon-11 film and it leaves the sample between 70 to 110 ^{o}C on heating. It is expected that the residual solvent remains in the amorphous phase and hence is insensitive to the X-ray diffraction data discussed in the earlier section. Figure 3.13a-c shows the FTIR spectra obtained from the cast film with 5% TFA. The spectra show variation in the amide A, amide II and progression bands during heating. The normalized absorbance of the amide A and amide II bands shown in Figure 3.13d and e increases in the temperature range from 70 to 110 ^{o}C and then decreases on further heating. The progression bands at 1160 and 1199 cm^{-1} arising from T_{10} and T_9 (CH_2 twisting) modes also show the effect of TFA as shown in Figure 3.13c and f. The wavenumber decreases with increasing temperature but distinctly shows deviation at about 90 °C. More significantly the absorbance of these peaks decrease very rapidly at about 90 °C, when the TFA leaves the sample. The rapid decrease in the absorbance indicates the constraint in the twisting motion of CH_2. In the case of nylon-11 – TFA system, in the solution the amide group in the nylon can be protonated[35,36] and can form an ion pair with TFA. During the evaporation of the solvent the ion pair disappears and the hydrogen bonding between nylon chains is gradually formed. The 5% TFA retained in the amorphous phase is also expected to form ion-pair with the amide group. On removal of the TFA on heating, the amide groups become free, which can subsequently form the hydrogen bond and consequently the intensity of the amide II and amide A absorbance increases and concomitantly the increased hydrogen bonding restricts the T_{10} and T_9 (CH_2 twisting) modes. The above results suggest that the formation of the γ phase in nylons may be by externally regulating the hydrogen bond formation during crystallization. In the case of nylon-6, the KI/nylon complex or the clay layers when nylon-6 is crystallized in the presence of clay layers control the hydrogen bonding formation. In the case of

nylon-11, the TFA-amide ion pair controls the formation of hydrogen bonding leading to the γ phase.

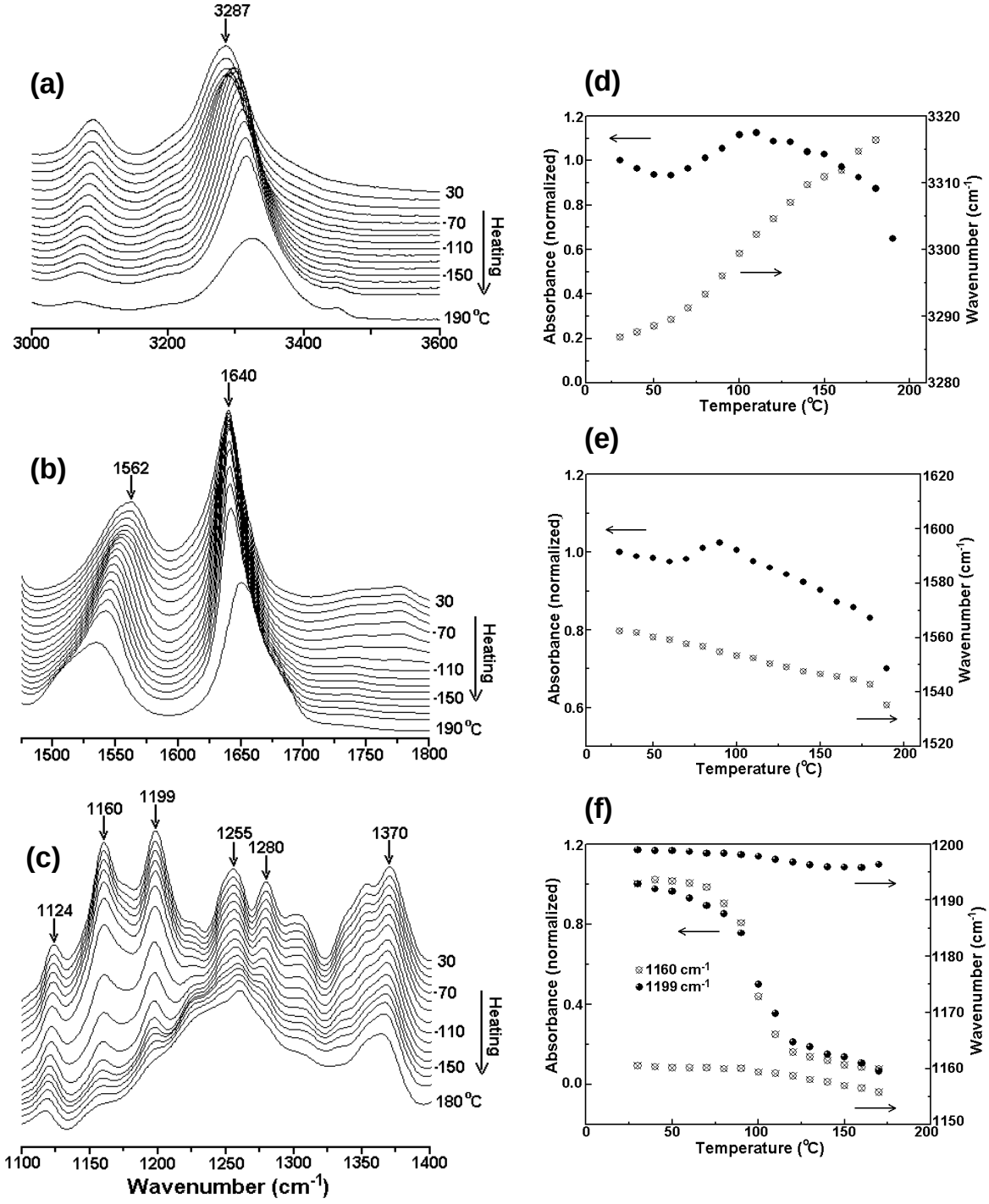

Figure 3.13: Variable temperature FTIR spectra of the TFA-cast nylon-11 film with 5% TFA during heating from room temperature to melt: (a) 3000–3600 cm^{-1}, (b) 1500–1800 cm^{-1}, and (c) 1100–1400 cm^{-1}. The variation of the wavenumber and normalized absorbance of the characteristic bands (d) 3000–3600 cm^{-1}, (e) 1500–1800 cm^{-1}, and (f) 1100–1400 cm^{-1}.

3.4 Conclusion

The high temperature XRD studies provided new information on the polymorphism of nylon-11. Nylon-11 may be crystallized into α, α', γ and pseudohexagonal phases by appropriate crystallization conditions. Nylon-11 crystallized in the α phase when precipitated in 1,4-butanediol and did not fully transform into the pseudohexagonal phase on heating. A complex polymorphism has been exhibited by nylon-11 melt-crystallized at 175 °C. The sample crystallized in the pseudohexagonal phase, and on cooling from the T_c, it transformed into the α' phase, which is different from the α phase, at about 100 °C. However, the transition temperature is dependent on the T_c. The smectic phase or the δ phase obtained on melt quenching appeared to be the pseudohexagonal phase. It was shown for the first time that the γ phase, obtained by casting nylon-11 in TFA, transformed into pseudohexagonal phase on heating above 110 °C.

For the first time, we reported the observation of change in the 001 *d* spacing during phase transition. The value and the variation of the *d* spacing of the 001 reflection is highly phase sensitive. The 001 d spacing showed a change in the value when the α and α' phase changed into the pseudohexagonal phase or vice versa. Similar changes were seen when the γ phase transformed into the pseudohexagonal phase on heating to melt. The above studies indicate that nylon-11 showed a change in the structural features above 110 °C on heating, which manifested as a change in the crystalline phase.

The variable temperature FTIR studies indicated that the α and α' phases had a similar conformation in the crystalline phase. The γ phase showed characteristic infrared bands at different positions from those of the α and α' phase. It was speculated from the HTFTIR studies on TFA-cast film with 5% TFA that the interaction of TFA with amide groups might be responsible for the formation of the γ phase.

3.5 References

1. Newman, B. A.; Chen, P. K.; Pae, K. D.; Scheinbeim, J. I. *J. Appl. Phys.* **1980**, *51* (10), 5161.
2. Mathur, S. C.**;** Scheinbeim, J. I.**;** Newman, B. A. *J. Appl. Phys.* **1984**, *56* (9), 2419.
3. Lee, J. W.**;** Takase, Y.**;** Newman, B. A.**;** Scheinbeim, J. I. *J. Polym Sci., Polym. Phys.* **1991**, *29*, 273.

4. Takase, Y.; Lee, J. W.; Scheinbeim, J. I.; Newman, B. A. *Macromolecules* **1991**, *24*, 6644.
5. Scheinbeim, J. I.; Lee, J. W.; Newman, B. A. *Macromolecules* **1992**, *25*, 3729.
6. Gao, Q.; Scheinbeim, J. I. *Macromolecules* **2000**, *33*, 7564.
7. Slichter, W. P. *J. Polym. Sci.* **1959**, *36*, 259.
8. Kinoshita, Y. *Macromol. Chem.* **1959**, *33*, 1.
9. Kawaguchi, A.; Ikawa, T.; Fujiwara, Y.; Tabuchi, M.; Konobe, K. *J. Macromol. Sci. Phys. B* **1981**, *20* (1), 1.
10. Kim, K. G.; Newman, B. A.; Scheinbeim, J. I. *J. Polym. Sci. Polym. Phys. Ed.* **1985**, *23*, 2477.
11. Newman, B. A.; Sham, T. P.; Pae, K. D. *J. Appl. Phys.* **1977**, *48*, 4092.
12. Schmidt, C. F.; Stuart, Z. *Naturforsch* **1958**, *13A*, 222.
13. Sasaki, T. *J. Polym. Sci. Part B: Polym. Lett*. **1965**, *3*, 557.
14. Brill, R. J. *J. Prakt. Chem.* **1942,** *161*, 49.
15. Ramesh, C. *Macromolecules* **1999**, *32*, 3721.
16. Biangardi, H. J. *J. Macromol. Sci.-Phys. B* **1990**, *29* (2/3), 139.
17. Vasanthan, N.; Murthy, N. S.; Bray, R. G. *Macromolecules* **1998**, *31*, 8433.
18. Ramesh, C. *Macromolecules* **1999**, *32*, 5704.
19. Murthy, N. S.; Curran, S. A.; Aharoni, S. M.; Minor, H. *Macromolecules* **1991**, *24*, 3215.
20. Yoshioka, Y.; Tashiro, K.; Ramesh, C. *Polymer* **2003**, *44*, 6407.
21. Yoshioka, Y.; Tashiro, K. *J. Phys. Chem. B* **2003**, *107*, 11835.
22. Yoshioka, Y.; Tashiro, K. *Polymer* **2003**, *44*, 7007.
23. Yoshioka, Y.; Tashiro, K. *Polymer* **2003**, *44*, 4337.
24. Yoshioka, Y.; Tashiro, K. *Polymer* **2004**, *45*, 6349.
25. Zhang, Q.; Mo, Z.; Zhang, H.; Liu, S.; Cheng, S. Z. D. *Polymer* **2001**, *42*, 5543.
26. Bunn, C. W.; Garner, E. V. *Proc. R. Soc. (London)* **1947**, *189*, 39.
27. Ramesh, C.; Keller, A.; Eltink, S .J. E. A. *Polymer* **1994**, *35*, 2483.
28. Sandeman, I.; Keller, A. *J. Polym Sci.* **1956,** *19*, 401.
29. Yu, H. H. *Mater. Chem. and Phys*. **1998**, *56*, 289.
30. Jakes, J.; Krimm, S. *Spectrochimica Acta* **1971**, *27A*, 19.
31. Abu-isa, I. *J. Polym. Sci. Part A-1* **1971,** *9*, 199.
32. Nair, S.S.; Ramesh, C. *Macromolecules* **2005,** *38*, 454.

33. Doskocilova, D.; Pivcova, H.; Schneider, B.; Cefelin, P. *Coll. Czech. Comm.* **1963,** *28,* 1867.
34. Skrovanek, D. J.; Painter, P.C.; Coleman, M. M. *Macromolecules* **1986,** *19,* 699.
35. Kricheldorf, H. R. *Die Makromol. Chem.* **2003,** *179,* 2695.
36. Bradbury, J. H.; Yuan, H. H. H. *Biopolymers* **2004,** *11,* 661.

CHAPTER 4

STUDIES ON THE CRYSTALLINE PHASES OF NYLONS -6,7 AND -6,9

4.1 Introduction

Crystalline transitions in even-even nylons attracted great deal of interest and are reviewed in detail in chapter 1. However, reports on the crystalline transition of even-odd or odd-even nylons are very scanty. One possible reason is the very limited commercial success of these nylons. In the case of even-even nylons or even nylons the principal phase is the α phase and is consisted of hydrogen-bonded sheets sheared progressively. The chains are in the all-*trans* conformation and the hydrogen bonds are confined to a plane. However in the case of even-odd nylons, the methylene units are unable to form saturated intrasheet hydrogen bonding scheme with linear hydrogen bonds and all-*trans* conformation for methylene units. In the case of nylon-6,5, the structural model is based on two hydrogen bond directions.[1] Similar type of structure is also reported for nylon-6,9.[2] Therefore, even-odd nylons present a different crystal structure from even-even nylons resulting in some different properties from even-even nylons.[1-4]

In the present chapter, we report the results of the detailed investigations made on the polymorphism of even-odd nylons, namely nylon -6,7 and -6,9 using variable temperature wide-angle X-ray scattering (WAXS). For the first time, we prepared the various crystalline forms of nylons -6,7 and -6,9 by different procedures and followed the crystalline transitions *in situ* by using a hot stage attached to an X-ray diffractometer. Also for the first time we examined the Fourier transform infrared spectroscopy (FTIR) of various phases on heating and correlated it with the high temperature wide-angle X-ray scattering (HTWAXS) data.

4.2 Experimental Section

4.2.1 Materials

Hexamethylene diamine and pimelic acid for the synthesis of nylon-6,7 were obtained from Aldrich, USA. Thionyl chloride for the synthesis was obtained from Spectrochem, India and was used after distillation. Nylon-6,9 pellets were directly obtained from Aldrich, USA. 1,4-Butanediol used for crystallization of the polymers was obtained from Merck, Germany.

4.2.2 Synthesis of Nylon-6,7

Nylon-6,7 was prepared by the melt polymerization technique as well as the interfacial polymerization technique.

4.2.2.1 Melt Polymerization technique

Nylon-6,7 salt was prepared from the monomers hexamethylene diamine (0.1 mol) and pimelic acid (0.101 mol) using methanol as solvent. A precise balance of the reactive groups was ensured in order to obtain high molecular weight polymer. The pH of an aqueous solution (1%) of the salt was measured and was found to be 7.6. The polymerization was carried out in two steps. In the first step, the nylon-6,7 oligomer was obtained from the salt by condensation at 235 °C for 10h. In the second step, the oligomer was subsequently melt polymerized at 280 °C for 4h under vacuum (0.010 mbar) to obtain high molecular weight nylon-6,7.

4.2.2.2 Interfacial Polymerization technique

Pimelic acid was converted to pimeloyl chloride for enhancing its reactivity. For this purpose the reaction between the diacid and thionyl chloride (1:3 mole) was carried out at a temperature of 75 °C for 6h. The FTIR spectrum showed that all the acid groups were converted to acid chloride. The excess thionyl chloride was removed by distillation and the pimeloyl chloride formed was purified by distillation under reduced pressure.

Pimeloyl chloride was taken in dichloroethane and hexamethylene diamine in sodium hydroxide (2M) solution. Sodium hydroxide acts as the hydrogen chloride acceptor. The organic phase was immediately added to the aqueous phase under high speed stirring. The polymerization took place at the interface. The polymer formed was initially washed with methanol and then with water and dried under vacuum at 60 °C.

4.2.3 Sample Preparation

The nuclear magnetic resonance (NMR), FTIR and the thermal studies carried out on nylon-6,7 prepared by the interfacial and melt polymerization techniques showed similar results. The nylon-6,7 polymer was dissolved in 1,4-butanediol at its refluxing temperature. On cooling very slowly to room temperature, the nylon-6,7 formed a precipitate, which was filtered and washed repeatedly in acetone to remove the 1,4-butanediol. This procedure gave a highly crystalline sample in the form of fine powder. Similarly, nylon-6,9 was crystallized by precipitating in 1,4-butanediol. Thus obtained crystalline powders were used for WAXS and FTIR studies. The techniques are described in detail in chapter 3.

4.2.4 Characterization

Inherent viscosities were measured at 30 ^{o}C in an automated Schott Gerate AVS 350 viscometer, using an Ubbelohde suspended level viscometer in formic acid (98-100%) at a polymer concentration of 0.5%. The η_{inh} was 1.16 dl/g for nylon-6,7 prepared by melt polymerization and 0.27 dl/g for nylon-6,7 prepared by interfacial polymerization. For nylon-6,9 pellets obtained commercially the η_{inh} was 0.69 dl/g.

The melting and crystallization behavior of the nylons -6,7 and -6,9 was analyzed by using a TA Instruments Q10 calorimeter. The sample weight was about 5 mg, and the heating and cooling rate was 10 °C/min. The calorimeter was calibrated using the standard protocol. The samples were scanned from 0 °C to 250 °C.

^{1}H and ^{13}C NMR measurements were performed in a Bruker DRX 500 spectrometer at 25 ^{o}C with a proton resonance frequency of 500 MHz and ^{13}C resonance frequency of 125 MHz. The samples were dissolved in deuterated trifluoroacetic acid (TFA-*d*) and deuterium oxide was used as an external locking agent. The spectra were internally referenced to tetramethyl silane.

4.3 Results and Discussion

4.3.1 Studies on Nylon-6,7

4.3.1.1 NMR Studies

The chemical shifts observed in the ^{1}H and ^{13}C NMR spectra of the synthesised nylon-6,7 shown in Figures 4.1 and 4.2, respectively, are in full agreement with the anticipated chemical composition. The chemical shifts at 3.52 and 2.70 ppm originate from the methylene protons adjacent to the amide group i.e., –CONHC$\underline{H}_2$– and –C$\underline{H}_2$CONH–, respectively. The other methylene protons in the repeat unit of the polymer show chemical shifts in the range 1.41 to 1.80 ppm. As shown in Figure 4.1, the ratio of integration (4:4:14) matches with the number of methylene protons in the repeat unit of the polymer, and hence confirms the structure. The peaks at 4.72 ppm and 11.25 ppm were due to the solvents D_2O and TFA-*d*, respectively.

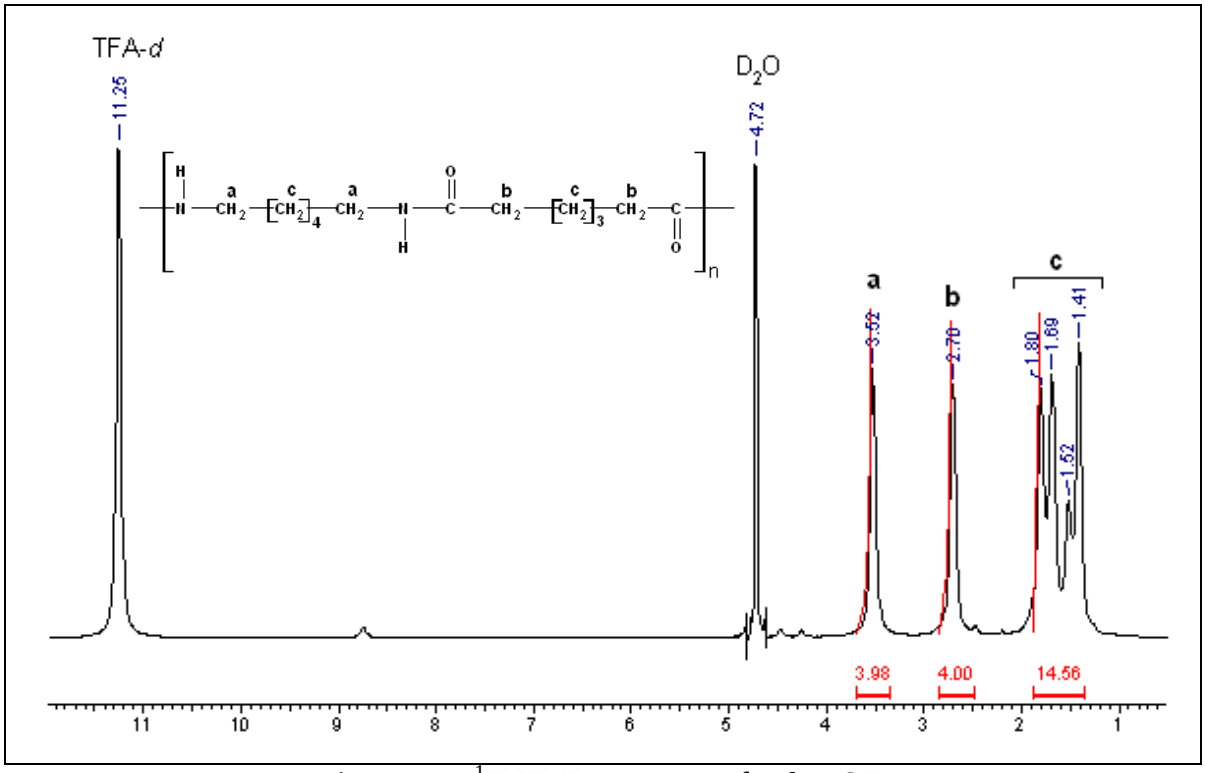

Figure 4.1: ^{1}H NMR spectrum of nylon-6,7.

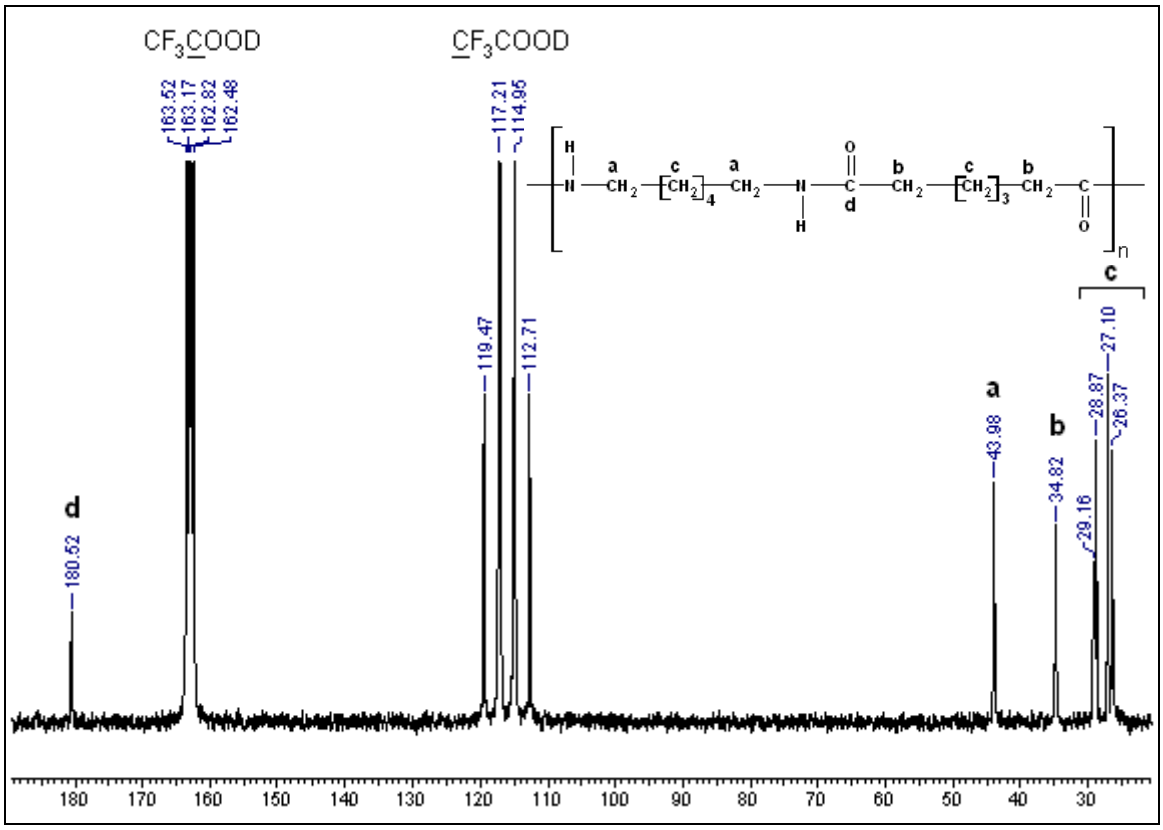

Figure 4.2: ^{13}C NMR Spectrum of nylon-6,7.

The ^{13}C NMR spectrum (Figure 4.2) was also found to be in agreement with the expected chemical structure. The chemical shift at 180.52 ppm corresponds to the carbonyl carbon of the amide group (–CONH–). The carbon atoms adjacent to the amide group show chemical shifts at 43.98 ppm (–CONHCH$_2$–) and 34.82 ppm (–CH$_2$CONH–). The chemical shifts below 30 ppm were assigned to the rest of the carbons of the alkylene segment. The peaks at 163 ppm and 116 ppm correspond to the carbon atoms of the carbonyl group and CF3 group of the solvent TFA-*d*.

4.3.1.2 Thermal Analysis

Figure 4.3 shows the DSC thermograms comprising a sequence of three scans performed with the nylon-6,7 sample crystallized in 1,4-butanediol. In the first run (a), the sample was heated (10 °C/min) through fusion to 240 ^{o}C, and left in the melt for 1 min, and was cooled (10 °C/min) to observe crystallization from the melt (b). The second heating (c) represents the thermogram of the melt-crystallized sample. Double melting peaks are seen for either 1,4-butanediol crystallized or melt-crystallized samples, a common observation in thermal studies of nylons.[5]

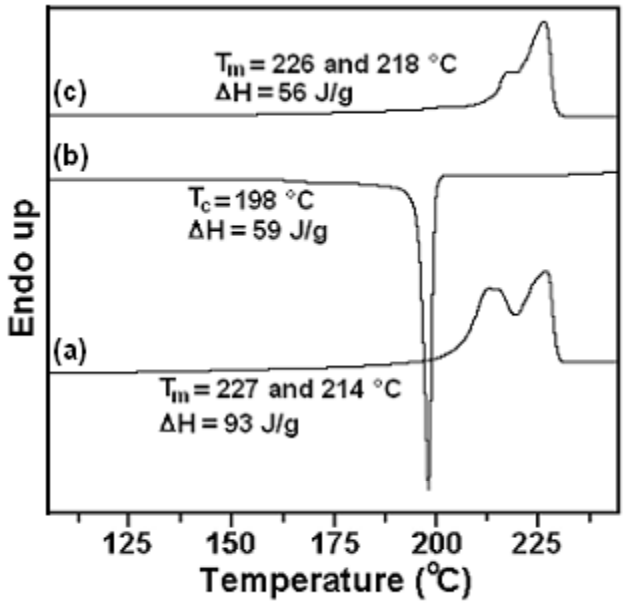

Figure 4.3: The DSC thermograms obtained during (a) first heating, (b) cooling, and (c) reheating, for nylon-6,7 crystallized in1,4-butanediol.

This phenomenon is associated with partial melting and recrystallization of the smaller and/or less perfect crystals with a lower melting point during the course of heating. The high temperature peak is associated with the more stable 'reorganized' state comprised of

thicker and/or more perfect crystals. The melt temperatures are lower than expected when compared with those of similar even-even nylons (i.e. 265 °C for nylon-6,6).[6]

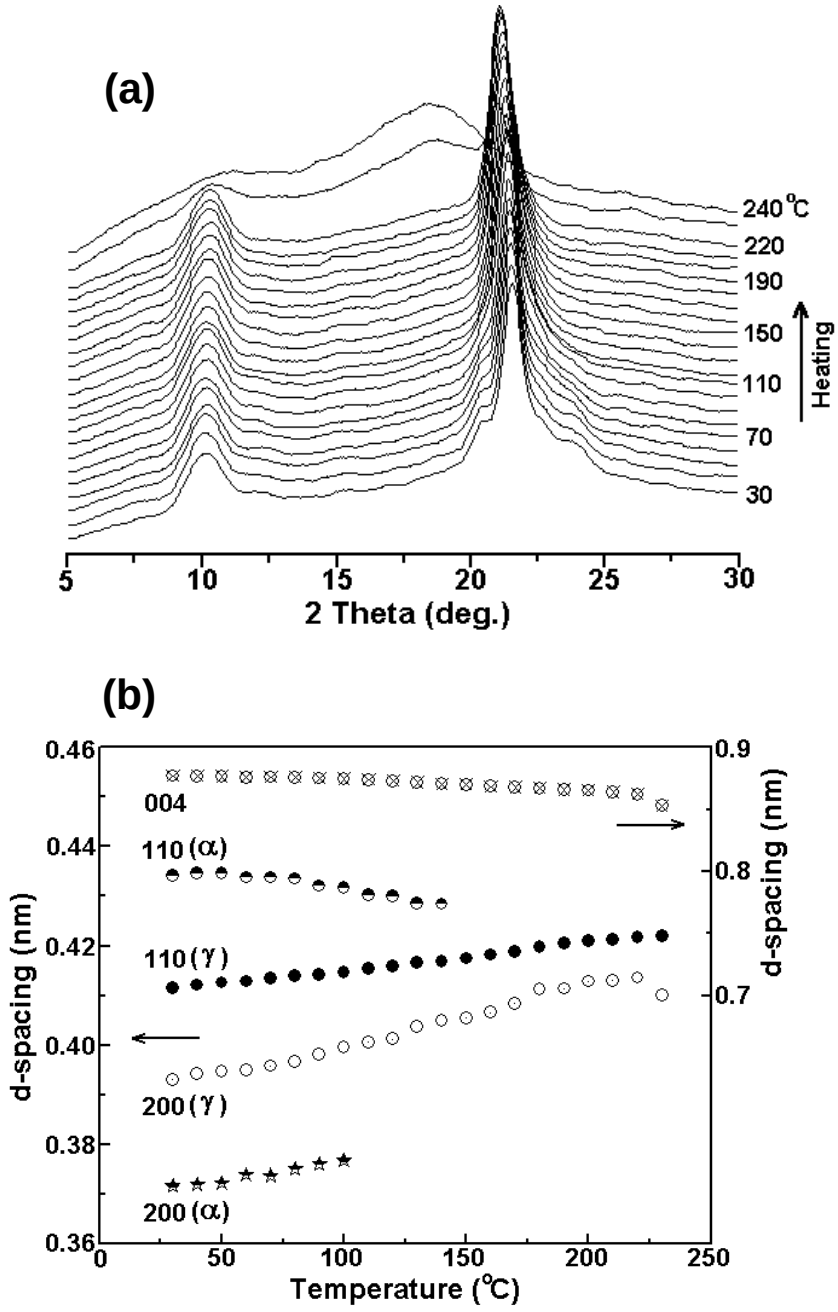

Figure 4.4: Behavior of (a) XRD patterns and (b) *d* spacings on heating from room temperature to melt for nylon-6,7 crystallized in 1,4-butanediol.

4.3.1.3 Variable Temperature WAXS Studies

The room temperature diffraction pattern and the patterns obtained on heating the nylon-6,7 crystallized in 1,4-butanediol is shown in Figure 4.4a. The room temperature

diffraction pattern shows diffraction peaks at 2θ = 20.44, 21.58, 22.61 and 23.94° and the corresponding *d* spacings are 0.434, 0.411, 0.393 and 0.371 nm respectively. The structure of nylon-6,7 is not yet solved in the literature, but the indexing is based on nylon-6,9.[2] Based on the *d* spacing values, the peaks at 2θ = 20.44 and 23.94° may be identified with the α phase. These peaks may be indexed as the 110 and 200 reflections of the monoclinic structure, respectively. The peaks at 2θ = 21.58 and 22.61° indicate the presence of the γ phase, and the reflections may be indexed as 110 and 200, respectively.[2] The γ phase is also having a monoclinic structure. The *d* spacings are similar to the γ phase of nylon-6. Kinoshita[4] also reported a γ phase structure for even-odd nylons. The α phase fraction is about 11 % and that of γ phase is about 39 %. The 004 reflection occurs at 2θ = 10.09°, corresponding to a *d* spacing of 0.876 nm. The behavior of the *d* spacings on heating from room temperature to melt is shown in Figure 4.4b, respectively. The two peaks due to the α phase move closer to the γ phase peaks on heating, and disappear at about 140 °C without merging with the γ phase. On the other hand, the peaks due to the γ phase remain as such, albeit, with small increase in the *d* spacing values and the sample melts in the γ phase. The 004 reflection at 2θ = 10.09° exhibits a small decrease with an increase in temperature. The small decrease in the 004 reflection *d* spacing is expected because of the enhanced motion of the methylene segments.[7,8]

The behavior of the diffractograms and *d* spacings of the melt-crystallized sample is different from the sample crystallized from the 1,4-butanediol solution described above. Figure 4.5a and b show the behavior of the diffractograms and the *d* spacings on cooling from the crystallization temperature (T_c) at 220 °C to room temperature. The diffractogram recorded after the completion of crystallization at 220 °C shows two peaks at 2θ = 20.83° and 21.24°. and the corresponding *d* spacings are 0.426 and 0.418 nm, respectively. Based on the *d* spacing values these peaks can be assigned to the γ phase, and indexed as the 110 and 200 reflections of the monoclinic structure, respectively. A third peak appears as a shoulder to the peak at 2θ = 20.83° and is at 2θ = 20.15°. This peak at 2θ = 20.15^o is indicative of the presence of an additional phase as this peak is not observed for the γ phase. The corresponding *d* spacing is 0.440 nm. The position of this new reflection is similar to the 100 reflection of the α phase. Nevertheless, its behavior on cooling differs from the α phase.[9,10] Following Murthy,[11] the new phase may be interpreted to arise from the intermediate phase and is termed the metastable phase to distinguish it from the α and

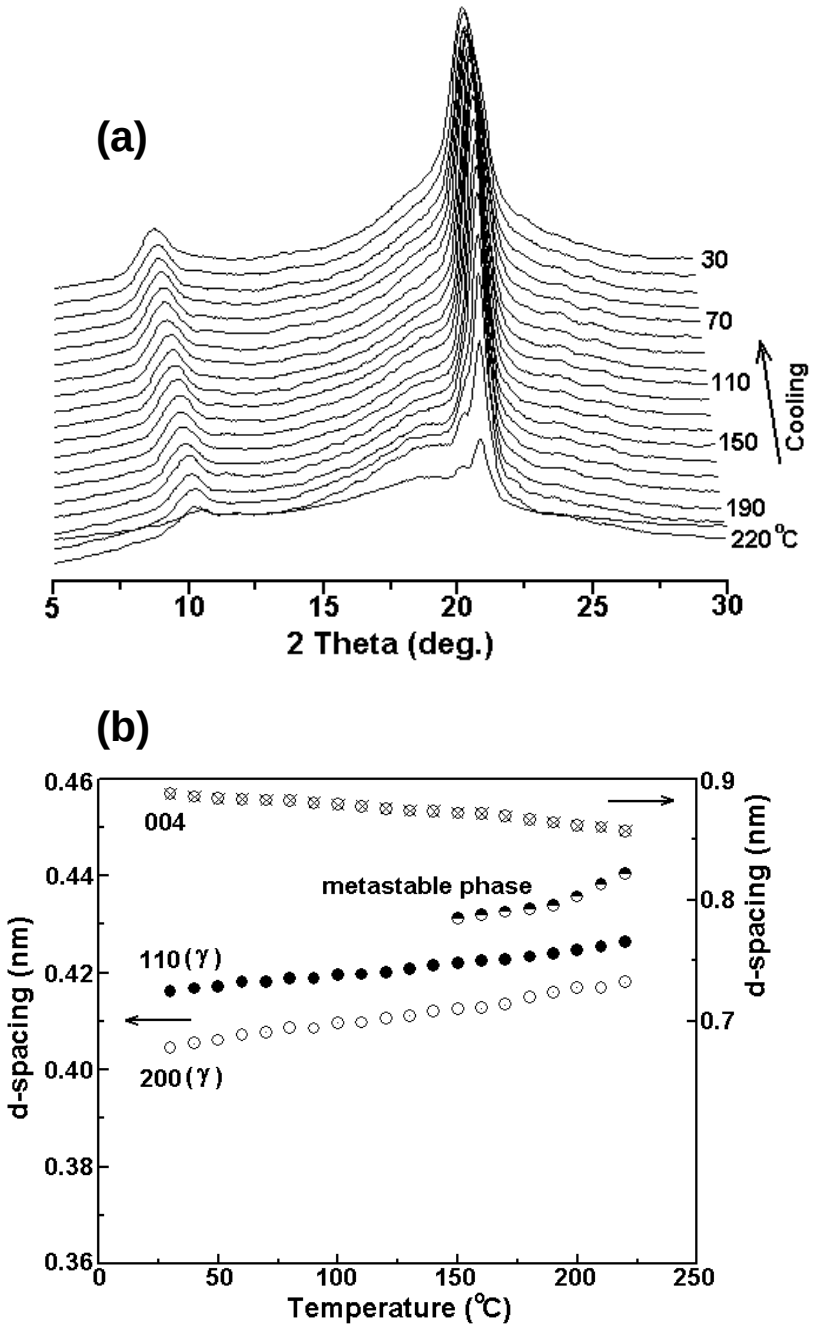

Figure 4.5: Behavior of (a) XRD patterns and (b) *d* spacings of nylon-6,7 melt-crystallized at 220 °C on cooling to room temperature.

γ phases. Detailed description of the metastable phase will be made in chapter 5. The 004 reflection shows a peak at 2θ = 10.32° corresponding to the *d* spacing of 0.857 nm. The characteristic peaks of the γ phase at 2θ = 20.83° and 21.24° show a small shift toward higher angles on cooling to room temperature as shown in Figure 4.5b. The metastable phase peak at 2θ = 20.15° shifts towards higher values and disappears around 150 °C. The room temperature diffraction pattern shows only the γ phase peaks. At room temperature

the 004 reflection occurs at a *d* spacing of 0.887 nm. The variations in diffraction patterns and *d* spacings on cooling from the T_c are found to be reversible on heating and hence will not be discussed in detail.

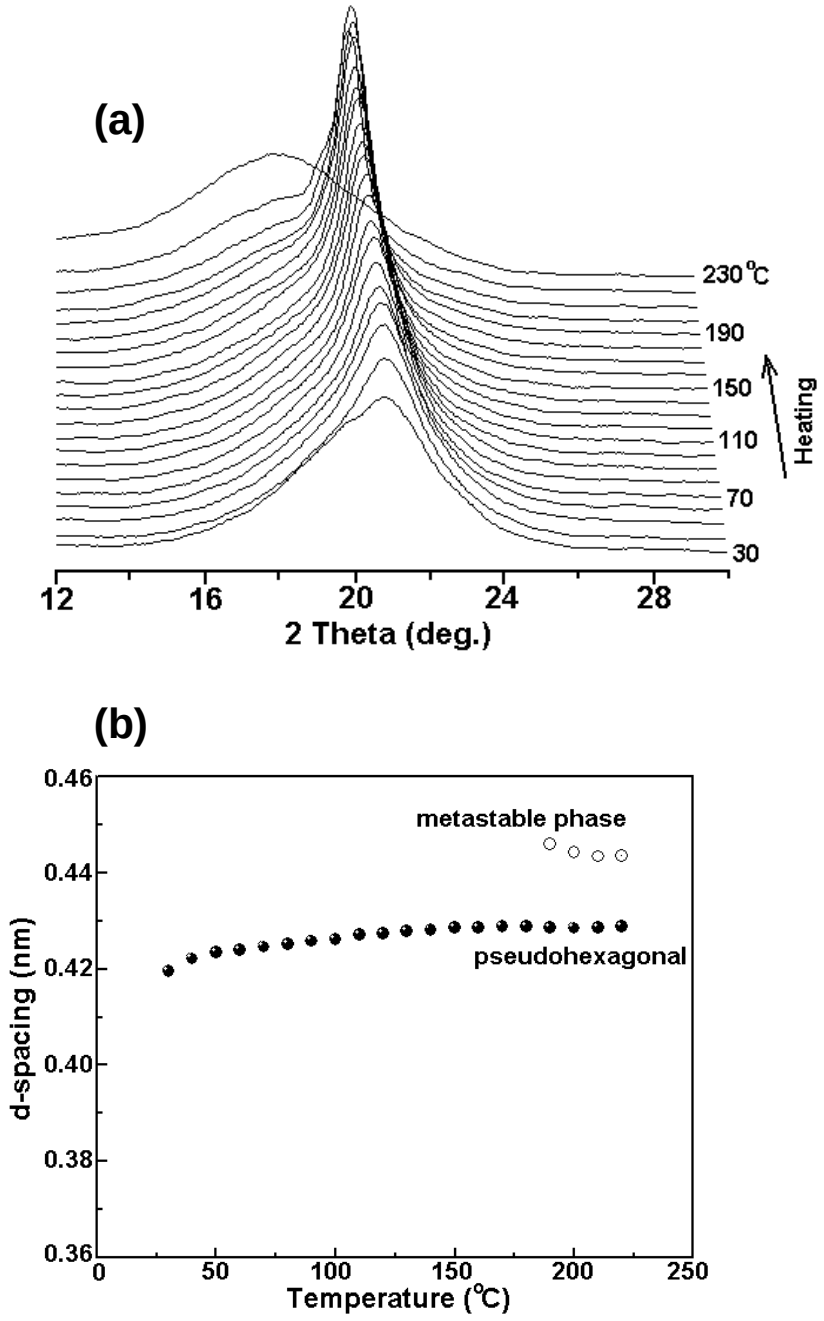

Figure 4.6: Behavior of (a) XRD patterns and (b) *d* spacings on heating from room temperature to melt for quenched nylon-6,7.

Figure 4.6a and b show the diffractograms and *d* spacings of the melt-quenched sample on heating from room temperature. The room temperature diffractogram looks very broad,

similar to the amorphous material. However, on profile fitting the crystalline peak become obvious at 2θ = 21.17° and the *d* spacing is 0.419 nm. The single peak nature of the diffractogram indicates that the sample crystallized in the psuedohexagonal phase. On heating the crystalline peak progressively becomes sharper, but the single peak nature is preserved until melting. Furthermore, at about 190 °C an additional peak appears at 2θ = 20.02° corresponding to the *d* spacing of 0.446 nm indicating the formation of metastable phase. The meatstable phase is stable till melting. Figure 4.6 b shows the variation of the *d* spacing with temperature and it shows a small increase with increase in temperature.

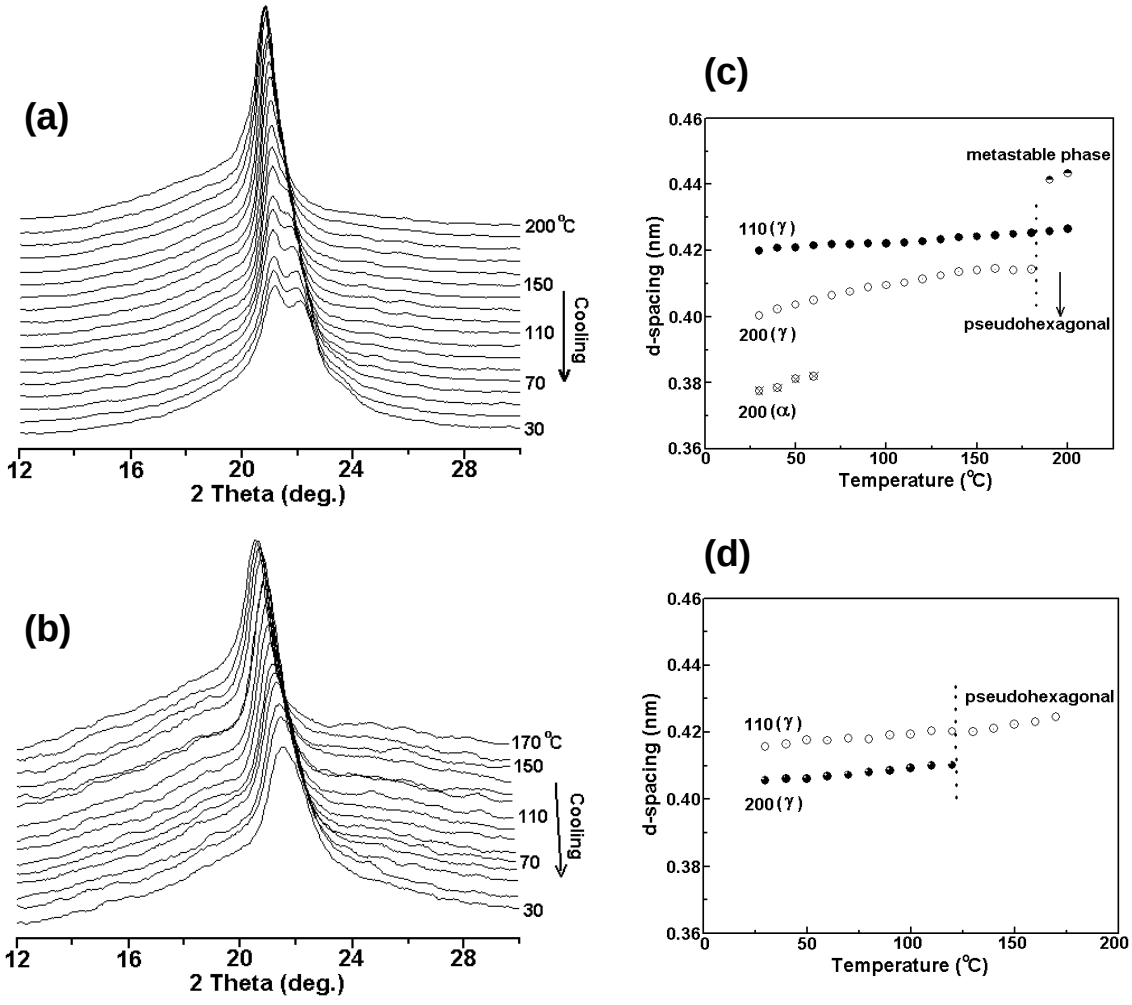

Figure 4.7: Behavior of XRD patterns of the melt-quenched nylon-6,7 sample on cooling from the holding temperatures (a) 200 °C, and (b) 170 °C to room temperature. The behavior of *d* spacings of the melt-quenched sample on cooling from the holding temperatures (c) 200 °C, and (d) 170 °C to room temperature.

The behavior of the sample is different, however, if the sample is not allowed to melt but held at temperatures below the melting temperature (T_m) and then cooled to room

temperature. The behavior of the diffractograms and *d* spacings obtained on cooling from the holding temperature 200 °C to room temperature is shown in Figure 4.7a and c. Firstly, the metastable phase, which appears as a shoulder to the psuedohexagonal phase, disappears at about 180 °C on cooling. But most importantly, immediately on cooling an additional peak appears at the higher angle side. The two peaks now appear at 2θ = 20.87 and 21.44° and the *d* spacings are 0.425 and 0.414 nm, respectively. The peak positions are similar to the γ phase and it may be concluded that the pseudohexagonal phase transforms into the γ phase immediately on cooling. On further cooling the *d* spacing decreases marginally with decreasing temperature. At room temperature the peaks appear at 2θ = 21.15 and 22.20°. These values are different from the peak position of the γ phase obtained by melt crystallization. Furthermore, on cooling below 70 °C, the peak due to the α phase occurs at 2θ = 23.27°. However the fraction of the α phase is very small as the peak at about 2θ = 20° is not obvious in the pattern. The behavior of the diffractograms is different if it is held at 170 °C and cooled to room temperature. The diffractograms and the variation of *d* spacing with temperature is shown in Figure 4.7b and d. In this case the psuedohexagonal phase is kept up to 130 °C. On cooling below 130 °C, the psuedohexagonal phase changes into γ phase. Also the sample does not exhibit the α phase on cooling.

4.3.1.4 Variable Temperature FTIR Studies

Infrared spectroscopy is sensitive to the conformational changes of the chains. FTIR spectra of nylons are well documented in the literature.[12] In the following section, the discussion will be focused on the data obtained from variable temperature FTIR studies on the various phases of nylon-6,7. There are four important regions in the FTIR spectra of nylons as described in chapter 3.

Figure 4.8a and b shows the spectral region from 550 to 800 cm^{-1} for the sample crystallized in 1,4-butanediol and the melt-crystallized sample, respectively. The region comprises the amide V and amide VI bands that stem from the out-of-plane vibration of the N–H and C–O bonds, respectively. The amide V and amide VI bands are also sensitive to the twisting angles around the NH–CH_2 and CO–CH_2 bonds, respectively.[13] Broadening and slight peak position shift (increase/decrease) of these bands with increasing temperature may correspond to the occurrence of twisting motion around the CH_2–amide bonds, as well as the change in hydrogen bonding strength. At room temperature the 1,4-

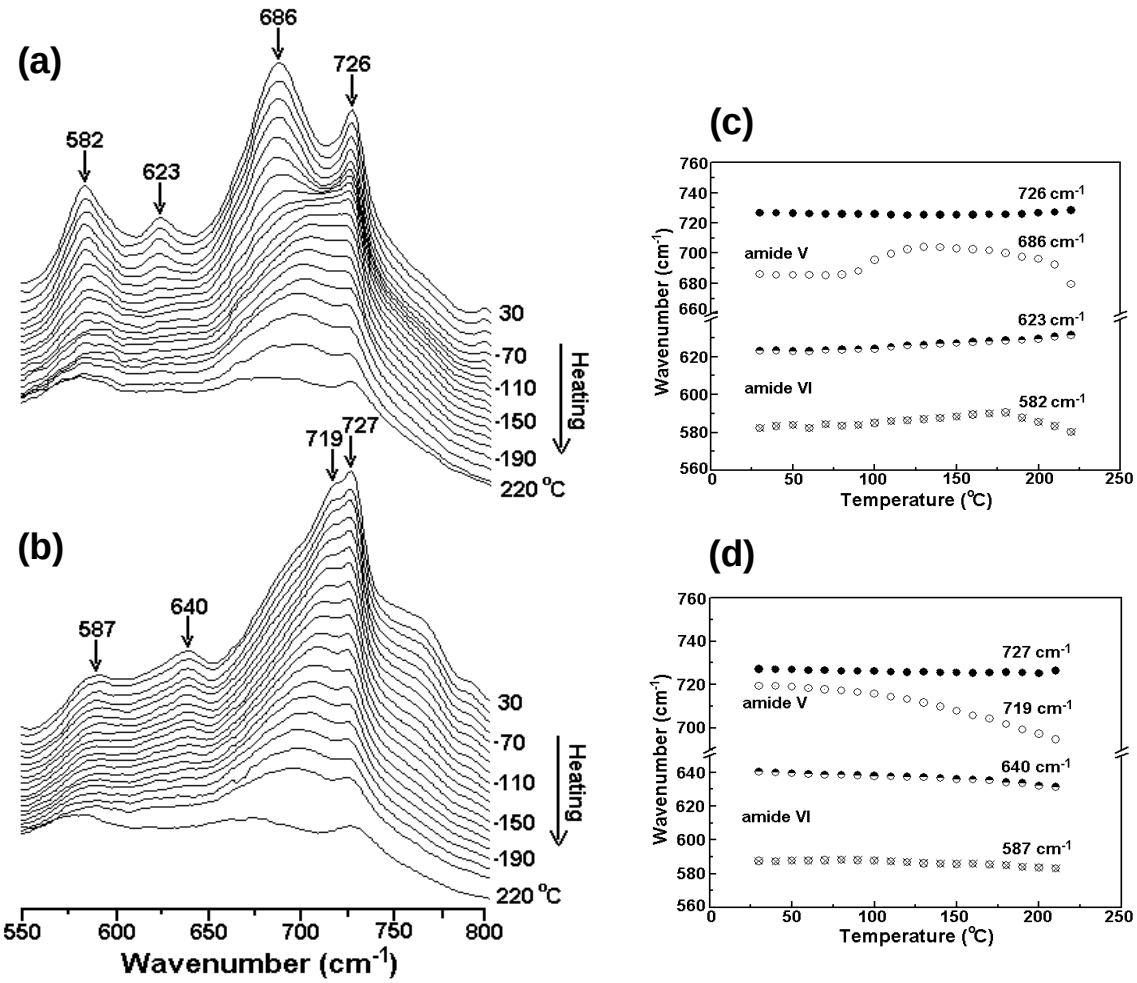

Figure 4.8: Variable temperature FTIR spectra of the region 500–800 cm^{-1} of nylon-6,7 during heating from room temperature to melt for (a) 1,4-butanediol crystallized, and (b) melt-crystallized samples. The variation of the wavenumber of amide V and amide VI bands during heating for (c) 1,4-butanediol crystallized, and (d) melt-crystallized samples.

butanediol crystallized sample, which is predominantly in the γ phase, shows the amide V band at 686 cm^{-1}. In the case of the γ phase of nylon-6, the amide V band occurs at 710 cm^{-1}.[14] Similar to the γ phase of nylon-6[15] the γ phase of the 1,4-butanediol crystallized nylon-6,7 sample shows the amide VI band at 623 cm^{-1} along with a distinct additional band at 582 cm^{-1}. The WAXS results indicate the presence of both the α and γ phases at room temperature. On heating, the amide VI bands at 582 and 623 cm^{-1} do not show any appreciable shift in wavenumber but the band intensity decreases appreciably. The amide V band at 686 cm^{-1} shows a very complicated behaviour as shown in Figure 4.8c. The wavenumber increases with increasing temperature up to 120 °C and on further heating it again decreases. It may be noted that the WAXS data showed that the small

fraction of the α phase vanished at about 140 °C. The band at 726 cm^{-1} assigned to the methylene-rocking mode, which arises from the orthorhombic packing cell of the methylene segments,[7,16,17] does not change with temperature. The behaviour of the melt-crystallized sample is different from the 1,4-butanediol crystallized sample as seen in Figure 4.8b. For this sample the amide V band occurs at 719 cm^{-1} and the amide VI bands at 587 and 640 cm^{-1}. These differences in the spectra show that the molecular conformations are different for the γ phase obtained by the 1,4-butanediol crystallized sample and the melt-crystallized sample, even though the WAXS patterns look alike. On heating the amide VI bands shows decrease in intensity without any shift in the position. But the amide V band shifts to lower wavenumber as shown in Figure 4.8d.

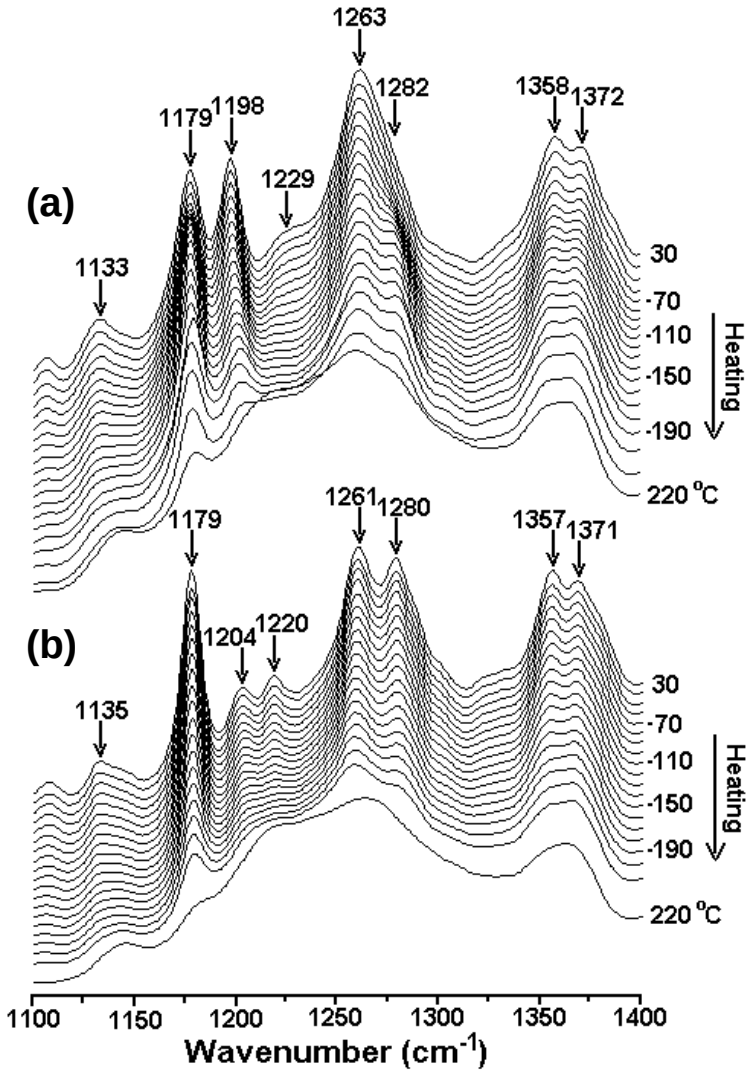

Figure 4.9: Variable temperature FTIR spectra of the region 1100–1400 cm^{-1} of nylon-6,7 during heating from room temperature to melt for (a) 1,4-butanediol crystallized, and (b) melt-crystallized samples.

The region from 1100 to 1400 cm^{-1} is characterized by the progression bands from the methylene sequence. At room temperature the bands appear at 1133, 1179, 1198, 1229, 1263, 1282, 1358, 1372 cm^{-1} for the 1,4-butanediol crystallized sample, and 1135, 1179, 1204, 1220, 1261, 1280, 1357, 1371 cm^{-1} for the melt-crystallized sample as shown in Figure 4.9 a and b, respectively. Upon heating almost all these bands show minor shift in position and decrease in absorbance. The 1198 cm^{-1} band assigned to CH_2 twisting is seen in the solution-cyrstallized sample, but is absent in the melt-crystallized sample. Similar to the γ phase of nylon-6,[14] the spectra of the melt- crystallized sample show bands at 1204 and 1220 cm^{-1}, which is characteristic of the γ phase. In both the samples the wavenumber of the band at 1179 cm^{-1} seems to remains constant on heating up to melting. However, the 1198 cm^{-1} band seen in the 1,4-butanediol crystallized sample seems to shift to slightly higher wavenumber with increase in temperature. The absorbance decreases with increasing temperature for the bands at 1179 and 1198 cm^{-1}. In the 1,4-butanediol crystallized sample the bands at 1263 and 1282 cm^{-1} show minor shift in position on heating and the intensity of the band at 1282 cm^{-1} develops on heating after about 110 °C. However in the case of the melt-crystallized sample the bands at 1261 and 1280 cm^{-1} seem to have comparable intensities at room temperature. The absorbance decreases with increasing temperature for these bands.

The regions sensitive to hydrogen bonding are from 1500 to 1800 cm^{-1} and from 3000 to 3600 cm^{-1}. The region 1500 to 1800 cm^{-1} is shown in Figure 4.10a and b for the 1,4-butanediol crystallized and melt-crystallized samples, respectively, and contains the amide I and amide II bands. The amide I band appears at almost the same position for both the samples, 1636 cm^{-1} for the 1,4-butanediol crystallized sample and 1637 cm^{-1} for the melt-crystallized sample. The amide I band arises from the stretching of the carbonyl groups and the band has contribution from the hydrogen bonded carbonyl groups in the crystalline region (ordered), the hydrogen bonded carbonyl groups in the amorphous region (disordered) and the non hydrogen bonded carbonyl groups (free). Because of the contribution from the different carbonyl groups outlined above, the band usually appears highly asymmetric. Visual inspection of the Figure 4.10a and b shows that the behavior of the amide I band looks very similar for both the samples at room temperature and on heating. The amide II band appears at 1547 and 1558 cm^{-1} for the 1,4-butanediol crystallized and melt-crystallized samples, respectively. The amide II band arises mainly

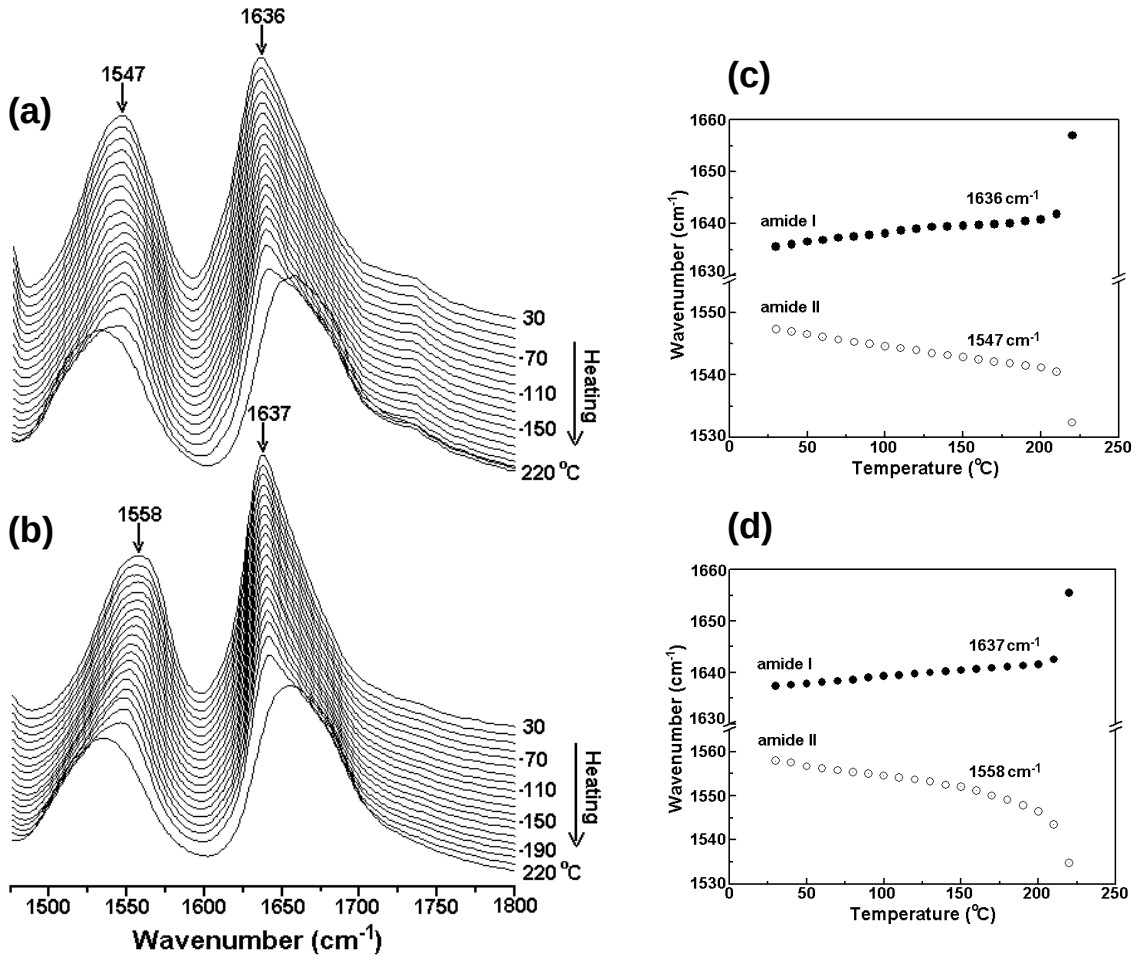

Figure 4.10: Variable temperature FTIR spectra of the region 1500–1800 cm^{-1} of nylon-6,7 during heating from room temperature to melt for (a) 1,4-butanediol crystallized, and (b) melt-crystallized samples. The variation of the wavenumber of amide I and amide II bands during heating for (c) 1,4-butanediol crystallized, and (d) melt-crystallized samples.

from the in-plane N–H bending and has contributions from ordered, disordered and free N–H groups. Consequently, the amide II band also appears highly asymmetric. Due to the uncertainty in the position of the individual bands, deconvolution of the peak into individual components is not attempted, and the band is treated as a single peak. Figure 4.10c and d shows the behavior of the band position during heating for the 1,4-butanediol crystallized and melt-crystallized samples, respectively. Both the samples show a similar trend in the wavenumber shift of the amide I and amide II bands. The amide I band of both the samples shifts slightly to higher wavenumbers on heating. The amide II band of both the samples, however, shifts to lower wavenumber on heating. The shift is more pronounced in the melt-crystallized sample.

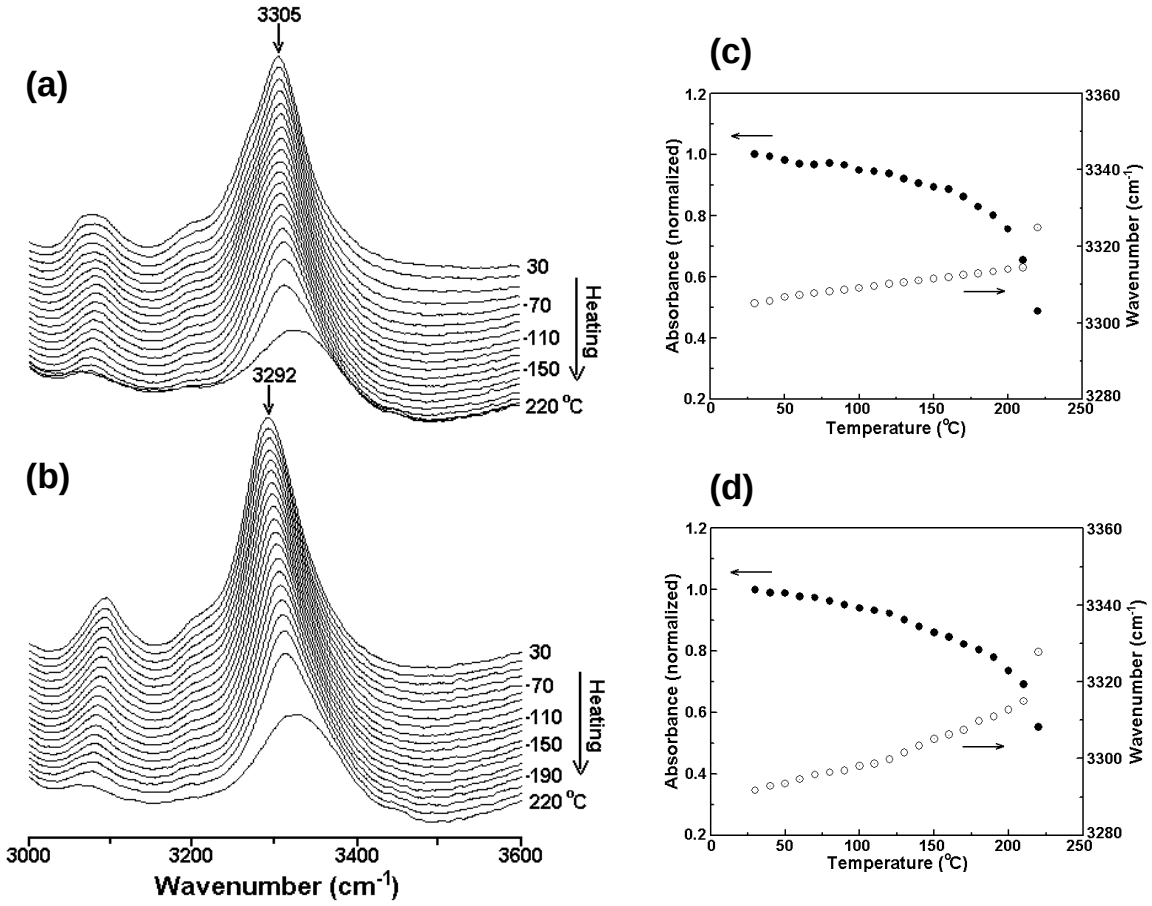

Figure 4.11: Variable temperature FTIR spectra of the region 3000–3600 cm^{-1} of nylon-6,7 during heating from room temperature to melt for (a) 1,4-butanediol crystallized, and (b) melt-crystallized samples. The variation of the wavenumber and normalized absorbance of amide A band during heating for (c) 1,4-butanediol crystallized, and (d) melt-crystallized samples.

The amide A band is assigned to the N–H stretching vibration and is sensitive to the strength of the hydrogen bond. The contribution to the amide A comes from i) free N–H stretch at 3444 cm^{-1} ii) bonded N–H stretch at 3300 cm^{-1} arising out of crystalline fraction iii) bonded N–H stretch at 3310 cm^{-1} arising out of amorphous fraction. Figure 4.11a and b shows the variation in the spectra during heating for the 1,4-butanediol crystallized and melt-crystallized samples, respectively. The region is too broad to deconvolute meaningfully into individual peaks and hence is discussed as a composite peak. The amide A band appears at 3305 cm^{-1} for the 1,4-butanediol crystallized sample which comprises both α and γ phases at room temperature. It shifts to a lower wavenumber of 3292 cm^{-1} for the melt-crystallized sample, which exists in the γ phase at room temperature. The amide A band, in general is sharp and skewed and cannot be approximated to Gaussian profile. However, it may be noted that in nylon-11 sample cast from 1,1,1,3,3,3-hexafloro-2-

propanol a symmetrical profile was observed.[18] Figure 4.11c and d shows the variation of the wavenumber and absorbance of the amide A band during heating for both the samples. In the case of the 1,4-butanediol crystallized sample, the peak position shifts to higher wavenumber in a linear fashion until melting and after melting the peak shifts to 3325 cm^{-1}. The normalized area decreases progressively with increase in temperature, however close to melting it decreases rapidly. The melt-crystallized sample shows a similar behavior; nevertheless minor variations are seen. The wavenumber increases with increase in temperature, but more pronounced increase is above 110 ^{o}C. After melting the peak shifts to 3328 cm^{-1}. The integrated absorbance decreases progressively with increase in temperature, with a rapid decrease near melting.

4.3.2 Studies on Nylon-6,9

4.3.2.1 NMR Studies

Figures 4.12 and 4.13 show the ^{1}H and ^{13}C NMR spectra of the commercially obtained nylon-6,9, respectively, and compare well with the ^{1}H and ^{13}C NMR spectra of nylon-6,7. The chemical shifts at 3.87 and 3.03 ppm originate from the methylene protons adjacent to the amide group i.e., –CONHC$\underline{H}_2$– and –C$\underline{H}_2$CONH–, respectively. The other methylene protons in the repeat unit of the polymer show chemical shifts in the range 1.75 to 2.08 ppm. As shown in Figure 4.12, the ratio of integration (4:4:18) matches with the number of methylene protons in the repeat unit of the polymer. The peaks at 4.72 ppm and 11.18 ppm were due to the solvents D_2O and TFA-*d*, respectively.

The ^{13}C NMR spectrum (Figure 4.13) shows a chemical shift at 180.89 ppm, which corresponds to the carbonyl carbon of the amide group (–$\underline{C}$ONH–). The carbon atoms adjacent to the amide group show chemical shifts at 44.09 ppm (–CONH$\underline{C}H_2$–) and 34.87 ppm (–$\underline{C}H_2$CONH–). The chemical shifts below 30 ppm were assigned to the rest of the carbons of the alkylene segment. The peaks at 163 ppm and 116 ppm correspond to the carbon atoms of the carbonyl group and $\underline{C}$F3 group of the solvent TFA-*d*.

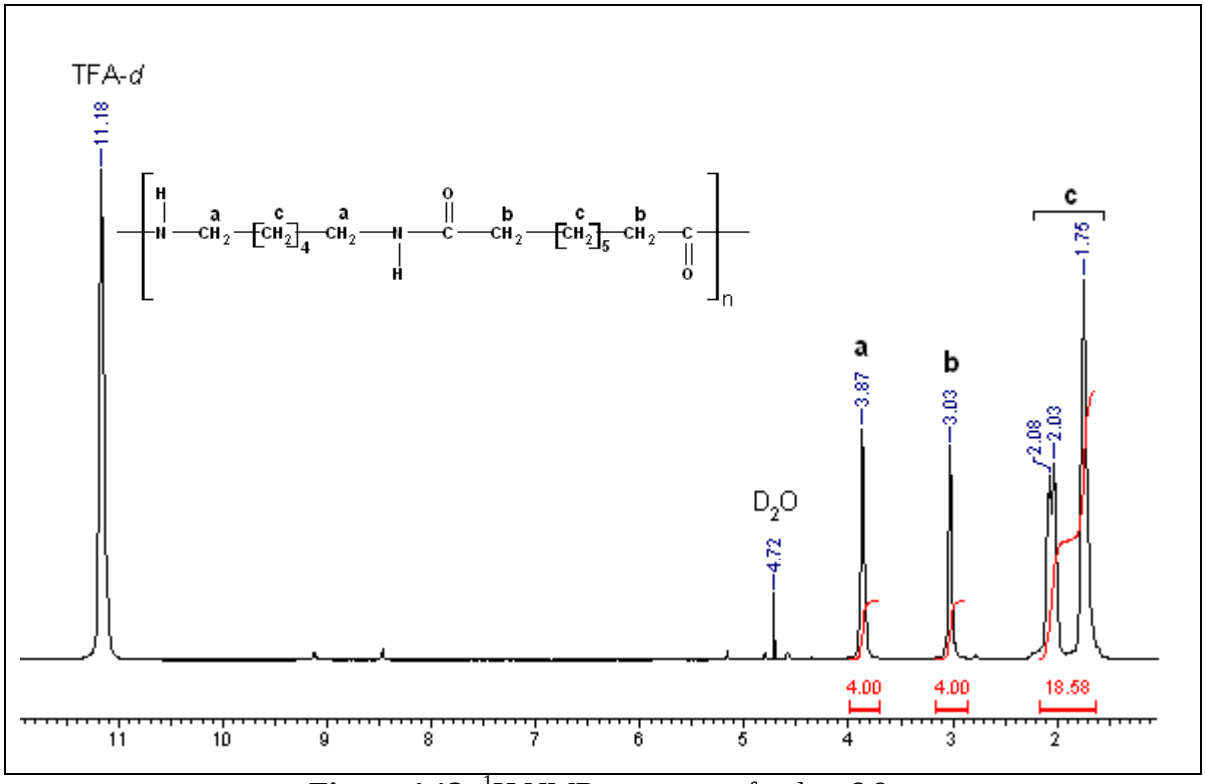

Figure 4.12: ^{1}H NMR spectrum of nylon-6,9.

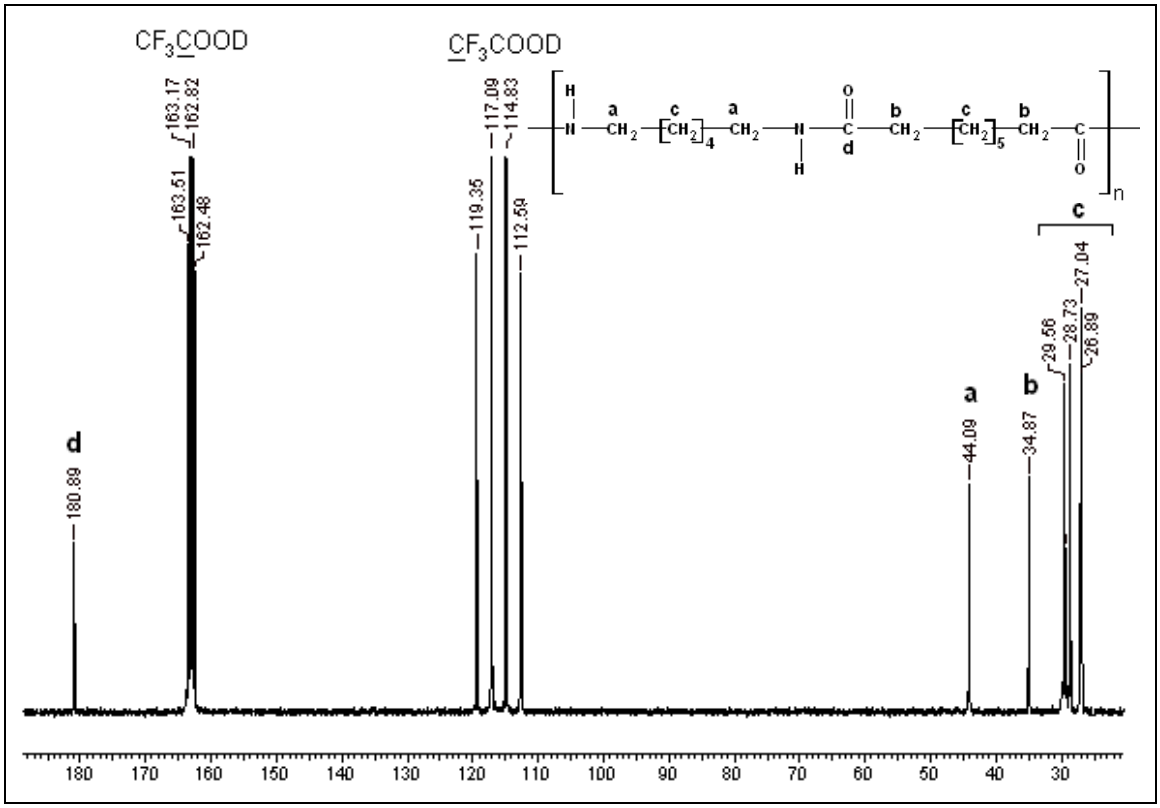

Figure 4.13: ^{13}C NMR Spectrum of nylon-6,9.

4.3.2.2 Thermal Analysis

Figure 4.14 shows the DSC thermograms comprising a sequence of three scans performed with the nylon-6,9 sample crystallized in 1,4-butanediol. In the first run (a), the sample was heated (10 °C/min) through fusion to 240 °C, and left in the melt for 1 min, and was cooled (10 °C/min) to observe crystallization from the melt (b). The second heating (c) represents the melt-crystallized sample. The first heat, which corresponds to the 1,4-butanediol crystallized sample, shows three melting peaks. This behavior can be associated with reorganization during heating of different populations of lamellar crystals. The transition observed on heating is reproducible, thus indicating thermal stability of the sample. Comparison between (a) and (c) indicates a greater reorganization during heating for the melt-crystallized samples or a preferential crystallization from the melt in the high-temperature state. Figure 4.14c shows only the high temperature peak (T_m = 209 °C) associated with the more stable 'reorganized' state comprised of thicker and/or more perfect crystals. The T_m of nylon-6,9 was found to be less than that of nylon-6,7 due to lower hydrogen bond density, which is determined by the methylene segment length between the amide groups.

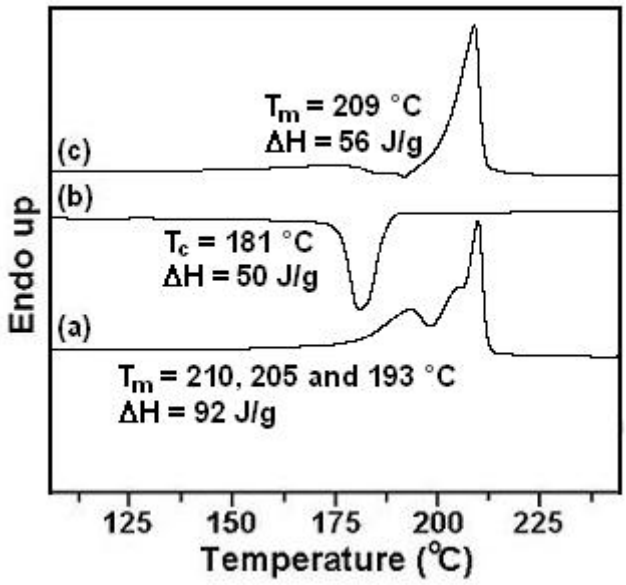

Figure 4.14: The DSC thermograms obtained during (a) first heating, (b) cooling, and (c) reheating, for nylon-6,9 crystallized in1,4-butanediol.

4.3.2.3 Variable Temperature WAXS Studies

The room temperature diffraction pattern of the nylon-6,9 sample crystallized in 1,4-butanediol shows the characteristic reflections of nylons at 2θ = 20.63 and 23.71°. In even-odd nylons, hydrogen bonds between the neighboring molecular chains are not saturated if the methylene units adopt the extended conformation in the crystals. Therefore, nylon-6,9 has a different crystal structure from the even-even nylons though the WAXS patterns are similar. These reflections may be indexed as 110 and 200, respectively, based on the monoclinic unit cell.[2] The results exclude the γ phase structure reported by Kinoshita[4] for even-odd nylons, that presents a characteristic diffraction at *d* spacing of 0.42 nm. The behavior of the diffractograms and the *d* spacings of the α phase on heating from room temperature to melt is shown in Figure 4.15a and b, respectively. It is seen from the figure that, on heating, the two-peak nature of the diffractogram is preserved until melting, indicating no crystalline transition before melting. The change in the *d* spacings of the 110 and 200 reflections with increase in temperature is similar to the behavior of *d* spacings in the even-even nylons such as nylon-6,6, nylon-6,10, and nylon-6,12. The *d* spacing of the 200 reflection shows a rapid increase after 120 °C and approaches the 110 reflection. However, above 190 °C the *d* spacing of the 200 reflection does not change but remains constant. The *d* spacings are 0.423 and 0.405 nm, respectively, for the 110 and 200 reflections. These values are similar to the *d* spacing of the γ phase. This indicates that the α phase transformed into the γ phase at about 190 °C. Interestingly, at about 190 ^{o}C a small peak appears at $2\theta = 20.60^{o}$, with a *d* spacing value of 0.431 nm. The *d* spacing of this peak increases with increase in temperature. As with nylon-6,7, this peak may be attributed to the formation of metastable phase at high temperatures and is stable until melting. The 004 reflection shows a peak at 2θ = 10.86° and the corresponding *d* spacing is 0.814 nm. On heating the *d* spacing increases with increase in temperature up to 190 °C. At 190 °C the α phase transforms into the γ phase, and the 004 *d* spacing changes from 0.855 nm into 0.955 nm. At this juncture, it is worth pointing out that the heating thermogram (Figure 4.14a) of the sample shows a minor endotherm at about 190 °C.

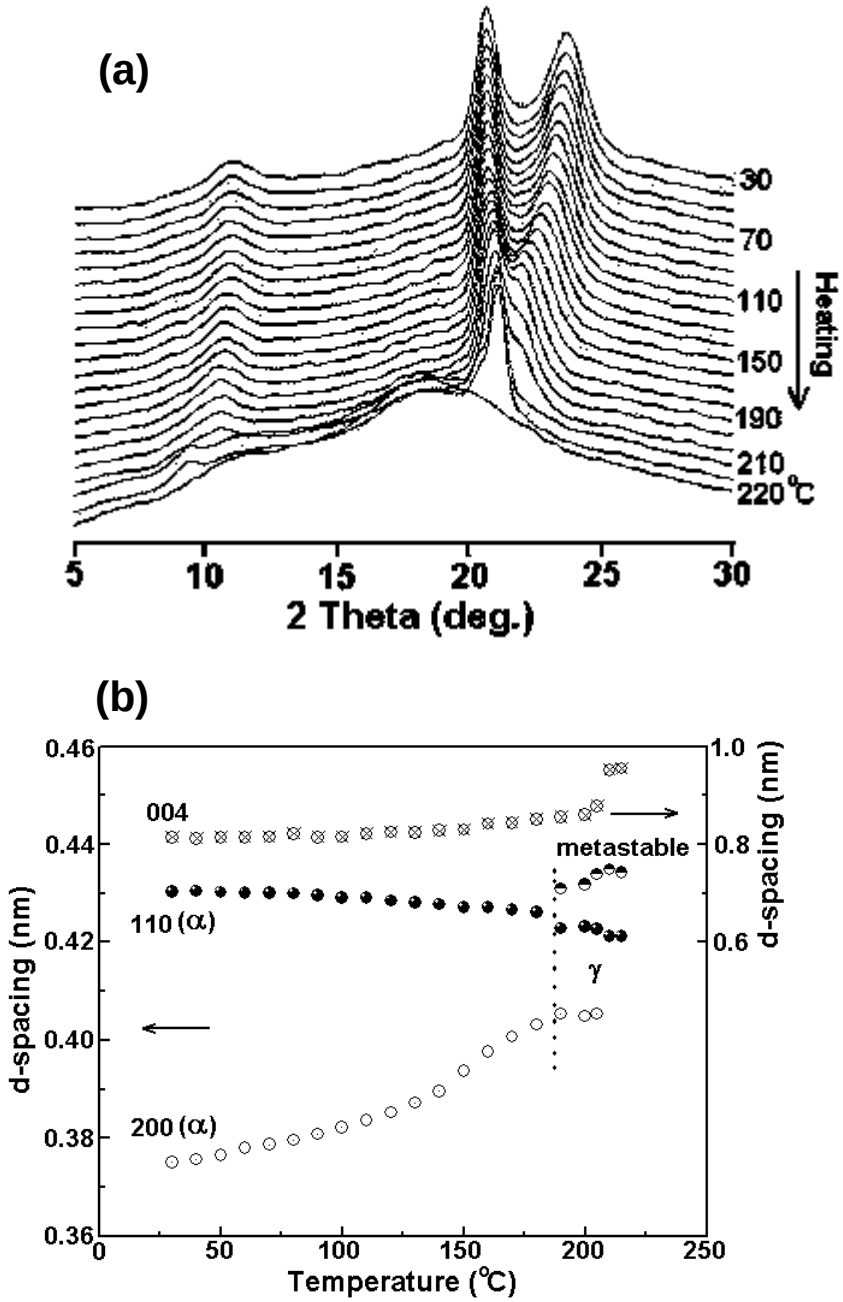

Figure 4.15: Behavior of (a) XRD patterns and (b) *d* spacings on heating from room temperature to melt for nylon-6,9 crystallized in 1,4-butanediol.

The behavior of the diffractograms and *d* spacings of the sample crystallized at 205 °C and on cooling from the T_c at 205 °C to room temperature are shown in Figure 4.16a-c, respectively. As seen in Figure 4.16a, though the diffractogram recorded after the completion of crystallization at 205 °C appears to have a single peak at 2θ = 20.98°, the profile fitting procedure clearly indicates the presence of two shoulder peaks at 2θ = 20.47 and 21.30°. The corresponding *d* spacings of the three reflections at 2θ = 20.47, 20.98 and

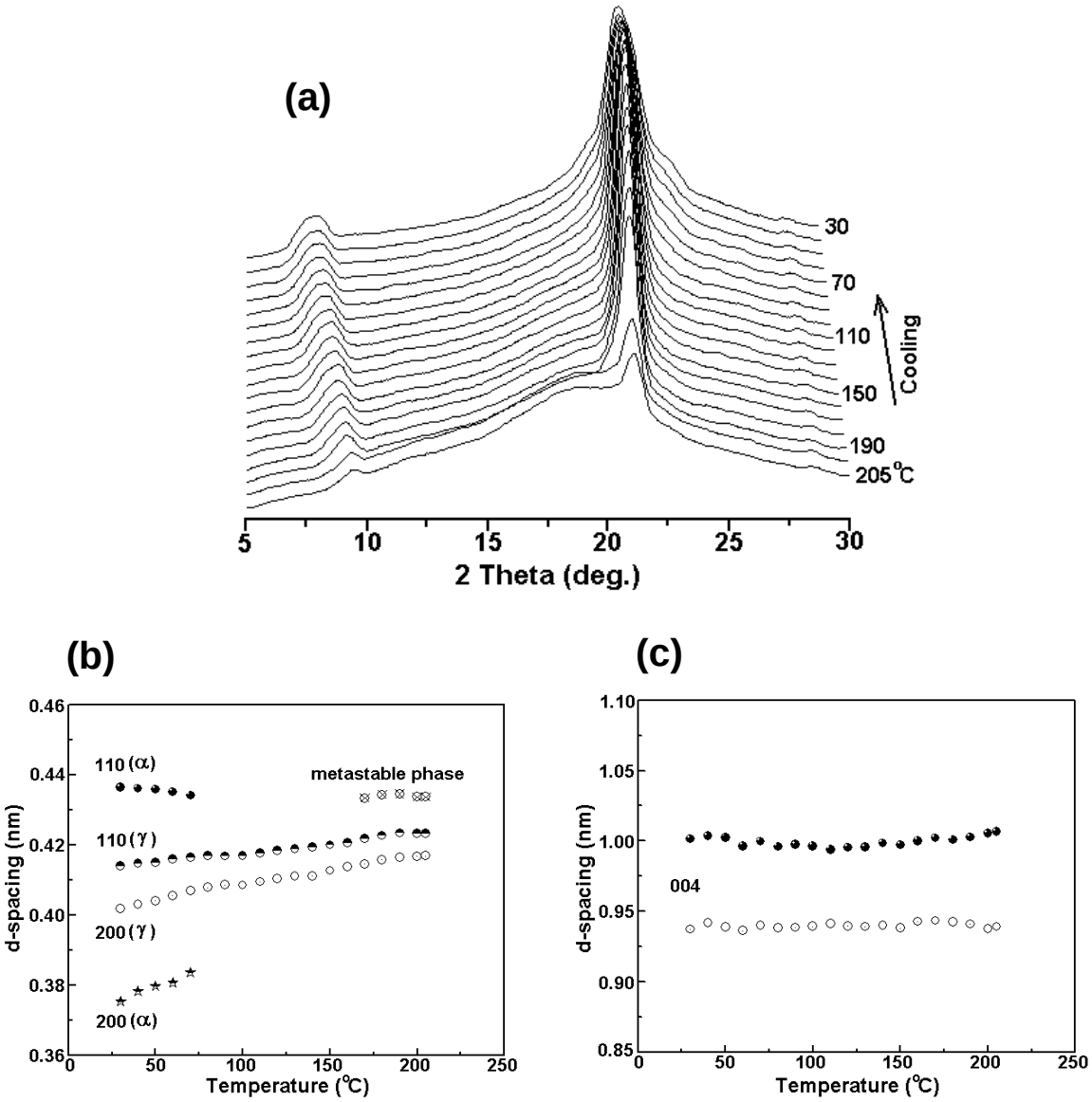

Figure 4.16: Behavior of (a) XRD patterns, (b) *d* spacings of nylon-6,9 melt-crystallized at 205 °C on cooling to room temperature, and (c) *d* spacings of the 001 reflection on cooling from T_c to room temperature.

21.30° are 0.434, 0.423, and 0.417 nm, respectively. The peaks at 2θ = 20.98 and 21.30° can be assigned to the 110 and 200 reflections of the γ phase, respectively. The peak at 2θ = 20.47° is indicative of the presence of the metastable phase and it can be concluded that during the isothermal crystallization at 205 °C, both the metastable and the γ phase are formed simultaneously. However the fraction of the metastable phase is very less compared to γ phase. The characteristic peaks of the γ phase at 2θ = 20.98 and 21.30° show a small shift toward higher angles on cooling to room temperature as shown in

Figure 4.16b. The peak due to the metastable phase at $2\theta = 20.47^{o}$ remains almost constant and disappears around 170 ^{o}C. Though the crystallization of nylon-6,9 is predominantly in the γ phase, on cooling to room temperature, the α phase is also formed to some extent. The peaks of the α phase are clearly seen at 70 ^{o}C. At room temperature the amount of the γ phase is about 35% and that of the α phase is about 5%. The 004 reflection shows two peaks at 2θ = 8.78 and 9.41° corresponding to the *d* spacings of 1.006 and 0.939 nm, thus indicating the presence of both the α and γ phases in the melt-crystallized sample. However the α phase is more obvious below 100 °C, when the peaks due to the α phase move out of the peaks due to the γ phase. The position of the peaks does not change on cooling to room temperature as shown in Figure 4.16c.

Parts a and b of Figure 4.17 show diffractograms and *d* spacings of the melt-quenched sample on heating from room temperature. The diffractogram recorded at room temperature appears to have a single broad peak, similar to the amorphous material. But profile fitting the broad peak makes the crystalline peak at $2\theta = 21.33°$ obvious, and the *d* spacing is at 0.416 nm. Single peak nature of the diffractogram indicates that the sample crystallized in the psuedohexagonal phase on quenching from the melt. On heating, the peak at $2\theta = 21.33°$ becomes sharper indicating that the crystals become more perfect, and the peak position shifts to lower angles. The *d* spacing remains constant after 150 °C and the sample melts in the psuedohexagonal phase. At about 160 °C, the peak due to the metastable phase at $2\theta = 20.07°$ starts appearing. The metastable phase remains stable till the sample is melted.

The behavior of the sample is different, however, if the sample is not allowed to melt but held at a temperature below the T_m and then cooled to room temperature. The diffractograms obtained on cooling from the holding temperature 175 °C is shown in Figure 4.18a. The metastable phase, which appears as a shoulder to the psuedohexagonal phase, disappears at about 160 °C on cooling. An additional peak appears at $2\theta = 21.63°$ immediately on cooling and the corresponding *d* spacing is 0.411 nm. The *d* spacing values 0.411 and 0.424 nm indicate that the psuedohexagonal structure transforms into γ phase immediately on cooling and the behaviour is similar to nylon-6,7. On cooling the *d* spacings decrease with decrease in temperature, as shown in Figure 4.18b. At room

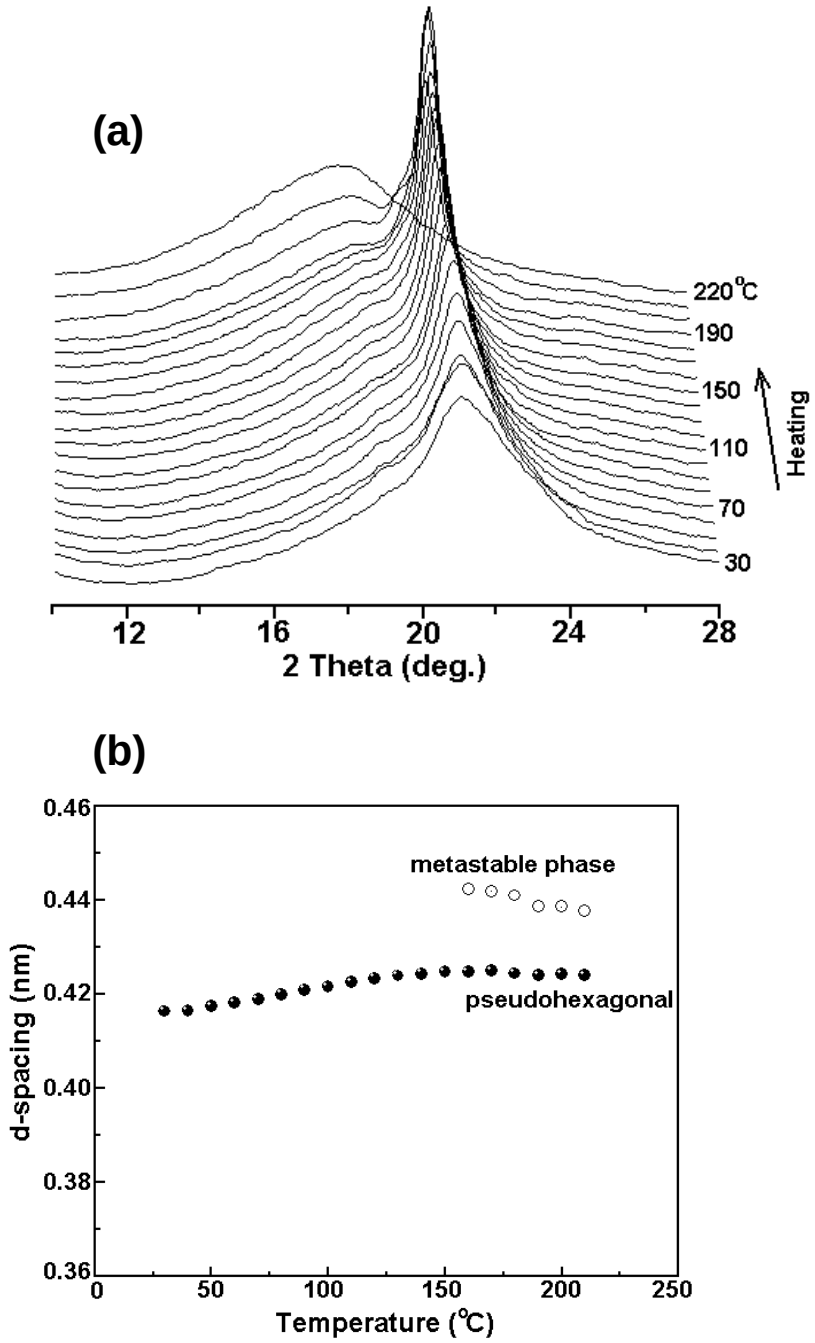

Figure 4.17: Behavior of (a) XRD patterns and (b) *d* spacings on heating from room temperature to melt for quenched nylon-6,9.

temperature the *d* spacings of the γ phase are 0.419 and 0.399 nm. Also at about 120 °C, a new peak appears at 2θ = 21.92° and this peak moves to higher values on cooling. At room temperature it occurs at 2θ = 23.34° and the *d* spacing is 0.381 nm. From the position of the peak it can be assigned to the α phase, however, the amount of material transformed into α phase is very less compared to the γ phase.

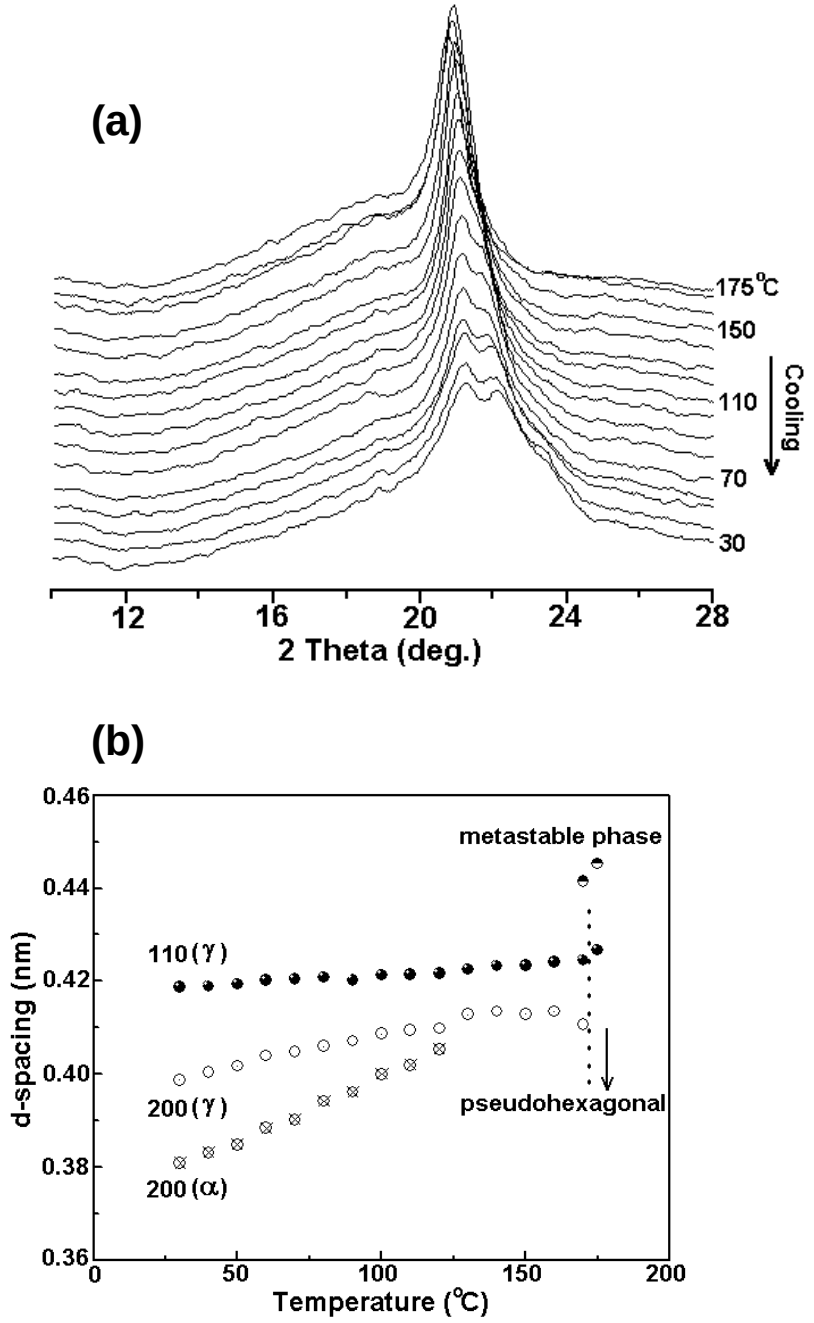

Figure 4.18: Behavior of (a) XRD patterns and (b) *d* spacings of the melt-quenched nylon-6,9 sample on cooling from the holding temperature 175 °C to room temperature.

4.3.2.4 Variable Temperature FTIR Studies

Figure 4.19a and b shows the spectral region from 500 to 800 cm^{-1} for the sample crystallized in 1,4-butanediol and the melt-crystallized sample, respectively. At room temperature the amide V and amide VI bands appear at 689 and 581 cm^{-1}, respectively, for the 1,4-butanediol crystallized sample, which indicates that it exists in the α phase. The

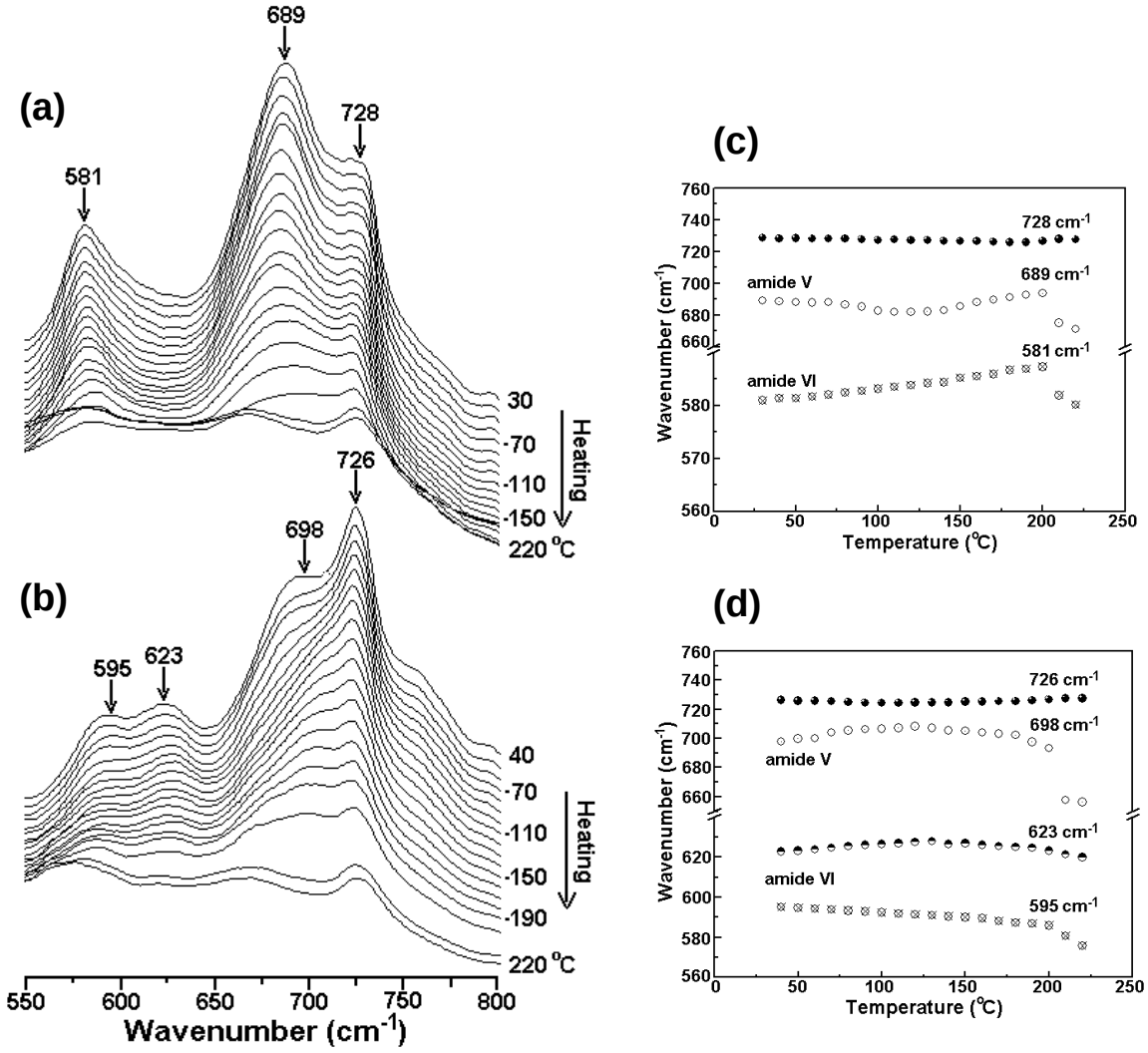

Figure 4.19: Variable temperature FTIR spectra of the region 500–800 cm^{-1} of nylon-6,9 during heating from room temperature to melt for (a) 1,4-butanediol crystallized, and (b) melt-crystallized samples. The variation of the wavenumber of amide V and amide VI bands during heating for (c) 1,4-butanediol crystallized, and (d) melt-crystallized samples.

variation of amide V and amide VI band positions on heating for the1,4-butanediol crystallized sample is shown in Figure 4.19c. On heating, the wavenumber of the amide V band shows a slight decrease and then increase and close to the T_m the wavenumber again starts to decrease. The wavenumber of the amide VI band, however, shows a gradual increase and again close to the T_m starts to decrease. The band at 728 cm^{-1} assigned to the methylene-rocking mode, appears to be invariant towards heating.[7,16,17]

The behaviour of the melt-crystallized sample is different from the 1,4-butanediol crystallized sample. The amide V band occurs at 698 cm^{-1}, which can be assigned to the γ phase. As in the case of γ phase of nylon-6, the amide VI band for the melt-crystallized sample occurs at 623 cm^{-1} along with a distinct additional band at 595 cm^{-1}.[15] These results indicate that the melt-crystallized sample at room temperature exists in the γ phase. However the WAXS results indicate the presence of the α and γ phases for the melt-crystallized sample at room temperature, which is not evident from the FTIR results. On heating the amide V band at 698 cm^{-1} shows a gradual increase up to about 80 °C and on further heating remains constant and starts to decrease close to melting. It may be pointed out here that the α phase seen in melt-crystallized sample at room temperature in the WAXS results, disappears at about 80 °C. The amide VI bands at 595 cm^{-1} and 623 cm^{-1} show similar behavior, they show a slight decrease with increasing temperature as shown in Figure 4.19d.

In the region 1100 to 1400 cm^{-1} characterized by the progression bands from the methylene sequence the bands appear at 1112, 1138, 1179, 1193, 1211, 1230, 1246, 1259, 1287, 1308, 1335, 1371 cm^{-1} for the 1,4-butanediol crystallized sample, and 1112, 1126, 1179, 1195, 1218, 1251, 1265, 1280, 1300, 1319, 1332, 1369 cm^{-1} for the melt-crystallized sample, at room temperature, as shown in Figure 4.20a and b, respectively. In the 1,4-butanediol crystallized sample the bands at 1179 and 1193 cm^{-1} seem to have comparable intensities at room temperature. However in the melt-crystallized sample the band at 1179 cm^{-1} is sharp and seems to have high intensity as compared to the band at 1195 cm^{-1} at room temperature. The 1193 and 1195 cm^{-1} bands are assigned to CH_2 twisting. Upon heating almost all these bands show minor shift in position and decrease in absorbance.

Another region of interest is from 1500 to 1800 cm^{-1}, which is sensitive to hydrogen bonding. The region is shown in Figure 4.21a and b for the 1,4-butanediol crystallized and melt-crystallized samples, respectively, and contains the amide I and amide II bands. The amide I band appears at almost the same position for both the samples, 1637 cm^{-1} for the 1,4-butanediol crystallized sample and 1636 cm^{-1} for the melt-crystallized sample. The amide I band arises from the stretching of the carbonyl groups. Because of the contribution from the different carbonyl groups the band usually appears highly asymmetric. Visual inspection of the Figure 4.21a and b shows that the amide I band for the 1,4-butanediol crystallized sample is broad and skewed, as compared to the amide I band for the melt-

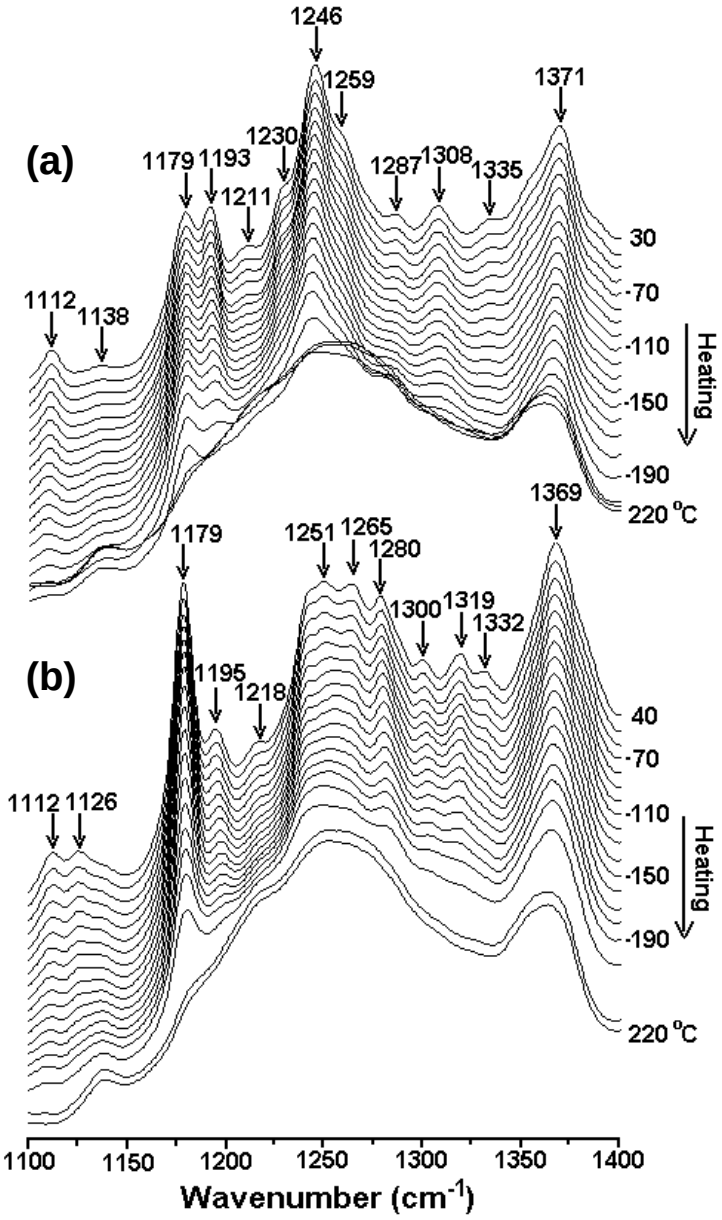

Figure 4.20: Variable temperature FTIR spectra of the region 1100–1400 cm^{-1} of nylon-6,9 during heating from room temperature to melt for (a) 1,4-butanediol crystallized, and (b) melt-crystallized samples.

crystallized sample, which is sharp and skewed. However their behavior looks very similar at room temperature and on heating. The amide II band appears at 1539 and 1549 cm^{-1} for the 1,4-butanediol crystallized and melt-crystallized samples, respectively. The band shifts to 1549 cm^{-1} for the γ phase. The amide II band arises mainly from the in-plane N–H bending and has contribution from the different N–H groups, consequently it also appears highly asymmetric. Due to the uncertainty in the position of the individual bands, the band

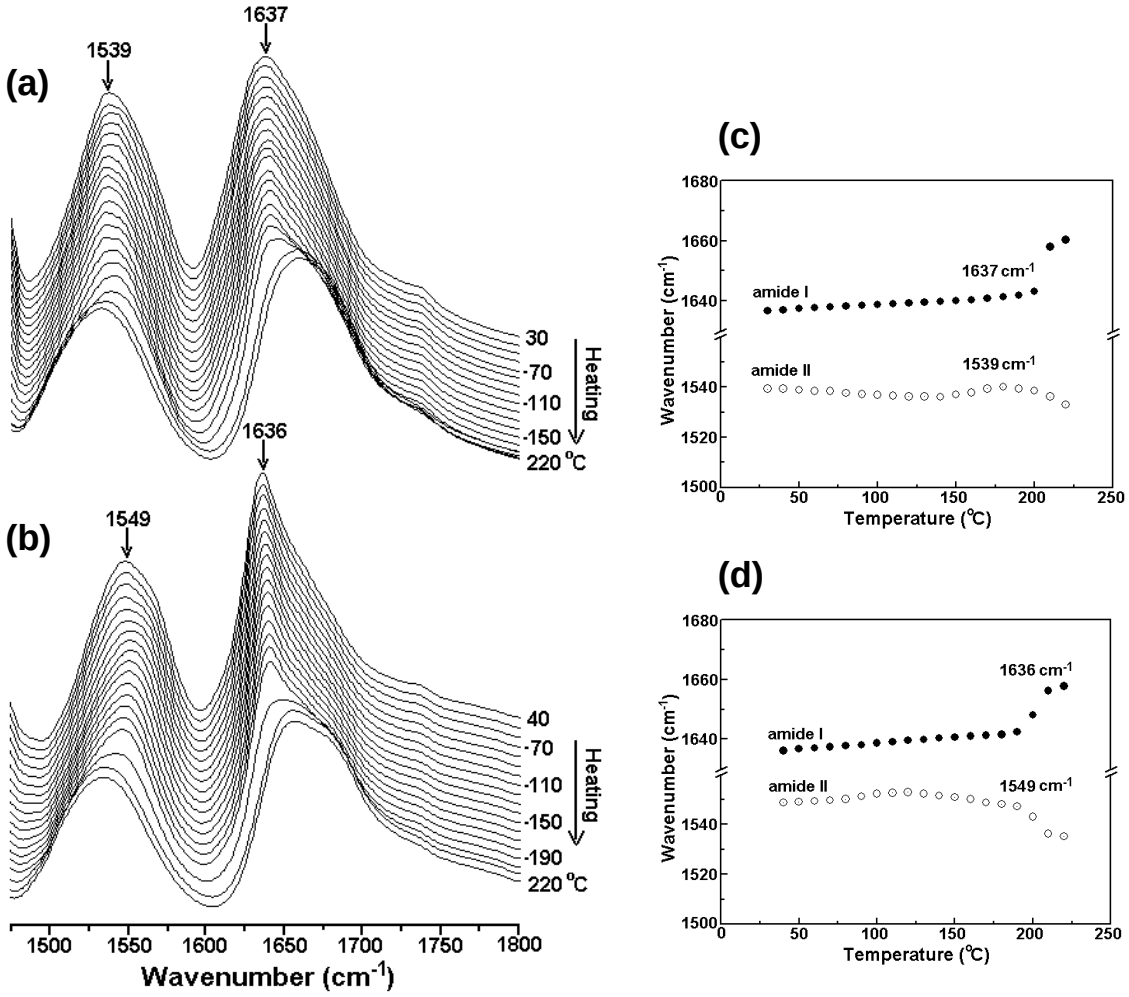

Figure 4.21: Variable temperature FTIR spectra of the region 1500–1800 cm^{-1} of nylon-6,9 during heating from room temperature to melt for (a) 1,4-butanediol crystallized, and (b) melt-crystallized samples. The variation of the wavenumber of amide I and amide II bands during heating for (c) 1,4-butanediol crystallized, and (d) melt-crystallized samples.

is treated as a single peak. Figure 4.21c and d shows the behavior of the band position during heating for the 1,4-butanediol crystallized and melt-crystallized samples, respectively. The amide I band of both the samples shows a similar behavior. It shows a slight shift to higher wavenumbers on heating. The amide II band for the 1,4-butanediol crystallized sample initially shows a slight decrease, then increases on further heating and again decreases close to the T_m. However, the amide II band for the melt-crystallized sample shows a slight increase initially during heating and on further heating starts to decrease up to melting.

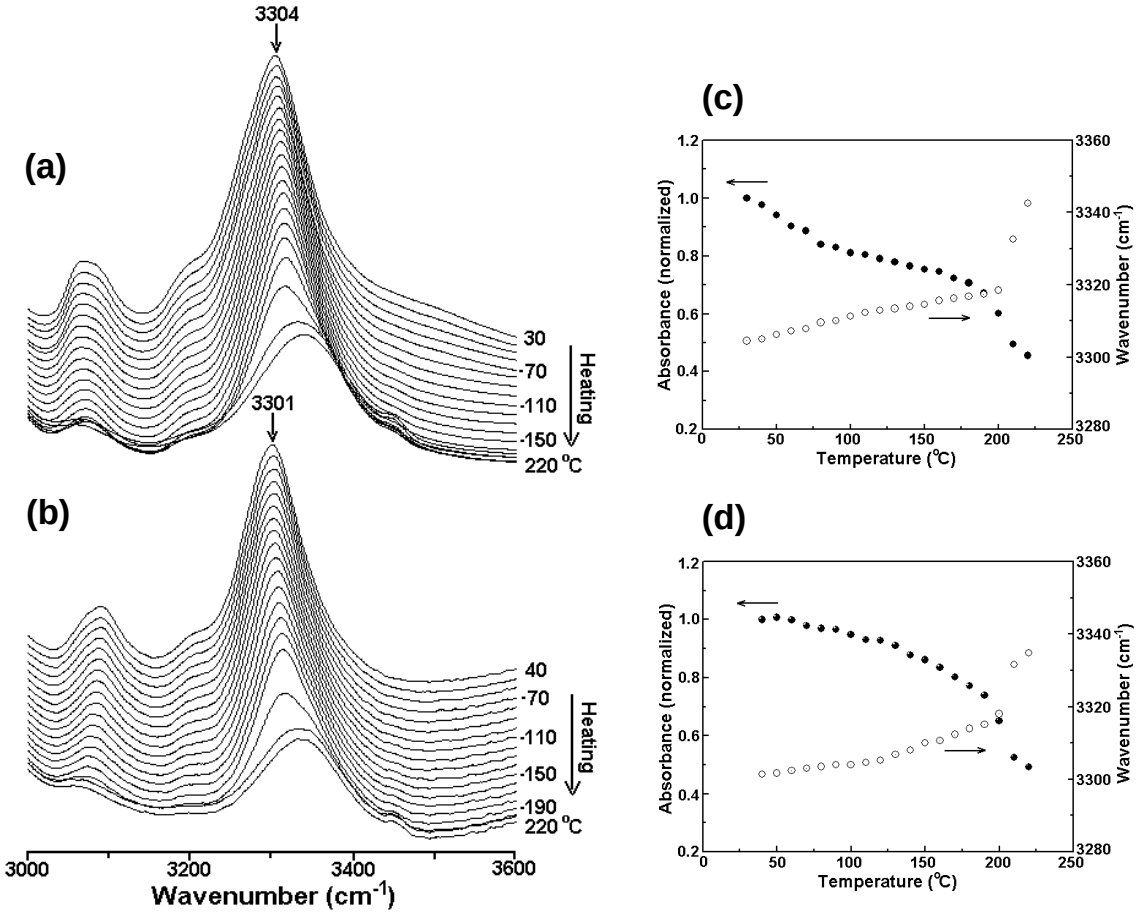

Figure 4.22: Variable temperature FTIR spectra of the region 3000–3600 cm^{-1} nylon-6,9 during heating from room temperature to melt for (a) 1,4-butanediol crystallized, and (b) melt-crystallized samples. The variation of the wavenumber and normalized absorbance of amide A band during heating for (c) 1,4-butanediol crystallized, and (d) melt-crystallized samples.

The amide A band assigned to the N–H stretching vibration, is also sensitive to the strength of the hydrogen bond. It has contribution from the different N–H groups. Hence the amide A band, in general is sharp and skewed. Figure 4.22a and b shows the variation in the spectra during heating for the 1,4-butanediol crystallized and melt-crystallized samples, respectively. The region is too broad and the position of the individual bands is uncertain. Hence deconvolution of the peak into individual components is not attempted, and the band is treated as a single peak. The amide A band position appears at 3304 cm^{-1} for the 1,4-butanediol crystallized sample and at 3301 cm^{-1} for the melt-crystallized sample, which is very close. Figure 4.22c and d shows the variation of the wavenumber and absorbance of the amide A band during heating for both the samples. In the case of the 1,4-butanediol crystallized sample, the peak position shifts to higher wavenumber in a

linear fashion until melting and after melting the peak shifts to 3343 cm^{-1}. The normalized area decreases with increasing temperature; initially the rate is more which slows down after 80 ^{o}C. Again close to melting it decreases rapidly. The melt-crystallized sample shows a similar behavior; nevertheless minor variations are seen. The wavenumber increases with increase in temperature, but more pronounced increase is above 120 ^{o}C. After melting the peak shifts to 3335 cm^{-1}. The integrated absorbance decreases progressively with increase in temperature, with a rapid decrease near melting. The FTIR spectra of the 1,4-butanediol crystallized and melt-crystallized samples show distinct differences similar to the WAXS studies.

4.4 Conclusion

Nylon-6,7 was synthesized by interfacial and melt polymerization techniques, and a detailed study was carried out on its crystalline transitions on heating and cooling using HTWAXS and HTFTIR. Crystalline transition studies were also carried out on nylon-6,9, a known even-odd nylon, with a chemical repeat unit close to nylon-6,7 using HTWAXS and HTFTIR. The results obtained were compared with that of nylon-6,7.

Nylon-6,7 precipitated in 1,4-butanediol crystallized predominantly into the γ phase with a small amount of α phase. On heating the γ phase remained invariant but the α phase transformed into the γ phase above 140 °C. The sample melted in the γ phase. Nylon-6,7 crystallized in the γ phase upon melt crystallization at 220 °C, and on cooling from the T_c it remained in the γ phase without any change. Apart from the γ phase, the metastable phase was also formed during melt crystallization. The metastable phase transformed into the γ phase on cooling at about 150 °C.

The melt-quenched sample, on the other hand, exhibited the psuedohexagonal phase. The psuedohexagonal phase was stable on heating. On heating, at about 190 °C, the metastable phase started appearing and coexisted with the psuedohexagonal phase until melting. If the psuedohexagonal phase was cooled without allowing it to melt, then it transformed into the γ phase. The transition temperature is dependent on the holding temperature. For the holding temperature 200 °C, the transition temperature was 180 °C and for the holding temperature 170 °C, the transition temperature was 130 °C.

Nylon-6,9 crystallized in the α phase when precipitated in 1,4-butanediol and on heating it transformed into the γ phase at about 190 °C. The γ phase was stable up to the melting temperature. During this transition a small amount of the material transformed into the metastable phase and was stable until melting. Upon melt crystallization at 205 °C nylon-6,9 crystallized in the γ phase. On cooling to room temperature the α phase was seen at about 70 °C. Melt-quenched nylon-6,9 crystallized into the psuedohexagonal phase and the phase was kept during heating. Similar to nylon-6,7, the metastable phase was formed at about 160 °C. On cooling from 175 °C, the psuedohexagonal phase transformed into the γ phase immediately.

The variable temperature FTIR studies indicated that in the case of nylon-6,7, the molecular conformation in the γ phases obtained by 1,4-butanediol crystallization and melt crystallization were different as evident from the spectral region 500 to 800 cm^{-1}. On the other hand nylon-6,9 crystallized in 1,4-butanediol showed spectra typical of the α phase, while the melt-crystallized sample showed spectra due to the γ phase.

4.5 References

1. Navarro, E.; Franco, L.; Subirana, J. A.; Puiggalı´, J. *Macromolecules* **1995,** *28,* 8742.
2. Franco, L.; Cooper, S. J.; Atkins, E. D. T.; Hill, M. J.; Jones, N. A. *J. Polym. Sci., Part B: Polym. Phys.* **1998,** *36,* 1153.
3. Navarro, E.; Subirana, J. A.; Puiggalı´, J. *Polymer* **1997,** 3*8,* 3429.
4. Kinoshita, Y. *Makromol. Chem.* **1959,** *33,* 1.
5. Wunderlich, B. *Macromolecular Physics;* Academic Press: New York, **1973.**
6. Miller, R. L. *Polymer Handbook,* 3rd ed.; Brandrup, J., Immergut, E. H., Eds.; Wiley-Interscience: New York, **1989;** Chapter VI.
7. Yoshioka, Y.; Tashiro, K.; Ramesh, C. *Polymer* **2003**, *44*, 6407.
8. Yoshioka, Y.; Tashiro, K. *J. Phys. Chem. B* **2003**, *107*, 11835.
9. Ramesh, C.; Gowd, E. B. *Macromolecules* **2001**, *34*, 3308.
10. Murthy, N. S.; Curran, S. A.; Aharoni, S. M.; Minor, H. *Macromolecules* **1991**, *24*, 3215.
11. Murthy, N. S. *Polym. Commun.* **1991**, *32,* 301.
12. Jakes, J.; Krimm, S. *Spectrochimica Acta* **1971**, *27A,* 19.

13. Jakes, J.; Krimm, S. *Spectrochimica Acta* **1971**, *27A,* 35.

14. Abu-isa, I. *J. Polym. Sci., Part A-1* **1971**, *9,* 199.

15. Nair, S.S.; Ramesh, C. *Macromolecules* **2005,** *38,* 454.

16. Snyder, R. G. *J. Chem. Phys*. **1979,** *71,* 3229.

17. Tashiro, K.; Sasaki, S.; Kobayashi, M. *Macromolecules* **1996,** *29,* 7460.

18. Skrovanek, D. J.; Painter, P.C.; Coleman, M. M. *Macromolecules* **1986,** *19,* 699.

CHAPTER 5

STUDIES ON THE CRYSTALLIZATION BEHAVIOR OF NYLON-6 IN THE PRESENCE OF LAYERED SILICATES USING VARIABLE TEMPERATURE WAXS AND FTIR

5.1 Introduction

Nylon-6 is commercially important and one of the prominent members of the polyamide class of semicrystalline polymers. The structure and morphology of nylon-6 have been extensively investigated. Nylon exhibits polymorphism, and the polymorph depends on the crystallization condition. At room temperature it shows two crystalline modifications, namely the α phase[1] and the γ phase.[2] However, the α phase is unstable at elevated temperatures and transforms into the α' phase, which is stable until melting.[3,4] On the other hand, the γ phase does not exhibit any crystalline transition on heating and is stable up to melting.[3] The α phase has a monoclinic structure[1] with a = 0.956 nm, b = 1.724 nm, c = 0.801 nm, and β = 67.5°. In the α phase, the hydrogen bonds are formed between anti-parallel chains.[1] The γ phase also has a monoclinic structure with a = 0.933 nm, b = 1.688 nm, c = 0.478 nm, and β = 121°, but the twisted chains allow hydrogen bonds to be formed between parallel chains.[2] The α phase is easily obtained by melt crystallization, while severe crystallization conditions need to be applied to obtain the γ phase. The α phase can be transformed into the γ phase by treatment with aqueous potassium iodide–iodine solution.[2,5-7] High-speed spinning also yields the γ phase.[7] In the case of nylon-6 fibers a metastable phase has also been reported and discussed in detail.[7]

Recently, it has been found that the γ phase is readily formed in nylon-6 nanocomposites, primarily the nylon-6–montmorillonite clay nanocomposites.[8-11] The relative fraction of α and γ phases is dependent on the layered silicate content as well as the interaction between nylon-6 and the silicate layers.[12] It has been shown that the silicate layers act as nucleating centers, and the interaction between the clay layers and the polymer changes its semicrystalline morphology.[13] It has been suggested that the clay surface induces kinetically favored formation of γ phase.[14] Wu and co-workers[15,16] have shown that higher cooling rates promote the crystallization of γ phase. They also reported higher amounts of γ phase when annealed at 200 °C as against 180 °C. Paul et al.[17] studied the crystallization behavior of nylon-6–clay nanocomposites and observed that in the case of injection-molded samples the γ phase predominates in the skin while the core contains both the phases, which is attributed to the different cooling rates of the skin and core regions.

Variable temperature wide-angle X-ray scattering (WAXS) is perhaps the most appropriate tool to study the crystalline phases and their transitions. The crystallization of

nylon-6–clay nanocomposite from the melt has been monitored by using a hot stage coupled to an X-ray diffractometer. We have observed for the first time the appearance of the metastable phase, apart from the γ phase, during the crystallization of nylon-6 in the presence of silicate layers. Further, for the first time, we report the examination of the γ phase of nylon-6 in the nanocomposite and the γ phase obtained by treating nylon-6 in KI/I_2 by variable temperature Fourier transform infrared spectroscopy (FTIR).

5.2 Experimental Section

Nylon-6 pellets (Akulon K2 2D grade, η_{inh} = 0.76 dL/g) were obtained from Century Enka, India. The clays, Cloisite 25A and Cloisite 30B, were obtained from Southern Clay Products. These clays were montmorillonites modified by dimethyl 2-ethylhexyl (hydrogenated tallow alkyl) ammoniums and methyl bis(2-hydroxyethyl) (hydrogenated tallow alkyl) ammoniums, respectively. Before melt mixing, nylon-6 and the clays were dried in a vacuum oven at 100 °C for 5 h. In most cases, melt mixing (100 rpm) of nylon-6 with the desired amount of clay was conducted in DSM Micro 5 twin-screw compounder at 230 °C for 5 min. The batch size was approximately 5 g. In one case the mixing was performed in Haake Rheocord 600p attached with a batch mixer (75 rpm, 230 °C for 5 min), and the batch size was approximately 50 g. The strands obtained were powdered in a SPEX 6750 freezer mill. The TGA-7 unit in the Perkin-Elmer thermal analysis system was used to determine the amount of clay present in the nanocomposites. The samples were heated under a flowing nitrogen atmosphere from 50 to 600 °C, at a heating rate of 10 °C/min, and the weight loss was recorded. The weight of the residue remaining at 600 °C was taken as the % clay content in the nanocomposite. The X-ray diffraction (XRD) experiments were performed using a Rigaku Dmax 2500 diffractometer with a copper target. The details are described in chapter 3. The samples were scanned between 2θ = 2 to 30° at a scan speed of 2°/min. The *in situ* melt crystallization studies were carried out as described in chapter 3.

The low cooling rate of the hot stage made it impossible to *in situ* crystallize below 200 °C because the sample crystallized prior to reaching the intended crystallization temperature (T_c). Hence, a different method was followed for crystallization at lower temperatures. Powders of the nylon/clay nanocomposites were sandwiched between two thin microscopic cover glasses, heated on a hot plate, melted, and pressed into a thin film. The sandwiched films were melted for about 5 min in an oil bath isothermally set at 240 °C

and then very rapidly transferred to another oil bath maintained at the T_c. After crystallization in the oil bath, the sample was recovered and transferred to the X-ray hot stage, and the change in structure was monitored during heating by scanning at regular temperature intervals. The crystallinity of the samples was calculated from the integrated intensity of the crystalline reflections and the amorphous scattering.

Room temperature and high temperature infrared spectra of these samples were taken using Perkin-Elmer FTIR spectrometer (model: Spectrum GX) with a DTGS detector at a resolution of 2 cm^{-1} in the range of 400–4500 cm^{-1}. The details are described in chapter 3. Nylon-6 in the α phase was obtained by dissolving nylon-6 in 1,4-butanediol at its refluxing temperature and subsequently cooling very gradually to room temperature. This procedure gave highly crystalline α phase in the form of fine powder. This powder was used for FTIR studies on the α phase as well as to obtain the γ phase. The powder was treated with KI/I_2 aqueous solution to convert the α phase into the γ phase according to the procedure reported elsewhere.[6] In the case of nylon-6–clay sample, the γ phase was obtained by the following method: A very thin film of the nylon-6–clay sample was melt-pressed in a small copper plate and allowed to cool to room temperature. The room temperature WAXS pattern showed that the sample crystallized fully into γ phase, and the crystallinity was 37%.

5.3 Results and Discussion

5.3.1 Variable Temperature WAXS Studies

The nanocomposites obtained are either intercalated or exfoliated depending on the type of clay used. The gallery height of Cloisite 25A and Cloisite 30B, as determined from the XRD experiments are 1.84 and 1.78 nm, respectively. Cloisite 25A yields always intercalated nanocomposites as evident from the characteristic clay layer peak at 2θ = 2.48° and 5.22°. On the other hand, Cloisite 30B-based nanocomposites appear to be exfoliated, as the characteristic clay peaks are absent in the X-ray diffractograms. The exfoliation in the case of Cloisite 30B is probably due to the presence of high hydroxyl content in the clay surface compared to Cloisite 25A. However, under the experimental conditions used, the crystallization behavior of nylon-6 is similar for both the nanocomposites. Hence, the crystallization data obtained from the intercalated system is presented here because additional information is available on the effect of nylon crystallization on the clay layers.

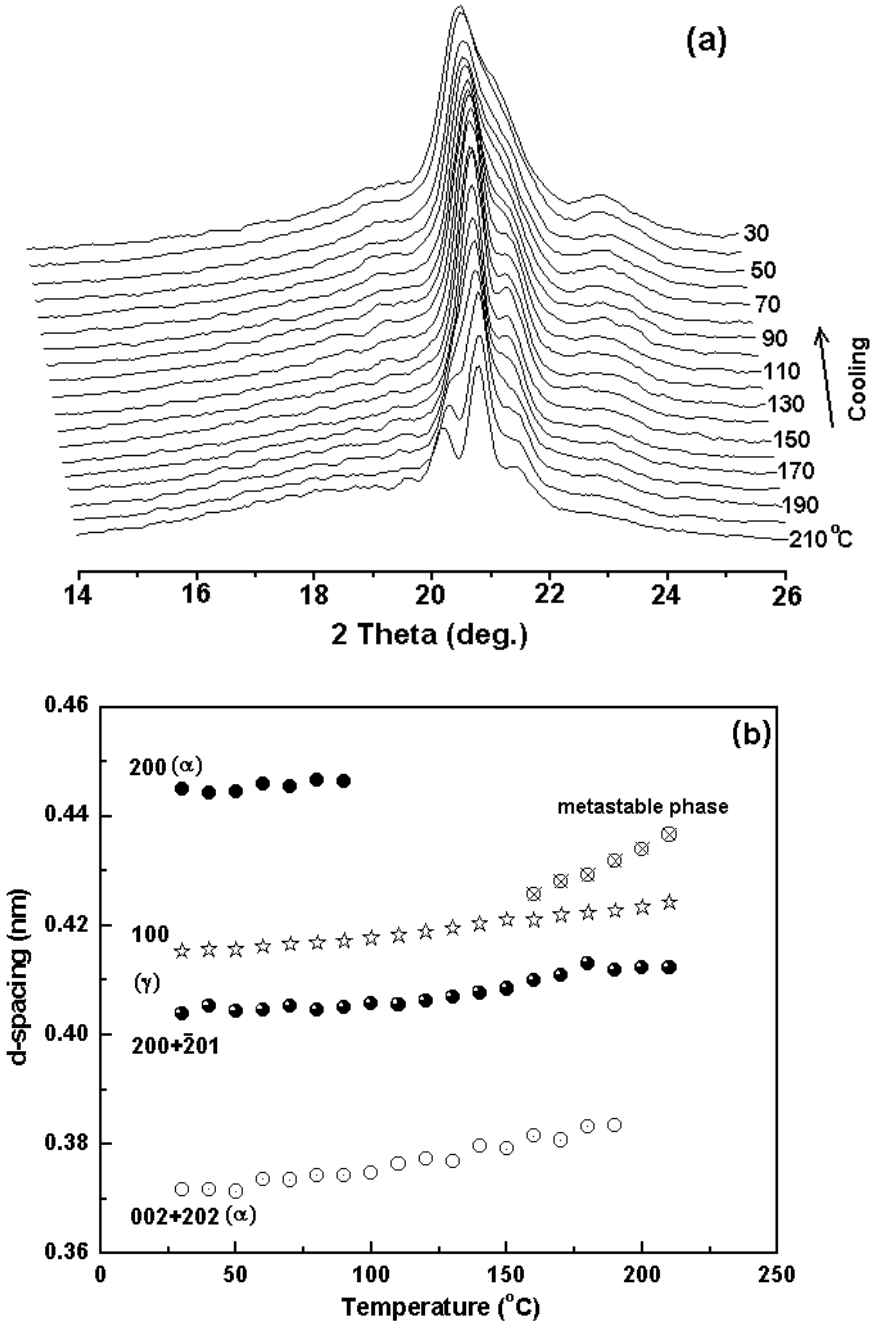

Figure 5.1: (a) Behavior of XRD patterns and (b) *d* spacings on cooling from T_c to room temperature of nylon-6 cloisite 25A nanocomposite (6%).

The structure development during isothermal crystallization of nylon-6–clay nanocomposite at 210 °C and subsequent cooling to room temperature has been followed *in situ* by WAXS. The behavior of the diffractograms and the *d* spacing on cooling from the T_c to room temperature is shown in parts a and b of Figure 5.1, respectively. The clay peaks observed at low 2θ ranges are not shown in the figure but will be discussed separately. The salient feature of Figure 5.1a is that thediffractogram recorded after the

completion of crystallization at 210 °C shows two sharp peaks at 2θ = 20.33° and 20.93°, and the corresponding *d* spacings are 0.437 and 0.424 nm respectively. A third peak appears as a shoulder to the peak at 2θ = 20.93 ^{o} and is at 2θ = 21.54°. The peaks at 2θ = 20.93° and 21.54° may be identified as 100 and 200/$\bar{2}$01 reflections of the γ phase. The peak at 2θ = 20.33° is observed for the first time and is indicative of the presence of an additional phase as this peak is not observed for the γ phase. The position of this new reflection is closer to the 200 reflection of the α phase. Nevertheless, its behavior on cooling differs from the α phase[3,4] and will be discussed in the following paragraph. Following Murthy,[7] the second phase may be interpreted to arise from the 200 reflection of an intermediate phase and is termed the metastable phase to distinguish it from the α and γ phases. Murthy[7] showed that the metastable phase can be converted into either the α or γ phase by suitable thermomechanical treatment. The deconvolution procedure could not locate the 002/202 peak of the metastable phase, and hence it is not considered during deconvolution process.

The characteristic peaks of the γ phase at 2θ = 20.93^{o} and 21.54° show a small shift toward higher angles due to thermal contraction on cooling to room temperature. On the other hand, the response of the metastable phase on cooling is more dramatic; the peak at 2θ = 20.33° shifts towards higher values and merges with the 100 reflection of the γ phase at around 150 ^{o}C. Below 150 °C the metastable phase could not be distinguished from the γ phase. This may be due to an anisotropic thermal contraction of the lattice planes corresponding to these two X-ray peaks. Though the crystallization of nylon-6 in the presence of clay is predominantly in the γ phase, the α phase is also formed to some extent. The trace of the α phase is first seen at 190 ^{o}C, as the 002/202 reflection of the α phase is seen distinctly at this temperature. On the other hand, the 200 reflection becomes apparent only after cooling below 100 ^{o}C. The *d* spacings of the α phase reflections are shown in Figure 5.1b along with that of γ phase. At room temperature the amount of the γ phase is 40% and that of the α phase is 9%. The variations in diffraction patterns and *d* spacings on cooling from T_c are found to be reversible on heating and hence will not be discussed in detail. The behavior of the γ phase obtained in the presence of silicate layers may be compared with the γ phase obtained by treating nylon-6 in KI/I_2 solution. In the

latter case, no metastable phase is observed at 160 ^{o}C on heating but remained as the γ phase until melting.[3]

It is worth comparing the *d* spacing of the γ phases crystallized in the presence of clay layers with that of the γ phase observed in neat nylon. The characteristic *d* spacings of the 100 and $200/\bar{2}01$ reflections of the γ phase of neat nylon-6 obtained by KI/I_2 treatment at room temperature are 0.415 and 0.40 nm, respectively.[3] These values do not change appreciably at 210 ^{o}C and are 0.419 and 0.404 nm. In the case of γ phase obtained in the presence of clay layers the *d* spacings are similar at room temperature. However, these values change to 0.424 and 0.412 nm at 210 ^{o}C indicating the existence of a definite difference between the γ phases obtained by the two methods.

A careful observation of the diffractograms in Figure 5.1a shows the continued crystallization of the material in the γ phase during cooling to room temperature. Simultaneously, there is an increase in the fraction of the α phase during cooling, albeit in low fractions. The crystallization of nylon-6 into the γ phase is assisted by the clay layers, and this is evident from the crystal size calculated from the reflections 100 and $200/\bar{2}01$. The crystal size, 28 nm, normal to the plane 100 is unusually large and shows that the clay layer acts as a template for epitaxial crystallization[18] of nylon-6. The large crystal size indicates that at 210 ^{o}C most of the crystallization occurs close to clay layers; but on cooling, crystallization could take place farther removed from the clay layers with reduced crystal sizes, thereby broadening the diffraction peaks. The amount of α phase fraction formed depends on the crystallization condition. The thin film sample allowed to crystallize on cooling to ambient temperature showed only the γ phase without any α phase at room temperature.

The XRD patterns of the sample crystallized in the silicon oil bath at 100 ^{o}C are shown in Figure 5.2. At room temperature the sample exhibits a typical γ phase along with a small amount of α phase, which is consistent with the observations of Fornes and Paul.[17] On heating, the α phase disappears at a lower temperature than the sample crystallized at 210 ^{o}C. The metastable phase appears at about 160 ^{o}C and coexists with γ phase until melting. These results further indicate that the metastable phase also crystallized along with γ phase

at 100 °C but could not be distinguished from the γ phase because the *d* spacings overlap in the temperature range from room temperature to 150 °C.

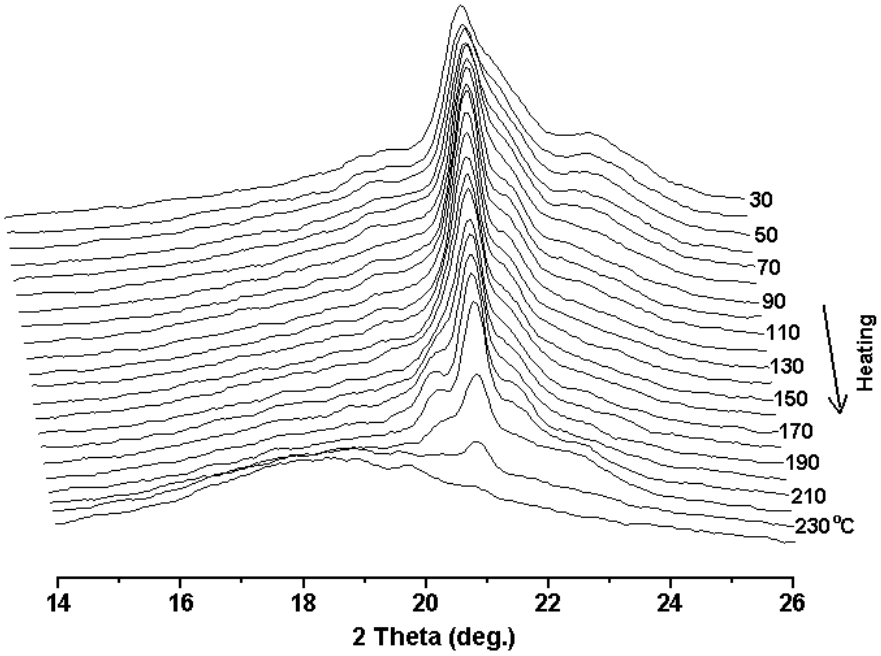

Figure 5.2: Behavior of XRD patterns on heating from room temperature to melt of nylon-6 cloisite 25A nanocomposite (5.5%) crystallized in a silicone oil bath at 100 °C. (Note: Sample prepared in Haake Rheocord).

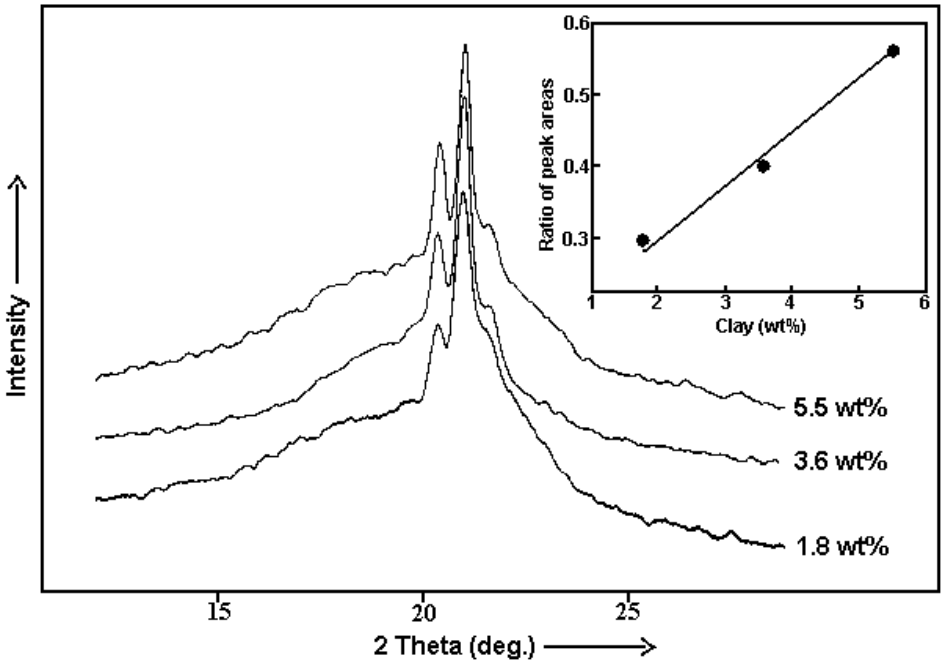

Figure 5.3: XRD patterns at the end of crystallization at 210 °C for various clay contents of nylon-6–clay nanocomposites. Inset shows the ratio of the 200 peaks of the metastable and γ phases at 210 °C.

However, the intensity of the 200 reflection of the metastable phase is lower than the intensity of the sample crystallized at 210 °C, indicating that the T_c is one of the factors that control the formation of the metastable phase. The amount of metastable phase crystallized also appears to depend on the clay content in the nanocomposite. The diffractograms recorded at the end of crystallization at 210 °C for various clay contents are shown in Figure 5.3. It may be commented that the amount of metastable phase depends on the amount of clay present in the nanocomposite and the T_c. At this stage it may be speculated that the metastable phase is the material directly crystallizing on the clay layers and can be seen only after heating above 150 °C. The metastable phase is shown to transform into the α or γ phase by suitable thermomechanical treatment;[7] apparently, in the present case the metastable phase is formed and stabilized by the clay layers.

The effect of crystallization of nylon-6 on the clay layers in the case of intercalated nanocomposites will be discussed here. Figure 5.4a shows the variation of diffraction patterns at low 2θ ranges, where characteristic peaks due to clay occur, during cooling from the T_c. The clay exhibits two peaks at 2θ = 2.48° and 5.22° corresponding to d spacings of 3.59 and 1.70 nm at the T_c, 210°C. These are the first- and second-order reflections from the clay layers.[19] The d spacing 3.59 nm corresponds to the distance between two adjacent clay layers and is called the gallery height. Figure 5.4b shows the variation of gallery height with temperature on cooling. The gallery height decreases with decreasing temperature; however, it decreases more rapidly on cooling from 190 to 130 °C and may be attributed to the crystallization of nylon-6 present within the gallery. At 210 °C the crystallization rate of nylon-6 within the gallery will be retarded due to the confined space, and it is kinetically favored to crystallize at lower temperatures on cooling. Apart from the changes in gallery height, the clay peaks become broader and decrease in peak height. These changes suggest some degree of disturbance in the clay layer stacking order due to polymer crystallization within the layers. However, these changes are reversible on heating as the material crystallized between the clay layers melts away.

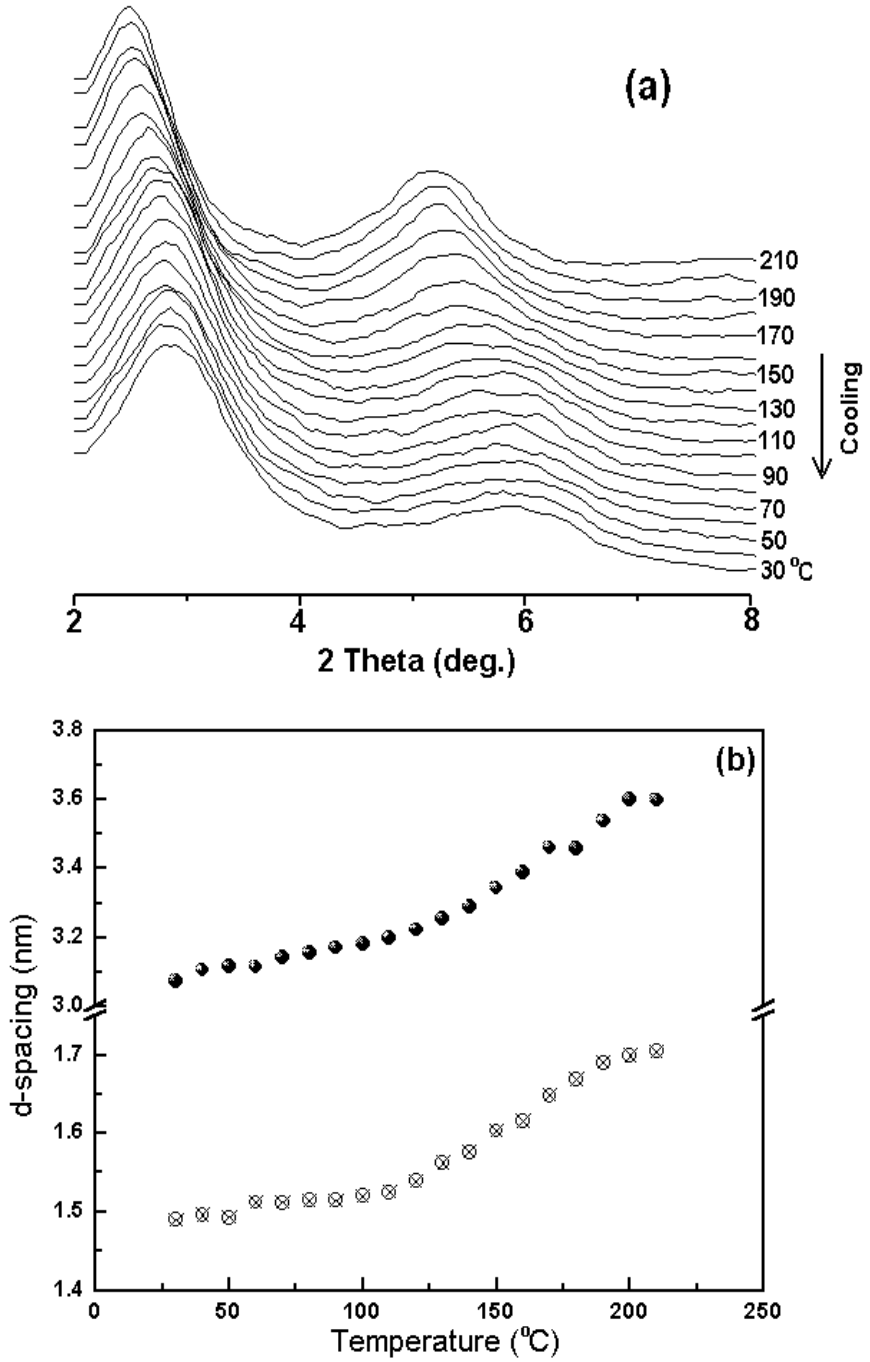

Figure 5.4: Behavior of (a) XRD patterns and (b) *d* spacings of clay at low 2θ ranges on cooling from T_c (210 °C) to room temperature for nylon-6 cloisite 25A nanocomposite (6%).

5.3.2 Variable Temperature FTIR Studies

The foregoing discussions are primarily focused on the structure based on the data obtained from variable temperature WAXS studies, and in the following section the discussion will be focused on the data obtained from variable temperature FTIR studies on the γ phase of nylon-6 in the presence and absence of clay layers. Variable temperature spectra of the α phase is also obtained and compared with the spectra of γ phase. It may be

pointed out that Murthy and co-workers[20] obtained the α phase by melt crystallization while in the present case the α phase is obtained by dissolving nylon-6 in 1,4-butanediol at its refluxing temperature and subsequent slow cooling to room temperature. The crystallinity of the sample at room temperature is 56%; the infrared spectra obtained at room temperature and on heating look similar to the variable temperature spectra reported by Murthy and co-workers,[20] and hence it will not be discussed here. It is interesting to note that when the α phase, with 56% crystallinity, is converted into the γ phase (KI/I_2) by treating in KI/I_2 solution at room temperature, the crystallinity decreases to 36%. The room temperature WAXS indicates the absence of the α phase in the sample. The large decrease in the crystallinity during phase transformation indicates the occurrence of major structural reorganization when the α phase converts into the γ phase. Variable temperature WAXS studies on these samples are reported in detail elsewhere,[3] and here we report for the first time the variable temperature FTIR spectra of the γ phase obtained by treating nylon-6 in KI/I_2 solution and the γ phase (clay) obtained by melt crystallization of nylon-6 clay nanocomposite.

The infrared spectroscopy studies on nylon-6 have been made, and the band assignments of α and γ phases are reported in literature.[21-28] The γ phase (KI/I_2) shows distinct absorbance peaks at 585, 623, 962, 975, 1234 and 1439 cm^{-1}. On the other hand, the α phase shows strong characteristic bands at 577, 928, 950, 959, 1201, 1416 and 1477 cm^{-1}. The γ phase (clay) shows absorbance bands at 588, 626, 962, 974, 1235 and 1439 cm^{-1}. The 463, 1020 and 3628 cm^{-1} bands are due to clay and are obvious only in the nylon-6–clay spectra. Figures 5.5 to 5.8 show the sections of spectra of α phase and γ phases wherein major differences are observed between the phases.

Figure 5.5a–c shows the spectral region from 400 to 800 cm^{-1} for the various phases and comprises amide V and amide VI bands. At room temperature the amide V and amide VI bands appear at 690 and 577 cm^{-1} respectively for the α phase. The amide V band shifts to 710 cm^{-1} for γ phase (KI/I_2). The amide VI band is shifted[28] to 623 cm^{-1} from 577 cm^{-1}. However, in Figure 5.5b the spectra show a distinct additional band at 585 cm^{-1} and may be assigned exclusively to the γ phase (KI/I_2) because the α phase is totally absent in this sample, as evidenced from the WAXS pattern at room temperature. This may also be assigned to the amide VI band because of the position, and hence in the case of the γ phase

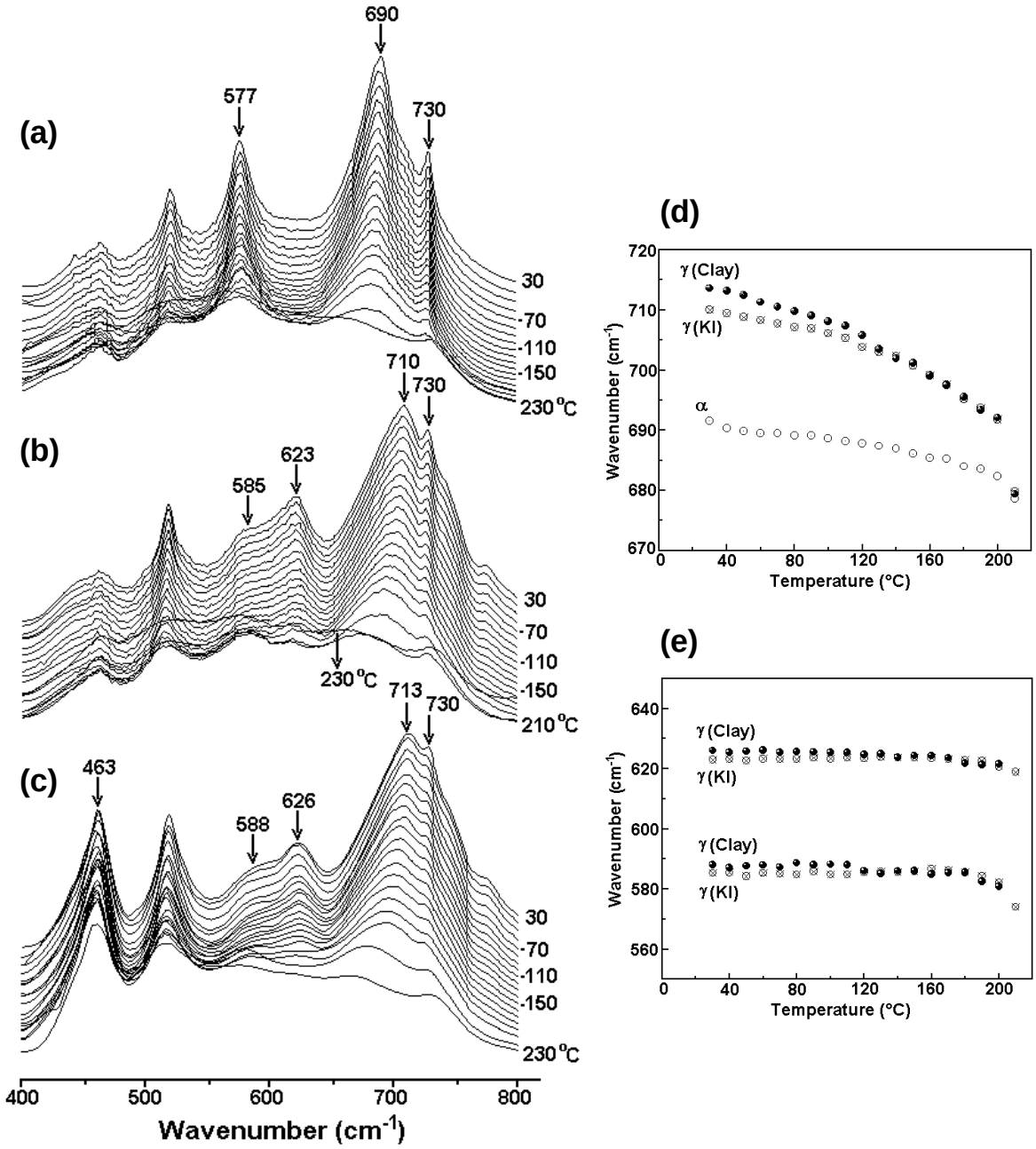

Figure 5.5: Variable temperature FTIR spectra of the region 400–800 cm^{-1} of nylon-6 during heating from room temperature to melt: (a) α phase; (b) γ phase obtained by treating α phase in KI/I_2 solution at room temperature; (c) γ phase obtained by melt crystallization of nylon-6–clay nanocomposite; (d) variation of the wavenumber of amide V band at 690 cm^{-1} for all the three phases during heating; (e) variation of the wavenumber of amide VI bands at 585 cm^{-1} and 623 cm^{-1} for the γ phases during heating.

amide VI has two distinct bands at 585 and 623 cm^{-1}. The spectra of the γ phase (clay), as seen from Figure 5.5c, are very similar to the spectra of the γ phase (KI/I_2), but with band shifts for the key amide bands. The amide V appears at 713 cm^{-1} while the two bands of

amide VI occur at 588 and 626 cm^{-1}. The variation of amide V band position on heating for α and γ phases is shown in Figure 5.5d. On heating, the wavenumber of amide V band decreases with increasing temperature; the decrease is more for the γ phase than the α phase. Both the γ phases have same wavenumber above 120 °C, and interestingly in the melt above 210 °C the phases vanish and all the samples show the same wavenumber, 678 cm^{-1}. The amide VI bands at 585 and the 623 cm^{-1} show very small decrease with feature is the band at 730 cm^{-1} assigned to the methylene rocking mode, which arises from the orthorhombic packing cell of the methylene segments.[29-31] The band at 730 cm^{-1} appears for all the three samples at the same wavenumber, indicating that the conformation of the methylene segments is similar for the α and γ phases, even though the hydrogen bonding schemes are different. The 730 cm^{-1} band disappears when the sample increase in temperature. Again, above 120 °C the γ phase (clay) and the γ phase (KI/I_2) have the same wavenumber. On heating close to the melting temperature (T_m), the wavenumber shows more rapid downward shift and these bands vanish in the melt. Another interesting melts at 210 °C. The band at 463 cm^{-1} is due to the clay and does not change even at 230 °C, while the nylon-6 is in the melt form at this temperature.

Figure 5.6 shows the spectra in the region from 900 to 1050 cm^{-1}. The α phase shows characteristic absorbance peaks at 928, 950, and 959 cm^{-1}. These bands do not appear for the γ phases, but new bands appear at 962 and 975 cm^{-1}. The band at 975 cm^{-1} is assigned to the CO-NH in-plane vibration.[23,26] The band appears at 974 cm^{-1} at room temperature for the γ phase (clay). On heating, the 975 cm^{-1} band of the γ phase (KI/I_2) shows a small shift to lower wavenumber, but the band at 974 cm^{-1}exhibits a shift toward the higher wavenumber. The band at 962 cm^{-1}appears to vanish well below the T_m; however, the deconvolution of the peaks indicates that the 962 cm^{-1} band exists up to the T_m, albeit, with greatly reduced intensity. The peak width increases with increase in temperature, but the normalized absorbance decreases. The γ phase (KI/I_2) and the γ phase obtained in the presence of clay show similar behavior in the half-width and the normalized absorbance, but minor variations can be seen. In the case of nylon clay nanocomposites the band at 1050 cm^{-1} is due to Si–O stretch of the clay layers.[32]

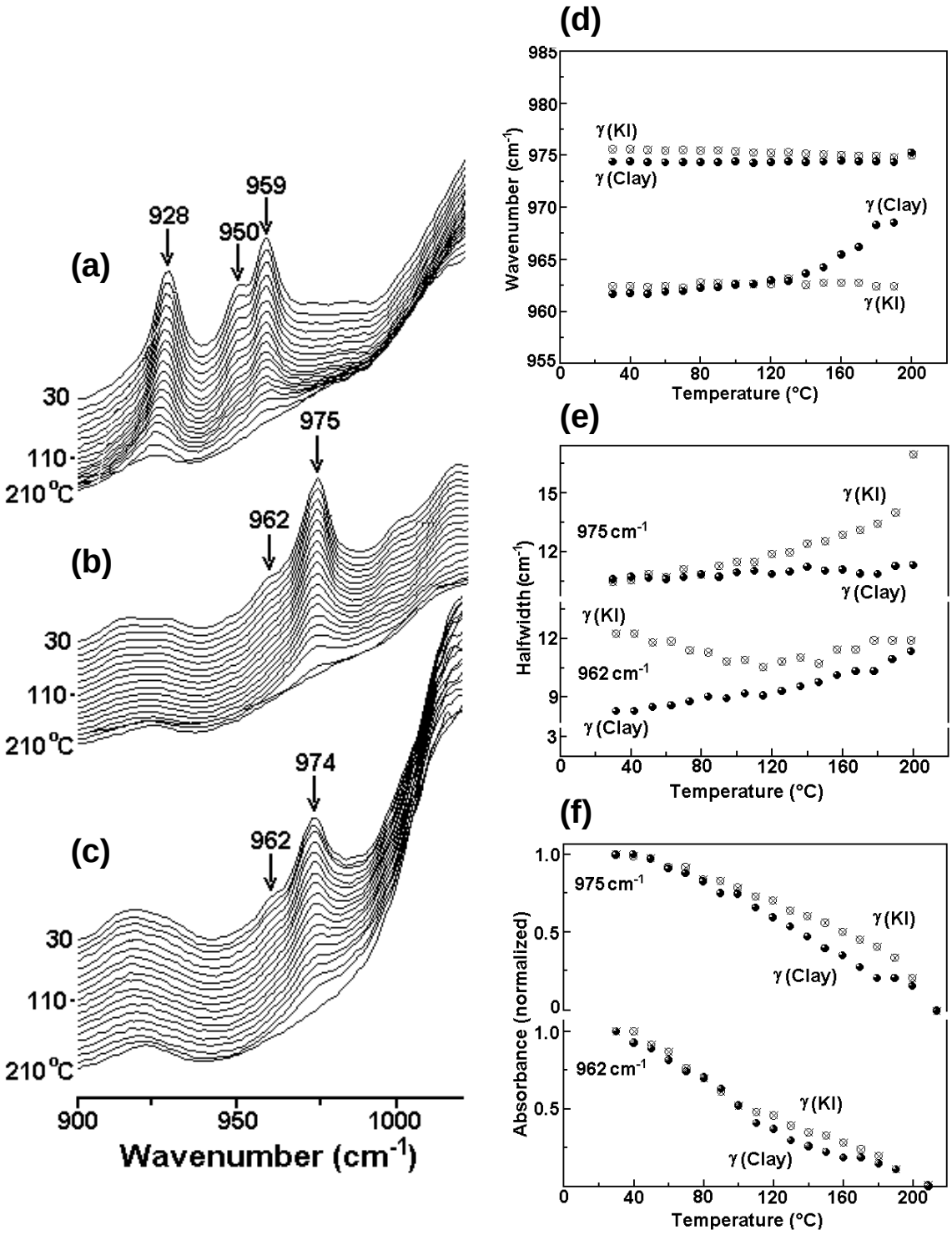

Figure 5.6: Variable temperature FTIR spectra of the region 900–1050 cm^{-1} of nylon-6 during heating from room temperature to melt: (a) α phase; (b) γ phase obtained by treating α phase in KI/I_2 solution at room temperature; (c) γ phase obtained by melt crystallization of nylon-6–clay nanocomposite. The variation of (d) wavenumber, (e) full width at half-maximum, and (f) normalized absorbance for the 962 and 975 cm^{-1} bands for the γ phases during heating.

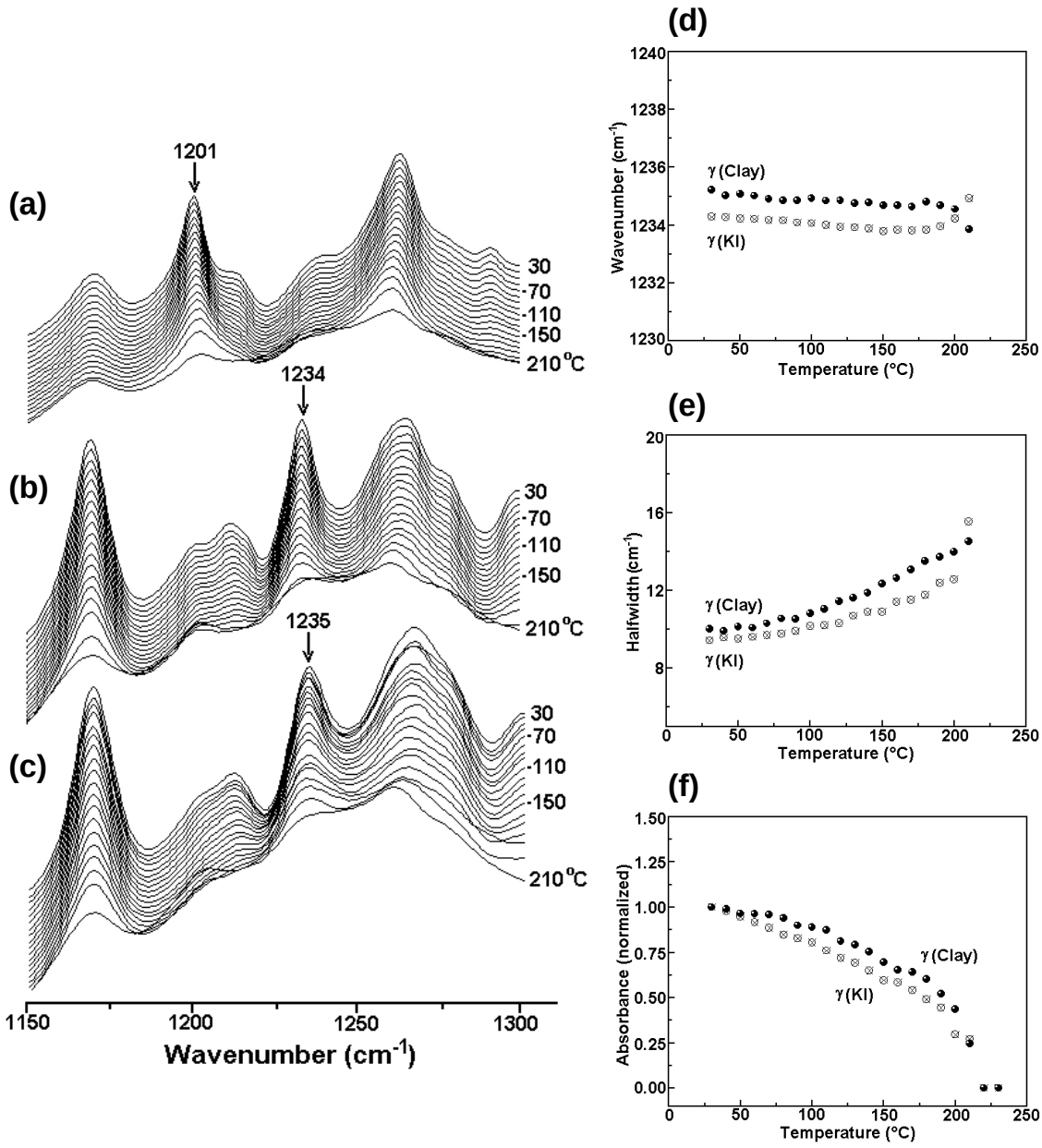

Figure 5.7: Variable temperature FTIR spectra of the region 1150–1300 cm^{-1} of nylon-6 during heating from room temperature to melt: (a) α phase; (b) γ phase obtained by treating α phase in KI/I_2 solution at room temperature; (c) γ phase obtained by melt crystallization of nylon-6–clay nanocomposite. The variation of (d) wavenumber, (e) full width at half-maximum, and (f) normalized absorbance for the 1234 cm^{-1} band for the γ phases during heating.

Another region of interest is from 1150 to 1300 cm^{-1}, and the γ phase shows a distinct characteristic absorbance at 1234 cm^{-1}, which is assigned to amide III and CH_2 wagging vibration.[22,26] Figure 5.7a–f shows the spectra in this region and the behavior of the wavenumber, peak half-width, and the normalized intensity of the characteristic γ phase

band. The band appears at 1234 and 1235 cm^{-1} for the γ phase (KI/I_2) and γ phase (clay), respectively. On heating, the wavenumbers show marginal decrease up to 180 °C. On heating above 180 °C, in the case of the γ phase (clay) the wavenumber shifts to lower value, but it increases in the case of the γ phase (KI/I_2). The half-width increases with increase in temperature, and above 150 °C the half-width shows more accelerated increase. However, the normalized absorbance decreases with increase in temperature. The key difference between the γ phase obtained by KI/I_2 treatment and the γ phase (clay) is the half-width of the band. The γ phase (clay) shows consistently higher half-width compared with the γ phase obtained by KI/I_2 treatment.

The region from 3100 to 3500 cm^{-1} is very sensitive to hydrogen bonding and is assigned to the hydrogen-bonded NH stretch (amide A). The contribution to the amide A comes from i) free N–H stretch at 3444 cm^{-1} ii) bonded N–H stretch at 3300 cm^{-1} arising out of crystalline fraction, and iii) bonded N–H stretch at 3310 cm^{-1} arising out of amorphous fraction. The region is too broad to deconvolute meaningfully into individual peaks and hence is discussed as a composite peak. Nevertheless, it provides valuable information and Figure 5.8 shows the variable temperature spectra of the α and γ phases along with the wavenumber variation with temperature for the band at 3300 cm^{-1}. Qualitatively, the spectra of the γ phases look similar, but the peak occurs at 3301 and 3305 cm^{-1} for the γ phases obtained by KI/I_2 and clay, respectively. Another observable difference is that in the case of γ phase (clay) the band appears broader than the γ phase (KI/I_2). The amide A band appears at 3301 cm^{-1} for the α phase and the band is sharper than the γ phases. On heating, the band shifts to higher wavenumber region, and all the samples have similar shape and wavenumber in the melt above 210 °C. The bands at 2868 and 2940 cm^{-1} need special mention; these bands are not related to crystalline fraction because these bands are present without much reduction in absorbance above the T_m. These bands are assigned to symmetric and asymmetric CH_2 stretch, respectively.[21,25] The nature of the crystalline phase seems to affect the peak position of these bands. At room temperature these bands appear at 2869 and 2940 cm^{-1} for the α phase. These bands shift to 2858 and 2929 cm^{-1} for the γ phase (KI/I_2) and to 2860 and 2933 cm^{-1} for the γ phase (clay). Interestingly, the values converge to 2860 and 2934 cm^{-1} in the melt for all the samples. The effect of interaction between the nylon and clay is also seen in the spectra of clay as well. The band due to hydrogen bonding is seen at 3633 cm^{-1} for the modified clay at room temperature.

This band shifts to 3628 cm^{-1} for the nylon-6–clay nanocomposite; shifting of the wavenumber toward lower frequency indicates the strengthening of the hydrogen bonding in the clay due to nylon-6.

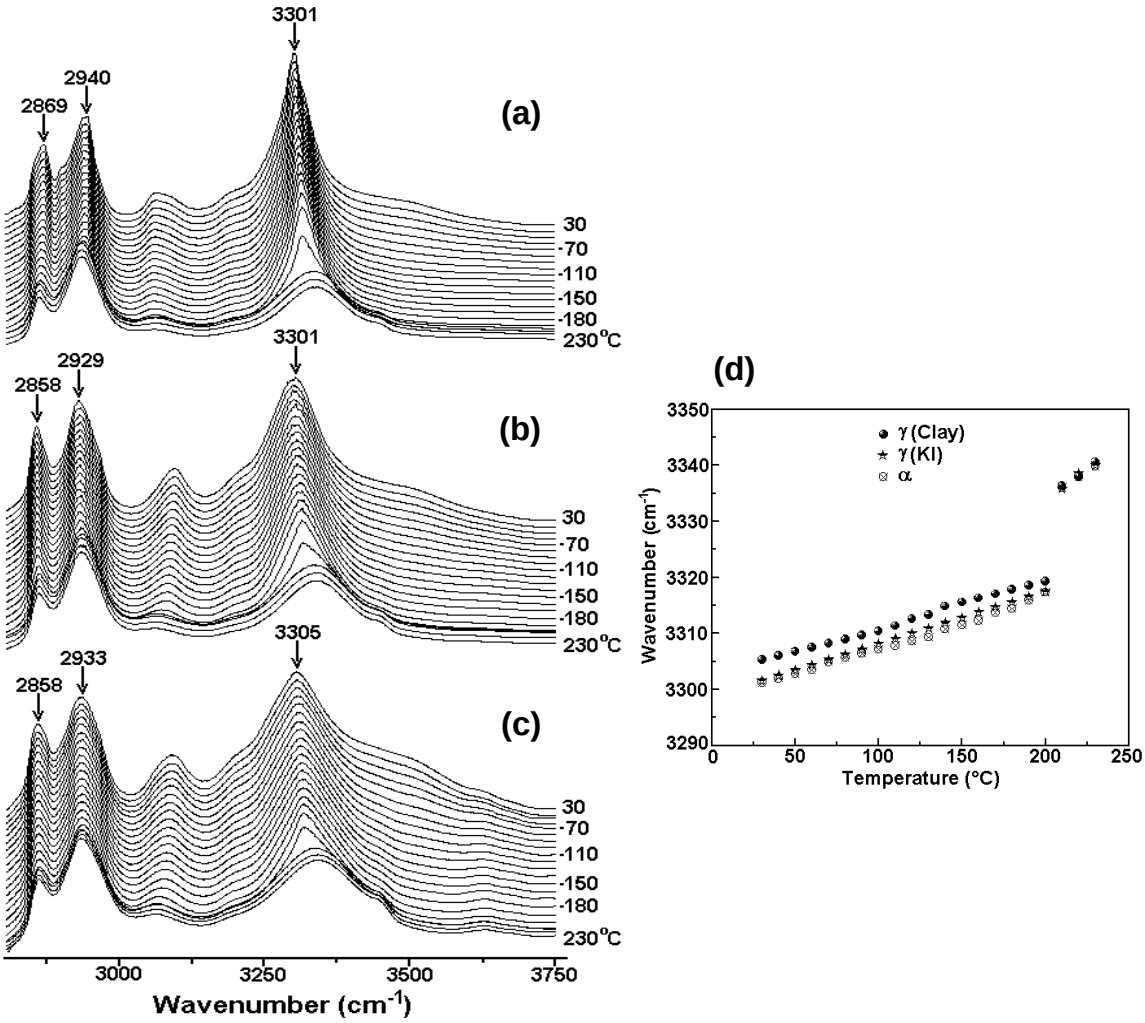

Figure 5.8: Variable temperature FTIR spectra of the region 2750–3750 cm^{-1} of nylon-6 during heating from room temperature to melt: (a) α phase; (b) γ phase obtained by treating α phase in KI/I_2 solution at room temperature; (c) γ phase obtained by melt crystallization of nylon-6–clay nanocomposite; (d) The variation of the wavenumber of amide A band at 3301 cm^{-1} with temperature for all the three samples.

The samples used for FTIR studies have only one phase present at room temperature, and the FTIR spectra may be considered to represent the respective phases. Further, the crystallinity of the samples having the γ phase is similar and is about 36%. The variable temperature FTIR spectra of the γ phase (clay) do not indicate the presence of metastable phase, even though WAXS studies showed its presence. The possible argument is that the

chain conformation in the metastable phase is similar to the γ phase and hence could not be identified in the FTIR spectra. The difference seen in the FTIR spectra of the γ phases is similar to the differences exhibited by the samples in the behavior of *d* spacing, even though the general feature of the γ phase is similar in both the samples. The difference may be attributed to the mechanism of γ phase formation, which is different for the two methods. In the case of the nanocomposite, the γ phase is formed by melt crystallization with clay layers controlling the hydrogen bonds. In the case of γ phase obtained by KI/I_2 treatment, the iodine forms a complex with the nylon, and the removal of iodine from the complex leads to the γ phase.[28]

5.4 Conclusion

The *in situ* XRD studies on the crystallization of nylon-6–clay nanocomposites provided new information on the crystallization of nylon-6 in the presence of clay layers. Nylon-6 in the nanocomposite is crystallized into the γ phase and metastable phase. The metastable phase depended on the amount of clay present in the system and is obvious in the X-ray diffractogram only after heating to 150 °C. The *d* spacings of the nylon-6 γ phase obtained in the presence of the clay showed differences from the pristine γ phase obtained by treating nylon-6 in KI/I_2 solution. The variable temperature FTIR studies also showed that the nylon–clay system gives characteristic infrared bands at different positions from those of the neat γ phase. These results suggest that in the case of nylon-6 the characteristics of the γ phase depend on the method of its formation.

5.5 References

1. Holmes, D. R.; Bunn, C. W.; Smith, D. J. *J. Polym. Sci*. **1955**, *17*, 159.
2. Arimoto, H.; Ishibashi, M.; Hirai, M.; Chatani, Y. *J. Polym. Sci., Part A:* **1965,** *3*, 317.
3. Ramesh, C.; Gowd, E. B. *Macromolecules* **2001**, *34*, 3308.
4. Murthy, N. S.; Curran, S. A.; Aharoni, S. M.; Minor, H. *Macromolecules* **1991**, *24*, 3215.
5. Stepaniak, R. F.; Garton, A.; Carlsson, D. J.; Wiles, D. M. *J. Polym. Sci., Polym. Phy. Ed.* **1979,** *17*, 987.
6. Miyasaka, K.; Makishima, K. *J. Polym. Sci., Part A-1* **1967,** *5*, 3017.
7. Murthy, N. S. *Polym. Commun.* **1991**, *32*, 301.

8. Kojima, Y.; Usuki, A.; Kawasumi, M.; Okada, O.; Fukushima, Y.; Kurachi, T.; Kamigaito, O. *J. Mater. Res*. **1993,** *8,* 1185.
9. VanderHart, D. L.; Asano, A.; Gilman, J. W. *Chem. Mater*. **2001**, *13*, 3781.
10. Lincoln, D. M.; Vaia, R. A.; Wang, Z. G.; Hsiao, B. S. *Polymer* **2001**, *42*, 1621.
11. Cho, J. W.; Paul, D. R. *Polymer* **2001**, *42*, 1083.
12. Lincoln, D. M.; Vaia, R. A.; Wang, Z. G.; Hsiao, B. S.; Krishnamoorti, R. *Polymer* **2001,** *42*, 9975.
13. Lincoln, D. M.; Vaia, R. A.; Krishnamoorti, R. *Macromolecules* **2004,** *37*, 4554.
14. Mathias, L. J.; Davis, R. D.; Jarrett, W. L. *Macromolecules* **1999,** *32*, 7958.
15. Wu, Q.; Liu, X.; Berglund, L. A. *Macromol. Rapid Commun.* **2001,** *22*, 1438.
16. Liu, X.; Wu, Q. *Eur. Polym. J.* **2002,** *38,* 1383.
17. Fornes, T. D.; Paul, D. R. *Polymer* **2003,** *44*, 3945.
18. Maiti, P.; Okamoto, M. *Macromol. Mater. Eng*. **2003**, *288*, 440.
19. Vaia, R. A.; Ishii, H.; Giannelis, E. P. *Chem. Mater.* **1993**, *5*, 1694.
20. Vasanthan, N; Murthy, N. S.; Bray R.G. *Macromolecules* **1998,** *31,* 8433.
21. Doskocilova, D.; Pivcova, H.; Schneider, B.; Cefelin, P. *Coll. Czech. Comm.* **1963,** *28,* 1867.
22. Schneider, B.; Schmidt, P.; Wichterle, O. *Coll. Czech. Comm*. **1962**, *27,* 1749.
23. Illers, K. H.; Haberkorn, H.; Simak, P. *Makromol. Chemie.* **1972,** *158,* 285.
24. Jakes, J.; Krimm. S. *Spectochemica Acta* **1971,** *27A,* 19.
25. Jakes, J.; Krimm. S. *Spectrochemica Acta* **1971,** *27A,* 35.
26. Rotter, G; Ishida, H. *J. Polym. Sci., Polym. Phys. Ed.* **1992,** *30,* 489.
27. Wu. Q; Liu. X.; Berglund, L. A. *Polymer* **2002,** *43,* 2445.
28. Abu-isa, I. *J. Polym. Sci., Part A-1* **1971**, *9*, 199.
29. Snyder, R. G. *J. Chem. Phys*. **1979,** *71,* 3229.
30. Tashiro, K.; Sasaki, S.; Kobayashi, M. *Macromolecules* **1996,** *29,* 7460.
31. Yoshioka,Y.; Tashiro, K.; Ramesh, C. *Polyme*r **2003,** *44,* 6407.
32. Loo, L. S.; Gleason, K. K. *Macromolecules* **2003,** *36*, 2587.

CHAPTER 6

SUMMARY AND CONCLUSIONS

6.1 Summary

The key findings and conclusions of the present thesis are summarized below.

Nylon-11 was crystallized into different crystalline phases by appropriate methods. The change in the structure during heating was monitored *in situ* by wide-angle X-ray scattering (WAXS). The α phase obtained by precipitating nylon-11 in 1,4-butanediol started transforming into the pseudohexagonal phase on heating, but the transformation was not fully completed before melting. The melt-crystallized sample at 175 °C gave the pseudohexagonal phase, which transformed into the α' phase on cooling to room temperature at about 100 °C. The *d* spacing of the 001 reflection also showed a change at the transition temperature. The melt-quenched sample showed the pseudohexagonal phase, which did not change during heating, but on cooling transformed into the α' phase. The γ phase was obtained by casting nylon-11 in trifluoro acetic acid (TFA), and it changed into the pseudohexagonal phase at about 110 °C on heating. The *d* spacing of the 001 reflection depended on the way in which it was obtained. The studies have shown that nylon-11 is one of the few nylons that exhibit an extensive degree of polymorphism. High temperature Fourier transforms infrared spectroscopy (HTFTIR) studies revealed, apart from the conformational differences between various phases of nylon-11, some information on the formation of the γ phase.

Nylon-6,7 was synthesized by interfacial and melt polymerization techniques, and a detailed study was carried out on its crystalline transitions on heating and cooling using HTWAXS and HTFTIR. Crystalline transition studies were also carried out on nylon-6,9, a known even-odd nylon, with a chemical repeat unit close to nylon-6,7 using HTWAXS and HTFTIR. The results obtained were compared with that of nylon-6,7.

Nylon-6,7 precipitated in 1,4-butanediol crystallized in the γ phase with a small amount of α phase which transformed into the γ phase above 140 °C, and the sample melted in the γ phase. The melt-crystallized sample at 220 °C also gave the γ phase, which was retained on cooling to the room temperature. However, an additional peak was observed close to the main γ phase peak, which was due to the metastable phase and it transformed into the γ phase on cooling at about 150 °C. The melt-quenched sample showed the pseudohexagonal phase, and at about 190 °C, the metastable phase started appearing and

coexisted with the psuedohexagonal phase until melting. If the psuedohexagonal phase was cooled without allowing it to melt, then it transformed into the γ phase.

The α phase obtained by precipitating nylon-6,9 in 1,4-butanediol transformed into the γ phase at about 190 °C on heating which was stable up to melting. During this transition a small amount of the material transformed into the metastable phase and was stable until melting. Upon melt crystallization at 205 °C nylon-6,9 crystallized in the γ phase, and the α phase was seen at about 70 °C on cooling to room temperature. Melt-quenched nylon-6,9 crystallized into the psuedohexagonal phase and similar to nylon-6,7, the metastable phase was formed at about 160 °C. On cooling the psuedohexagonal phase transformed into the γ phase immediately.

The HTFTIR studies indicated that in the case of nylon-6,7, the molecular conformation in the γ phases obtained by 1,4-butanediol crystallization and melt crystallization were different. On the other hand nylon-6,9 crystallized in 1,4-butanediol showed spectra typical of the α phase, while the melt-crystallized sample showed spectra due to the γ phase.

The crystallization of nylon-6–clay nanocomposite was studied by variable temperature WAXS and FTIR. Nylon-6 was found to crystallize into the γ phase at 210 °C, as indicated by its characteristic peaks in WAXS. However, an additional peak was observed close but on the lower angle side of the main γ phase peak, indicating the presence of a metastable phase. The clay content in the nanocomposite as well as the crystallization conditions dictated the extent of metastable phase that developed. The temperature dependence of the *d* spacing of the γ phase obtained in the presence of clay layers showed difference from the γ phase obtained by treating nylon-6 in KI/I_2 solution. Variable temperature FTIR studies were conducted on the γ phases for the first time, and it showed definite but subtle differences in the spectra of the phases obtained by the two methods.

6.2 Conclusions

The major conclusions arising out of the present work are given below.

- Nylon-11 showed a change in the structural features above 110 °C on heating, which manifested as a change in the crystalline phase. The WAXS studies clearly

indicated that the in the case of nylon-11, the α and α' phases are distinctly different. The smectic phase or the δ phase obtained on melt quenching appeared to be the pseudohexagonal phase. Nylon-11 is the first nylon to exhibit variation in the pseudohexagonal phase packing mode depending on the starting phase. In the case of nylon-11, it was speculated from the variable temperature FTIR studies on TFA-cast film with 5% TFA, that the interaction of TFA with amide groups controls the formation of hydrogen bonding leading to the γ phase.

- The characteristics of the γ phase of nylons -6,7 and -6,9 are similar, probably owing to their chemical structural similarity. Nevertheless, nylon-6,9 could crystallize into the α phase under appropriate crystallization conditions, but nylon-6,7 always crystallized in the γ phase only. HTFTIR studies indicated that the molecular conformation in the γ phase is dictated by the crystallization conditions.

- Similarly, the subtle differences in the FTIR spectra of the γ phase of nylon-6 crystallized in the presence of clay layers and the γ phase obtained by the treatment in KI/I_2 indicates the minor variation in the molecular conformations in these phases.

- The studies presented above clearly show that the γ phase is a very stable crystalline modification of nylons and does not undergo any crystalline transitions on heating. On the other hand α phase of nylons undergoes crystalline transition on heating. The molecular conformation in the crystal lattice of γ phase is different from that of the α phase.

- It has been shown for the first time that the γ phase is accompanied by the metastable phase in all the nylons studied in this thesis. The metastable phase is seen at high temperature and the amount of the metastable phase is relatively less compared with the γ phase.

6.3 Future Perspectives

- The key focus of the present study is on the γ phase. The properties and characteristics of the metastable phase are less understood at this stage. It would be of interest to study in detail the metastable phase.

- Most nylons have the α phase when used in commercial applications. Hence it is of interest to study the physical and mechanical properties of nylons having the γ phase.

- It would be interesting to systematically vary the methylene sequence in the nylon structure and study the effect of methylene sequence on the polymorphisms and crystalline transitions in nylons.

List of Publications

1. Crystalline Phases in Nylon-11: Studies Using HTWAXS and HTFTIR

   Smitha S. Nair, C. Ramesh and K. Tashiro

   Macromolecules **2006,** *39*, 2841

2. Studies on the Crystallization Behavior of Nylon-6 in the Presence of Layered Silicates Using Variable Temperature WAXS and FTIR

   Smitha S. Nair and C. Ramesh

   Macromolecules **2005**, *38*, 454

3. Studies on the Clathrate (δ) Form of Syndiotactic Polystyrene Crystallized by Different Solvents Using Fourier Transform Infrared Spectroscopy

   E. Bhoje Gowd, **Smitha S. Nair,** C. Ramesh and K. Tashiro

   Macromolecules **2003**, *36*, 7388

4. Crystalline Transitions of the Clathrate (δ) Form of Syndiotactic Polystyrene during Heating: Studies Using High-Temperature X-ray Diffraction

   E. Bhoje Gowd, **Smitha S. Nair** and C. Ramesh

   Macromolecules **2002**, *35*, 8509

5. Polymorphism in Nylon-11: Characterization using HTWAXS and HTFTIR

   Smitha S. Nair, C. Ramesh and K. Tashiro

   Macromolecular Symposia, in press